

University of Alberta

Determinants of Histone H1 dynamics *in vivo*

by

Nikhil Raghuram

A thesis submitted to the Faculty of Graduate Studies and Research
in partial fulfillment of the requirements for the degree of

Doctor of Philosophy
in
Experimental Oncology

Department of Oncology

©Nikhil Raghuram
Spring 2013
Edmonton, Alberta

Permission is hereby granted to the University of Alberta Libraries to reproduce single copies of this thesis and to lend or sell such copies for private, scholarly or scientific research purposes only. Where the thesis is converted to, or otherwise made available in digital form, the University of Alberta will advise potential users of the thesis of these terms.

The author reserves all other publication and other rights in association with the copyright in the thesis and, except as herein before provided, neither the thesis nor any substantial portion thereof may be printed or otherwise reproduced in any material form whatsoever without the author's prior written permission.

Abstract

Chromatin plays a pivotal role in regulating critical DNA dependent processes, such as transcription. Chromatin and associated epigenetic modifications form the molecular basis of differentiation and development and are misregulated in disease states, such as cancer. Histone H1 molecules are key players in epigenetic mechanisms and are involved in the formation and stabilization of higher order chromatin structures, as well as having gene specific effects in transcription. Post-translational modifications, such as core histone acetylation and H1 phosphorylation, modify H1 binding and thus alter H1 function, although the underlying molecular mechanisms are unknown.

We have used live cell imaging techniques, such as FRAP, to elucidate the complex binding events of H1 in response to chromatin modifying events during transcription. Using this approach, we have described the changes in H1 dynamics upon induction of core histone acetylation and how cooperativity of H1 binding is changed upon this modification. Using classical biochemical experiments and imaging techniques, we have shown a novel interaction between phosphorylated H1 molecules and a nuclear prolyl-isomerase, Pin1. This establishes phosphorylation-dependent proline isomerization of H1 as a key regulatory event during transcriptional initiation. Pin1 and core histone acetylation impart changes in one or more of the binding steps of H1, impeding H1 function. This can have consequences on the stability of higher orders of chromatin structure. Our studies provide mechanistic insight towards the epigenetic regulation of H1 and chromatin structure in transcriptional processes.

Acknowledgements

I wish to acknowledge Dr. Michael Hendzel for his excellent supervision and support over the years. I thank him for taking me under his wing as an undergraduate student and providing me with a perfect environment for conducting research. I would like to thank my committee members, Dr. Luis Schang and Dr. Gordon Chan, for their support and encouragement over the years. Much of the work in thesis has been inspired by fruitful discussions with Dr. Hendzel and members of my committee, and I am grateful for their keen involvement in my work and success. Thanks to Dr. John Th'ng for his valuable advice and friendship over the years. I would also like to thank members of the lab, Darin McDonald, Kristal Missiaen, Dr. Ismail H Ismail, Dr. Hilmar Strickfaden, Stuart Campbell, Dr. Leah Young, and Christi Andrin for their guidance and friendship over the years. They have made the long years of my PhD life enjoyable and I am greatly indebted for that. Dr. Roseline Godbout has been instrumental in instilling a sense of dedication and determination in my work and I am truly grateful to having her around. Dr. Xuejun Sun's knowledge and work ethic has been inspirational, and Gerry Barron has provided valuable companionship and guidance in the Cell Imaging Facility. I would also like to thank CIHR, ACB, AFHMR and the Endowed Studentship for providing scholarships. Finally, I would like to thank my dear parents, grandparents and my younger brother for their love and support over the years without which none of this would have been possible.

Chapter I - Introduction	1
1.1 Epigenetics and cancer.....	2
1.2 The eukaryotic nucleus and its organization.....	3
1.3 The nucleosome.....	4
1.4 Higher orders of chromatin structure.....	4
1.5 Core histones.....	7
1.6 Linker histones.....	7
1.6.1 Linker histone variants.....	8
1.6.2 Expression pattern of variants.....	8
1.6.3 Localization.....	10
1.6.4 Structural features.....	11
1.6.5 H1 in other organisms.....	17
1.7 Role of histone H1 in higher order chromatin fiber formation.....	18
1.7.1 H1 and the structure of the 30nm chromatin fiber.....	23
1.8 Histone H1- a gateway to chromatin.....	30
1.9 Globular domain of H1.....	31
1.10 H1 C-terminal domain	32
1.11 The CTD of H1 is intrinsically disordered.....	33
1.12 The N-terminal domain of H1.....	35
1.12.1 Protein interactions mediated by the NTD of H1.....	36
1.13 Cooperativity in histone H1 binding to chromatin.....	36
1.14 Histone H1 and the regulation of gene expression	37
1.14.1 H1 is a gene specific regulator of transcription.....	39
1.15 Core histone acetylation, chromatin and transcription.....	40
1.15.1 Histone code.....	40
1.15.2 N-terminal tails and their role in chromatin condensation.....	41
1.15.3 Secondary structure of core histone NTD	43
1.15.4 Core Histone acetylation.....	43
1.15.5 Core histone acetylation and transcription.....	45
1.15.6 Core histone acetylation and nucleosome assembly during S-phase.....	46
1.15.7 Core histone acetylation and chromatin structure.....	47
1.15.8 HDAC inhibitors.....	50
1.15.9 Distinct kinetic pools of acetylated histones.....	51
1.15.10 Class I acetylation and histone H1	54
1.16 Histone H1 phosphorylation	55
1.16.1 Histone H1 phosphorylation and cancer	58
1.16.2 How H1 phosphorylation is thought to affect H1 binding.....	58
1.16.3 Chromatin condensation and H1 phosphorylation.....	59
1.16.4 Transcription and H1 phosphorylation levels.....	62
1.17 Proline Isomerization.....	64
1.17.1 Cyclophilins.....	68
1.17.2 FKBP.....	69

1.17.3	PTPA.....	70
1.17.4	Parvulins.....	70
1.18	Pin1.....	71
1.18.1	Regulation of Pin1 through the WW domain.....	74
1.18.2	Catalytic domain of Pin1.....	75
1.18.3	Pin1 substrates.....	76
1.18.4	Pin1 regulation of Cdc25.....	77
1.18.5	Regulation of transcription by Pin1.....	78
1.18.6	Regulation of chromatin structure by Pin1.....	79
1.18.7	Role of Pin1 in cancer and disease.....	80
1.19	Fluorescence recovery after photobleaching (FRAP).....	80
1.19.1	Photobleaching.....	81
1.19.2	Recovery.....	82
1.19.3	Mathematical modeling of FRAP curves.....	86
1.20	Thesis Focus.....	88

Chapter II – Experimental Procedures.....90

2.1	Cell culture.....	91
2.2	Isolation of nuclei and histones.....	91
2.3	Electrophoresis.....	92
2.4	Nucleosome reconstitution.....	93
2.5	Roscovitine treatment/Acid extraction of histones.....	93
2.6	Mobility shift assay for detecting phosphorylated H1.....	94
2.7	Co-immunoprecipitation.....	94
2.8	H1 phosphorylation/dephosphorylation assays.....	95
2.9	Volumetric measurement of lac arrays.....	96
2.10	Fluorescence recovery after photo-bleaching.....	97
2.11	Kinetic modeling of H1 dynamics <i>in vivo</i>	98
2.12	Fluorescence Resonance Energy Transfer (FRET).....	100
2.13	Transmission Electron Microscopy.....	100
2.14	Immunofluorescence.....	101
2.15	Buffers and Recipes.....	102

Chapter III – Core histone acetylation affects the cooperative behavior and high-affinity binding of histone H1 to chromatin.....105

3.1	Abstract.....	106
3.2	Introduction.....	107
3.3	Results.....	110
3.3.1	Comparison of binding affinities among H1 variants.....	110
3.3.2	Changes in histone phosphorylation and acetylation post TSA treatment.....	114
3.3.3	Analysis of histone H1 dynamics post induction of core histone acetylation (TSA 1hr).....	115

3.3.4	Histone H1 dynamics with hyperacetylated core histone.....	119
3.3.5	Heterochromatin vs. Euchromatin.....	122
3.3.6	H1 hybrids and their response to hyperacetylation.....	126
3.3.7	Hyperacetylation changes the cooperativity of H1 binding to chromatin.....	129
3.4	Discussion.....	136
3.5	Supplementary Material.....	141
3.5.1	Assessing the change in cooperativity of H1 binding to chromatin following hyperacetylation.....	141
3.5.2	Supplementary Figures.....	146

Chapter IV – Pin1 promotes chromatin condensation and regulates histone H1 dephosphorylation and chromatin binding.....154

4.1	Abstract.....	155
4.2	Introduction.....	156
4.3	Results.....	158
4.3.1	Pin1 interacts with histone H1.....	158
4.3.2	Pin1 promotes the dephosphorylation of H1.....	161
4.3.3	Phosphorylation of H1 and Pin1 cause conformational changes in H1 CTD.....	167
4.3.4	Pin1 modulates the dynamics of H1.1 and H1.5.....	171
4.3.5	Distinct effects of Ser at position 152 vs. 183 in H1.1....	175
4.3.6	Distinct effects of Thr at position 152 vs. 183 in H1.1....	180
4.3.7	Pin1 depletion relaxes chromatin and causes decondensation.....	181
4.3.8	Role of Pin1 in transcription.....	189
4.4	Discussion.....	195
4.4.1	- Histone H1 interacts with Pin1.....	195
4.4.2	- Pin1 as a chromatin modifier.....	196
4.4.3	- Histone H1 phosphorylation, Pin1 and transcription.....	198
4.5	– Supplementary Figures.....	201
4.6	– Supplementary unpublished results and discussion.....	214
4.6.1	– H1 dynamics at sites of replication.....	214
4.6.2	– Focal accumulation of Pin1 alters chromatin condensation.....	219
4.6.3	– Focal accumulation of Pin1 recruits RNA Polymerase II.....	224
4.6.4	– Focal accumulation of Pin1 does not lead to transcriptional elongation.....	226

Chapter V – Perspectives.....231

5.1	Synopsis	232
5.2	Comprehensive model.....	233

5.3	Applicability to other post-translational modifications	
	DNA methylation and H1	236
5.4	Implications of the model –	238
5.4.1	Core histone hyperacetylation and phosphorylation dependent proline isomerization of H1 modulate the ‘site-exposure’ of chromatosomes.....	238
5.4.2	Chromatin decondensation and transcription.....	238
5.5	- Future directions.....	250
5.5.1	Understanding the role of the NTD of H1.....	250
5.3.2	Understanding the role of Thr in H1	252
5.3.3	Does Pin1 recruit RNA Polymerase II to sites of transcription?.....	255
	References	259

List of Tables –

Table 3. 1 – Detailed kinetic modeling data (TSA analysis).....	118
Supplementary Table I – Mathematical modeling data of H1.1, H1.5 and H1.1mut.....	213

List of Figures -

Figure 1.1 – Condensation of DNA from a 2nm fiber (naked DNA) to higher orders of chromatin fiber structures.....	6
Figure 1.2 – Protein sequence alignment of different H1 variants.....	13
Figure 1.3 – Structure of H1 and location of H1 binding.....	15
Figure 1.4 – Changes in chromatin structure upon addition of linker histones and salt conditions.....	21
Figure 1.5 – Proposed models of the 30nm chromatin fiber.....	27
Figure 1.6 – Changes in 30nm structures upon H1 binding.....	29
Figure 1.7– Location and sequence conservation of Thr-Pro and Ser-Pro residues among H1 variants.....	57
Figure 1. 8 – Proline isomerisation at the structural level.....	67
Figure 1.9 – Structural domains of human Pin1.....	73

Figure 1.10 – From FRAP to mathematical modeling.....	85
Figure 3.1 - Comparison of t_{50} (a) and t_{90} (b) values of the six H1 variants before and after treatment with HDAC inhibitor, TSA.....	113
Figure 3.2 - FRAP recovery profiles post induction of core histone acetylation (TSA treatment for 1hr).....	117
Figure 3.3 - FRAP recovery profiles post induction of core histone hyperacetylation (TSA treatment for 18 hrs).....	121
Figure 3.4 - Comparison of t_{50} and t_{90} values between heterochromatin and euchromatin enriched H1 variants.....	125
Figure 3.5 - Comparison of t_{50} , t_{90} , and kinetic parameters of H1 hybrids following core histone hyperacetylation (TSA 18hrs).....	128
Figure 3.6 - Behavior of individual domains of H1 to hyperacetylation.....	133
Figure 3.7 – Cooperativity in H1 binding is reduced following hyperacetylation.....	134
Figure 3.8 - Impact of hyperacetylation on LA and HA sites.....	135
Supplementary Figure 3.1 – TSA increases core histone acetylation levels.....	146
Supplementary Figure 3.2 – Linker histone and core histone phosphorylation status upon TSA treatment.....	148
Supplementary Figure 3.3 – Analyzing whether addition of Hoechst 33342 affects H1 mobility.....	149
Supplementary Figure 3.4 - FRAP recovery profiles of H1 variants post induction of core histone acetylation (TSA treatment for 1hr) enriched in euchromatin....	150
Supplementary Figure 3.5 - FRAP recovery profiles of H1 variants post induction of core histone acetylation (TSA treatment for 1hr) enriched in heterochromatin.....	151
Supplementary Figure 3.6 - FRAP recovery profiles of H1 variants post induction of core histone hyper-acetylation (TSA treatment for 18hrs) enriched in euchromatin.....	152

Supplementary Figure 3.7 - FRAP recovery profiles of H1 variants post induction of core histone hyper-acetylation (TSA treatment for 18hrs) enriched in heterochromatin.....	153
Figure 4.1 – Pin1 interacts with histone H1.....	160
Figure 4.2 – Pin1 promotes H1 dephosphorylation.....	165
Figure 4.3 – Pin1 and H1 phosphorylation change the structure of the CTD.....	170
Figure 4.4 – Pin1 stabilizes GFP-H1.1 and GFP-H1.5 dynamics.....	174
Figure 4.5 – Pin1 primarily acts at phosphorylated position S183 on H1.1.....	179
Figure 4.6 – Pin1 ^{-/-} cells have a relaxed chromatin structure.....	185
Figure 4.6(A) – Ultrastructure of Pin1 knockout cell	187
Figure 4.6(B) – Ultrastructure of Pin1 wt cell	188
Figure 4.7 – Pin1 and H1 phosphorylation are marks of transcriptionally competent chromatin.....	193
Figure 4.8 – Pin1 stabilizes H1 binding at sites of transcription.....	194
Supplementary Figure 4.1 – Activity of Cdk2 extracted from Pin1wt and Pin1 ^{-/-} cells.....	201
Supplementary Figure 4.2 – Pin1 promotes H1 dephosphorylation of Ser residues <i>in vivo</i>	202
Supplementary Figure 4.3 – FRET controls and FRET efficiency.....	203
Supplementary Figure 4.4 – Effect of Cyclosporine and Rapamycin on H1 dynamics.....	204
Supplementary Figure 4.5 – Core histone and H1 composition in Pin1wt vs. Pin1 ^{-/-} cells.....	205
Supplementary Figure 4.6 - Mobility shift assay for detecting phosphorylated H1.....	206
Supplementary Figure 4.7 – Mathematical modeling data derived from H1.1mut FRAP curves.....	207
Supplementary Figure 4.8 – Quantification of Pin1 and pS173 levels at lac	

arrays.....	209
Supplementary Figure 4.9 – Accumulation of RNA Polymerase II at sites of transcription and the affect of a-amanitin on its levels.....	210
Supplementary Figure 4.10 – Chromatin decondensation upon transcriptional activation.....	211
Supplementary Figure 4.11 - Dynamics of H1.1 and H1.2 at sites of transcription.....	212
Supplementary Figure 4.12 – H1.1 dynamics at sites of replication.....	217
Supplementary Figure 4.13 – Focal accumulation of Pin1 and Pin1 <i>mut</i> causes chromatin decondensation at lac arrays.....	222
Supplementary Figure 4.14 – Focal accumulation of Pin1 leads to recruitment of RNA Polymerase II in an isomerase independent manner.....	225
Figure 4.15 – Focal accumulation of Pin1 or Pin1 <i>mut</i> does not lead to transcriptional elongation.....	227/8
Figure 4.16 – Transcriptional activation at sites of Pin1 accumulation leads to increased chromatin decondensation.....	230
Figure 5.1 – Changes in nucleosomal structure upon induction of transcription-associated post-translational modifications of histones.....	235
Figure 5.2 – Current model describing the changes in chromatin structure upon transcriptional induction or the hierarchical model of transcription-induced changes to chromatin.....	241
Figure 5.3 – Dynamic chromatin conformation model.....	248

List of Symbols and Abbreviations used

aa	Amino acid
Ala	Alanine
APS	Ammonium Persulphate
Arg	Arginine
ATM	Ataxia telangiectasia mutated
ATP	Adenosine Triphosphate
AUT	Acetic acid/urea/Triton X-100
BAF	Barrier to Autointegration Factor
b_l	Population of H1 bound with low affinity
b_s	Population of H1 bound with high affinity
bp	basepair
BSA	Bovine serum albumin
CFP	Cyan Fluorescent Protein
CTD	C-Terminal Domain
Cdk/cdk	Cyclin dependent kinase
CMV	Cytomegalovirus
CsA	Cyclosporin A
Cys	Cysteine
DAPI	4',6-diamidino-2-phenylindole
D_{eff}	Effective diffusion coefficient
ddH ₂ O	deionized distilled water
DMEM	Dulbecco's modified eagle's media
Dnmt	DNA Methyltransferase
DNA	Deoxyribose nucleic acid
DNase	deoxyribonuclease
DTT	Dithiothreitol
EDTA	ethylenediaminetetraacetic acid
(e)GFP	(enhanced) Green Fluorescent protein
EM	Electron Microscopy
Glu	Glutamic acid
Gly	Glycine
Hepes	(4-(2-hydroxyethyl)-1-piperazineethanesulfonic acid)
HMG	High Mobility Group
HP1	Heterochromatin protein 1
HPLC	High-performance liquid chromatography
f	Freely diffusing population
FACT	Facilitator of transcription
FBS	Fetal Bovine Serum
Fig	Figure
FKBP	FK506 Binding protein
FRAP	Fluorescent Recovery After Photobleaching
FRET	Fluorescent (Or Forster) Resonance Energy Transfer
HA	High affinity (H1 population)
HAT	Histone acetyltransferase

HCl	Hydrochloric acid
HDAC	Histone deacetylases
HDACi	Histone deacetylase inhibitor
IPTG	Isopropyl- β -D-thio-galactoside
kD	Kilodalton
KS-test	Kolmogorov-Smirnov test
LA	Low-affinity (H1 population)
LacR	Lac Repressor
LSM	Laser Scanning microscope
Lys	Lysine
MAPK	Mitogen-activated protein (MAP) kinases
mcherry	monomeric cherry fluorescent protein
MEF	Mouse Embryonic Fibroblasts
min	minute
MMTV	Mouse Mammary Tumour Virus
mut	mutant
NA	Numerical Aperture
NAD	Nicotinamide adenine dinucleotide
NIB	Nuclei Isolation Buffer
NIMA	never in mitosis A)-1
NRL	Nucleosomal repeat length
NTD	N-Terminal Domain
PAGE	Polyacrylamide gel electrophoresis
PBS	Phosphate buffered saline
PCNA	Proliferating cell nuclear antigen
PCR	Polymerase chain reaction
PKA/PKC	Protein Kinase A/C
PPIase	Peptidyl-prolyl isomerase
PP2A	Protein phosphatase 2
Pro	Proline
PTPA	Phosphotyrosyl phosphatase activator (PTPA)
Rb	Retinoblastoma protein, or pRb
RIPA	<u>Radio Immuno-precipitation buffer</u>
RNA	Ribonucleic acid
RFP	Red Fluorescent protein
RNAPolII	RNAPolymerase II
SAHA	Suberoylanilide hydroxamic acid
SET	Su(var)39, Enhancer of Zeste, Trithorax
SDS	Sodium dodecyl Sulphate
siRNA	Small Interfering ribonucleic acid
SEM	Standard Error Mean
Ser	Serine
SD	Standard Deviation
τ_R	Residence Time
τ_T	Transition Time

tTA-ER	tetracycline transcriptional activator - hormone binding domain of the estrogen receptor (ER)
TBS	Tris-buffered Saline
TBST	TBS with 0.1% Tween-20
TDMS	Top-Down Mass Spectrometry
TEM	Transmission electron microscope
TEMED	Tetramethylethylenediamine
Thr	Threonine
TopoII α	type IIA topoisomerase
Tris	tris(hydroxymethyl)aminomethane
TSA	Trichostatin A
Tyr	Tyrosine
t _{1/2}	T ₅₀ Time required to achieve half of maximum value
UV	Ultraviolet
WT	Wildtype
X	Fold
YFP	Yellow Fluorescent protein

Units of measurement used

°C	degree Celsius
L	Liter
μ l	Microliter
μ m	Micrometer
μ M	Micromolar
m	meter
nm	nanometer
s (or sec)	second
pH	$-\log[H^+]$

Chapter I - Introduction

1.1 – Epigenetics and cancer

Epigenetics is a term coined by Conrad Hal Waddington in 1942 who described it as the study of epigenesis, or the ‘causal mechanisms’ of development, underpinning the relationship between genes, their products and the processes that brings the phenotype into being (Van Speybroeck, 2002; Waddington, 1942). The term ‘epigenetics’ has since evolved as the study of stable or heritable changes in gene expression profiles that occur without changes in DNA sequence. However, it must be kept in mind that most epigenetic changes, unlike genetic changes, are reversible in nature. For example, converting fully differentiated cells to stem-cell like phenotype through epigenetic mediated induced pluripotency has dispelled our long-held belief that differentiation is unidirectional and that these processes are reversible under appropriate conditions (Yamanaka, 2009).

Epigenetic regulators include the plethora of histone modifications, DNA methylation, as well as recent discoveries with non-coding RNAs that play a role in the epigenetic phenomena. They play a fundamental role in many processes such as differentiation, senescence, aging, X-chromosome inactivation as well as in disease states such as cancer. Global DNA hypomethylation and promoter hypermethylation has been observed in almost every type of human cancer, the latter correlating with silencing of tumor suppressors as well as providing tumor cells with selective growth advantage (Baylin & Herman, 2000; Costello et al, 2000; Feinberg & Vogelstein, 1983; Goelz et al, 1985). The epigenetic landscape of cancer cells is further characterized by altered histone modifications of crucial genes and a global reduction in monoacetylation and trimethylated H4 molecules

(Fraga et al, 2005). Furthermore, the role that epigenetics play in carcinogenesis, has recently been recognized by the fact that tumor cells could develop a cancer stem cell like phenotype through epithelial to mesenchymal transitions, which are mediated primarily through epigenetic means (Mani et al, 2008).

Such epigenetic aberrations occur at frequencies similar to genetic mutations of tumor suppressors, which are traditionally held as a causal link for oncogenesis (Baylin & Herman, 2000; Jones & Laird, 1999). Epigenetic aberrations are now held to be responsible for virtually every step of the oncogenic pathway from initiation to progression of tumors (Jones & Baylin, 2002) underlying the importance of studying such events. These and other studies have been instrumental in the introduction of a number of DNA methyltransferase inhibitors and histone deacetylase inhibitors into clinical trials for cancer treatment and have been shown to have promising anti-tumor properties (Yoo & Jones, 2006).

1.2 The eukaryotic nucleus and its organization

In all eukaryotic nuclei, genomic DNA exists in a highly compacted state through its association with proteins known as histones. Histones help offset the strong negative charges present on the DNA molecule and provide a scaffold onto which DNA can be wound (Wolffe, 1998).

The packaging of DNA together with histones involves a series of distinct hierarchical events that essentially compacts the entire 2m of genomic DNA into the 5-10 μ m constrains of the nucleus. This ordered nucleoprotein complex is known as chromatin (Wolffe, 1998).

1.3 The nucleosome

The basic structural and functional repeating element of chromatin is termed the nucleosome. The nucleosome is comprised of 147bp of DNA wound 1.65 in a left-handed superhelical turn around the histone octamer (Luger et al, 1997; Richmond et al, 1984). The histone octamer comprises of two copies of each core histone – H2A, H2B, H3 and H4 (Kornberg & Thomas, 1974). Binding of the linker histone, or histone H1, organizes an additional 20bp of DNA into a structure known as the chromatosome. This highly conserved structural entity forms the fundamental unit of higher order structures of chromatin (Van Holde, 1988; Widom, 1998). Nucleosomal arrays stabilized by histone H1 are traditionally referred to as chromatin fibers. It must be noted that the assembly of DNA into these structures does not render them static, but these are highly dynamic, conformationally mobile, multi-protein complexes regulating a host of processes such as transcription, replication and DNA repair (Anderson & Widom, 2000; Van Holde, 1988; Widom, 1998; Wolffe, 1998).

The nucleosome fulfils three major functions. One, it imparts a structural bend in the DNA at the atomic level and neutralizes part of its negative charge. Secondly, the binding of DNA to histones curtails the accessibility of DNA to other DNA binding proteins such as transcription factors. Thirdly, the nucleosome forms the building blocks for the formation of higher order chromatin structure that further engage DNA into higher orders of DNA compaction (Luger et al, 1997).

1.4 - Higher orders of chromatin structure

Higher order chromatin structure consist of arrays of nucleosomes, or chromatosomes, in an orderly, defined yet dynamic orientation in three-dimensional space (Woodcock & Ghosh, 2010). *In vitro*, arrays of nucleosomes fold into distinct 30nm chromatin fibers dependent upon the ionic strength of the media, the presence of N-terminal tails of the core histones, and the presence of linker histones (Bednar et al, 1998; Carruthers et al, 1998) (see Figure 1.1). Binding of the nucleosomes increases the DNA packing ratio (length of DNA/length into which it is packed) to 6:1, while a 30nm fiber increases the compaction of DNA to 40:1. Mitotic chromosomes, which represent highly condensed chromatin structures have DNA compacted to 10,000:1. The mechanism by which such dense chromatin structures are attained or the very nature of these structures itself is still under investigation. It must be noted that the structure of chromatin varies in a spatio-temporal manner, with dense structures of chromatin prevalent in heterochromatin, while 'relaxed' chromatin is present in euchromatin. Additionally, as cells undergo mitosis, chromatin structures are maximally condensed following which chromatin decondenses in the daughter cells.

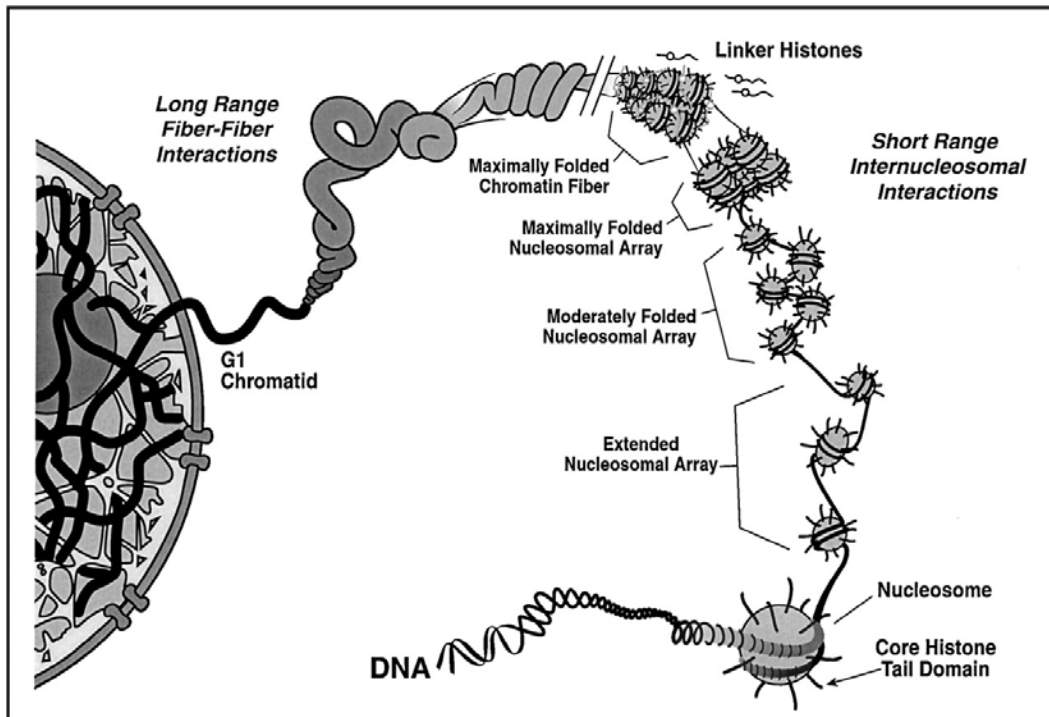


Figure 1.1 – Condensation of DNA from a 2nm fiber (naked DNA) to higher orders of chromatin fiber structures. Figure illustrates the hierarchy of folding that is responsible for condensing the entire length of the genomic DNA into the constraints of the nucleus. Binding of histones organizes DNA into a structure known as the nucleosome and arrays of nucleosomes in an extended conformation are also known as the 10nm fiber. Binding of linker histones further condenses this structure to form a 30nm chromatin fiber. Linker histones and the NTD of core histones play a key role in the formation and stabilization of higher order structures. Processes that result in, or indeed the structure or conformation of chromatin fibers higher than the 30nm chromatin fiber are not known. Figure adapted from (Hansen, 2002), and reproduced with permission from Annual Reviews of Biophysics and Biomolecular Structure.

1.5 - Core histones

Each of the core histones (H2A, H2B, H3 and H4) consists of a structured C-terminal histone fold domain and an unstructured N-terminal domain. The latter play key roles in interacting with a host of proteins involved in modifying the accessibility of proteins to DNA, along with being sites of modifications in a number of cellular processes such as transcription, DNA damage signaling events, replication, recombination (Van Holde, 1988; Widom, 1998; Wolffe, 1998). The tail domains, compared to the fold-domain, are very flexible and are thought to rearrange spatially under different chromatin modifications (Hansen, 2002). The N-terminal domains are key requirements for the formation of higher order structures even in the presence of linker histones (Schwarz et al, 1996; Tse & Hansen, 1997). They are thought to mediate both short-range nucleosomal interactions, as well as long-range interactions that are key in maintaining the 30nm fiber.

1.6 – Linker histones

Linker histones are a family of structural proteins associated with chromatin that bind and influence chromatin fiber stability and dynamics. They are fairly small (~21KDa) proteins and are composed of predominantly basic amino acids (Godde & Ura, 2008; Noll & Kornberg, 1977; Shaw et al, 1976; Whitlock & Simpson, 1976). Linker histones are found in near 1:1 stoichiometry with nucleosomes, and have been found to be essential for mammalian cell survival (Fan et al, 2003; Fan et al, 2005). A 50% decrease in global H1 levels was found to alter chromatin

structure by increasing the chromatin decondensation that paralleled a decrease in nucleosomal spacing (Fan et al, 2005).

1.6.1 - Linker histone variants - Lower eukaryotes, such as yeast, possess only one subtype of histone H1 (Ali et al, 2004). Mammalian cells on the other hand, have seven to eight different subtypes or variants of H1 (Albig et al, 1997a), encoded by different genes. The variants were primarily resolved with the help of cation-exchange chromatography (Kinkade & Cole, 1966; Parseghian et al, 1993), two-dimensional gel electrophoresis (SDS-PAGE and AUT) (Lennox & Cohen, 1983). The existence of multiple variants of H1 was further confirmed with the help of reverse-phase HPLC (RP-HPLC), capillary electrophoresis and top-down mass spectrometry (TDMS) (Rundquist & Lindner, 2006; Zheng et al, 2010).

H1 variants were initially named based on their chromatographic properties (reviewed in (Parseghian & Hamkalo, 2001)), however, were later renamed based on the order that they were cloned and sequenced by Doenecke (Albig et al, 1997b). There have been at least ten homologous H1 proteins described to date. These include H1.0, H1.1, H1.2, H1.3, H1.4, H1.5, H1t, H1Foo, spermatid specific H1-like protein HILS1 and H1x.

1.6.2 - Expression pattern of variants - H1.2, H1.3, H1.4 and H1.5 are present in all somatic cells, while H1.1's expression is restricted to thymus, testis, spleen, neuronal cells, and lymphocytic cells (Franke et al, 1998; Parseghian & Hamkalo, 2001; Parseghian et al, 1994; Rasheed et al, 1989). The expression of H1.0, the replacement subtype, is mainly restricted to cells that are in G0 phase of the cell cycle, or in terminally differentiated cells (Doenecke et al, 1997; Panyim &

Chalkley, 1969a; Zlatanova & Doenecke, 1994). H1t, H1Foo and H1LS1 are highly developmental and tissue specific, with H1t being restricted to male germ-cells (Seyedin et al, 1981), and H1Foo is specific to oocyte, zygote and early embryo (Tanaka et al, 2001; Tanaka et al, 2005). H1LS1, the spermatid specific H1, is thought to replace H1t during spermiogenesis (Yan et al, 2003). H1x is a relatively newer member of the H1 family (Happel et al, 2005) and is found to be expressed in all tissues examined (Yamamoto & Horikoshi, 1996).

Among the different variants, the expression pattern of H1.0 has received most attention, in part, due to its stringent regulation. H1.0 is seen to accumulate in cells following terminal differentiation (Gjerset et al, 1982; Zlatanova & Doenecke, 1994). The functional relevance of H1.0 accumulation in differentiated cells is currently unknown. However, mice completely lacking the H1.0 gene were found to be viable and fertile, suggesting that H1.0 was dispensable, at least for normal mouse development (Sirotkin et al, 1995).

The expression pattern of H1.1-H1.5 is linked to the cell-cycle, while expression of H1.0 and H1.x are generally considered to be independent of cell cycle status (Doenecke et al, 1994). The expression of H1.0 remained unchanged in the presence of DNA replication inhibitors (Zlatanova, 1980) suggesting its expression being independent of cell cycle. Studies in murine erythroleukemia cells showed H1.0 gene transcription to occur throughout the cell cycle, however their levels did peak in mid to late S-phase (Grunwald et al, 1991). This is in contrast to replication dependent H3 expression that begins in early S-phase (Grunwald et al, 1991). More importantly, chemical inducers of differentiation,

led to high levels of H1.0 accumulation in these cells, once again linking H1.0 to differentiation (Grunwald et al, 1991). Furthermore, the mRNAs of both H1.0 and H1.x are polyadenylated (Doenecke et al, 1994; Yamamoto & Horikoshi, 1996) and the genes themselves exist outside the main histone cluster of genes. In direct contrast, most of the histone genes and the somatic H1 variants the gene expression profiles of which are linked to DNA replication have a characteristic 3'-hairpin like mRNA structure, which is necessary for S-phase dependent processing of mRNA (Doenecke et al, 1994; Marzluff, 2005; Zlatanova & Doenecke, 1994). Additionally, most of the replication dependent H1 genes are clustered, while replication independent H1 genes are spread around. For example, while most of the somatic H1 genes and H1t map to chromosome 6 (Albig et al, 1993), H1.0 maps to chromosome 22 (Doenecke et al, 1994), and H1x maps to chromosome 3 (Sulimova et al, 2002).

Despite the spectrum of H1 variants available to a cell, there appears to be limited heterogeneity, at least in HeLa cells, where only H1.2 and H1.4 are the predominant variants expressed and H1.5 is expressed at a much lower ratio compared to its other counterparts (Zheng et al, 2010). Whether the limited heterogeneity is a characteristic of differentiated or tumorigenic cells, is currently unknown. Furthermore, there are also single amino acid polymorphisms (Ala to Thr substitution in H1.2 at position 142) that are known to occur (Zheng et al, 2010) adding further diversity to H1 proteins within the nucleus.

1.6.3 - Localization The variants also differ in their localization within the nucleus. Some variants, such as H1.1 and H1.2 are more enriched in euchromatin,

while other variants, such as H1.0, H1.4 and H1.5 prefer heterochromatic sites (Th'ng et al, 2005). H1.x. on the other hand has been shown to accumulate in the nucleolus (Happel et al, 2005), however, its function in the nucleolus has not yet been determined.

1.6.4 - Structural features - The human variants share a common structure that consists of a central globular winged helix domain, a short N-terminal domain (NTD) and long unstructured C-terminal domain (CTD) (Figure 1.3) (Albig et al, 1997b). Much of the heterogeneity among the members is present in the NTD and CTD, while the globular domain is fairly well conserved. The different members also possess distinct kinetic properties, which reflects differences in their binding affinity to chromatin. These could be attributed to differences in either the net charge on H1, or the length of the CTD, or the number and relative positions of the S/TPKK phosphorylation motifs on different H1 family members (Hendzel et al, 2004; Th'ng et al, 2005). These S/PTKK sites are of particular importance to H1 binding since they are substrates for enzymes such as Cdk2 (will be discussed in detail, below). H1.0, the shortest linker histones, has a very high density of basic amino acids in its CTD. It is also the only variant to exclusively possess TP sites and no SP sites on its CTD, even though it has very high percentage of serines (10% of the protein), just not next to a proline residue. It is also the only variant in the H1 family to have a methionine and histidine in the mature form of the protein (Zlatanova & Doenecke, 1994). All the variants have similar content of alanines, (which varies from 15% in H1.0 to 27% in H1.4) and prolines (varies

from 7.7% in H1.0 to 10% in H1.2), imparting a significant hydrophobicity in the H1 molecule.

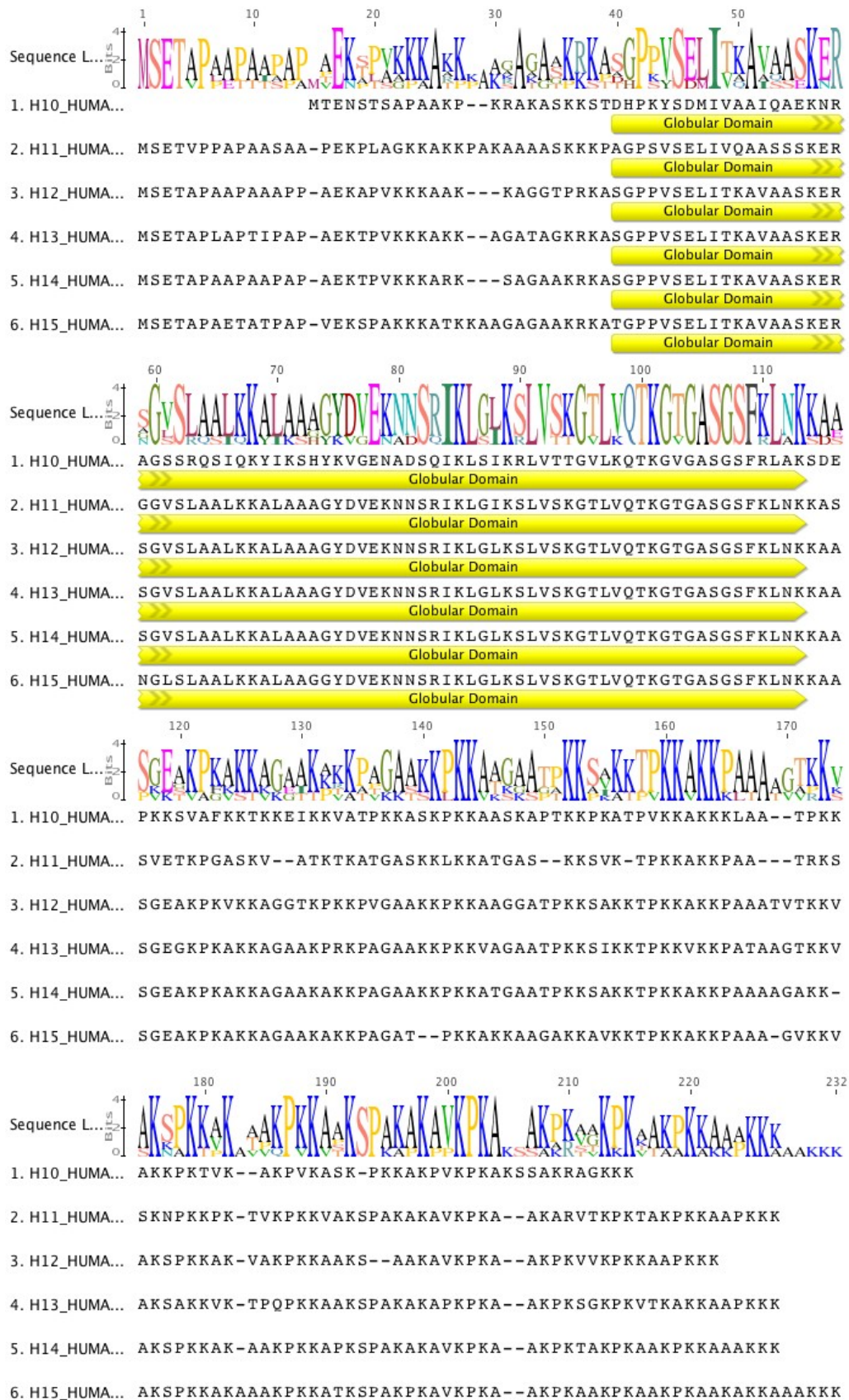


Figure 1.2 – Protein sequence alignment of different H1 variants. Protein alignment of the major somatic human H1 variants shows that the globular domain houses the majority of conserved sequences. Variability in sequences amongst variants arises from the two tails of H1. Furthermore, lysines are the major amino acid residue in the CTD, followed by alanine, imparting significant positive charge and hydrophobicity to the domain. It is interesting to note that among the conserved amino acid residues in the CTD, proline residues are among the most prominent. This observation is true even in the six variants of chicken H1 where 11 out of 13 proline residues are conserved (Clark et al, 1988). The significance of this conservation is not known. Furthermore, as can be seen from the consensus sequence shown as a sequence logo, there is a high degree of AKP or AKKP motifs found in the CTD. It must be noted that while alanine and lysine have high helix-forming propensity, proline has the least (Pace & Scholtz, 1998), suggesting a dynamic equilibrium of various structures in the CTD. These putative proline kinked AK alpha-helix motif, referred to as the AKP Helix (Kasinsky et al, 2001), are thought to form amphipathic helical structures in the presence of DNA that may aid in inter-molecular H1 interactions, and/or assist in binding to linker DNA (Subirana, 1990). Additional common features include the presence of a lower charge density in the CTD region that is most proximal to the globular domain, including the presence of negatively charged glutamic acid, compared to the rest of the CTD (Subirana, 1990). The function of this short region, known as the CTD hinge, is unknown. Furthermore, there is limited functional knowledge on the presence on Lysine triplets at the end of all H1 variants, or as to why most lysine residues on H1 appear as lysine doublets. This feature is shared by H1 variants in many organisms (Subirana, 1990). This Figure was generated using the Geneious Software, with protein sequences obtained from Uniprot/NCBI database.

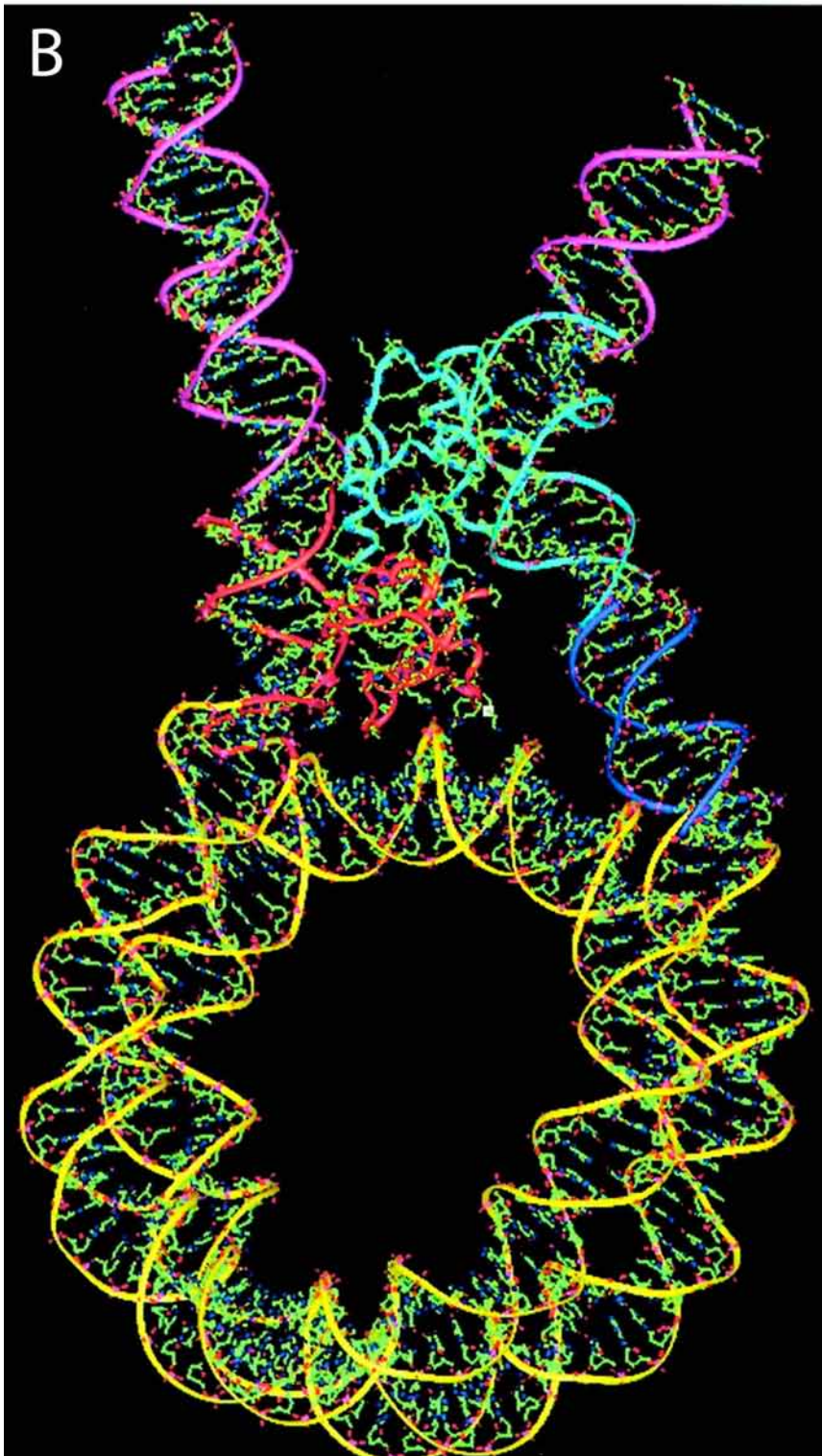
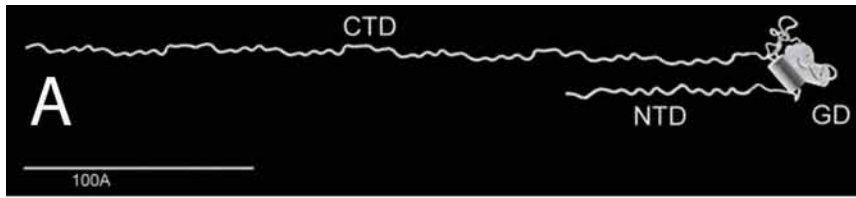


Figure 1.3 – Structure of H1 and location of H1 binding (A). This is an illustration of H1 highlighting the tripartite structure of H1 drawn to scale. The CTD of H1 is very long (comprising of approximately 100 amino acids) compared to the NTD (30 residues). Both the NTD and the CTD of H1 are intrinsically disordered and are unstructured in solution, compared to the globular domain. Figure adapted from (McBryant & Hansen, 2012) and reproduced with permission from Springer.

(B) Computer modeling of the chromosome alluding towards the strategic location of H1 at the entry and exit points of DNA. The globular domain (in red) binds at the nucleosome dyad axis while the CTD of H1 (shown in cyan) establishes extensive contacts with the linker DNA bringing the two strands together. This forms a unique ‘stem’ like structure that is thought to direct higher order folding of chromatin. Figure adapted from (Bharath et al, 2002) and reproduced with permission from Oxford University Press.

1.6.5 - Histone H1 in other organisms – Compared to core histones, linker histones are less evolutionarily conserved with the CTD and NTD housing much of the heterogeneity. However, it must be kept in mind that even the first DNA condensing proteins, such as those found in *Chlamydia* (eubacteria), are rich in lysine, proline and alanine, similar to those found in human H1 (Kasinsky et al, 2001) This suggests that there are ‘simple compositional constraints’ of amino acids in proteins that interact and condense DNA (Kasinsky et al, 2001). While the H1 like proteins in *Chlamydia* and *Trypanosoma* were similar in amino acid composition, they lacked the globular domain that is a feature of most animal, plant and fungal H1 (Ramakrishnan et al, 1993). Thus, the DNA condensing proteins in *Chlamydia* resembled the CTD of mammalian H1. It is interesting to note that most of these ‘H1-like’ proteins analyzed in bacteria comprised of approximately 125 amino acids, which is very similar to the length of the CTD of human H1 variants (Kasinsky et al, 2001). Among eukaryotic cells, the yeast *Saccharomyces cerevisiae* is unique in that its H1 has two globular domains (Patterton et al, 1998).

While H1 has been found to be dispensable for *Saccharomyces cerevisiae*, *Aspergillus nidulans*, and *Tetrahymena*, they are essential for higher organisms such as mice, and *Drosophila* (Downs et al, 2003; Patterton et al, 1998; Ramon et al, 2000; Shen et al, 1995) (Lu et al, 2009b). *Drosophila melanogaster* has a single H1 variant, dH1, and is essential for heterochromatin assembly and structural organization of polytene chromosomes, with cells lacking dH1 displaying higher genomic instability (Vujatovic et al, 2012). Histone H1 in

Drosophila, mice and humans have been shown to play key roles in chromatin structure formation and regulation of gene expression (Fan et al, 2005; Vujatovic et al, 2012). The role of H1 in these processes will be explored in the following sections.

1.7 – Role of histone H1 in higher order chromatin fiber formation

Binding of histone H1 stabilizes and organizes an additional 20bp of DNA into the nucleoprotein complex (Varshavsky et al, 1976; Whitlock & Simpson, 1976). Histone H1 occupies a strategic location at the entry and exit sites of nucleosomal DNA forming a unique stem-like structural motif (Bednar et al, 1998). The structure effectively brings the linker DNA together and “closes” off the nucleosome, thereby constraining the DNA entry/exit angle. This apposition is thought to orient the position of successive nucleosomes hence determining the pattern of inter-nucleosomal contacts (Bednar et al, 1998; Robinson & Rhodes, 2006) (Figure 1.4). Interestingly, it has been shown that the length of the stem-like structure is dependent upon the charge of the H1 variant (Bednar et al, 1998) alluding towards the possibility of differential chromatin condensing abilities for different variants.

In vitro experiments have been instrumental in our understanding of the role of histone H1 in influencing chromatin structure. In the absence of H1 and under low salt conditions, nucleosomal arrays form extended, decondensed or partially folded arrays (commonly referred to as the ‘beads on a string’ structure) lacking inter-nucleosomal contacts (Thoma, 1979). As the salt concentration is increased to 2mM MgCl₂ or 100mM NaCl, inter-nucleosome contacts increase

leading to the formation of secondary or higher orders of chromatin structure. However, these structures are unstable, heterogeneous, form clumps and fail to fold into the 30nm fibers, which is a feature of native chromatin (Bednar et al, 1998; Hansen, 2002). Binding of histone H1 imparts stability and homogeneity to nucleosomal arrays forming a compact 30nm fiber (Carruthers et al, 1998; Hansen, 2002). In addition, higher orders of chromatin structure can be formed in much lower salt concentrations in the presence of H1 (Hansen, 2002).

Similar results were obtained in cells housing a 50% reduction of H1 levels where global changes in chromatin structure along with a reduction in nucleosome repeat length were observed (Fan et al, 2005). Specifically, polynucleosomes extracted from H1 deficient cells were found to be heterogeneous and less compact (Fan et al, 2005). Furthermore, *Xenopus* chromosomes depleted of H1 (an embryonic, maternally derived variant also known as B4) are aberrantly elongated and “stringy” (Maresca et al, 2005). This morphological defect was thought to be the main cause of the observed chromosome mis-alignment and mis-segregation in these extracts (Maresca et al, 2005). A similar effect is seen in *Drosophila* cells where H1 is required for proper polytene chromosomal structure and formation of the chromocentre (Lu et al, 2009b). Polytene chromosomes that otherwise display a distinct banding pattern of intensely stained bands and dark interband regions lose this pattern upon depletion of H1 (Lu et al, 2009b). Furthermore, chromosomal arms were found to form chromatin clumps devoid of any defined structure and were thinner in appearance in the absence of H1 (Lu et al, 2009b).

These results were confirmed with the help of single-molecule force spectroscopy, which was used for analyzing the mechanical properties of the 30nm chromatin fiber with nanometer and sub-pico-Newton resolution (Chien & van Noort, 2009; Cui & Bustamante, 2000). While H1 was shown to have no affect on the stiffness of the fiber, it improved the mechanical stability of chromatin fibers (Kruithof et al, 2009). Stiffness is described as the force needed to cause unit displacement in length of the fiber, and is inversely proportional to compliance. The 30nm fiber was found to be highly compliant, such that small changes in force could cause large changes in fiber length. This is thought to ensure thermal ‘breathability’ of the chromatin fiber (Kruithof et al, 2009). The increase in mechanical stability of the 30nm fiber was attributed largely, to the ability of fibers reconstituted with H1 to resist unstacking of nucleosomes under applied force (Chien & van Noort, 2009; Kruithof et al, 2009). These results suggest that the principle role played by H1 is to orient successive nucleosomes, such that they stack in the most energetically favorable manner. Furthermore, it also suggests the inherent dynamicity of the chromatin fiber, which is not diminished under the stabilizing effect of H1.

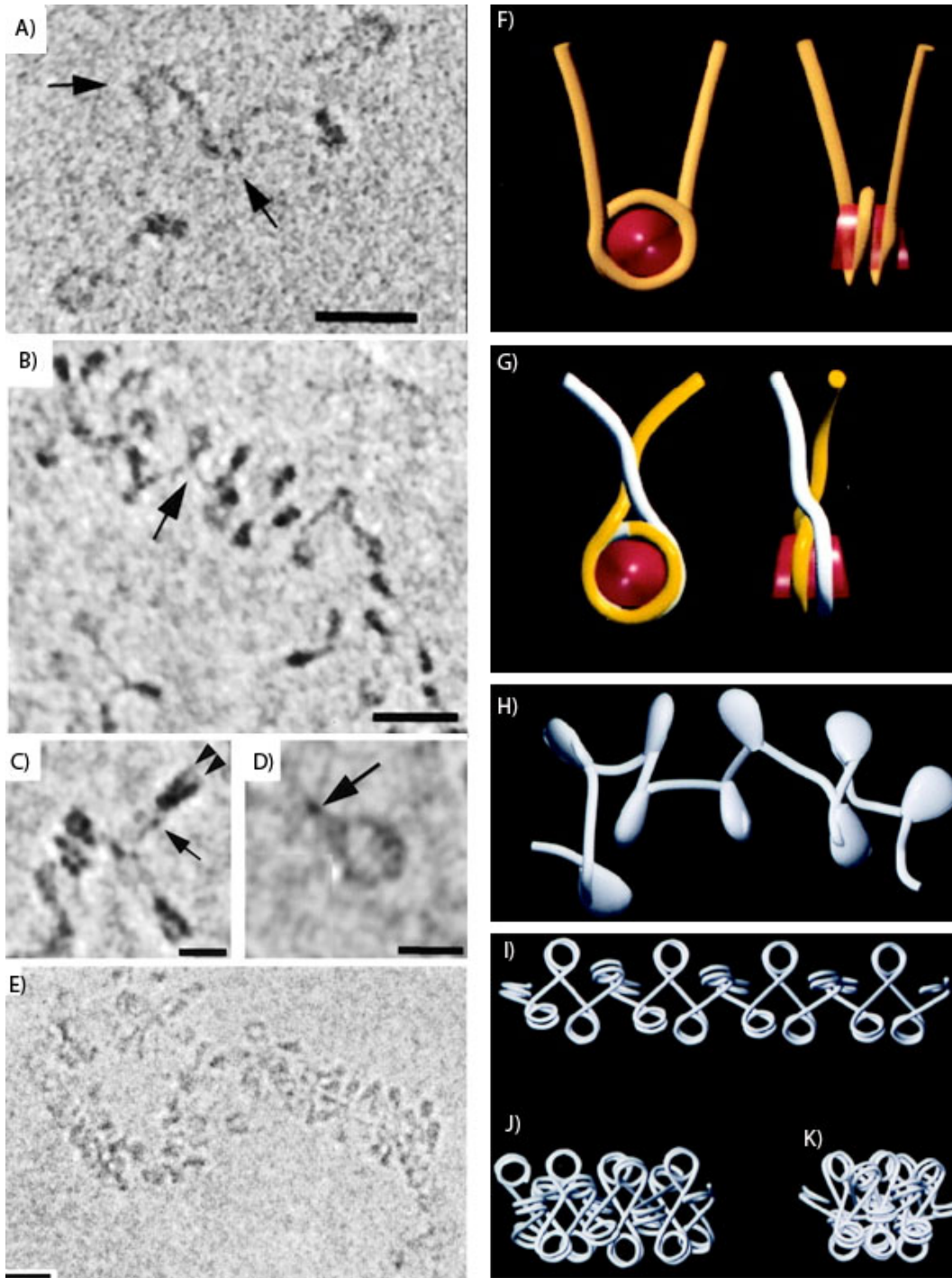


Figure 1.4 – Changes in chromatin structure upon addition of linker histones and salt conditions. (A) Electro-cryomicroscopy of unstained, unfixed chromatin fibers isolated from chicken erythrocytes, in low salt (5mM mono-valent) in the absence of linker histones. These fibers clearly show the divergence of the linker DNA, which may be a result of mutual electrostatic repulsive forces. The possible path of the linker DNA in the absence of linker histones is shown in (F). At the same ionic concentration, linker histones induce a “stem” like conformation of the linker DNA (shown by the arrows). One potential path of the linker DNA in such a conformation is shown in (G). The abundance of positively charged amino acids in the CTD of H1 are thought to stabilize the DNA molecules at this intersection. (C) The arrowheads show the two gyres of DNA looping around the nucleosomes, while the arrow points towards the stem-motif induced by H1. (D) Another view of the stem-motif that shows the DNA being brought together prior to their divergence. (E) Electron cryomicroscopy of chromatin fibers isolated from chicken erythrocytes in 15mM (monovalent ions) show that upon increasing the salt concentration, successive nucleosomes come in close contact with one another, in part due to a reduction in the entry-exit angles of linker DNA (from 85° to 45°). (H) 3D model of the zigzag nucleosomal array in low salt (5mM) which shows the nucleosomes as pear shaped structures. Note that the stem like structure induced by H1 is positioned towards the interior of the fiber structure. (I) Model structures of the chromatin fiber as the ionic strength is increased from 5mM (monovalent) (I) to 15mM (J) to 80mM (K), which correlates with decreasing linker DNA entry-exit angles from 85° (I) to 45° (J) to 35° (K). Figure adapted from (Bednar et al, 1998) and reproduced with permission from PNAS.

1.7.1 - H1 and the structure of the 30nm chromatin fiber – *In vitro* reconstituted chromatin fibers have provided us with valuable insight into the structure of the 30nm chromatin fiber. *In vitro* salt concentrations and the presence of H1 play an important role in influencing the topology of the fiber (Hansen, 2002), and as such, the structure of the 30nm fiber *in vitro* is a subject of much controversy in the field (reviewed in (Robinson & Rhodes, 2006)).

Richmond and colleagues carried out electron microscopy on tetranucleosomes imaged at a resolution of 9Å and showed that in the absence of H1, nucleosomal arrays form a structure that can be computationally modeled to a two-start helical structure with the linker DNA stretching across two stacks of nucleosomal cores in a zigzag fashion (Schalch et al, 2005). The structure has a diameter of about 25nm and a compaction ratio of 5-6 nucleosomes/11nm (Schalch et al, 2005). However, it must be kept in mind that these experiments were conducted in the presence of high salt concentrations (20-60mM MgCl₂, 150mM KCl) thereby bypassing the need for H1 (Schalch et al, 2005). Furthermore, the two-start helical model is modeled on linker DNA length of 20bp that connects two nucleosomes (Schalch et al, 2005). Longer or non-uniform linker DNA lengths would cause local perturbations in the structure thereby disrupting nucleosome-nucleosome contacts (Robinson & Rhodes, 2006). It must be noted that structures formed with such short nucleosome repeat lengths (NRL) have a very limited dependence on H1 for compaction. For example, the sedimentation coefficient of nucleosomal arrays with 167bp repeat length, increase from 125 to 142 S in the presence of H1, while nucleosomal arrays with

NRL of 197bp, more than double the sedimentation coefficients indicating greater compaction in the presence of H1 (Routh et al, 2008). It is interesting to note that arrays with 167bp NRL also bind H1 at lower stoichiometry (0.5:1 H1: nucleosome), which may be due to the insufficiency of linker DNA between adjacent nucleosomes (Routh et al, 2008).

In the presence of physiological amounts of H1 (one per nucleosome) and longer NRL, chromatin fibers adopt a slightly different topography. In the presence of low salt concentrations (1.6mM MgCl₂), a left handed one-start helix is formed (Robinson et al, 2006) (Figure 1.5). The diameter of the fiber is dependent upon the NRL, although this dependence does not vary linearly. The diameter of the fiber remains constant as the repeat length increases from 177 to 207bp at 33nm, while a dramatic increase to 43nm is seen when the repeat length is increased to 217bp (Robinson et al, 2006). Analysis of the NRL from a large number of cell types, tissues and organisms, has revealed it to center around 180-200bp (Widom, 1992). This is in contrast to the 167bp NRL used in the Richmond model described above (Schalch et al, 2005). Electron microscopy of reconstituted chromatin fibers with H1 and NRL at 177, 187, 197 or 207bp showed that such fibers had a diameter of 33nm and was significantly more compact than the earlier model of the 30nm fiber, encompassing 11 nucleosomes/11nm (Robinson et al, 2006). Unlike the 167bp NRL arrays, 197bp NRL arrays have a requirement for H1 to achieve higher compaction and bind H1 in a 1:1 stoichiometry (Routh et al, 2008). In the absence of H1, these arrays form

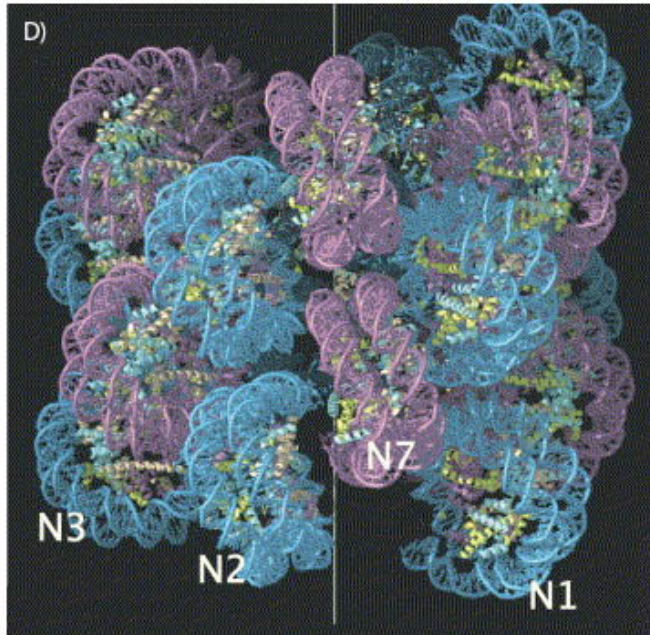
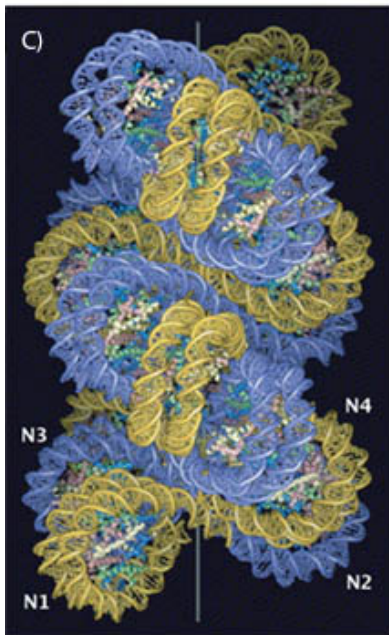
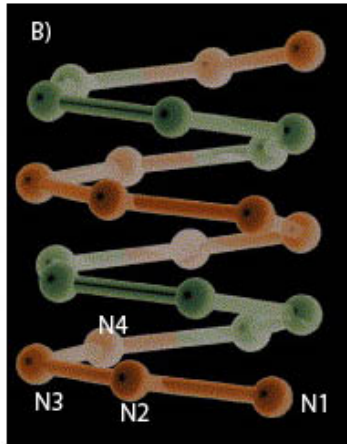
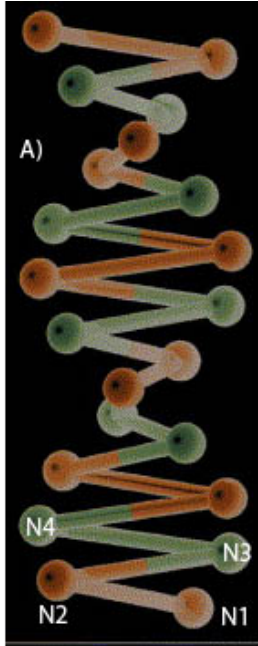
unfolded, ‘puddles’ of nucleosomes, while addition of H1 transforms these structures to well-defined, compact structures (Routh et al, 2008) (Figure 1.6).

The greater compaction does not mean that these fibers are rigid. In fact, force spectroscopy studies on such fibers show that chromatin fibers with 197bp repeats are *less* stiff (or more compliant) than fibers with 167bp NRL (Kruithof et al, 2009). Note that the latter adopts a two-start helix, as noted above. This implies that the higher compliance of the one-start helical model affords it greater thermal breathing, while maintaining a high degree of compaction. In other words, the two-start model is compact, yet highly dynamic.

Interestingly, reconstitution of chromatin fibers with even higher repeat lengths, such as those found in sea urchin sperm having a high nucleosome repeat length of 237bp (Spadafora et al, 1976), 45nm chromatin fibers encompassing approximately 16 nucleosomes/11nm, are formed (Robinson et al, 2006). Substitution of a sea urchin specific H1 variant does not change the diameter of the 30nm fiber, suggesting that substituting different H1 variants may not influence the physical dimensions of the chromatin fiber (Robinson et al, 2006).

These results show that linker histones and nucleosome repeat lengths play a crucial role in modulating the degree of compactness of the chromatin fiber. It is thought that chromatin fibers housing lower levels of H1/nucleosome, such as transcriptionally active fibers, may adopt a chromatin fiber conformation similar to the two-start helical model (Robinson & Rhodes, 2006). Structures that require a high degree of chromatin condensation, such as mitotic chromosomes and transcriptionally inactive chromatin, would be expected to adopt a conformation

similar to the one-start model, allowing greater compaction (Robinson & Rhodes, 2006) (Bassett et al, 2009; Travers, 2009). It is still unknown whether such transitions are possible *in vivo*, and at what energetic costs. Furthermore, it must be kept in mind that such models are based upon static images obtained either in fixed EM samples or X-ray crystal structures and hence are not representative of the dynamicity that this commonly associated with chromatin fibers *in vivo*. Furthermore, these models utilize the 601 nucleosomal arrays that have a very strong nucleosome positioning sequence (Lowary & Widom, 1998) and strict restrictions on nucleosome repeat length (Robinson et al, 2006; Schalch et al, 2005). It is likely that variations in repeat lengths and nucleosomal dynamicity will impart a substantial microheterogeneity in the structure of the chromatin fiber. As already mentioned, it has been shown that the chromatin fiber is very compliant and even the one-start helical model has a high degree of thermal breathing (Kruithof et al, 2009). Thus, it is questionable whether large-scale transitions between one-start helix and two-start helical model are even required during chromatin disruptive processes such as transcription.



Two-start Helix (Richmond Model)

One-start Helix (Robinson & Rhodes model)

Figure 1.5 – Proposed models of the 30nm chromatin fiber. (A) Topology of the two-start helical model, and a space-filled model (C) of the same is illustrated. Also known as the Richmond model of the 30nm chromatin fiber (Schalch et al, 2005), this structure packs 5-6 nucleosomes/11nm, with nucleosome 1 (N1) packing on top of nucleosome 3 (N3), with a fiber diameter of 25nm. Straight linker DNA (20bp) connects stacks of radially arranged nucleosomes in a zigzag arrangement. This structure was obtained following computational modeling of a crystal structure of tetranucleosomes in the absence of linker histones and in the presence of high ionic strength (40mM MgCl₂). (B) Topology and space filled model (D) of the one-start helical model of the 30nm fiber, as proposed by Robinson and Rhodes (Robinson et al, 2006). This model is a left-handed one-start helix that was obtained following computational modeling of EM measurements of long nucleosomal arrays in the presence of H1. The model encompasses 11nucleosomes/11nm with 40bp of linker DNA, with a diameter of 33nm. In this model, nucleosomes from successive gyres (shown in orange and green) interdigitate with one another, which allows a high compaction ratio. It is important to note that both the Robinson/Rhodes model and the Richmond model are based on the structure adopted by the 601-nucleosome positioning sequences (Robinson et al, 2006; Schalch et al, 2005). This ensures the same nucleosome repeat length across the entire structure. Natural DNA sequences, however, may differ in the nucleosome repeat lengths and will introduce irregularities in the structure of the fiber. Figure adapted from (Robinson & Rhodes, 2006) and reproduced with permission from Elsevier.

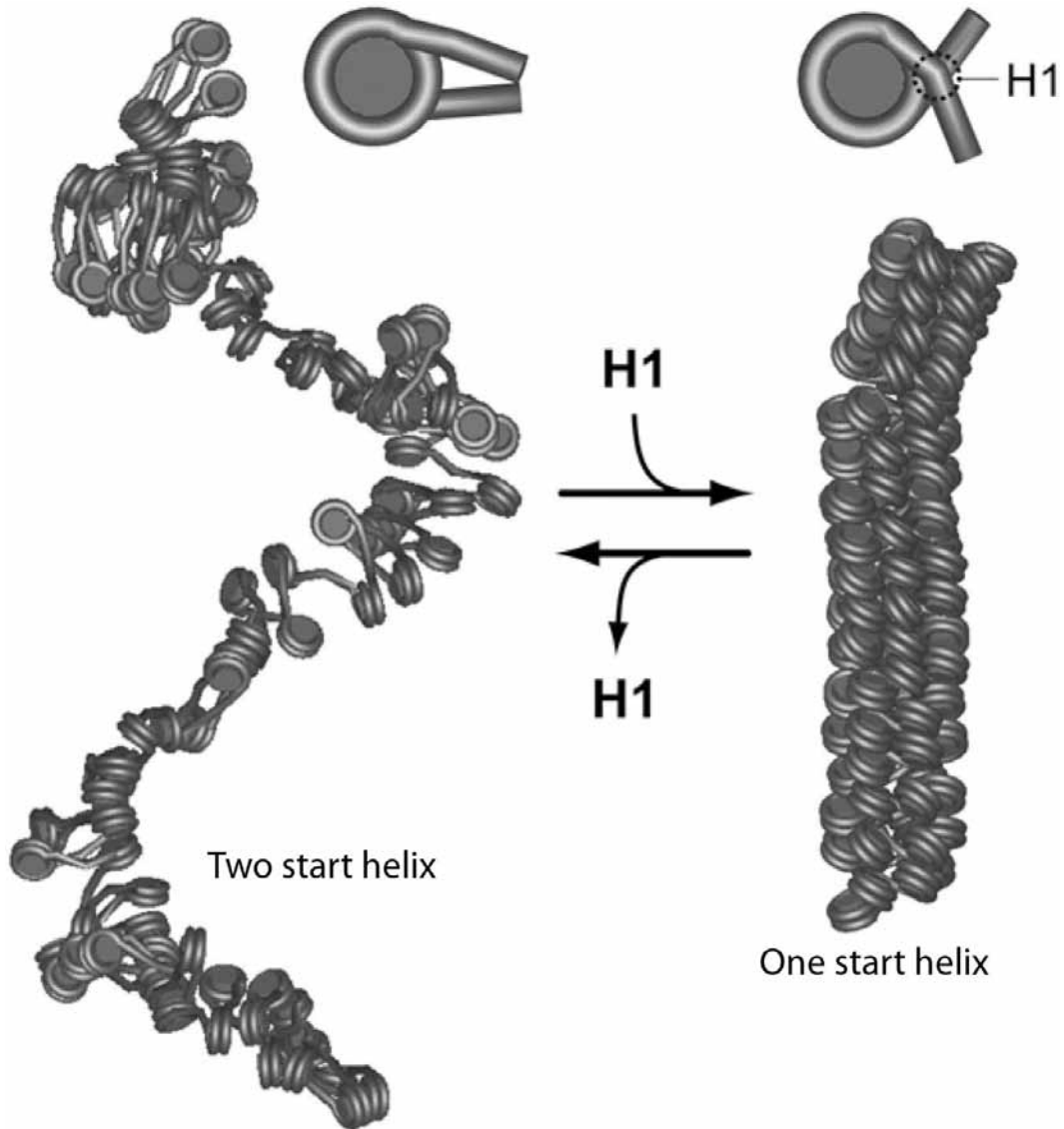


Figure 1.6 – Changes in 30nm structures upon H1 binding. The figure illustrates a model of the 30nm structure transition upon H1 binding. These are based on Monte-Carlo simulations of the two 30nm structures at thermal equilibrium (298K). In the absence of H1, the linker DNA is much more accessible to proteins, whereas with H1 binding and stabilization of the fiber architecture, leads to a closed conformation. This is due to the change in the trajectory of the linker DNA, reducing its entry and exit angle, which induces a transition from the two start helix to a one-start helical structure. Figure adapted from (Kepper et al, 2008) and reproduced with permission from Biophysical Journal.

1.8 – Histone H1- a gateway to chromatin

H1s ability to stabilize chromatin fiber is a well characterized and extensively studied architectural role. However, recent evidence allude toward another important function for H1, and that is its ability to interact with a number of non-histone proteins, thereby acting as a gateway to chromatin and chromatin changes (McBryant et al, 2010). These interactions fall under three categories – (1) Site specific competitors, such as UBF, that compete with H1 for binding to specific sites on DNA, (2)- global competitors of H1 – proteins such as HMG proteins that compete with H1 for chromatin binding, in a dose dependent manner (Catez et al, 2002; Catez et al, 2006) and (3) – proteins that bind H1 directly, such as NASP that are thought to function as chaperones to H1 facilitating the loading of H1 to nucleosomal arrays (Finn et al, 2008). Interestingly, the tails of H1 have been shown to play an important role in mediating these interactions. For example, the activity of DNA fragmentation factor 40 (DFF40) is dependent upon the presence of H1CTD (Widlak et al, 2005). Another DNA binding protein Barrier to Autointegration Factor (BAF) was found to bind specifically to H1.1 CTD (Montes de Oca et al, 2005). The binding of NASP to H1 is also dependent on either the NTD or the CTD. The NTD of H1.4 was also shown to interact with HP1 following methylation of its K26 residue (Daujat et al, 2005), thereby alluding towards a possible mode of regulating H1 interaction partners through post-translational modifications.

The ability of H1 to interact with different proteins is still an under-appreciated role for H1, compared to its well-known role of stabilizing chromatin. Our studies have characterized a novel interaction between H1 and Pin1, and will be discussed in detail in Chapter 4. Such studies that look at H1 and its interaction with other proteins are essential for our understanding of the roles they play in regulating chromatin structure during processes such as transcription.

1.9 – Globular domain of H1

The globular domain of H1 is thought to be essential for proper positioning and binding to the nucleosome. It has been shown to afford the same level of nucleosome protection from micrococcal nuclease as the complete H1 protein (Allan et al, 1980), however lacks the ability to condense nucleosomal arrays (Allan et al, 1986). This domain is highly conserved amongst the H1 variants. Globular domains isolated from different variants of H1, however, showed different affinities to chromatin and a lower overall affinity to chromatin in the absence of the C-terminal domain of H1 (Thoma et al, 1983). This suggests that while the globular domain plays a role in influencing H1 binding to chromatin, the C-terminal domain is the primary determinant of its affinity (Hendzel et al, 2004).

The structure of the globular domain of H1 has been studied with the help of NMR (Cerf et al, 1993; Cerf et al, 1994) and X-Ray crystallography (Ramakrishnan et al, 1993) and shows the presence of three classical alpha-helices in a typical ‘winged-helix DNA binding domain’. This structuring allows conserved lysine and arginine residues to interact with DNA. The spatial

clustering of these positively charged residues results in two distinct DNA binding sites on the globular domain, known as Site I and Site II (Brown et al, 2006). These sites are thought to provide H1 with the ability to bind and bridge different DNA molecules together, such as those found in nucleosomal DNA, DNA crossovers or four-way junctions (Krylov et al, 1993; Ramakrishnan et al, 1993; Varga-Weisz et al, 1993). Computer modeling of the globular domain binding to DNA places its primary DNA binding site (Site I) in close proximity to the major groove of the entering DNA, while the secondary binding site (Site II) is in close proximity to the nucleosomal DNA at the dyad axis (Bharath et al, 2003).

1.10 – H1 C-terminal domain

The C-terminal domain has been shown to be the primary determinant of high affinity binding to chromatin. Deletion of the CTD causes the H1 molecule to bind with very low-affinity to chromatin, with the kinetics approaching that of free-diffusion (Hendzel et al, 2004). Variants of H1 differ in the lengths of the CTD, with H1.1 and H1.2 having short CTD, while H1.5 has a long CTD (Th'ng et al, 2005). The length of the CTD also correlates with the binding affinity of H1 to chromatin (Th'ng et al, 2005). H1.1 and H1.2 have comparatively lower affinities to chromatin, while H1.5 has a much stronger affinity to chromatin. One exception to this rule is H1.0, which has a short CTD but binds with an affinity comparable to that of H1.5. This could be explained, in part, due to the high charge density on H1.0 (46 residues in 97 residues are basic in nature) that facilitates high affinity binding (Th'ng et al, 2005).

Furthermore, the CTD has a high degree of positively charged residues with up to 40% of the CTD made entirely of lysine/arginine residues, while the rest are made up of alanine (~25%) and prolines (~12%). However, each variant is composed of differing ratios of positively charged amino acids, which confers different net charges to these variants (Th'ng et al, 2005).

The CTD comprises of roughly half of the entire H1 molecule and is the domain that houses the majority of heterogeneity amongst the variants. For example, there are differences in both the number and the relative positioning of the critical DNA binding residues such as the S/TPKK DNA binding motifs (Lu & Hansen, 2004) and the phosphorylation sites found within these motifs (Moreno & Nurse, 1990). While H1.1 has just one TP site and one SP site, H1.5 has two of each on its CTD (Th'ng et al, 2005).

The physical properties of the CTD as well as the phosphorylation of H1 will be discussed in much greater detail in the following sections.

1.11 - The CTD of H1 is intrinsically disordered

Intrinsic disorder refers to the lack of a defined secondary structure (α -helices or β -sheets) under native conditions. These regions within a protein, however, adopt characteristics of secondary structure upon interaction with DNA or proteins (Hansen et al, 2006; Lu et al, 2009a). Up to a third of eukaryotic proteins have been proposed to be intrinsically disordered proteins that acquire structure only upon interaction with their target proteins (Ward et al, 2004).

Studies of the CTD of H1 using either circular dichroism and IR spectroscopy have showed that the CTD is conformationally flexible and is

devoid of a secondary structure in solution (Clark et al, 1988; Roque et al, 2005). In the presence of DNA, however, the CTD of H1 acquires stable and ordered secondary structures that include α -helices and β -sheets (Roque et al, 2005; Roque et al, 2007). The process of coupled binding and folding of the CTD upon interaction with DNA is thought to be the central mechanism through which high affinity H1 binding to chromatin is achieved. More recently, it has been shown that phosphorylation of H1 on the CTD can further alter the proportion of α -helices and β -sheets (Roque et al, 2008) thus alluding towards a potential mechanism for regulating this process.

It should be noted, however, that only sub-domains within the CTD acquire an ordered structure upon interaction with DNA, while the rest of the CTD can remain disordered (Roque et al, 2005). This phenomenon is also termed as “dynamic fuzziness”, where regions within a protein can exist in a dynamic equilibrium between different conformations (order vs. disorder), with disorder maintaining its presence even in the bound state (McBryant & Hansen, 2012). For example, only two discontinuous regions (residues 98-122 and 147-170 in H1^o) are essential for modifying chromatin structure when bound to DNA (Lu et al, 2009a; Lu & Hansen, 2004). The amino acid composition in these regions is more important than the primary sequence itself, since randomizing the sequence in these regions did not abrogate the chromatin condensing function of H1 (Lu et al, 2009a). These experiments show that specific subdomains within the CTD are able to strategically engage linker DNA, which has the effect of stabilizing the structure in those domains, and simultaneously condensing chromatin structure.

Sub-domains that do not engage DNA remain unstructured (McBryant & Hansen, 2012).

1.12 – The N-terminal domain of H1

The role and function of the NTD of H1 is poorly understood, compared to its CTD counterpart. However, recent evidence suggests that the NTD of H1 may also play a role in influencing the binding affinity of H1 molecules for chromatin. The NTD of H1 is relatively short, 36 amino acids compared to approximately 100 amino acids of in the CTD (Bohm & Mitchell, 1985). The NTD can be divided into two sub-domains, N-I and N-II, with the N-terminal half of the NTD (N-I) being rich in hydrophobic residues, such as alanine and proline while being devoid of basic residues, while the domain closer to the globular domain (N-II) is rich in basic residues (Bohm & Mitchell, 1985). While both of the sub-domains of NTD are devoid of a structure in solution, N-II can form a non-amphipathic α -helix in the presence of DNA (Vila et al, 2001). The basic residues on the NTD are arranged in a manner such that they form two positively charged ‘faces’ oriented in opposite directions (Vila et al, 2001). These are thought to bind non-consecutive segments of DNA, allowing H1NTD to bridge linker DNA together. In H1.2, N-II, has a unique Gly-Gly structural motif, which effectively further subdivides this domain into two alpha-helices (Vila et al, 2002). The presence of two glycine residues affords greater conformational flexibility, which is thought to be important in bridging DNA together (Vila et al, 2002). While the NTD of H1 has no effect in folding nucleosomes into higher order fibers, it could play a role in positioning the linker histone molecule within chromatin, as well as

anchoring the globular domain (Allan et al, 1986). Furthermore, recent experiments in which the NTD of two variants were swapped revealed that the NTD might also determine the relative affinities of these variants to chromatin (Vyas & Brown, 2012b).

1.12.1 - Protein interactions mediated by the NTD of H1 - The NTD of H1b (H1.5) specifically interacts with differentiation-specific transcription factor, Msx-1. H1.5 and Msx-1 are thought to bind specific regulatory elements such as *MyoD* as a complex, in effect maintaining a repressed chromatin structure (Lee et al, 2004). *In vitro* studies have also shown an association between HP1 and methylated H1.4 (K26)(Daujatz et al, 2005).

1.13 – Cooperativity in histone H1 binding to chromatin

Several models for H1 binding to chromatin have been proposed (Brown et al, 2006; Raghuram et al, 2009). While some models attribute the globular domain to make the initial contact with linker DNA and orient the H1 molecule to its proper position at its binding site, others have ascribed this role to the CTD. However, recent evidence has shown that the C-terminal domain establishes initial contact with the linker DNA, followed by the binding of either site I or site II of the globular domain (Stasevich et al, 2010). The CTD is also thought to bring the two linker DNAs closer so as to allow the two sites on the globular domain to bind. High affinity H1 binding is established through the acquisition of the CTD structure (Stasevich et al, 2010). The binding of the CTD and the globular domain were found to be cooperative in nature, i.e., the binding of one domain (CTD) increased the affinity of the other domain (globular domain) (Stasevich et al,

2010). This allows the entire H1 molecule to bind with much greater affinity to chromatin than the sum of its individual domains (Stasevich et al, 2010).

In chapter 3, we explore how post-translational modifications such as core histone acetylation can change the cooperativity of H1 binding to chromatin. In the following sections, we explore the role of H1 in transcriptional regulation and the changes in chromatin structure associated with transcriptional activation.

1.14 – Histone H1 and the regulation of gene expression

Chromatin has been shown to be repressive to transcriptional machinery, acting as a structural barrier to RNA Polymerase II progression *in vitro* (Armstrong, 2007; Huang & Bonner, 1962; Lorch et al, 1987; Lorch et al, 1992). Given its role in stabilizing higher order chromatin structure, histone H1 was thought to impede access to chromatin modifiers and the transcription machinery acting as a general repressor of transcription (Archer et al, 1991; Carruthers et al, 1998; Workman & Kingston, 1992; Zlatanova & Van Holde, 1992). For example, deposition of linker histones onto *in vitro* reconstituted nucleosomal arrays inhibited initiation and elongation, resulting in a dramatic increase in premature termination of transcripts (O'Neill et al, 1995). *In vitro* transcription assays on chromatin templates revealed that at a stoichiometry of 0.5-1 linker histones per nucleosome, H1 caused a measurable decrease in basal level of transcription (Laybourn & Kadonaga, 1991). Transcriptional activators, however, were able to overcome this H1-mediated repression (Laybourn & Kadonaga, 1991). When the level of H1 is increased to 1-1.5 linker histone per nucleosome, a sharp decline in transcription rate was observed, even in the presence of transcriptional activators (Laybourn &

Kadonaga, 1991). This suggested that H1 plays an important role in both basal and activated transcription rates in a stoichiometric dependent manner (Laybourn & Kadonaga, 1991). This is consistent with the observation that transcriptionally inactive dry maize embryos have a higher linker histone to nucleosome ratio of 2:1, which is rapidly reduced to 1:1 upon germination induced transcriptional activation (Ivanov, 1989). Furthermore, cross-linking experiments (DNA-protein) have shown an approximately 50% reduction in the amount of H1 cross-linked to actively transcribed genes (Bresnick et al, 1992; Dedon et al, 1991; Kamakaka & Thomas, 1990). This led to a model whereby H1 eviction was thought to be a key step in transcriptional elongation (Koop et al, 2003).

However, studies have shown transcription to occur even in condensed structures, structures that would require the stabilization afforded by H1. Studies from the Belmont group (University of Illinois) (Chuang et al, 2006; Hu et al, 2009; Tumber et al, 1999) and other studies (Muller et al, 2004; Sharp et al, 2006) have shown that transcription can occur in chromatin structures that are fairly condensed. For example, using bacterial artificial chromosomes, it was shown that transcription could take place in chromatin structures that are four-fold more compact than a 30nm fiber (Hu et al, 2009). In fact, it has been established that H1 is present on both active and inactive Balbiani Ring structures and there was no evidence for loss of H1 molecules during gene unfolding and activation (Ericsson et al, 1990). The Balbiani ring system undergoes a rapid condensation into a 30nm fiber in the absence of transcription (Ericsson et al, 1990). When transcriptionally activated, these fibers locally decondense into a 5nm filament

(unfolded nucleosomes). Even in these fully extended chromatin fibers, the presence of histone H1 molecules was detectable by immunoelectron microscopy (Ericsson et al, 1990). Similar experiments carried out on *Drosophila* polytene chromosomes confirmed the presence of H1 along the entire length of the chromosome at both bands (30nm, condensed chromatin, transcriptionally silent) and puffs (10nm filament, decondensed, transcriptionally active) (Hill et al, 1989).

Similar results were obtained in an *in vitro* transcription assay using reconstituted chromatin assembled using purified core histones, H1 and histone chaperons, which resulted in chromatin structures that approximated the 30nm fiber in compaction (Li et al, 2010). In order to successfully transcribe this structure, basal transcription machinery had to be supplemented with HATs, SWI/SNF complex, FACT, Mediator, PARP-1. Interestingly, it was shown that H1 molecules were present throughout a complete cycle of RNA Polymerase II elongation and the preceding changes to chromatin that is associated with transcriptional activation (Li et al, 2010).

These and other results suggest the presence of H1 at sites of transcription, although at reduced levels. More importantly, these experiments allude towards the important regulatory role that chromatin and H1 can play in transcriptional processes.

1.14.1 - H1 is a gene specific regulator of transcription - Experiments in knock out models, where H1 or H1 variants were selectively depleted, revealed gene-specific effects on expression. In a knockout strain of *Tetrahymena thermophila*

where histone H1 was knocked out, transcription from RNA Polymerase I and III were unaffected while most RNA Polymerase II transcripts were unchanged following depletion of H1 (Shen & Gorovsky, 1996; Shen et al, 1995). Most of the genes that were susceptible to changes in H1 levels were non house-keeping or inducible genes, such as *ngoA* and *CyP*, whose levels change upon growth conditions (Shen & Gorovsky, 1996). While some genes such as *ngoA* were repressed by H1, other genes such as *CyP* were activated by H1 (Shen & Gorovsky, 1996). Similarly, analyzing the transcriptome of mammalian cells harboring a 50% decrease in global H1 levels (triple knock out of H1c (H1.2), H1d (H1.3), H1e (H1.4)), a differential change in gene expression was found (Fan et al, 2005). While some genes were upregulated, others were suppressed. There was limited functional redundancy in these variants, with knockout of specific variants leading to specific defects in development (Alami et al, 2003).

These studies instead support H1s role as a gene-specific regulator of transcription. One of the mechanism through which H1 can accomplish this role is by strategically positioning the nucleosome in a manner that facilitates or prevents the binding of transcriptional activators/repressors (Koop et al, 2003). Gene-specific regulation of transcription by H1 variants warrants further investigation since the exact mechanism behind many of such events are unknown and there is limited amount of information of such an effect in human cells (Sancho et al, 2008).

1.15 – Core histone acetylation, chromatin and transcription

1.15.1 - Histone code

The histone code model postulates that post-translational modifications on histone tails such as methylation, acetylation, phosphorylation, sumoylation, ADP-ribosylation, deimination, proline isomerization and ubiquitylation play a central role through which cells are able to modify the structure and function of chromatin (reviewed in (Kouzarides, 2007)). These multiple histone tail modifications are thought to act in sequence or in combination to direct unique downstream functions (Strahl & Allis, 2000). The modifications can act either directly on the chromatin state by altering its ability to fold, or can serve as docking sites for other chromatin associated proteins that typically possess enzymatic activities (Kouzarides, 2007; Strahl & Allis, 2000).

1.15.2 - N-terminal tails and their role in chromatin condensation

As per the histone code hypothesis, there are two functions that the NTD of core histones are thought to play. First, is their ability to function as a hub for protein-protein interactions and second, is to directly influence the structure of the chromatin fiber.

The role of the N-termini in protein-protein interaction was first established in yeast models, where it was shown that SIR3, SIR4 and TUP1 interacted with the amino termini of histones, rather than DNA, to repress transcription (Kingston et al, 1996; Roth, 1995). The list of proteins that interact with the N-terminal tail has expanded to include the *Drosophila* NURF complex, the yeast SWI/SNF complex, the RSC complexes, HMG-14 proteins and nucleosome assembly proteins such as the yNAP-1 proteins (Edmondson et al, 1996; Hecht et al, 1995; Hecht et al, 1996; Trieschmann et al, 1998). Proteins that

bind to modified residues do so with the help of specialized domains, such as the bromodomain (that binds to acetylated lysine), or the chromodomain (that binds methylated lysine). These domains are thought as the ‘readers and interpreters of the histone code’ (reviewed in (Lee & Workman, 2007)).

The role of the N-terminal tails in regulating chromatin structure have largely been derived from several *in vitro* experiments utilizing nucleosomal arrays assembled from DNA and purified histones (Simpson et al, 1985). Nucleosomal arrays have been shown to be in equilibrium between highly condensed and decondensed state at physiological salt concentrations (Fletcher & Hansen, 1996; Hansen, 2002). The condensed state is a result of a series of hierarchical folding coupled with oligomerization. Arrays that lack the N-terminal domains have significantly reduced level of condensation with a marked reduction in both folding and oligomerization (Fletcher & Hansen, 1995; Garcia-Ramirez et al, 1992; Moore & Ausio, 1997; Schwarz et al, 1996; Tse & Hansen, 1997). The core histone tails also differ in their ability to affect the condensation state. For example, the formation of the moderately folded conformation can be induced in the presence of only the H3/H4 tail, while oligomerization can take place in the presence of either H2A/H2B tail or the H3/H4 tail (Tse & Hansen, 1997). These results conclusively show that the N-terminal tails of core histones are responsible for both short-range and long-range inter-nucleosome interactions, as well as mediating oligomerization through inter-fiber interactions (Hansen et al, 1998; Tse & Hansen, 1997). Furthermore, oligomerization and formation of higher ordered chromatin fibers are thought to occur through separate mechanisms

mediated by the NTD of core histones. While chromatin condensation is primarily mediated through protein-protein interaction of the NTD of adjacent nucleosomes, oligomerization involves both protein-protein interactions as well as protein-DNA interactions (Tse & Hansen, 1997).

1.15.3 - Secondary structure of core histone NTD

The NTD of core histones, like the CTD of H1, are intrinsically disordered. They acquire structure following interaction with DNA and/or protein (Hansen et al, 2006). Studies using circular dichroism have shown that the NTD of H3 and H4 are comprised of ~50% alpha helices when bound to nucleosomal DNA (Baneres et al, 1997). However, it must be noted that, *in vivo*, the NTD of core histones are unlikely to interact with the nucleosomal DNA based on several cross-linking experiments, and may instead interact with linker DNA (reviewed in (Hansen, 2002)). Histone acetylation increases the α -helical content of the histone tails, suggesting a mechanism by which histone acetylation might be able to influence chromatin structure (Wang et al, 2000). For example, an increase in alpha-helical content due to acetylation of H4K16, in theory, would lead to a 4Å decrease in the separation between DNA and the NTD (Wang et al, 2000).

1.15.4 - Core Histone acetylation

Core histone acetylation is associated with a number of cellular processes such as transcription, DNA replication and DNA repair (Annunziato & Seale, 1983b; Bird et al, 2002; Chahal et al, 1980; Nelson et al, 1979; Vidali et al, 1978). A steady state level of core histone acetylation is maintained by the antagonistic activities of histone acetyltransferases (HATs), which are responsible for the transfer of an

acetyl moiety to the ϵ -amino group of lysine residue through an amidation reaction, and histone deacetylases (HDACs), which remove them (Shahbazian & Grunstein, 2007). There are three main families of HATs, which are grouped based on their catalytic domain– GNAT (Gcn5 N-acetyl transferase), MYST (Morf, Ybf2, Sas2 and Tip60) and CBP/p300. HATs are multi-subunit complexes and their specificity and activity depends on the subunits in the complex (Lee & Workman, 2007).

There are 18 HDACs that have been identified in humans involved in processes such as transcription (Ozawa et al, 2001; Sun et al, 2002; Won et al, 2002; Zhang et al, 2002). The HDAC family of proteins can be subdivided into three sub-families – Class I, Class II and NAD-dependent Sir family of HDACs (Class III). While Class I and Class II HDACs catalyze a Zn-dependent hydrolysis of acetyl-lysine amide bond, Class III HDACs catalyze the deacetylation through the transfer of the acetyl moiety onto the sugar residue of NAD (Gallinari et al, 2007). The classification of HDACs into the three classes is based on the homology to their yeast counterparts, with Class I HDACs sharing homology to the yeast RPD3 gene, Class II HDACs sharing homology to the Hda1 yeast deacetylase, and the Sirtuins or Class III HDACs are homologues of the yeast Sir2 gene (reviewed in (Thiagalingam et al, 2003)).

Although there is considerable overlap in terms of substrate specificity between the HATs, some residues may be preferentially acetylated compared to others. The SAGA complex (with Gcn5 as the catalytic domain) preferentially targets H3K9 acetylation, while NuA3 complex targets H3K14 residues (John et

al, 2000). Even members of the same family can show different site specificities, for example while CBP prefers H4K12, p300 targets H4K8 (McManus & Hendzel, 2003). Furthermore, genetic studies involving P300 and CBP knockout mice, as well as functional studies analyzing the role of these proteins in retinoic acid-induced differentiation, have alluded towards their non-redundant and distinct functions within the cell (Kawasaki et al, 1998; Yao et al, 1998).

1.15.5 - Core histone acetylation and transcription – Core histone acetylation, a common feature of transcriptionally active sites, is thought to be one of the mechanisms through which these chromatin sites decondense allowing greater accessibility to DNA dependent proteins (Allfrey et al, 1964; Davie & Hendzel, 1994; Loidl, 1988; Ridsdale et al, 1990; Vidali et al, 1988). For example, core histone acetylation is a feature of the transcriptionally active *Tetrahymena* macronucleus, and not the inactive micronucleus (Gorovsky et al, 1973). Furthermore, many transcriptional co activators have HAT activity (Brownell et al, 1996), while transcriptional repressors associate with HDACs (Taunton et al, 1996b). H4K16, H3K9 and H3K14 are specific sites on the N-terminal tail that are associated with activation of gene expression (Lee & Workman, 2007; Shahbazian & Grunstein, 2007).

Histone acetylation, however, is not sufficient for inducing gene expression. For example studies using ϵ -acetyl antibodies revealed that while core histone acetylation was found in both transcriptionally active and transcriptionally poised chromatin across the 33kbp β -globin transcription unit, additional steps/factors were needed for transcriptional elongation (Hebbes et al, 1994b; Hebbes et al,

1992; Hebbes et al, 1988a). These may include chromatin modifiers (such as SWI/SNF complex), transcription factors (such as FACT, Mediator), PARP-1, as well as the basal transcription machinery that facilitate high levels of transcription (reviewed in (Sims et al, 2004)). Similarly, while chromatin decondensation and an increase in core histone acetylation at the developmentally regulated *Hoxb9* locus is responsible for setting up a transcriptionally poised state, transcriptional elongation of this gene is observed days later (Chambeyron & Bickmore, 2004).

1.15.6 - Core histone acetylation and nucleosome assembly during S-phase—

Assembly of nucleosomes occurs during DNA replication in the S-phase of the cell cycle and requires the assistance of histone chaperones. Newly synthesized histones are transiently acetylated prior to deposition onto DNA, a mechanism that is thought to aid the interaction with chaperones and prevent premature association with DNA. Following deposition, the acetylated marks are rapidly removed (Annunziato & Seale, 1983a; Jackson et al, 1976; Ruiz-Carrillo et al, 1975; Shahbazian & Grunstein, 2007).

Both H3 and H4 are acetylated at multiple sites during S-phase. For example, newly synthesized H4 molecules are acetylated at lysines 5 and 12 prior to its deposition onto nascent DNA, a process that is conserved in organisms from *Tetrahymena*, *Drosophila* to humans (Chicoine et al, 1986; Sobel et al, 1995). Deacetylation of these histones is observed within an hour of acetylation and is essential for proper chromatin maturation (Annunziato & Seale, 1983b; Jackson et al, 1976).

H3K56 acetylation is an abundant modification in *Saccharomyces cerevisiae* on newly synthesized H3 molecules (S-phase) and disappears in G2 phase (Masumoto et al, 2005). This modification, which is thought to occur at the entry-exit points of nucleosomal DNA, has been shown to promote replication coupled nucleosome assembly, as well as being important for genomic integrity and replication-linked DNA damage response in yeast (Li et al, 2008; Masumoto et al, 2005; Ozdemir et al, 2006).

1.15.7 - Core histone acetylation and chromatin structure – On the nucleosomal level, histone acetylation does not have a significant effect on the structure or stability of individual nucleosomes (Ausio & van Holde, 1986). However, acetylation does increase the susceptibility of nucleosomes to DNase I as well as increase the binding of transcriptional factors to DNA (Ausio & van Holde, 1986; Simpson, 1978). The mechanism behind this could be due to increased ‘site-exposure’ of the nucleosomes upon acetylation (Anderson et al, 2001; Polach & Widom, 1995). The ‘site-exposure model’ helps explain the conformational dynamics of nucleosomes as being in equilibrium between two transient states that differ by the extent to which the DNA is coiled. While the native state allows for maximal DNA binding to the nucleosome, transient uncoiling of the DNA is thought to allow binding of transcriptional factors and other DNA dependent proteins to bind. The equilibrium constant has been shown to be dependent upon the sequence of DNA (Anderson & Widom, 2000; Anderson & Widom, 2001) and the presence of core histone tail domains (Polach et al, 2000). Furthermore, core histone acetylation increases the equilibrium

constant (1.5 fold), although this increase is not nearly as dramatic as when the N-terminal tails are completely removed (1.5-14 fold increase) (Anderson et al, 2001).

Core histone acetylation does have a significant impact on higher order chromatin structures. Following exposure to sodium butyrate, a HDAC inhibitor, interphase chromatin in HeLa cells were shown to form thinner fibers with an average diameter of 20nm alluding towards the formation of moderately “relaxed” fibers (Annunziato et al, 1988). In the absence of H1, oligonucleosomes assembled with hyperacetylated histones were found to remain in an unfolded extended conformation at physiological ionic strength, while non-acetylated oligomers were found to form moderately folded nucleosomal conformations (Garcia-Ramirez et al, 1995). Active gene chromatin fragments containing acetylated histones were also found to resist H1 induced chromatin condensation and aggregation allowing them to remain in a less-folded state (Ridsdale et al, 1990). Consistent with these studies, oligomers assembled from acetylated histones were able to support a 15-fold increase in the transcription rate compared to those assembled from non-acetylated histones (Tse et al, 1998). While it must be noted that acetylation leads to a relaxation in the folding of nucleosomal arrays, oligomerization of the arrays is only partially affected, suggesting that oligomerization and folding are mediated by distinct mechanisms through the NTD of core histones (Tse & Hansen, 1997; Tse et al, 1998).

It must be noted that some acetylation marks may have a much stronger effect on chromatin architecture than other marks. For example, using

recombinant H4 molecules acetylated at Lys16 (H4K16), it was shown that a single acetylation event was able to abolish MgCl₂ dependent compaction of a nucleosomal array, similar to the defect seen in H4 entirely lacking its NTD (Shogren-Knaak et al, 2006). A similar defect was seen even for oligomerization, suggesting that H4K16 was responsible for both condensation and oligomerization of the chromatin fiber (Shogren-Knaak et al, 2006).

Core histone acetylation can also have an indirect effect on chromatin structure, by acting as docking stations for remodeling factors and histone chaperones. In yeast, for example, the chromatin remodelers SWI/SNF complex and histone acetyltransferase GCN5 are thought to act together in order to relieve transcriptional repression (Pollard & Peterson, 1997). In a recent *in vitro* study utilizing highly purified proteins, it was shown that histone acetylation mediated by p300 leads to the eviction of histones from the promoter DNA (Sharma & Nyborg, 2008). This process was found to be independent of ATP dependent chromatin remodelers, but was instead dependent on the histone chaperone Nap1, highlighting a mechanism of acetylation-linked histone eviction (Sharma & Nyborg, 2008). Several other *in vitro* and *in vivo* experiments have shown that HATs and histone chaperons exist in distinct protein networks that act in concert to regulate transcriptional processes (reviewed in (Hansen et al, 2010)). The association of chromatin remodelers and histone chaperones with HATs is thought to expedite the dissociation of DNA from the nucleosome, independent of the site-exposure model, ensuring rapid access of DNA to transcription factors (Luger & Richmond, 1998).

1.15.8 - HDAC inhibitors – HDAC inhibitors (HDACi) have been used in number of biochemical assays to study to the role of histone acetylation in various processes such as the use of sodium butyrate in transcriptional studies (Mathis et al, 1978). Structurally, HDACi fall into distinct categories, such as hydroxamates, cyclic peptides, aliphatic acids, and benzamides (reviewed in (Dokmanovic et al, 2007). Trichostatin A (TSA) is one of the first natural hydroxamates that was shown to inhibit HDACs (inhibits class I and II) (Yoshida et al, 1990). TSA is a potent, reversible inhibitor that is effective even at nanomolar concentrations (Yoshida & Horinouchi, 1999). Prolonged incubation with the drug leads to cell cycle arrest at G1 and G2/M checkpoints as well as apoptosis at higher concentrations (Kim et al, 2000; Sawa et al, 2001). TSA, however, has very selective effects on gene expression with only 2% of the expressed genes undergoing a change in their expression profiles (2-fold change) upon addition of TSA (Van Lint et al, 1996).

Vorinostat (suberoylanilide hydroxamic acid, SAHA), which is structurally similar to TSA, is one of the first HDACi to be approved by the FDA for the treatment of cutaneous T-cell lymphoma (Kelly & Marks, 2005). SAHA has shown therapeutic potential in phase II clinical trials in solid as well as hematologic cancers (Garcia-Manero et al, 2012; Kelly et al, 2005; Kirschbaum et al, 2011; Qiu et al, 2000), however the exact mechanism of its anti-tumor effect is still unknown.

A greater understanding of the anti-cancer properties of HDACi as well as the molecular mechanisms involved in this process is important in improving their

therapeutic efficacy. In Chapter 2, we examine the role that an HDACi, TSA, plays in influencing the structure of chromatin and how this changes the molecular dynamics of histone H1.

1.15.9 - Distinct kinetic pools of acetylated histones. Histone acetylation occurs on multiple residues on core histones, albeit at different rates. The rates of acetylation can be measured, since acetylation imparts a change in mass and charge (neutralizes a lysine residue) on the histone molecule. Experimental setup includes preincubating cells with [³H] acetate for a short pulse and chasing it with HDACi, Sodium Butyrate (Cousens et al, 1979; Covault & Chalkley, 1980). Core histones are then run on AUT gels that allow resolution of histone and acetylated forms, the latter appear as distinct ‘ladders’ (Alfageme et al, 1974) (see Suppl. Figure 3.1, page 155). These experiments revealed that core histone acetylation is a dynamic process comprising of distinct populations of histones that are acetylated/deacetylated at different rates. Hepatoma tissue culture cells, when treated with sodium butyrate, exhibit one population of core histones that are rapidly hyperacetylated ($t_{1/2} = 7$ min for H4 monoacetylation), while the majority of histones (85%) are acetylated slowly ($t_{1/2} = 200-300$ min for H4 monoacetylation) (Covault & Chalkley, 1980). The kinetics of deacetylation also follows a similar kinetic profile with rapid deacetylation rates observed with a $t_{1/2}$ of 3-7 min, while a second pool of histones are deacetylated with a $t_{1/2} = 30$ min (Covault & Chalkley, 1980). While the rates measured in the presence of butyrate may not reflect actual *in vivo* rates of acetylation, the biphasic nature of acetylation rates may hold physiological relevance. For example, histones

involved in rapid dynamics of histone acetylation are associated with transcriptionally active chromatin (Boffa et al, 1990; Hendzel et al, 1991; Ip et al, 1988).

The kinetics and the fraction of histones undergoing this fast, reversible, change in acetylation status depends upon the organism and their stage in differentiation. For example, in immature chicken erythrocytes, approximately 3.7% of the histones are actively acetylated and deacetylated, while in mature chicken erythrocytes, this number drops to 2.1% (Zhang & Nelson, 1986). The rest of the chicken erythrocyte genome is either monoacetylated or unacetylated, and is considered 'frozen' with respect to their acetylation status (Brotherton et al, 1981). Furthermore, while mature erythrocytes have two distinct pools of histones undergoing rapid acetylation (a fast population $t_{1/2} = 12$ min and a slow pool $t_{1/2} = 300$ min, for monoacetylated H4), immature erythrocytes house only the rapidly acetylated histones (Zhang & Nelson, 1988a). *Saccharomyces cerevisiae*, on the other hand, have the majority of their core histones in an acetylated state with an estimated 13 acetylated lysines per nucleosome, creating a transcriptionally competent and accessible chromatin state (Waterborg, 2000). In addition, almost 51% of all yeast chromatin undergo rapid rates of acetylation/deacetylation with the half-life for H4 acetylation recorded at around 15 min (Waterborg, 2001).

A further classification can be made based upon the extent of dynamic acetylation seen in immature chicken erythrocytes. Upon addition of sodium butyrate, one group of H4 molecules are rapidly hyper-acetylated (tetra-acetylated) and rapidly deacetylated upon removal of the inhibitor ($t_{1/2} = 5$ min for

tetraacetylated H4) (Zhang & Nelson, 1988a; Zhang & Nelson, 1988b). This group of actively acetylated species is referred to as Class I acetylation (Davie & Hendzel, 1994; Hendzel & Davie, 1991). Another group of H4 histones reach only the mono- or di-acetylated state upon treatment with Sodium butyrate and are slowly deacetylated ($t_{1/2} = 90$ min for H4 mono-acetylated) (Zhang & Nelson, 1988a; Zhang & Nelson, 1988b). These are referred to as the Class II group of acetylation (Davie & Hendzel, 1994; Hendzel & Davie, 1991). It has been shown that approximately 50% of the newly methylated H4 molecules also participate strongly in class I dependent rapid acetylation and deacetylation (Hendzel & Davie, 1991), providing a link between the process of histone methylation, acetylation, and transcriptional activation. Furthermore, transcriptionally active and transcriptionally competent genes are enriched in class I tetra-acetylated H4 species (Hendzel et al, 1991; Spencer & Davie, 2001). Class II acetylated H4 species, on the other hand, are associated with repressed, transcriptionally competent and active genes (Hendzel et al, 1991). Given that transcriptionally active genes house rapidly acetylated species of H4, it is possible to map these regions following brief treatment with HDACi. Using antibodies against highly acetylated H3 and SC-35 (a non-small nuclear ribonucleoprotein spliceosome which is used a surrogate marker for interchromatin granule cluster (Spector et al, 1991)) it was shown that highly acetylated histones, along with associated histone acetyltransferases and histone deacetylases frequently enrich on the periphery of interchromatin granule clusters (Hendzel et al, 1998).

1.15.10 - Class I acetylation and histone H1 – It is known that the bulk of chromatin fragments extracted from chicken erythrocytes, aggregate and precipitate in 150mM NaCl, possibly due to oligomerization of the fibers (Ridsdale et al, 1990; Ridsdale et al, 1988; Spencer & Davie, 2001). However, in such chromatin fractionation studies, the 150mM NaCl soluble fraction was shown to be enriched in class I acetylated histones and primarily contained transcriptionally active/competent genes (Hendzel et al, 1991; Ridsdale & Davie, 1987; Zhang & Nelson, 1988b). These soluble fractions do contain linker histones; however, the levels of H1 are lower (30% lower) than those found in unfractionated chromatin (Ridsdale & Davie, 1987). This raised the question as to whether the class I fractions had an altered level of condensed chromatin, given their reduced H1 content (Ridsdale et al, 1988). In order to address this, polynucleosomes extracted from different chromatin fractions and stripped of endogenous H1 were assessed for their ability to aggregate in the presence of increasing amounts of exogenously added H1. Polynucleosomes that are otherwise soluble in 150mM NaCl aggregate upon addition of H1, until the dominant species in the soluble fraction are the mono-nucleosomes (Ridsdale et al, 1988). While repressed genes in chicken erythrocytes (such as ovalbumin) are rapidly precipitated, active genes (such as the H5 gene) resisted H1 induced precipitation at 150mM NaCl (Ridsdale et al, 1988). As already mentioned, the chromatin soluble fraction at this salt concentration consists of highly acetylated species. Taken together, these results suggest that core histone acetylation altered the capacity of H1 to condense chromatin fibers (Ridsdale et al, 1990).

In chapter 3, we study the dynamics of histone H1 when core histone acetylation is induced. Our experimental strategy consisted of increasing the abundance of both class I acetylated histones, as well as class II acetylated histones. This was achieved by using two different durations of treatment with HDACi, Trichostatin A.

1.16 – Histone H1 phosphorylation

Histone H1 phosphorylation is maintained by the antagonistic activities of two enzymes Cdk1/Cdk2 and protein phosphatases (Paulson et al, 1996). H1 phosphorylation increases with the cell cycle with low levels found during G1 (Gurley et al, 1978; Hohmann, 1983). The levels increase as cell progress through S-phase while maximum levels are found at the G2-M transition (Ajiro et al, 1981a; Ajiro et al, 1981b; Bradbury et al, 1974a; Gurley et al, 1974; Hohmann et al, 1976). The kinases recognize a consensus sequence of (S/T)PXZ, where X is any amino acid and Z is a basic amino acid (Macleod et al, 1977; Moreno & Nurse, 1990). These sites of phosphorylation are present predominantly in the C-terminal domain of H1, while some variants such as H1.4 and H1.5 have additional sites at the N-terminal domain as well (Figure 1.7) (Langan, 1978a; Langan, 1978b; Sarg et al, 2006). These sites are used differentially as cells progress through the cell-cycle with serine residues used exclusively in interphase (Sarg et al, 2006; Zheng et al, 2010). Threonine residues are additionally phosphorylated in mitosis resulting in high levels of H1 phosphorylation at this stage (Sarg et al, 2006; Zheng et al, 2010).

The molecular mechanism behind how H1 phosphorylation affects its function is still a matter of debate in the literature. Recent evidence points towards a structural effect, whereby H1 phosphorylation alters the conformation of the C-terminal domain, as measured by IR spectroscopy, leading to a higher percentage of β -sheets and a lower proportion of α -helices, compared to the non-phosphorylated version (Roque et al, 2008).

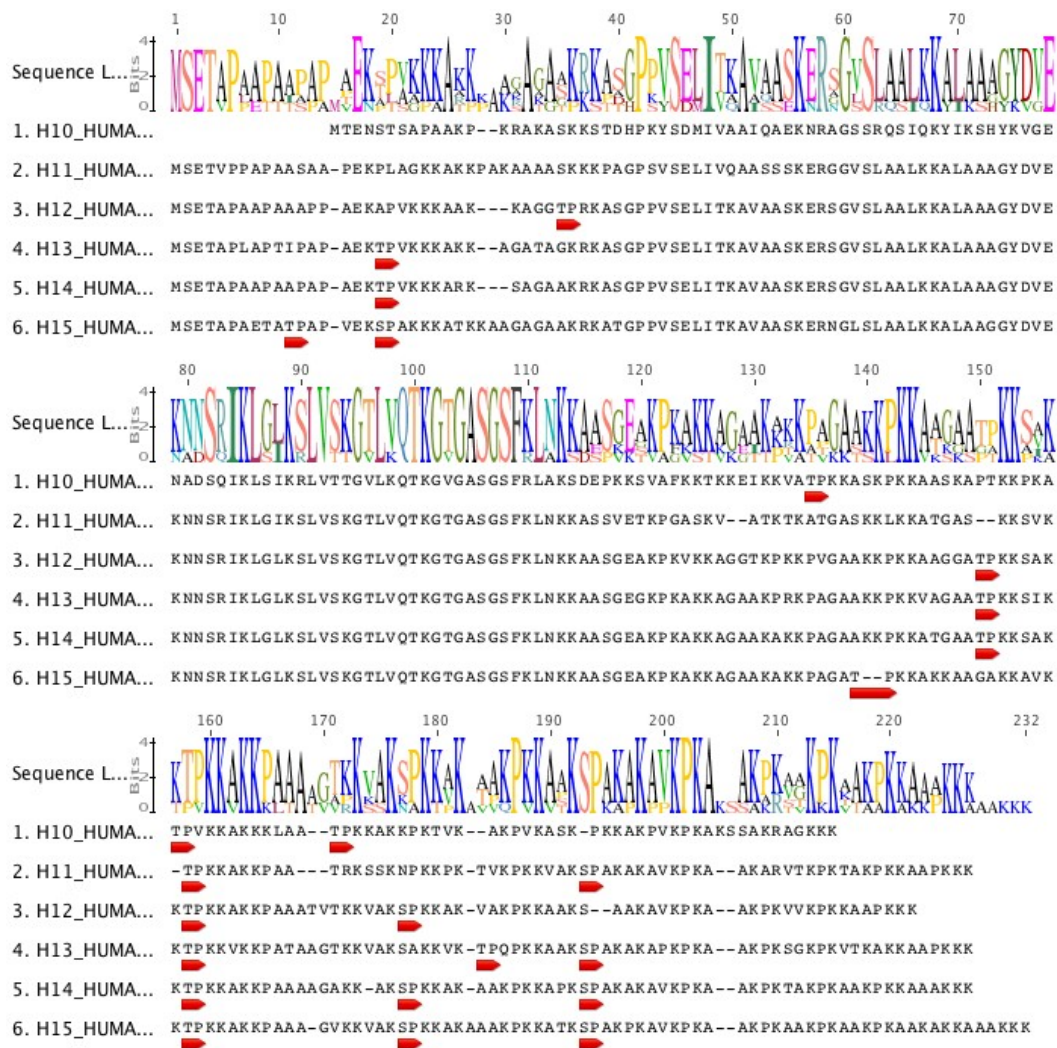


Figure 1.7– Location and sequence conservation of Thr-Pro and Ser-Pro residues among H1 variants. Among all the major human somatic variants of H1, a general trend can be seen with respect to the location of Thr-Pro and Ser-Pro residues (shown here with a red bullet). Thr-Pro residues tend to be located either in NTD or in the CTD, closer to the globular domain. Apart from H1.5, almost all SP sites are located in the CTD closer to the carboxy-terminal end. Furthermore, careful inspection of the sequences shows features that are unique to the variants. For example, H1.0 is unique in that has 3xThr-Pro sites and no Ser-Pro sites. All variants have a fairly well conserved Thr-Pro site at position 158 (of the consensus sequence). Furthermore, H1.3 and H1.4 share a very high degree of sequence identity (86%), however, a single amino acid difference (Ser-Pro at position 173 in H1.4 is Ser-Ala in H1.3), renders H1.3 to have one less cdk2 consensus site, compared to H1.4. Image was generated using the Geneious software.

1.16.1 - Histone H1 phosphorylation and cancer – The chromatin structure in oncogene transformed cells is remarkably different from that in normal cells. For example, *ras*- and *c-myc*- transformed cells have relaxed chromatin structure that correlates with a high degree of H1 phosphorylation (Chadee et al, 1995; Laitinen et al, 1990; Laitinen et al, 1995). High levels of H1 phosphorylation are also observed in cells transformed with *fes*, *mos*, *raf*, *myc* or MAP kinases (Chadee et al, 1995). Activation of the MAP Kinase pathway is thought to lead to the phosphorylation of the proto-oncogene *c-myc*, which then activates expression of cyclins E, A, which in turn elevate the levels of H1 phosphorylation (Chadee et al, 1995; Daksis et al, 1994; Davis, 1993; Filmus et al, 1994; Hunter & Pines, 1994; Jansen-Durr et al, 1993). Furthermore, fibroblasts lacking tumor suppressor Rb, correlate with increased H1 phosphorylation and decondensed chromatin state (Herrera et al, 1996). Accordingly, elevated levels of H1 phosphorylation were found in Lewis lung carcinoma cells of mice, compared to the normal cells (Lennox et al, 1982).

1.16.2 - How H1 phosphorylation is thought to affect H1 binding – Early studies on H1 structure showed that phosphorylation of H1 (by cAMP dependent kinase) on the globular domain destabilizes the globular domain, as analyzed by temperature dependent NMR studies (Rattle et al, 1977). These studies also showed that phosphorylation of H1 destabilized the *in vitro* binding of H1 to DNA (Rattle et al, 1977). H1 dynamics, as measured by FRAP, is markedly reduced when ATP reserves in the cell is depleted (Lever et al, 2000). This alludes towards a stronger binding to chromatin in the non-phosphorylated state of

H1 (Lever et al, 2000). Studies in *Tetrahymena* H1, an evolutionary divergent version of H1 devoid of a globular domain, revealed that when the individual serine phosphorylation sites were mutated to alanine, H1 bound to chromatin with a higher affinity (Dou et al, 2002; Dou & Gorovsky, 2000). Furthermore, mutation of serine residues to glutamic acid destabilized H1 binding to chromatin, both in *Tetrahymena* and mammalian cells (Dou et al, 2002; Hendzel et al, 2004). This led to a model where phosphorylated residues on H1 were thought to create a ‘charge patch’ and that electrostatic repulsions between the DNA backbone and the phosphate groups on H1 were primarily responsible for destabilizing H1 binding (Dou & Gorovsky, 2000; Dou et al, 1999). This model, however, fails to explain why a maximally phosphorylated H1 molecule in mitosis can bind and maintain the high degree of chromatin condensation observed. Additionally, the phosphorylated residues are housed in a domain that has greater than 40% of its amino acids made entirely of either lysine or arginine, reducing the effects of direct electrostatic contributions to H1 binding (Raghuram et al, 2009). Consistent with this hypothesis, CTD peptides were shown to undergo small changes in affinity for DNA *in vitro* following phosphorylation at T/SPKK sites (Roque et al, 2008). Our results (Chapter 4) allude towards the novel role played by proline isomerization, mediated by Pin1, which might explain how H1 phosphorylation is able to affect the binding of H1 to chromatin.

1.16.3 - Chromatin condensation and H1 phosphorylation – The impact of H1 phosphorylation on chromatin structure has been controversial. Studies from the Bradbury lab analyzing the level of H1 phosphorylation in *Physarum*

polycephalum slime mould, suggested that phosphorylation of H1 mediated by a H1 phosphokinase may be involved in the initiation of chromosome condensation thereby triggering mitosis (Bradbury et al, 1974a; Bradbury et al, 1974b). This led to the hypothesis that H1 phosphorylation could cause chromatin condensation given its strong correlation with the cell-cycle (Bradbury et al, 1973). Consistent with this hypothesis, treatment of condensed mitotic chromosomes with Staurosporine, a non-specific kinase inhibitor (Lawrie et al, 1997), led to rapid chromatin decondensation together with a rapid decrease in H1 phosphorylation levels (Th'ng et al, 1994). Further evidence for the relationship between H1 phosphorylation and chromatin condensation was established in studies with temperature sensitive growth mutants isolated from C3H mouse mammary carcinoma cell lines (Matsumoto et al, 1980). At the non-permissive temperature (39°C), these mutants were unable to initiate chromatin condensation, arresting in the G2 phase of the cell cycle (Matsumoto et al, 1980; Yasuda et al, 1981). These mutants were unable to achieve high levels of H1 phosphorylation that was thought to be necessary to achieve chromatin condensation during mitosis (Matsumoto et al, 1980). However, it must be noted that the molecular mechanism behind the lack of H1 phosphorylation in these cells is still unknown, although it has been shown that it is not due to the temperature sensitivity of a histone kinase (Mori et al, 1993; Yasuda et al, 1981). Interestingly, at the non-permissive temperature, ubiquitylated H2A is significantly reduced, suggesting that the thermo-labile protein maybe an E1 ubiquitin activating enzyme (Marunouchi et al,

1980; Matsumoto et al, 1983). The relationship between H1 phosphorylation and H2A ubiquitylation is unknown.

However, Gorovskys studies with *Tetrahymena* protozoans alluded towards a non-mitotic role for H1 phosphorylation, which did not directly correlate with chromatin condensation. *Tetrahymena* consists of a amitotically dividing, transcriptionally active macronucleus, and a mitotically dividing, transcriptionally silent micronucleus (Gorovsky, 1973; Gorovsky et al, 1978). The macronuclei divide without any marked changes in chromatin structure (Flickinger, 1965; Nilsson, 1970). The macronuclear H1 was found to be extensively phosphorylated, yet, did not initiate mitosis, or promote chromatin condensation as seen in eukaryotic cells (Allis & Gorovsky, 1981; Gorovsky et al, 1974). More importantly, they observed increased H1 phosphorylation when cells were subjected to stresses, such as heat shock, alluding towards the involvement of H1 phosphorylation with gene expression (Allis & Gorovsky, 1981). It must be noted, however, that the linker histone associated with micronuclei and macronuclei are very different in terms of structure and sequence (Johmann & Gorovsky, 1976). ‘Micronuclei H1’ is composed of three peptides (named α , β , γ) that bind to the linker region of chromatin (Allis & Gorovsky, 1981; Gorovsky & Keevert, 1975). The macronuclei H1 is evolutionary divergent from mammalian H1, lacking a globular domain and, hence, is much smaller (Wu et al, 1986).

In vitro studies in which chromatin stripped of endogenous H1 were reconstituted with either phosphorylated H1 or non-phosphorylated H1, showed that while reconstitution of chromatin with phosphorylated H1 had minimal effect

on the state of compaction of chromatin *in vitro*, it did cause a significant reduction in the stability of the chromatin fiber (Kaplan et al, 1984). This is consistent with the finding that *Rb* deficient fibroblasts have a relaxed chromatin structure along with increased Cdk2 activity and H1 phosphorylation levels (Herrera et al, 1996). Similarly, when Cdk2 was targeted to a specific chromosomal site, large-scale chromatin decondensation was observed that correlated with increased H1 phosphorylation (Alexandrow & Hamlin, 2005). Thus, while increased H1 phosphorylation correlates (and may cause) chromatin condensation in mitosis, H1 phosphorylation in interphase cells correlates with a relaxed chromatin structure.

1.16.4 - Transcription and H1 phosphorylation levels – One of the earliest indicators that H1 phosphorylation could play a role in regulating gene expression came from studies in which the linker histones extracted from animals fed with hormones, such as glucagon, insulin and thyrotropin to stimulate transcription, were found to be phosphorylated (Lamy et al, 1977; Langan, 1969). These studies led to the hypothesis that H1 phosphorylation could serve as a mechanism to evict H1 from chromatin allowing easy access to transcription factors and other proteins (Hohmann, 1983). Correlation of increased H1 phosphorylation and gene activity have been extended to studies in *Tetrahymena* where H1 phosphorylation was seen to accumulate non-randomly at sites of active transcription (Lu et al, 1995b) and more recently, in mammalian cells where H1 phosphorylation, specifically pS187 H1.4 levels, were enriched at active rDNA promoters (Zheng et al, 2010).

In *Tetrahymena* cells, histone H1 phosphorylation was found to regulate gene expression by creating a charge patch (Dou & Gorovsky, 2000). Strains of *Tetrahymena* in which all the phosphorylation sites of H1 were mutated to alanine or glutamic acid showed that phosphorylation of H1 served to remove it from sites of transcription (Dou et al, 1999). The gene expression profiles in these H1 mutant strains were similar to the gene expression profiles observed when H1 was depleted (Dou et al, 1999), while some genes were suppressed, others were activated (Dou et al, 1999).

In vitro studies on H1 phosphorylation and transcription have focused primarily on the MMTV promoter assays (Koop et al, 2003). Histone H1 phosphorylation was found to specifically increase at promoter or hormone response elements (part of the MMTV promoter) upon transcriptional activation (Koop et al, 2003). In the *in vitro* assays, H1 phosphorylation was not sufficient to promote elongation suggesting that H1 phosphorylation was a key feature of transcriptionally competent chromatin (Koop et al, 2003). Furthermore, phosphorylation of H1 did not lead to a reduction in the total amount of H1 present on the promoter; rather H1 levels were reduced only during transcriptional elongation (Koop et al, 2003).

In vivo, a reduction of H1 phosphorylation led to a reduction in transcription elongation at the MMTV locus and resulted in chromatin condensation (Stavreva & McNally, 2006). Furthermore, while transient (1hr) hormone induced activation of the MMTV promoter led to H1 phosphorylation, prolonged (24hrs) hormone activation promoted H1 dephosphorylation and

promoter deactivation (Lee & Archer, 1998). The dephosphorylation of H1 prevented transcription from the array even in the presence of hormone and major MMTV transcription activators (Lee & Archer, 1998). Transcriptional competency at these arrays was restored upon hormone removal, which also restored in H1 phosphorylation back to basal levels (Lee & Archer, 1998). These studies highlight the central role of H1 phosphorylation in transcriptional activation. In Chapter 4, we build upon the idea that H1 phosphorylation is an important step in transcriptional activation. We show that H1 phosphorylation is present at transcriptionally competent chromatin, consistent with the *in vitro* studies discussed above. Furthermore, we analyze the regulation of H1 phosphorylation at these transcriptionally active sites and other proteins that are involved in this process, namely, peptidyl prolyl isomerases such as Pin1.

1.17 - Proline Isomerization

Histone H1 phosphorylation occurs primarily on Ser/Thr-Pro residues on the CTD of H1. Such Ser/Thr-Pro motifs play key roles in the regulation of multiple different pathways and are the target of a large superfamily of kinases known as Pro-directed protein kinases that include CDKs, extracellular signal-regulated kinases (ERKS), glycogen synthase kinase-3 (GSK3), stress activated kinases, p38 kinases and polo-like kinases (PLKs) (Blume-Jensen & Hunter, 2001; Lu et al, 2003; Lu et al, 2002a; Lu & Zhou, 2007; Nigg, 2001). The importance of the proline residue immediately downstream of the residue that is phosphorylated by these kinases, is due to the fact that these form substrates to yet another group of enzymes known as Peptidyl-prolyl cis/trans isomerases (PPIase). PPIases are

molecular chaperons that are responsible for catalyzing the isomerization of the peptidyl prolyl bond ($\omega=0^\circ$ *cis* to $\omega=180^\circ$ *trans*) (Figure 1.8) (Ramachandran & Sasisekharan, 1968) thereby providing a change in the conformation of the protein (Fischer & Aumuller, 2003). Almost all amino acids, except proline, favor the energetically favorable *trans* conformation. However, due to the unique imide-peptide bond in proline, the energy difference between *cis*- and *trans*- conformations is reduced. This allows prolines to exist in either *cis*- or *trans*- conformations. Indeed, the *cis*- conformation has been observed in 5-6% of protein structures (Pal & Chakrabarti, 1999; Stewart et al, 1990), however, this number could be much higher in proteins that have intrinsically disordered regions. The energy barrier between the *cis*- and *trans*- conformations (14-24 Kcal/mol), albeit being reduced in Xaa-Pro bonds (Xaa is any amino acid) is still high for a spontaneous change in transition under physiological conditions. The slow reaction (0.002/s at 25°C (Christoph, 1981)) can be significantly enhanced (by several orders of magnitude) in the presence of PPIases (Zhou et al, 2000) thus providing cells with the option of having both *cis*- and *trans*- isomers of proteins in a matter of milliseconds (Lu et al, 2007). It is thought that the ability of a single protein to exist in two conformationally distinct structures may allow it to perform different functions based on its conformation (Lu et al, 2007). Such a regulatory mechanism is known as the 'proline switch' - a non-covalent, post-translational modification of proteins that can influence its function in time and space (Lu et al, 2007).

The PPIases are further subdivided into four families, Cyclophilins, FK506 Binding Proteins (FKBP), Parvulins and PP2A activators (PTPA) (Jordens et al, 2006; Lu & Zhou, 2007).

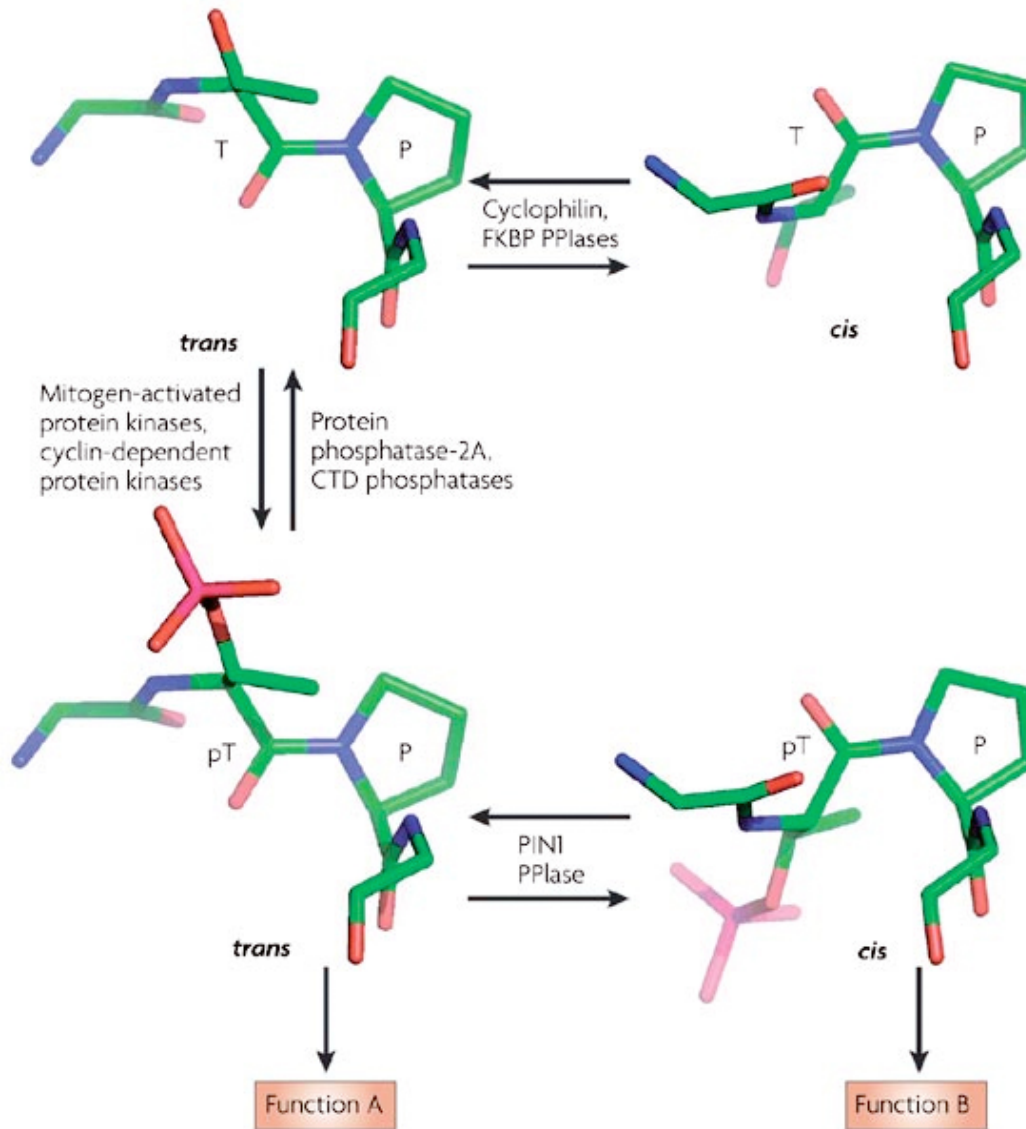


Figure 1. 8 – Proline isomerisation at the structural level. This is an illustration of proline isomerisation using Thr-Pro as a model substrate. Pro is unique in that it can undergo isomerization about its ω -bond angle that can be rotated from 0° (*cis*) to 180° (*trans*). These reactions are catalyzed by prolyl-isomerases (Cyclophilins, FKBP's and Pin1). Pin1 is unique among the prolyl-isomerases in that it has a strong preference for phosphorylated Ser/Thr-Pro bonds. Other PPIases, such as Cyclophilins and FKBP's do not have such a preference. Note the change in structure that is imparted following proline isomerisation. Since structure largely defines function, it is thought that the acquisition of two possible structures following isomerization, can potentially lead to two possible functions for the same protein. Figure adapted from (Lu et al, 2007) and reproduced with permission from Nature Publishing Group.

1.17.1 - Cyclophilins – The discovery of cyclophilins can be traced back to studies analyzing the *in vivo* target of an immunosuppressive drug, Cyclosporin A, CsA (Handschumacher et al, 1984). Cyclophilins are ubiquitous proteins and are highly conserved during evolution with at least eight different forms being found in humans (Galat, 2003). Cyclophilins are involved in a multitude of cellular processes, from protein folding, mitochondrial protection and regulation of apoptosis (reviewed in (Gothel & Marahiel, 1999)). The immunosuppressive actions of CsA are due to the formation of a ternary complex between CsA, cyclophilin and calcinuerin, which inhibits calcinuerin activity and T-cell proliferation (Liu et al, 1991). Cyclophilin A is over expressed in many cancers such as hepatocellular carcinoma, non-small cell lung cancer, pancreatic cancers and glioblastoma multiforme (Han et al, 2010; Howard et al, 2005; Li et al, 2006; Lim et al, 2002). Cyclophilins have been shown to have a direct effect on gene silencing. The yeast homolog of Cyclophilin A, Cpr1, interacts with and possibly promotes the assembly of the Sin3-Rpd3 HDAC complex through proline isomerisation of critical residues in Rpd3 (Arevalo-Rodriguez et al, 2000). Cyclophilins have been implicated in other chromatin modifying complexes, such as the Set3 complex (Arevalo-Rodriguez & Heitman, 2005). More recent evidence alludes to the direct association of some cyclophilins (Cyp71) with specific chromatin modifications in *Arabidopsis thaliana* (Li et al, 2007). Cyp71 consists of 4 WD40 domains in its N-terminal domain through which it is able to directly interact with H3 and promote the levels of H3K27 methylation of the

target gene loci leading to transcriptional silencing (Li et al, 2007). These results show that cyclophilins can have a direct impact on chromatin structure and gene expression profiles through their associations with histones.

1.17.2 - FKBP – FK506 Binding proteins, or FKBP, like cyclophilins, are very abundant, ubiquitously expressed and evolutionary conserved proteins involved in the protein folding process, with up to 18 isoforms present in humans (Galat, 2003; Galat, 2004; Suzuki et al, 2003). FKBP were initially identified as the target for another immuno-suppressive drug, FK506 and rapamycin (Harding et al, 1989; Siekierka et al, 1989). FKBP have been implicated in a number of processes, including regulation of transcription and chromatin modifications (reviewed in (Dilworth et al, 2012)). For example, both FKBP and Cyclophilin A have been shown to interact with a zinc-finger transcription factor YY1 (Yang et al, 1995), while FKBP25 directly interacts with HDAC1 and HDAC2 (Yang et al, 2001). Yeast FKBP12 interacts with chromatin associated high mobility group 1,2 homology HMO1 (Dolinski & Heitman, 1999). Direct evidence for the involvement of FKBP with chromatin comes from yeast Fpr4, which interacts specifically with the NTD of H3 and H4 and modulates the isomerization of two specific prolines (H3P30, 38) on the N-terminal tail of H3 (Nelson et al, 2006). Furthermore, Fpr4 was able to inhibit the methylation of H3K36 by regulating the isomerization of the prolyl bond at H3P38 (Nelson et al, 2006). Fpr4 was also shown to localize on the promoters and coding regions of genes, playing an important role in the transition from uninduced to an induced gene state (Nelson et al, 2006). These results establish a crucial link between proline isomerization,

which is a non-covalent histone modification, and histone lysine methylation, which is a covalent histone modification, in gene regulation. Furthermore, they describe a novel role for peptidyl-prolyl isomerases in regulating chromatin and transcriptional activity. Our studies, described in Chapter 3, detail the contribution of the parvulin class of isomerases, specifically Pin1, in modifying chromatin and its role in transcriptional processes.

1.17.3 - PTPA –Ser/Thr phosphatase 2A (PP2A) activator, alternatively called the phosphotyrosyl phosphatase activator (PTPA) was initially isolated as proteins that stimulated the otherwise weak phosphotyrosyl phosphatase activity of PP2A (Cayla et al, 1994; Janssens et al, 1998). They are newly discovered members of the peptidyl-prolyl isomerase group, and unlike other isomerases, their active site is an all- α -helix fold located at the interface of substrate-induced dimer interface (Leulliot et al, 2006). The yeast homolog, Rrd1, has been shown to associate with the CTD of the Rpb1 (the largest subunit of RNAPol II), and cause isomerisation of the CTD in response to stress signals (Jouvet et al, 2010; Poschmann et al, 2011). The role of these enzymes in higher eukaryotes is yet to be characterized.

1.17.4 - Parvulins - This class of prolyl isomerases are named after their initial discovery in *E.coli* as small 10kDa proteins (*Parvulus* – ‘very small’ in latin) that were resistant to both cyclosporin A and FK506 (Rahfeld et al, 1994a; Rahfeld et al, 1994b). The three main members of the human Parvulin class of PPIases include, Pin1, Par14 and Par17 (Mueller et al, 2006). Pin1 and Par14 are fairly well characterized and share a conserved C-terminal PPIase domain similar in sequence and structure (Sekerina et al, 2000). The differences however, rest in the

NTD of these proteins, with Pin1 housing a WW domain (discussed below), while Par14 has an unstructured domain rich in basic amino acids and is thought to bind DNA with high affinity (Surmacz et al, 2002). Human Par14 was shown to have PPIase activity towards non-phosphorylated, proline containing peptides, and shares about 30% of sequence identity with human Pin1 (Uchida et al, 1999). Surprisingly, the NTD of Par14 bears a striking resemblance to the primary sequence of HMG proteins (HMG17), raising the possibility that these proteins might directly contribute to DNA dependent processes such as regulation of gene expression (Surmacz et al, 2002). Most of the studies involving the Parvulins, however, have been on Pin1, and will be discussed below.

1.18 - Pin1

Pin1 (Protein interacting with NIMA (never in mitosis A)-1) is a member of the Parvulin family and its uniqueness lies in the fact that it specifically recognizes phosphorylated Ser/Thr-Pro residues and catalyzes the interconversion of the peptidyl prolyl bond (Lu et al, 1996; Lu & Zhou, 2007; Wulf et al, 2005). Pin1 is a highly abundant, small protein (163AA) that contains an N-terminal phospho-protein binding domain, known as the WW domain (1-39AA). The isomerase or the catalytic domain rests in the C-terminal domain (45-163AA) (Lu et al, 1996; Lu et al, 1999) (Figure 1.9).

The interaction of Pin1 with its substrates introduces a post-phosphorylation regulatory step, whereby Pin1 can modulate the structure of phosphorylated proteins potentially affecting their function, subcellular localization, stability, phosphorylation status or interaction with other proteins (Lu et al, 1999;

Ranganathan et al, 1997; Yaffe et al, 1997). Furthermore, protein kinases such as MAPK, Cdk2 and protein phosphatases such as PP2A have been shown to be conformation specific, targeting only the *trans*- isomer and not the *cis*- isomer (Brown et al, 1999; Weiwad et al, 2000; Zhou et al, 2000).

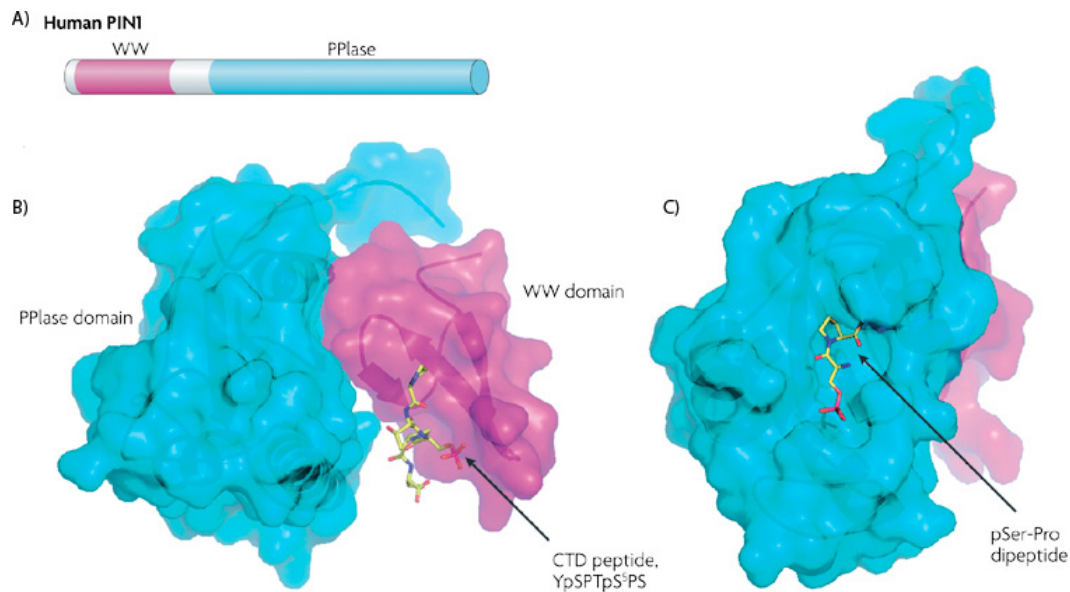


Figure 1.9 – Structural domains of human Pin1. (A) Pin1 contains an N-terminal WW domain that recognizes pSer-Pro/pThr-Pro residues, while the C-terminal domain is the catalytic PPlase domain that is responsible for the interconversion of *cis*- and *trans*-peptidyl prolyl bond. (B) X-ray structure of the WW domain bound to a model substrate. Structural features that enable selectivity and specificity of the WW domain include critical residues, such as Ser16, Arg17 and Tyr 23 that form a phosphate-binding pocket stabilizing the phosphorylated substrate, while Tyr23 and Trp 34 form a hydrophobic clamp stabilizing the proline residue on the substrate. (C) X-ray structure of the C-terminal catalytic domain bound to a model substrate. The domain forms a barrel shaped structure, allowing positively charged residues Lys63, Arg 68 and 69 to mediate electrostatic stabilization of the phosphate group on the substrate. Figure adapted from (Lu & Zhou, 2007) and reproduced with permission from Nature Publishing Group.

1.18.1 - Regulation of Pin1 through the WW domain – The WW domain, named after two conserved Trp residues, is a 38-40 amino acid structural motif that folds into three anti-parallel β -sheet structure and is found in many proteins involved in signaling pathways (reviewed in (Sudol, 1996)). The WW domain can be subdivided into five distinct groups based on their proline rich sequence substrate specificity. Group I WW domains bind ‘PPxY’ motifs (Chen et al, 1997), Group II bind ‘PPLP’ motifs (Ermekova et al, 1997), Group III are specific for ‘PGM’ motifs (Bedford et al, 1998), while group IV WW domains bind phospho-Ser/Thr-Pro residues. The WW domain of Pin1 falls under this category (Lu et al, 1999). Group V WW domain comprises of proteins, such as FBP30, that recognize Pro-Arg motifs (Bedford et al, 2000).

The WW domain in Pin1 is defined by the presence of two invariant Trp at either ends of the WW domain at position 11 and 34, along with a central hydrophobic patch made of aromatic amino acids (Ranganathan et al, 1997). The WW domain of Pin1, initiates the binding of Pin1 to its target substrates (Zhou et al, 1999). The role of this domain can best be described as a binding module that recognizes the pSer/Thr-Pro bonds and targets the catalytic PPIase domain to its substrates (Lu et al, 1999). Interaction between Pin1 substrates and the WW domain is mediated through critical amino acids present in its binding pocket. These include Ser16, Arg17, Tyr23 and Trp34 (Lu et al, 1999). The crystal structure of Pin1 and a peptide derived from the CTD of phosphorylated RNA Polymerase II revealed that Ser 16 and Arg 17 residues form a phosphate binding pocket, while the aromatic pair of Tyr, Trp form a hydrophobic clamp that interacts with the proline

residue (Verdecia et al, 2000). Importantly, it was found that the substrate always exists in a *trans*-peptidyl conformation both in the crystal structure and *in vitro* NMR studies (Verdecia et al, 2000; Wintjens et al, 2001). Ser 16 on Pin1 can be phosphorylated either by PKA or PKC *in vitro*, which completely abolishes its ability to interact with its substrates (Lu et al, 2002b). Furthermore, the WW domain of Pin1 has been shown to regulate the localization of Pin1 to specific structures within the nucleus called nuclear speckles. Phosphorylation of the Ser16 residue on the WW domain through PKA activation (forskolin treatment), disrupted the localization of Pin1 to these speckles (Lu et al, 2002b). These results show that the function of Pin1 can be regulated by phosphorylation of critical residues on its WW domain.

1.18.2 – Catalytic domain of Pin1 – The C-terminal PPIase domain of Pin1 is characterized by four anti-parallel β -sheets surrounded by four α -helices (Ranganathan et al, 1997). The active site is comprised of a set of hydrophobic residues (Leu-122, Met-130, Phe 134) that stabilize the hydrophobic proline and the peptide bond that undergoes the isomerization (Ranganathan et al, 1997; Yaffe et al, 1997). However, the distinguishing feature is the presence of a triad of basic residues (Lys-63, Arg 68 and Arg 69) that is thought to stabilize the phosphate group of the phosphorylated substrate (Ranganathan et al, 1997). These residues project outward and are present at the entrance of the PPIase domain and play a key role in conferring the unique substrate specificity for Pin1 (Ranganathan et al, 1997; Yaffe et al, 1997). At the same analogous position in FKBP and cyclophilin, for example, the basic patch is replaced with a hydrophobic patch,

which may explain the preference for hydrophobic residues N-terminal to the proline amino acid for these enzymes (Albers et al, 1990; Ranganathan et al, 1997). Lys 63 and Cys 113 are highly conserved in the Parvulin class of PPIases and have been shown to play central role in the isomerase activity of Pin1 (Yaffe et al, 1997; Zhou et al, 2000). The exact mechanism through the prolyl bond isomerases is still a subject of debate in the literature, although there are at least four different potential mechanisms that could account for this rapid reaction (reviewed in (Lu & Zhou, 2007)).

The CTD of Pin1 is also subject to post-translational modifications. Large-scale proteomic analysis of proteins phosphorylated by ATM/ATR detected by mass-spectroscopy, showed Ser108 (SQ motif) of Pin1 to be phosphorylated upon DNA damage (Matsuoka et al, 2007). Based on the crystal structure of Pin1 (Ranganathan et al, 1997), this modification resides on a loop connecting alpha-helix 1 and 2, and is located away from the active site of Pin1. The functional relevance of this modification is unknown.

1.18.3 - Pin1 substrates – Pin1 has been shown to interact with a wide number of substrates with a wide array of functions. These include proteins involved in cell cycle regulation such as cyclin D1 (Liou et al, 2002) and Cyclin E (Yeh et al, 2006), proteins involved in maintaining genome integrity such as p53 (Wulf et al, 2002), proteins involved in cellular differentiation such as Oct4 (Nishi et al, 2011) and Nanog (Moretto-Zita et al, 2010), proteins involved in apoptosis such as Bcl-2 (Pathan et al, 2001). The isomerase activity of Pin1 on its substrates can have different consequences, for example, while Pin1 enhances Cyclin E degradation

(Yeh et al, 2006), Pin1 stabilizes p53 and enhances its binding to promoters (Zheng et al, 2002). The regulation of some of Pin1s substrates, such as cdc25 and RNA Polymerase II will be discussed in detail.

1.18.4 – Pin1 regulation of Cdc25 – The regulation of Cdc25 by Pin1 is of importance to our studies, due to the mechanistic similarities of Pin1 regulation of histone H1 phosphorylation (Chapter 4). Cdc25 is a Cdc2 phosphatase that plays an important role in the entry into mitosis (Dunphy & Kumagai, 1991; Gautier et al, 1991; Strausfeld et al, 1991). During the transition from interphase to mitosis, the N-terminal domain of Cdc25 gets hyperphosphorylated, which allows its translocation to the nucleus where it becomes a substrate for Pin1 (Crenshaw et al, 1998; Kumagai & Dunphy, 1992; Shen et al, 1998; Stukenberg & Kirschner, 2001). Even a sub-stoichiometric amount of Pin1 (1:0.0005) is able to induce a conformational change in Cdc25, a change which inhibits its inherent phosphatase activity (Stukenberg & Kirschner, 2001). Pin1 plays an additional role in determining the function of Cdc25. The major pSer/Thr-Pro phosphatase, PP2A, (Che et al, 1998; Clarke et al, 1993; Karaiskou et al, 1999), only dephosphorylate residues when the peptidyl-prolyl bonds are in the *trans*- conformation (Zhou et al, 2000). Pin1, which catalyzes the isomerization about the prolyl-bond, increases the activity of PP2A towards its substrates (cdc25) thereby facilitating their dephosphorylation rates (Zhou et al, 2000). Pin1 thus imparts a post-phosphorylation regulatory step, mediated by proline isomerization, which is an important mechanism regulating protein function. Depletion of Pin1 from

Xenopus egg extracts leads to premature entry into mitosis accompanied by hyperphosphorylation of Cdc25 (Winkler et al, 2000).

In Chapter 4, we demonstrate a similar post-phosphorylation regulatory step exists for the regulation of histone H1 phosphorylation. In the absence of Pin1, we observed an increase in H1 phosphorylation level and a dependence of Pin1 for PP2A induced H1 dephosphorylation rates. As already discussed, H1 phosphorylation influences the structure and function of H1 molecules.

1.18.5 - Regulation of transcription by Pin1 –Pin1 plays an important role in gene expression through its actions on the C-terminal domain of the largest subunit of RNA Polymerase II, Rpb1, which is composed of 52 tandem repeats of YSPTSPS (Xu & Manley, 2007b). The CTD of RNA Polymerase II acts as a docking site for various proteins involved in efficient capping, splicing, cleavage, and polyadenylation of mRNAs *in vivo* (Hirose & Manley, 1998; McCracken et al, 1997; Proudfoot et al, 2002). The binding of proteins involved in this wide-spectrum of activities depends on the phosphorylation state of RNA Polymerase II, which varies with the transcription cycle (O'Brien et al, 1994). The maximally phosphorylated RNA Polymerase II has more than 100 potential Pin1 binding sites, in the 2 SP motifs present in the tandem repeat (Xu & Manley, 2007a). Indeed, Ess1 (the yeast homolog to human Pin1) is one of the major binding partners for hyperphosphorylated RNA Polymerase II CTD (Morris et al, 1999). Pin1 enhances the phosphorylation of RNA Polymerase II by cdc2/cyclin B *in vitro* (Xu & Manley, 2007b). The hyperphosphorylated form of RNA Polymerase II is thought to dissociate from chromatin and reorganize into distinct nuclear

speckles (Xu & Manley, 2007b). Furthermore, Pin1 was able to exert an inhibitory role in transcriptional initiation, while having no effect on transcriptional elongation (Xu & Manley, 2007b), however the mechanism behind Pin1 regulating RNA Polymerase II initiation is still unknown. Recent evidence further implicates EssI to interact with TFIIB, as well as with CTD phosphatases and 3'-end processing complexes, adding further complexity to the role of prolyl-isomerases in transcriptional regulation (Krishnamurthy et al, 2009). In addition, Pin1 also interacts with a host of transcription factors. For example, Pin1 affects the stability of cjun (Wulf et al, 2001), p53 (Zheng et al, 2002), SMRT (Stanya et al, 2008), and increases the recruitment of cofactors of STAT3 (Lufei et al, 2007), and translocation of β -catenin (Ryo et al, 2001), and regulates the dephosphorylation of cFos (Monje et al, 2005) and cMyc (Yeh et al, 2004).

1.18.6 - Regulation of chromatin structure by Pin1 – Pin1 was originally identified as an essential regulator of mitosis in both yeast and mammalian cells, and its depletion was shown to induce mitotic arrest (Lu et al, 1996). In mitosis, Pin1 plays an important role in regulating the mitotic phosphorylation of TopoII α (Xu & Manley, 2007a; Xu & Manley, 2007c). Pin1 is thought to bind the 5 S/TP sites of TopoII α in its CTD that are specifically phosphorylated during mitosis (Wells & Hickson, 1995; Xu & Manley, 2007c). Mitotic extracts, depleted of Pin1, were shown to be unable to induce chromatin condensation in permeabilized S-phase cells suggesting that Pin1 was necessary for chromatin condensation (Xu & Manley, 2007c), however the biochemical mechanism behind this process is unknown.

1.18.7 - Role of Pin1 in cancer and disease – Pin1 has been shown to play a crucial role in many processes, such as cell cycle, transcription, splicing, aging, DNA damage and developmental processes (reviewed in (Lu et al, 2003; Lu et al, 2002a; Lu & Zhou, 2007)). Consequently, deregulation of Pin1 is associated with a variety of pathological states such as cancer, Alzheimer’s disease, autoimmune and inflammatory diseases (Lee et al; Lu, 2004; Lu & Zhou, 2007). Over expression or dysregulation of Pin1 induces centrosome amplification, chromosome instability and cellular transformation by activating a number of oncogenic pathways, while inactivating tumor suppressors. Pin1 has been shown to be overexpressed in cervical, breast, prostate, brain, lung and colon cancers (Bao et al, 2004). Elevated Pin1 expression correlates with clinical staging of prostate cancer (Ayala et al, 2003). Pin1 can be used as an independent prognostic marker, with patients harboring higher Pin1 expression levels experiencing a shorter recurrence-free survival time (Ayala et al, 2003).

1.19 – Fluorescence recovery after photobleaching (FRAP)

FRAP experiments were first used almost 35 years ago to analyze the lateral diffusion of integral membrane proteins in living cells (Axelrod et al, 1976b; Edidin et al, 1976). Since then, FRAP has successfully been used to study the molecular flux of many nuclear proteins and has shaped our understanding of the chromatin as being highly dynamic and conformationally robust. Compared to *in vitro* techniques such as filter binding assays (Riggs et al, 1970) or capillary electrophoresis (He et al, 2004) that provide us with *in vitro* binding affinities of proteins, FRAP provides a measure of the *in vivo* binding affinity of proteins

(reviewed in (McNally, 2008)). This is of great significance, since *in vitro* experiments fail to completely replicate the crowded nature of the nuclear microenvironment and may not factor in the contributions of other proteins/chaperons that may influence binding (Sprague et al, 2004).

FRAP experiments help us to analyze the *in vivo* diffusion coefficient (D) of molecules (Axelrod et al, 1976a). The unconstrained diffusion coefficient of molecules is described by the Einstein-Stokes formula $D = kT/6\pi\eta r$ (Arrio-Dupont et al, 1997; Carrero et al, 2004b), where k is the Boltzmann constant, T is the temperature, η is the viscosity and r is the hydrodynamic radius of the molecule. Under the experimental conditions where T and η is kept constant, D is inversely proportional to r (reviewed in (Reits & Neefjes, 2001)). If the molecule is thought of as a sphere, then D is inversely proportional to $M^{1/3}$, where M is the molecular mass. The rate of protein movement through diffusion is reflected in its D value. , since it is a measure of the root mean squared displacement of a protein over time (Lippincott-Schwartz et al, 2001). Deviations from the predicted D value can provide us with valuable insight to whether molecules form large complexes or exist in multimeric or oligomeric structures. Additionally the dynamics of the molecule can also be hindered by interactions with other proteins or DNA, which can be quantified by experiments such as FRAP (Reits & Neefjes, 2001). FRAP experiments can be divided into two phases – photo-bleaching and recovery phase.

1.19.1 - Photobleaching - FRAP experiments consist of irreversibly photobleaching a defined area within a cell or organelle with the help of a high-

powered laser beam (Peters et al, 1974). Photobleaching is a process through which a fluorophore irreversibly loses its fluorescence, possibly due to a chemical interaction with oxygen or surrounding molecules in its excited state, such that it ceases to be fluorescent upon its return to the ground state (Hinterdorfer & Van Oijen, 2009). For example, photobleaching of YFP molecules *in vitro* leads to the decarboxylation of the YFP molecule leading to a non-fluorescent state (McAnaney et al, 2005). The exact process of photobleaching *in vivo*, however, is yet to be elucidated. The aim of photobleaching is to disrupt the steady-state distribution of fluorescent molecules, allowing us to analyze the kinetics with which the steady-state is reestablished following photobleaching (Carrero et al, 2004a). The kinetics are analyzed during the recovery phase of the FRAP experiment as detailed below.

1.19.2 - Recovery – After photobleaching, a timelapse image series is recorded until the relative fluorescence reaches equilibrium. The recovery phase of FRAP experiments is made possible due to the exchange between fluorescent and non-fluorescent molecules and is dictated by the kinetics of the molecules as well as the fraction of molecules that are mobile (Reits & Neeffjes, 2001).

The diffusion coefficient, D , of a protein based on two dimensional diffusion equation, is obtained with the equation, $D = \omega^2 \gamma_D / 4\tau_{1/2}$, where ω is the radius of the laser beam, γ_D depends upon the beam shape (for circular beams it is a constant value of 0.88) and $\tau_{1/2}$ is half the time it takes for complete recovery (Axelrod et al, 1976a; Lippincott-Schwartz et al, 2001).

However, binding interactions with macromolecules such as DNA or chromatin can considerably slow down a molecule leading to a 50- to 100-fold slower kinetics than predicted based on the molecular weight and diffusion of an inert molecule such as GFP (Phair & Misteli, 2000). For example, given its strong association with chromatin, core histone H3 (molecular weight of H3.3 is 15.3kDa) take a much longer time to attain pre-bleach levels of fluorescence, (Kimura & Cook, 2001), compared to proteins such as SF2/ASF (molecular weight is 27.7kDa) have very rapid dynamics within the cell (Phair & Misteli, 2000). Thus, FRAP experiments provide us with the *apparent* or *effective* mobility of proteins that is a combination of the absolute mobility of the protein as defined by its diffusional mobility and its mobility based on the specific interactions of the protein with other proteins/substructures (Misteli, 2001). The kinetics of most nuclear proteins, including H1, can be described as transient binding and unbinding interactions that results in a slowed, saltatory movement of the protein throughout the nucleus (Misteli, 2001).

FRAP experiments on H1 revealed the presence of at least two distinct kinetic populations of H1 in the nucleus (Figure 1.10) (Carrero et al, 2004b; Misteli et al, 2000). The recovery can be explained by a freely diffusing pool of H1 that exchanges with H1 that is bound to chromatin with low affinity, while a second pool of H1 comprises of H1 molecules that are strongly bound and does not contribute significantly to the recovery of the FRAP curve in the analyzed period of time (Misteli et al, 2000). The H1-GFP tagged molecules were bound to chromatin for over 220s before dissociating and moving on to the next binding

site (Misteli et al, 2000). This suggested that unlike free diffusion, where absolute diffusion coefficient could be easily determined using the equation given above, in molecules such as H1, the binding-unbinding turnover kinetics were rate-limiting and mathematical modeling of the FRAP curves were needed in order to quantify the binding events.

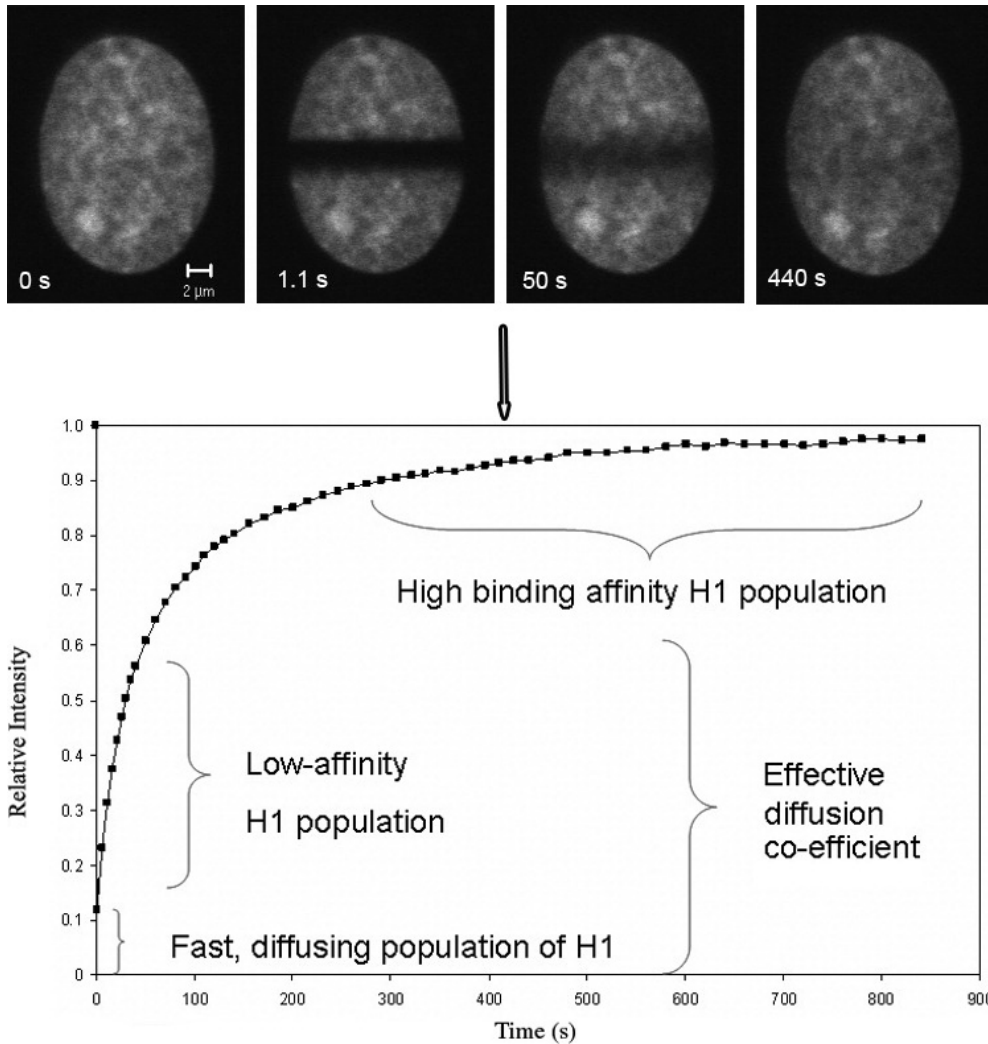


Figure 1.10 – From FRAP to mathematical modeling. Top series of panels illustrates a typical $10T_{1/2}$ cell expressing GFP-H1.0. A rectangular region of $1.5\mu\text{m}$ was photobleached. The recovery of fluorescence was measured at defined time intervals until equilibrium was reached. Fluorescence intensity is then normalized with the intensity at time zero, set to a maximum of 1, which is then plotted against time on the x-axis, as shown. Note that the normalized (or relative) intensity starts approximately at 0.1 (or 10%). This is due to the freely diffusing H1 population that reaches equilibrium even before the first image of the recovery phase is recorded. The recovery from 10% to approximately 80% takes about 200 seconds, and the major contributors of this phase of recovery are the low-affinity H1 population. The effective diffusion coefficient is a kinetic parameter that describes the behavior of both the freely diffusing population and the low-affinity H1 population. The next phase of the recovery from 80% to equilibrium levels are determined by the dynamics of the high-affinity population and takes from 200s to 900s. Residence time, transition time are temporal parameters associated with this kinetic population of H1. Figures adapted from (Raghuram et al, 2009) and reproduced with permission from NRC Research Press.

1.19.3 - Mathematical modeling of FRAP curves - The apparent mobility as measured by FRAP can be used to decipher the nature of interactions of the protein and this is primarily accomplished with the help of mathematic modeling of the FRAP curves (Carrero et al, 2004a; Carrero et al, 2004b; Phair & Misteli, 2001). Mathematical modeling simulates the process of FRAP and helps us to quantify hypothesized binding events in terms of mathematical descriptors in order to explain the mobility of proteins (Mueller et al, 2010; Phair & Misteli, 2001). The mathematical descriptors or modeling parameters for characterizing the dynamics of H1 include effective diffusion coefficient, residence time, transition time and the percentage of molecules that are bound with high affinity to chromatin. Residence time (τ_R) refers to the amount of time H1 spends in a high affinity state and is indirectly proportional to the unbinding rate or k_u , such that $\tau_R = 1/k_u$. The transition time (τ_T) is the time spent between two high-affinity interactions and is indirectly proportional to the binding rate, k_b such that $\tau_T = 1/k_b$. The effective diffusion coefficient takes into account the kinetics of the freely diffusing population and the population of H1 that is bound to chromatin with low-affinity (Carrero et al, 2004b).

The dynamics of H1 has been described using the compartmental model as well as the reaction diffusion model (Carrero et al, 2004a; Phair et al, 2004a; Phair et al, 2004b). The compartmental model effectively divides the nucleus into three physical compartments – the photobleached region, and the two unbleached regions on either side of the photobleached region, and the mathematical equations relate to the movement of the molecules in and out of these

compartments. The reaction diffusion model on the other hand, describes the reversible binding and unbinding of molecules in a one-dimensional system. Both of these models describe the binding process in the same mathematical terms (k_b and k_u), while differing in their description of the diffusion coefficient. The compartmental model is simplistic and provides us with only a rough estimate of the diffusion coefficient. The compartmental model, however, is more appropriate for proteins that show a distinct biphasic behavior, such as nuclear actin (Carrero et al, 2003) and many other nuclear proteins (Phair et al, 2004b).

The FRAP curves of H1, unlike GFP-actin, does not exhibit a stark biphasic curve. Instead, it appears as a curve produced due to a single diffusing population. The dynamics can be described with the help of the reaction-diffusion model that assumes that the chromatin structure that H1 binds, is relatively immobile on the time-scale observed and that the chromatin is spatially homogenous (Carrero et al, 2004b). Following the acquisition of the FRAP curve, the curve is fit to the mathematical solution of the reaction-diffusion model allowing us to estimate the modeling parameters listed above (Carrero et al, 2004b). The results of the mathematical modeling estimates that approximately 88% of the H1 population is comprised of H1 molecules that are bound to chromatin with low affinity as well as those who are diffusing freely through the nucleus (Carrero et al, 2004b). The remaining 12% of the population consists of H1 molecules bound with high affinity to chromatin (Carrero et al, 2004a; Carrero et al, 2004b). This is expressed as an *effective* diffusion coefficient. Furthermore, using the Einstein-Stoke law described earlier, the freely diffusive pool of H1 can be estimated to

being around 0.2% of the total H1 population (Carrero et al, 2004b). This suggests that at a given time, most of the H1 population is bound to chromatin, consistent with the role of H1 as a chromatin architectural protein.

1.20 - Thesis Focus -

Post-translational modifications, such as core histone acetylation and H1 phosphorylation, play an important role in many processes crucial to life, such as transcription. They alter the structure of chromatin fiber so that proteins such as transcription factors can gain access to DNA. We hypothesized that these modifications would impede the binding of H1 molecules to the chromatin fiber, thereby affecting its mobility and function.

Core histone acetylation has the ability to relax higher order chromatin structures and *in vitro* data previously had suggested that it prevented the ability of H1 to condense chromatin. However, it wasn't known how core histone acetylation would impact H1 dynamics *in vivo*. Furthermore, it wasn't known whether individual variants would respond differently to core histone acetylation, or whether they would all behave in a similar manner in a hyperacetylated chromatin environment. Additionally, upon treatment with histone deacetylase inhibitors, two distinct kinetic phases of acetylation have been observed, with one population of H4 molecules undergoing rapid rates of acetylation and deacetylation, while the majority of H4 molecules are involved in slow rates of acetylation and deacetylation. The contribution of these two distinct classes of acetylation in affecting histone H1 mobility/chromatin binding was also unknown. This is

especially important given that the rapidly acetylated histones are associated with transcriptionally active chromatin states.

Phosphorylation of H1 has been associated with transcription and cell cycle events although the mechanism behind how H1 phosphorylation affects H1 function, or whether or not it causes chromatin condensation has remained elusive. Furthermore, it is debatable as to whether the charge patch hypothesis accurately explains the role of H1 phosphorylation towards destabilizing H1 function. There are only a limited number of studies analyzing the regulation of H1 phosphorylation levels *in vivo*, or the kinetics of H1 phosphorylation itself. H1 phosphorylation has been shown to be enriched at sites of transcription, however, its function at these sites is unknown.

Our studies were designed with the objective of understanding the dynamics of H1 molecules and their function during transcriptional processes. The regulation of H1 dynamics by these post-translational modifications will provide us with an understanding of how chromatin is modified in processes such as transcription. This is important since most of the changes observed in processes such as oncogenesis are epigenetic in nature.

Chapter II – Experimental Procedures

2.1 - Cell Culture

Mouse embryonic fibroblasts (10T1/2 cells) and Ciras-3 cells (H-ras transformed 10T1/2 cells) were maintained in alpha-modified minimum essential media, supplemented with 10% fetal bovine serum and 1% L-Glutamine. Cells were treated with Trichostatin A (purchased from Sigma and dissolved in DMSO) at a concentration of 100ng/ml, for either 1hour or 18hrs.

Pin1^{-/-} and Pin1wt cells were cultured in DMEM (GIBCO). U2Os 263 cells were grown in High Glucose DMEM supplemented with 100µg/ml Hygromycin B. Transfections were done using Effectene (Qiagen) transfection reagents, according to the manufacturer's protocol. Cells transfected with mcherry-tTA-ER were treated with 1µM Tamoxifen (Sigma, dissolved in Ethanol) for either 1hr or 3hrs to activate transcription. For α-amanitin analysis, the 263 cells were transfected overnight with mcherry-tTA-ER and then pre-treated with α-amanitin (100µg/ml, overnight) following, which they were treated with Tamoxifen.

2.2 - Isolation of nuclei and histones

Nuclei were isolated as described in (Shechter et al, 2007), with some modifications. Briefly, 70-80% confluent cells were washed with ice-cold phosphate buffered saline (PBS). Nuclei were isolated using ice-cold nuclear isolation buffer (250mM Sucrose, 150mM NaCl, 20mM Tris pH 8, 2mM MgCl₂, 1mM CaCl₂, and 0.1% NP-40) supplemented with PhosSTOP (from Roche) a phosphatase inhibitor cocktail, Pepstatin (Roche), DTT and Complete protease inhibitor cocktail (Roche). Histones were extracted with 0.4N sulphuric acid, precipitated with ice-cold acetone (overnight) followed by centrifugation at

10,000x g for 10min at 4°C. They were then washed three times with acetone and air-dried.

2.3 - Electrophoresis

For SDS gels, precipitated extracts were dissolved in 3xSDS loading buffer (0.195M Tris, pH 6.8, 6% SDS, 3% β-mercaptoethanol, 30% glycerol) and loaded onto on an 18% acrylamide gel. A typical 18% gel (10ml, 2 gels) comprised of 2.5ml of 4xSeperating Buffer (1.5M Tris, pH 8.7, 0.4% SDS), 4.5ml 40% Acrylamide, 3ml ddH₂O, 100μl 10%APS, 10μl TEMED. Gels were and then transferred onto nitrocellulose membranes and transferred at 110V, 0.37A at room temperature. For Western Blot analysis, blots were stained with CPTS and blocked with 5% BSA (in TBS). Alternatively, for phosphorylated and total protein analysis, blots were instead stained with Pro-Q Diamond Blot stains and SYPRO Ruby Protein Blot stain (Molecular Probes), respectively.

Antibodies against acetyl-lysine were purchased from Cell-Signaling Technology, mouse mAB 9681. Antibodies against pS187, pS173, pT146 were used at a dilution of 1 in 5000 (5% BSA, TBST). Secondary antibodies were used at a concentration of 1 in 12,000 (1% BSA, TBST) and were either Alexa Fluor 680 goat anti-rabbit IgG (Invitrogen) or Alexa Fluor 750 goat anti-mouse 750 IgG (Invitrogen).

For AUT gels, precipitated proteins were redissolved in acid-urea sample buffer (100mM Tris-acetate, pH 8.8, 20% glycerol, 8M Urea, 5% β-mercaptoethanol, 2% Thiodiglycol, 1% cysteamine HCl, and Pyronin Y) and electrophoresed in acetic acid-urea-Triton X-100 (AUT) gels as described (Panyim & Chalkley,

1969b; Yoshida et al, 1990). Gels were run at 4°C, for 3hrs with 0.1N Acetic acid as the running buffer. Note that the polarity of the electrodes was reversed for AUT gels. Gels were then stained with Coomassie Brilliant blue.

2.4 - Nucleosome reconstitution

Nucleosomes were reconstituted using the Epimark Nucleosome assembly kit (NEB) with some minor modifications (Steger & Workman, 1999). 50pmol of nucleosomes were incubated with 50pmol of DNA (208bp of containing the *Lytechinus variegatus* 5SrDNA) at 2M NaCl, 1µg BSA in a final volume of 20µl at 37°C for 15min. The reaction mixture was serially diluted to 1.5, 1, 0.8, 0.7, 0.6, 0.5, 0.4, 0.25 and 0.2M NaCl using 50mM Hepes pH7.5, 1mM EDTA, 5mM DTT, complete Protease inhibitors (Roche) for 30°C (15min for each dilution). One final dilution was carried out in Tris pH 7.5, 1mM EDTA, 0.1%NP-40, 5mM DTT, complete protease inhibitors, 20% glycerol and 100µg/ml BSA to bring the final salt concentration to 0.1M NaCl. Reconstitutions were analyzed by electrophoresis on 5% acrylamide nucleoprotein gels.

2.5 - Roscovitine treatment/Acid extraction of Histones

Pin1^{-/-} and wt cells were treated with Roscovitine (30µM) for the times indicated. Cold nuclei isolation buffer was added directly to cells, and incubated at 4°C for approximately 10 min. The cells were then washed, and spun at 3200xg to isolate the nuclei. Histones were extracted using 0.4N H₂SO₄ + Protease inhibitors, DTT, and PhoSTOP (1hr, 4°C). Extracts were then spun at 10,000g and the supernatant was then precipitated with -20°C acetone (overnight). The precipitated histones

were then resuspended in SDS loading buffer and separated on 15% Acrylamide gels. H1 was detected using pS173, pS187 and pT146 (Abcam, 1:250).

2.6 - Mobility shift assay for detecting phosphorylated H1

Pin1^{-/-} and Pin1^{wt} cells were transfected with either H1.1-FLAG or the appropriate H1.1^{mut} FLAG. The following day, histones were extracted using 0.4N H₂SO₄, as described above. Phostag ligands bind with strong affinity to phosphate molecules, and when cross-linked in an acrylamide gel, can provide specific mobility shifts based on the presence/absence of phosphorylation (Kinoshita et al, 2009). Phostag SDS-PAGE gels (100μM Phostag, 10% Acrylamide gels) were prepared as per manufacture's protocol. Gels were run at constant current (20mA). The gels were then washed extensively with transfer buffer+4mM EDTA to chelate the Mn²⁺, rinsed with water, and then washed with transfer buffer without EDTA. Proteins were then transferred to a nitrocellulose membrane (110V,0.37mA, 90 min) and then probed with anti-FLAG (M2, Sigma) at 1:50,000 dilution.

2.7 - Co-immunoprecipitation

Approximately 1x10⁶ cells were centrifuged at 1300Xg and resuspended in ice-cold Nuclei Isolation Buffer (250mM Sucrose, 150mM NaCl, 20mM Tris pH 8, 1.5mM MgCl₂, 0.2mM CaCl₂, 0.1% IGEPAL CA630), supplemented with PhosSTOP (Roche) and Complete protease inhibitor (Roche). These were then centrifuged at 3200xg, and the nuclei were resuspended in modified RIPA buffer (Tris pH 7.4, 1% NP-40, 150mM NaCl) along with PhosSTOP, protease inhibitors and an endonuclease, Benzonase (Novagen). After 4hrs, the reaction was stopped

by adding 1mM EDTA. After 30min incubation at 4°C, the extract was spun down at 13,000xg to remove aggregates. The extract was then treated with antibody pre-bound to Dynabeads (Invitrogen) overnight. For co-IP with T98G cells stably expressing GFP-H1.1, extracts were treated with 50µl GFP-TRAP (ChromoTEK). The antibody-beads mixture were then separated using a magnetic rack, washed three times, following which 3xSDS loading buffer was added directly to the beads. Samples were then run on a standard 15% or 18% acrylamide gel, transferred onto a nitrocellulose membrane. Pin1 (G-8) antibody (SantaCruz), was used at a dilution of 1:1000, anti-H1 (Novus) was used at 1:250 dilution, anti-GFP (Abcam, Ab290) was used at 1:10,000 dilution, anti-RNA Polymerase II (8WG16, Promega) was used at 1 in 1000 dilution. Secondary antibodies were conjugated with infrared specific dyes (Alexa Fluor 680, Alexa Fluor 750), and all blots were scanned on the Odyssey Infrared Imaging system (LICOR Biosciences).

2.8 - H1 phosphorylation/dephosphorylation assays

Approximately 1.5×10^7 cells were centrifuged at 1300xg for 4min at 4°C, resuspended in RIPA buffer, 1mM EDTA along with PhosTOP protease inhibitors and phosphatase inhibitors (the latter was excluded in dephosphorylation assays). The extract was spun at 14,000xg for 10 min at 4°C, the supernatant was treated with either anti-Cdk2 antibody (M2, Santa Cruz, sc-163, 2.4µg) or anti-PP2Ac (1D6, Millipore, 4µg) overnight at 4°C. Dynabeads were then added the next day for 2hrs at 4°C, following which the beads were separated magnetically, washed three times with fresh RIPA buffer, once with 40mM Tris 7.6, and then

resuspended either in phosphorylation buffer (40mM Tris 7.6, 2mM DTT, 10mM MgCl₂) or in dephosphorylation buffer (40mM Tris 7.6, 2mM DTT, 1.5mM MgCl₂). Purified calf-thymus H1 (Calbiochem, resuspended in water at a concentration of 1mg/ml, 3µg of H1/reaction) was added to the reaction mixture with or without ATP (8.5mM). The reaction mixture was then incubated at either 30°C (for kinase reaction) or 37°C (dephosphorylation) for the given time. Adding 3XSDS-loading buffer stopped the reaction and H1 was resolved on a denaturing 18% Acrylamide gel. Cy3/Cy5 labeled H1 was phosphorylated in a similar manner, except, the reaction was allowed to progress for 90min, following which the reaction was stopped with the addition of EDTA. To verify phosphorylation, labeled H1 were resolved on a denaturing 18% acrylamide gel, transferred to nitrocellulose and stained with ProQ Diamond Phosphoprotein Blot Stain (Molecular Probes) to detect phosphorylated H1 molecules or SyproRuby Protein blot stain to detect total H1 protein. The blots were visualized using 302nm UV light.

Live Cell Imaging

2.9 - Volumetric measurements of lac arrays

Cells expressing either mcherry LacR or mcherry-ER-tTA were plated on a live cell imaging dishes and were then imaged using a Zeiss 710 LSM 63x Plan-Apochromatic 1.4 Oil DIC M27 objective with an objective warmer maintained at 37°C. A Piezo stage (Piezostem Jena, Zeiss) was used allowing rapid acquisition of z-stacks at a rate of 50 images (9.8µm in z-direction)/ 9 seconds (total

acquisition time), with a pixel dwell time of 0.79 μ s and pinhole set at 48 μ m. A 561nm laser operating at 1-2% laser output was used to excite the mcherry signal. The images were then analyzed on Imarisx64 7.3.0 Surface rendering algorithm. The images were thresholded based on 30% of the maximum absolute intensity recorded (approximately equal to one standard deviation), and the volume of the surface generated was then recorded.

2.10 - Fluorescence recovery after photo-bleaching

Mouse Embryonic fibroblasts were cultured on number 1.5 glass coverslips in tissue culture media. They were then transfected with individual H1 variant constructs (Th'ng et al, 2005) using Effectene (Qiagen) transfection reagent (as per manufacturers protocol). Approximately 24 hours after transfection, the binding affinity of histone H1 molecules were analyzed by FRAP. The coverslips were placed on a glass slide with a small well made of vacuum grease designed to hold the media in. The coverslip was placed on top of this well and sealed by applying gentle pressure. Alternatively, glass-bottom culture dishes (MatTek) may also be used for growing and transfecting the cells. These dishes can be directly placed on the heated stage. FRAP was carried out using a Laser-scanning confocal microscope (LSM510 NLO Carl Zeiss) using a 488nm laser operating at 100% for bleaching (30 iterations) and 0.5% for acquiring images. Pixel dwell time was maintained at 1.26 μ s. A 40x 1.3 oil objective lens equipped with a heated stage and objective warmer maintained at 37°C was utilized. For global H1 analysis, a rectangular region (1.5 micrometer in length) was photobleached, encompassing both euchromatin and heterochromatin regions of the nucleus and

recovery was monitored at regular time intervals (Carrero et al, 2004b). Only the cells that expressed GFP-H1 at low concentrations were analyzed to avoid complications with H1 over-expression. For heterochromatin vs. euchromatin H1 analysis, cells were pre-treated with Hoechst 33342 (200 ng/ml) for ½ hour and then replaced with fresh growth media. Hoechst itself did not have a statistically significant effect on H1 binding. Regions that stained intensely were the heterochromatin regions, while the remaining was classified as euchromatin. Two 1-micrometer diameter spots were simultaneously photo-bleached in heterochromatin and euchromatin regions, respectively. Images were corrected for cell movement and rotation using ImageJ software complemented with a specific algorithm plug-in (StackReg (Thevenaz et al, 1998)). Intensity measurements were done with Metamorph software. Statistical tests for t_{50}/t_{90} and plotting of the FRAP curves were performed using GraphPad Prism version 5.00 for Windows, GraphPad Software, San Diego California USA.

For H1 FRAP at sites of transcription, cells were co-transfected with GFP H1 and mcherry-ER-tTA or mcherry-LacR. Following the addition of Tamoxifen, the mcherry signal was used as a guide to locate the arrays. This was used as a mark to photobleach a spot (0.07 μ m in diameter) that corresponded to the arrays. Another non-array spot was simultaneously photobleached, and served as an internal control. The recovery of both the photobleached spots was monitored at regular time intervals.

2.11 - Kinetic modeling of H1 dynamics *in vivo*

A mathematical model was developed based on our previous studies (Carrero et al, 2004a; Carrero et al, 2004b), and the solution of the reaction-diffusion equation was fitted to those obtained from experimental FRAP data, allowing the estimation of multiple kinetic properties from a typical FRAP curve. The equations assume that histone H1 moves randomly throughout the nucleus and undergoes a reversible binding-unbinding interaction with chromatin. This analysis allowed an estimation of effective diffusion, binding and unbinding rates, and binding affinity. We also measured the proportion of the high affinity (HA) population and found an effective diffusion coefficient that accounts for a low affinity (LA) subpopulation and the freely diffusing subpopulation. To determine the values of these parameters, the raw data from the FRAP experiment (.txt files) are imported into the MATLAB FRAP interface. They are then normalized, using the built-in normalization protocol. The normalized data is then imported into the 'Reaction diffusion' interface, where variables such as the bleach width (1.5 μ m), iterations (500), and the correction factor are entered. The curve is adjusted manually at first to closely approximate the FRAP curve, following which the curve estimation is carried out which mathematically approximates the different parameters of the equation to their closest value. The numbers are manually tabulated for every FRAP experiment conducted. We then submitted the data to a two sample Kolmogorov-Smirnov test (KS-test) to determine if the set of estimated effective diffusion coefficients and binding affinities from the control groups differed significantly from those of the treatment groups. The reason for using non-parametric statistics for data analysis is the non-normal distribution

exhibited by the parameters distributions. Detailed mathematical equations, etc, can be found elsewhere (Carrero et al, 2004a; Carrero, 2009).

2.12 - Fluorescence resonance energy transfer (FRET)

FRET was carried out on H1Cy3Cy5 either in solution or when added to reconstituted nucleosomes that were placed on live cell imaging dishes (total volume of 150 μ l). A glass coverslip was placed on top to prevent evaporation. The sample was then imaged on a Zeiss 710 LSM equipped with a Plan-Apochromat 40x/1.3 Oil DIC M27 objective and a heat stage that was maintained at 37°C). The sample was excited with a 514nm or 633nm laser, both operating at 5% laser output. Emission spectra (5nm slit-width) were obtained using a 523-727nm filter when excited with 514nm and a 639-727nm filter when excited with the 633nm laser. Pixel dwell time was maintained at 2.55 μ s and pinhole was set at 600 μ m. FRET was calculated using the RatioA method (Clegg, 1992; Poirier et al, 2009), using peak heights and with extinction coefficient $\epsilon_A(630) = 150,000$ (Cy5), $\epsilon_A(514) = 5000$ (Cy5), $\epsilon_D(514) = 75,000$ (Cy3) and $d^+=1$. R_0 was set at 5.4nm (Fang et al, 2011)

2.13 - Transmission Electron Microscopy

Pin1^{-/-} and Pin1wt cells (a gift from Dr. Kun Ping Lu) were grown as adherent single layer cell cultures on MatTek 35 mm glass bottom dishes in DMEM medium supplemented with 10% FBS. Cells were washed first with 1xPBS and were fixed in 4% paraformaldehyde, prepared in 1xPBS and then washed three times (for 5min each) with 1xPBS. Cells were then postfixed with 2% glutaraldehyde (2hrs). The cells were then washed three times with 1xPBS (5min

each), following which they were stained with 1% Uranyl acetate for 30 min. Subsequently, the cells were dehydrated on a shaker with 20%, 40%, 60%, 80%, 90%, 98%, 100% ethanol diluted in ddH₂O (30min/step). The samples were then pre-embedded in Quetol 651® resin and 100% ethanol mixture 1:1 for 1hr, according to the manufacturer's protocol. Following which the sample was embedded in Quetol 651 for 1hr and then in Quetol Mix (see Buffer preparations). The embedded cells in Quetol mix, were then cured for 24h at 60°C. The cells were detached from the cover slip using multiple rounds of freezing and thawing in liquid nitrogen. Small blocks containing the cell-layer were cut out of the polymerized resin using a jewelry saw and glued with a drop of remaining resin onto a mounting block. Ultrathin sections of 100 nm thicknesses were cut at an ultramicrotome (Leica EM UC5). The floating sections were then picked up on a 300 mesh copper grid and after vaporizing a thin carbon layer onto the sections, the cells were imaged with a JEOL 2100 microscope operating at 200 kV. Pictures were taken using the 2k by 2k camera of a Gatan Tritium Energy filter at a magnification of 2000x – 5000x.

For image analysis, 2D images (600px X 600px, 1.171µm) were imported into MATLAB and Fourier transformations were carried out. Power spectra's, which are the square of the modulus of the Fourier transform, were rotationally averaged. The profiles were normalized by total intensity, averaged (n=36) and plotted against spatial frequency.

2.14 - Immunofluorescence

Cells were grown on Fisherbrand coverglass (18x18-1.5) overnight. Cells were fixed with 4% paraformaldehyde in 1XPBS for 10 min, permeabilized with 0.5% Triton X-100 for 5min. For pS173 H1 antibody, cells were fixed with 1% paraformaldehyde for 10 min. Coverslips were then washed with PBS, inverted onto 50-100 μ l of primary antibody in PBS, and incubated for at least 30 min. Coverslips were then washed with 0.1%Triton X-100 and then with PBS, prior to incubation with secondary antibody coupled with a flourophore. Cells were then mounted on slides using a 90% glycerol-PBS based medium containing 1mg of paraphenylenediamine/ml and 0.5 μ g DAPI/ml. Pin1 was detected using a monoclonal antibody (G-8, SantaCruz) at 1:500 dilution, pS173 antibodies were used at 1:400 dilution.

2.15 - Buffers and Recipes

Nuclei Isolation buffer (100 μ l)

250mM Sucrose (8.6g)

150mM NaCl (0.87g)

20mM Tris pH 8.0 (2ml of 1M Tris 8.0)

1.5ml MgCl₂ (150 μ l of 1M MgCl₂)

0.2ml CaCl₂ (20 μ l of 1M CaCl₂)

0.1% NP-40 or IGEPAL (100 μ L)

The solution was filter sterilized following preparation and kept at 4 $^{\circ}$ c

Radio Immuno-precipitation buffer (RIPA) 100ml

0.79g Tris, pH to 7.4

0.9g NaCl

1ml of IGEPAL

200µl 0.5M EDTA

AUT Separating Buffer (15%, 30ml)

15ml of Acrylamide 29:1

3.75ml 4% TEMED/ 43.1% Acetic acid

12g Urea

3ml Riboflavin in water (0.004%)

0.6ml 0.3M Triton-X 100 in PBS

0.3ml Thiodiglycol

The solution is heated with stirring until dissolved. It must be stored away from light at 4°C.

AUT Stacking Buffer (30ml)

7.5ml Acrylamide (29:1)

12g Urea

0.3ml TEMED

3ml Riboflavin (0.004%)

3.75ml 3M Potassium Acetate

0.6ml 0.3M Triton-X 100

0.3ml Thiodiglycol

The solution is heated with stirring until dissolved. It must be stored away from light at 4°C.

Phostag Separating buffer (10ml)

2.5ml 4xSeparating buffer (1.5M Tris, pH 8.7, 0.4% SDS)

2.5ml 40% Acrylamdie (29:1)

5ml ddH₂O

200µl Phostag (product is dissolved in 100µl methanol and 3.2ml H₂O)

200µl 10mM MnCl₂

10µl TEMED

100µl 10% Ammonium persulphate (APS)

Quetol Mix

3.5ml Quetol 651

5.4ml NSA (Nonenyl Succinic Anhydride)

1.1ml NMA (Methyl-5-Norbornene-2,3-Dicarboxylic anyhydride)

0.18ml DMP-30 (2,4,6-Tri(dimethylaminomethyl) phenol)

**Chapter III - Core histone hyperacetylation impacts cooperative behavior
and high affinity binding of histone H1 to chromatin***

*A version of this chapter has been published as Raghuram *et al.* 2010 Biochemistry, Volume 49, Pages 4420-4431. Reprinted (adapted) with permission from American Chemical Society. Copyright © 2010, American Chemical Society.

- All of the experiments, figures and the manuscript were prepared by Nikhil Raghuram.

3.1 - Abstract

Linker histones stabilize higher order chromatin structures and limit access to proteins involved in DNA-dependent processes. Core histone acetylation is thought to modulate H1 binding. In the current study, we employed kinetic modeling of H1 recovery curves obtained during fluorescence recovery after photobleaching (FRAP) experiments to determine the impact of core histone acetylation on the different variants of H1. Following brief treatments with histone deacetylase inhibitor, most variants showed no change in H1 dynamics. A change in mobility was detected only when longer treatments were used to induce high levels of histone acetylation. This hyperacetylation imparted marked changes in the dynamics of low-affinity H1 population, while conferring variant-specific changes in the mobility of H1 molecules that were strongly bound. Both the CTD and globular domain were responsible for this differential response to TSA. Furthermore, we found that neither the CTD nor the globular domain, by themselves, undergo a change in kinetics following hyperacetylation. This led us to conclude that hyperacetylation of core histones affects the cooperative nature of low-affinity H1 binding, with some variants undergoing a predicted decrease by almost two orders of magnitude.

3.2 - Introduction

Histone H1 or “linker histones” are of paramount importance in the formation and stabilization of higher order chromatin structure (Ramakrishnan, 1997; Thoma, 1979; van Holde & Zlatanova, 1996; Widom, 1998; Zlatanova & van Holde, 1996). There are at least six variants of histone H1 in mammalian somatic cells (H1.0, H1.1, H1.2, H1.3, H1.4 and H1.5) (D'Incalci et al, 1986; Kinkade & Cole, 1966; Lennox & Cohen, 1983). They differ in their amino acid sequences, molecular weights, turnover rates (Pehrson & Cole, 1982), timing and pattern of expression (Higurashi et al, 1987; Khochbin & Wolffe, 1994), and efficiency of condensing DNA (Khadake & Rao, 1995; Liao & Cole, 1981a; Liao & Cole, 1981b; Nagaraja et al, 1995). The latter could be attributed to small but significant differences in the amino acid sequences of the C-terminal domain, which affects the DNA binding properties of each variant (Th'ng et al, 2005).

Positioned at the entry and exit points of DNA in the nucleosome, their highly basic C-termini interact with linker DNA to promote folding of the nucleosomal chain into highly organized chromatin fibers. Histone H1-containing nucleosomes constrain two left-handed superhelical turns comprising of 168 bp of DNA (Kornberg & Lorch, 1999). A strong association of histone H1 with the nucleosome is thought to keep the DNA wrapped sufficiently tight to limit its accessibility to transcription factors and other nuclear proteins. This limited accessibility has implications on transcription, replication, recombination and DNA repair (Strahl & Allis, 2000).

Transcriptional activation is associated with changes to chromatin structure (Wolffe & Hayes, 1999; Wolffe & Kurumizaka, 1998; Wu, 1997). Since histone H1 compacts DNA leading to limited nuclear dynamics, histone H1 was attributed the function of a global repressor of transcription (Laybourn & Kadonaga, 1991; Schlissel & Brown, 1984; Thomas, 1999; Zlatanova & Van Holde, 1992). This assertion was countered by studies demonstrating that the influence of H1 on transcription is contingent upon the gene and may not always be repressive (Crane-Robinson, 1999; Folco et al, 2003; Koop et al, 2003; Shen & Gorovsky, 1996; Takami et al, 2000; Thomas, 1999; Wolffe et al, 1997).

A more recent study showed that a two-fold reduction in H1 levels in embryonic stem cells led to an at least two-fold change in gene expression in only a few genes, although this impaired differentiation and resulted in death of mutant embryos in mid-gestation (Fan et al, 2003; Fan et al, 2005). Selective repression of genes has also been reported in histone H1 knockout mice (Fan et al, 2003; Fan et al, 2005). Linker histones have also been implicated in the precise positioning of nucleosomes (Koop et al, 2003), which may explain the selectivity of histone H1 in the regulation of specific genes.

The posttranslational modifications of histones by lysine acetylation is thought to reduce the binding of the histone H1 proteins to the nucleosome (Perry & Annunziato, 1989; Perry & Annunziato, 1991), leading to a more accessible chromatin structure (Hebbes et al, 1994a; Struhl, 1998). Genes in a transcription-competent state are characterized by increased core histone acetylation (Hebbes et al, 1988b; Loidl, 1988; Reeves, 1984; Vidali et al, 1988), whereas

hypoacetylation is associated with gene silencing. Displacement of histone H1 by core histone acetylation not only alters chromatin condensation, but may also regulate the activity of transcription factors and enzymes involved in DNA repair and recombination (Roth et al, 2001; Wolffe & Hayes, 1999).

A steady state of histone acetylation is maintained by the antagonistic effects of two enzymes – histone acetyltransferases (HATs) (Roth et al, 2001) and histone deacetylases (HDACs) (Taunton et al, 1996a). Core histone acetylation occurs primarily at multiple highly conserved lysine residues, and occurs in a site-specific manner (reviewed in (Shahbazian & Grunstein, 2007)). Hyperacetylation of core histones prevents chromatin from folding into the 30nm fiber and reduces the ability of chromatin to self-assemble into higher-order structures (Annunziato et al, 1988; Tse et al, 1998). Recent work that substituted glutamine to mimic acetyl-lysine residues on core histones, suggested that acetylation of H2B and H4 caused the greatest hindrance to nucleosomal self-association (Wang & Hayes, 2008), switching between a relatively open state of chromatin and a closed one by reducing nucleosomal interactions and occluding the interactions between linker DNA and core histone tails (Shahbazian & Grunstein, 2007). Acetylation of a single residue, lysine 16 of histone H4, could inhibit the formation of the 30nm in nucleosomal arrays in vitro (Shogren-Knaak et al, 2006), although the role that linker histones play in regulating this switch is not clear (Robinson & Rhodes, 2006).

We have previously used FRAP to establish the importance of the C-terminal domain of histone H1 in binding to chromatin (Hendzel et al, 2004). In addition,

we have shown that the individual histone H1 subtypes vary considerably in their chromatin binding affinity (Th'ng et al, 2005) (reviewed in (Raghuram et al, 2009)). Mathematical modeling of FRAP recovery curves suggests that there are at least three different sub-populations of histone H1 in vivo, characterized as molecules bound with high affinity (which we will now term as HA sites), low-affinity (LA) and freely-diffusing H1 molecules (Carrero et al, 2004a). In our current study, we have analyzed the influence of inhibition of HDACs by TSA on the mobility of N-terminal GFP-tagged constructs of all major somatic variants of H1 (H1.0-H1.5) as measured by FRAP. Contrary to previously published studies (Misteli et al, 2000), we find that treatment with TSA for short durations (1-2 hrs) does not lead to significant change in H1 dynamics. The hyperacetylation of the core histones induced by lengthy (18 hrs) treatment with TSA induces a marked change in the binding of LA H1 molecules. Individual binding domains of H1 (CTD and globular domain), however, do not change their kinetics upon hyperacetylation. This leads us to conclude that hyperacetylation acts by decreasing the cooperativity with which H1 binds chromatin, thereby pushing the vast population of H1 molecules into a state that maintains a much less stable association with chromatin.

3.3 - Results

3.3.1 - Comparison of binding affinities among different H1 variants.

Mathematical modeling revealed that histone H1 was not a single kinetic population. Rather, we obtained evidence for a HA binding population and a second, larger population, with an effective diffusion coefficient that was several

orders of magnitude too slow to be a diffusing molecule (Carrero et al, 2004a; Carrero et al, 2004b). Because most histone H1 is visually associated with chromatin, we can conclude that this effective diffusion coefficient actually reflects a separate bound population, which we will refer to as LA. For simplification, the time required for fifty percent recovery (t_{50}) is used as a surrogate marker for this population, which is the predominant form of histone H1 for every variant examined. We use a second measure, the time to 90% recovery, as a surrogate measure for changes in the smaller HA population. The use of these surrogate markers is based on mathematical modeling revealing that there are two distinct kinetic populations of the protein.

In order to characterize the changes in H1 dynamics in response to core histone acetylation, we studied the kinetics of H1 in cells with a basal level of core histone acetylation (control cells) compared with those containing hyperacetylated core histones. Previously, we showed that using SK-N-SH neuroblastoma cells, H1.1 and H1.2 had the weakest binding to chromatin whereas H1.4 and H1.5 bound strongly (Th'ng et al, 2005). Here, using 10T1/2 mouse embryonic fibroblast cells, we confirm a similar distribution (control cells in Figure 3.1). Based on the recovery profile of H1 variants in these cells, H1.2 had high rates of recovery, low t_{50} (21 ± 4 seconds) and t_{90} values (170 ± 40 seconds). H1.0, H1.4 and H1.5 behaved similarly and exhibited slow recovery kinetics, with a t_{50} of 62 ± 18 s, 76 ± 24 s and 74 ± 18 s, and t_{90} of 637 ± 156 s, 667 ± 168 s and 638 ± 165 s, respectively. H1.1 and H1.3 had properties that reside between these two extremes. The t_{50}

values in H1.1 and H1.3 were 40 ± 9 s and 36 ± 11 s respectively while the t_{90} values were 382 ± 117 seconds in H1.1 to 292 ± 105 s in H1.3.

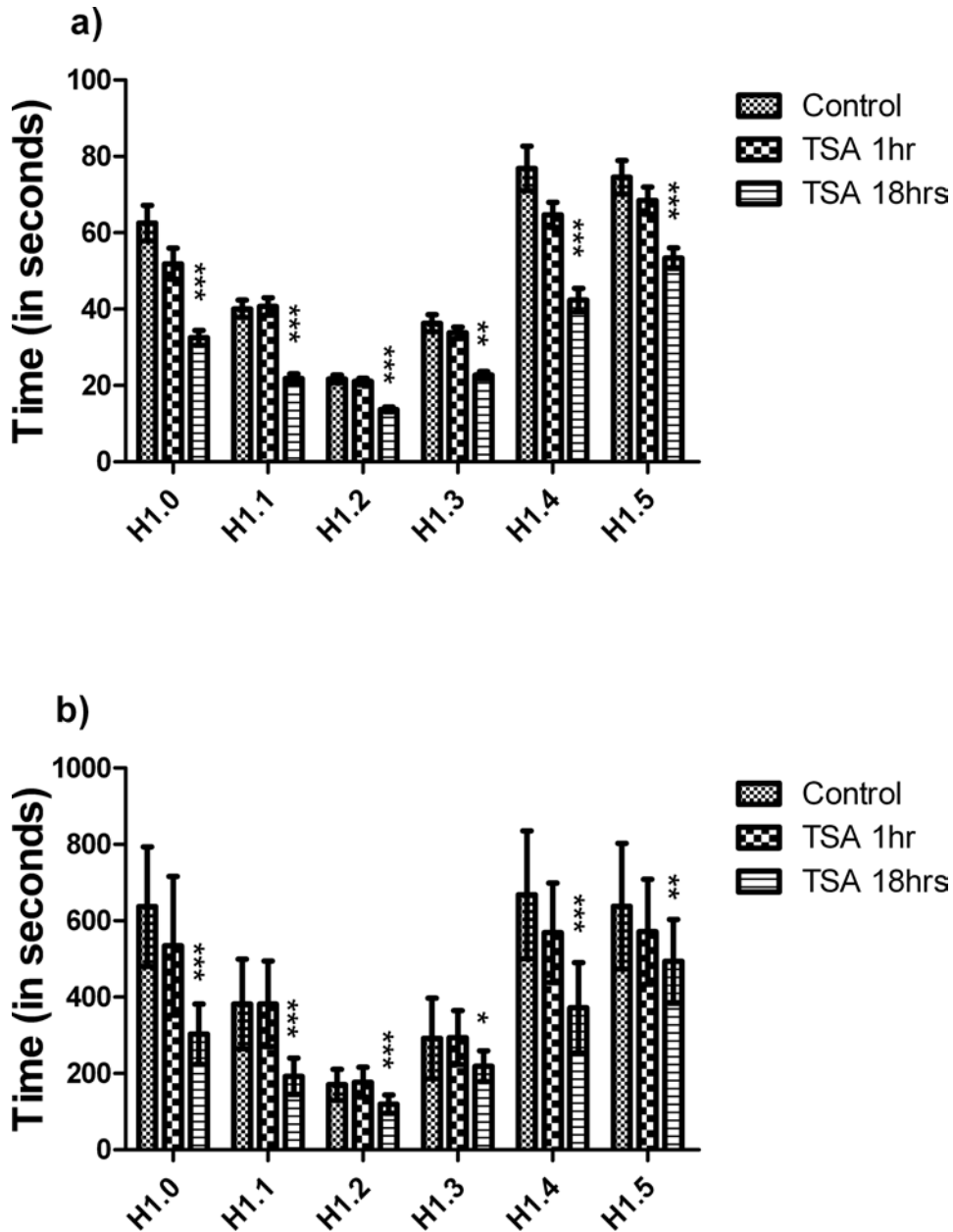


Figure 3.1 - Comparison of t_{50} (a) and t_{90} (b) values of the six H1 variants before and after treatment with HDAC inhibitor, TSA. Based on the relatively high t_{50} and t_{90} values, we can group H1.0, H1.4 and H1.5 as a high-affinity H1 group, whereas H1.1 and H1.3 constitute a mid/medium-affinity group. H1.2 constitutes the low-affinity H1 group. Major changes in t_{50} and t_{90} values were found only after 18hrs of treatment with TSA. Each bar represents an average (\pm SEM) from 15 different FRAP experiments. Significance between control vs. TSA (1hr or 18hrs) was analyzed using unpaired t-test (95% confidence interval). [Notation for significance (***) $p < 0.001$, (**), $0.001 < p < 0.01$, (*) $0.01 < p < 0.05$].

3.3.2 - Changes in histone phosphorylation and acetylation post TSA treatment

To gain insight into the molecular dynamics of histone H1 in response to TSA treatment, we examined the acetylation and phosphorylation status of the core histones and H1 following such treatment. Mouse embryonic fibroblasts were treated with 100ng/ml of TSA for 0.5hrs, 1hr or 18hrs. Cells were then harvested and the isolated histones were analyzed using acetic acid-urea-Triton X100 (AUT) gel electrophoresis (Supplementary Figure 3.1a, 3.1b). Some increase in histone acetylation was detectable within the first half hour of TSA treatment, as indicated by the relative increase of mono-acetylated H4 and the corresponding decrease in unacetylated H4. After one-hour treatment with TSA, there is an increase in mono-, di- and a small amount tri-acetylated H4 species. After 18-hrs of TSA treatment, mono-, di-, tri- and tetra-acetylated H4 species were abundant. Treatment of TSA for 48 hours did not lead to a further appreciable increase in H4 acetylation. Immunoblotting analysis using an antibody directed against acetyl-lysine was carried out to further characterize the changes in acetylation in core histones (Supplementary Figure 3.1c, 3.1d). TSA treatment for 0.5 hrs increased overall acetylation levels in core histones by 1.4 fold, and a further increase to 2-fold (over control cells) was observed following 1hr treatment with TSA. After 18hrs, there was a 7-fold increase in core histone acetylation over the untreated control cells. The antibody was unable to detect acetyl-lysine residues on histone H1 in either control or hyperacetylated cells. TSA exerts cellular effects other than inhibition of HDAC, including an inhibition of proliferation through the induction of p21 WAF1/Cip1 (Kim et al, 1999),

which inhibits the histone H1 kinase cdk2. This additional activity complicates the study on the impact on histone H1 binding, since phosphorylation of H1 has been shown to destabilize H1 binding and its inhibition would be expected to increase the binding affinity of histone H1. These secondary effects, which are characterized by induction of genes susceptible to changes in histone acetylation status, would be observed only after prolonged treatment with TSA (greater than 6hrs). Consistent with that expectation, changes to the phosphorylation of H1 or that of core histone phosphorylation status were not observed with brief treatments with TSA. With prolonged treatment of 18hrs, we found the levels of core histone phosphorylation to be similar to those observed in control cells. The level of H1 phosphorylation, however, was lower after 18 hours of TSA treatment as compared to control cells (Supplementary Figure 3.2 a, b). Notably, the expression of H1.0 is also upregulated in these cells. Phosphorylated histones from the ras-transformed Ciras-3 mouse cells were included as a positive control, where phosphorylation is observed on histone H1, H2A and H3.

3.3.3 - Analysis of histone H1 dynamics post induction of core histone acetylation (TSA 1hr).

Based on the above results, the most significant change in chromatin that we observe upon TSA treatment (1hr) is an upregulation of global histone acetylation levels. We proceeded to test the impact of TSA treatment on histone H1 binding using FRAP. MEFs were incubated with TSA for one hour and were then subject to FRAP experiments. The results show that a brief treatment with histone deacetylase inhibitors does not lead to any significant increase or decrease in

histone H1 binding. All variants fail to show a change that reaches statistical significance (Figure 3.1 & 3.2).

While t_{50} and t_{90} can provide some information on the changes in LA and HA binding sites, they are not as informative as extracted kinetic information obtained from mathematical modeling. Using the latter approach, we are able to obtain information on changes in pool sizes, the amount of time H1 molecules spend bound to the chromatin (residence time/Res.T), the amount of time spent in the weakly bound and freely diffusing states before engaging in a high affinity binding event (transition time/T trans). Changes in the effective diffusion coefficient provide a measure of binding to LA sites (Carrero et al, 2004a; Carrero et al, 2003). Specifically, increased effective diffusion rates require that the binding to LA sites be reduced in duration and/or that there be fewer LA sites available for binding, resulting in an increased freely diffusing pool.

Consistent with the trend seen in t_{50} and t_{90} values, no change in any kinetic parameter proved to be statistically significant following treatment with TSA for 1hr (Table 3.1).

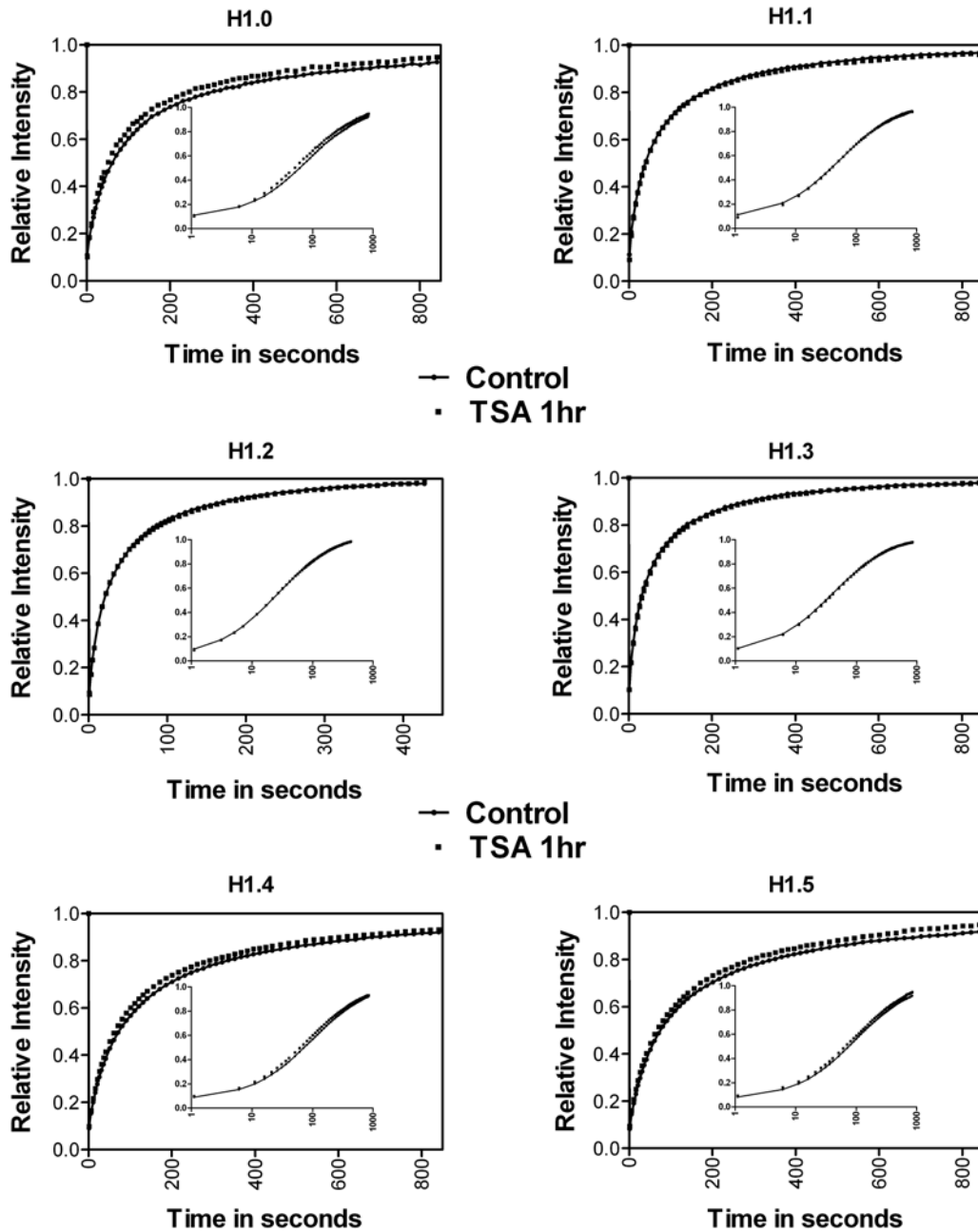


Figure 3.2 - FRAP recovery profiles post induction of core histone acetylation (TSA treatment for 1hr). Each FRAP recovery curve shown here is an average from 15 different FRAP experiments, repeated over three times. The plots show the relative intensity versus time (in seconds) for each of the six H1 subtypes. The inset re-plots the recovery profiles as the relative intensity versus the log of time. This better illustrates the recovery at earlier time points (1-100 seconds). Note that in most variants there is no change in recovery profiles following 1hr TSA treatment.

H1 Variant		Control				TSA 1hr				TSA 18hrs			
		Deff (μ^2/s)	B%	Res. (s)	T T trans. (s)	Deff (μ^2/s)	B%	Res. (s)	T T trans. (s)	Deff (μ^2/s)	B%	Res. (s)	T T trans. (s)
H1.0	<i>median</i>	0.008	20	624	2498.5	0.009	20	606	2043	0.013	16	346	2189
	<i>p-value</i>					0.65	0.86	0.59	0.54	0.004	0.54	0.01	0.34
H1.1	<i>median</i>	0.01	19	349	1406.5	0.009	18	439	2376	0.02	18	149	659.8
	<i>p-value</i>					0.35	0.10	0.35	0.35	0.001	0.51	0.01	0.05
H1.2	<i>median</i>	0.016	18	157	787.35	0.017	16	179	1070	0.024	13	141	980.8
	<i>p-value</i>					0.46	0.84	0.46	0.12	0.001	0.03	0.19	0.19
H1.3	<i>median</i>	0.01	18	330	1422.5	0.011	16	312	1559	0.017	18	219	956.3
	<i>p-value</i>					0.28	0.23	0.72	0.95	0.001	0.62	0.03	0.10
H1.4	<i>median</i>	0.005	19	716	2967.3	0.006	19	661	3278	0.009	19	392	1875
	<i>p-value</i>					0.14	0.71	0.93	0.94	0.001	0.48	0.04	0.24
H1.5	<i>median</i>	0.005	17	667	3170.7	0.006	21	518	1549	0.008	22	502	1919
	<i>p-value</i>					0.18	0.16	0.13	0.12	0.01	0.27	0.10	0.04

Table 3. 1 – Detailed kinetic modeling data. Kinetic parameters were obtained after modeling each FRAP curve based on the model described in Carrero, et al. Effective diffusion coefficient is associated with the freely-diffusing, low-affinity population, while residence time is an indicator of the affinity of the strongly bound population. The level of significance was determined by a two-sample Kolmogorov-Smirnov tests.

3.3.4 - Histone H1 dynamics with hyperacetylated core histones

To investigate the effects of core histone hyperacetylation on H1 mobility, we performed FRAP analysis after treating cells with TSA for 18 hours (overnight incubation) (Figure 3.3).

H1.1 and H1.2 revealed a statistically significant decrease in t_{50} and t_{90} values ($p < 0.001$) (Figure 3.1). This suggests that both the loosely bound sub-population, which predominates in the t_{50} measurement, and the strongly bound sub-population, reflected in the t_{90} measurement, were altered by core histone hyperacetylation. Both subtypes share a similar FRAP recovery profile-- the two curves (control and TSA 18hrs) converged at later time points. Histone H1.3 showed modest changes in mobility following core histone hyperacetylation. The t_{50} and t_{90} revealed a statistically significant decreases, although the drop in t_{90} was not as dramatic as seen in other variants. The strongly binding H1 variants, H1.0, H1.4 and H1.5, were also affected by the 18-hour TSA treatment. There were statistically significant ($p < 0.001$) drops in the t_{50} values in all the three variants, suggesting that the loosely bound sub-population increases its mobility upon TSA treatment. H1.0, H1.4 and H1.5 show a concomitant statistically significant drop in t_{90} values as well ($p < 0.001$ in H1.0 and H1.4 and $p = 0.003$ in H1.5). Interestingly, there is less apparent convergence in the recovery curves from control and TSA-treated cells for these more tightly binding histone H1 subtypes.

We then proceeded to mathematically model the FRAP curves enabling us to better understand the changes in kinetic behavior of H1 molecules post induction of core histone hyperacetylation. The hyperacetylation observed after an 18-hour

treatment with TSA led to significant changes in the kinetic parameters, although the changes were not uniform amongst all variants (detailed information can be found in Table I). The results of kinetic modeling show that there are significant increases in effective diffusion coefficient in all the variants analyzed (a p-value of less than 0.001 in H1.1, H1.2, H1.3 and H1.4, 0.004 in H1.0 and 0.01 in H1.5).

The changes to the HA population were variant dependent. With the exception of histone H1.2, there was no statistically significant change in the proportion of H1 at HA sites after 18hrs of TSA treatment ($p=0.03$). Although the proportion did not change in most variants, the residence time dropped significantly in H1.0, H1.1, H1.3 and H1.4 (1.5-2 fold decrease compared to control cells). A decrease in residence time indicates a decrease in affinity to the HA sites, and is inversely proportional to the dissociation rate of HA molecules to the freely diffusing/LA states.

Another similar time-dependent parameter obtained is the time H1 molecules spend cycling back and forth between the freely diffusing population and LA state before converting to a HA stably bound H1 population. This is known as the transition time, and the higher the transition time, the lower the association rate of HA H1 molecules. The only H1 variants in which a change in this parameter was observed were H1.1 and H1.5 ($p=0.049$ in H1.1 and $p=0.044$ in H1.5).

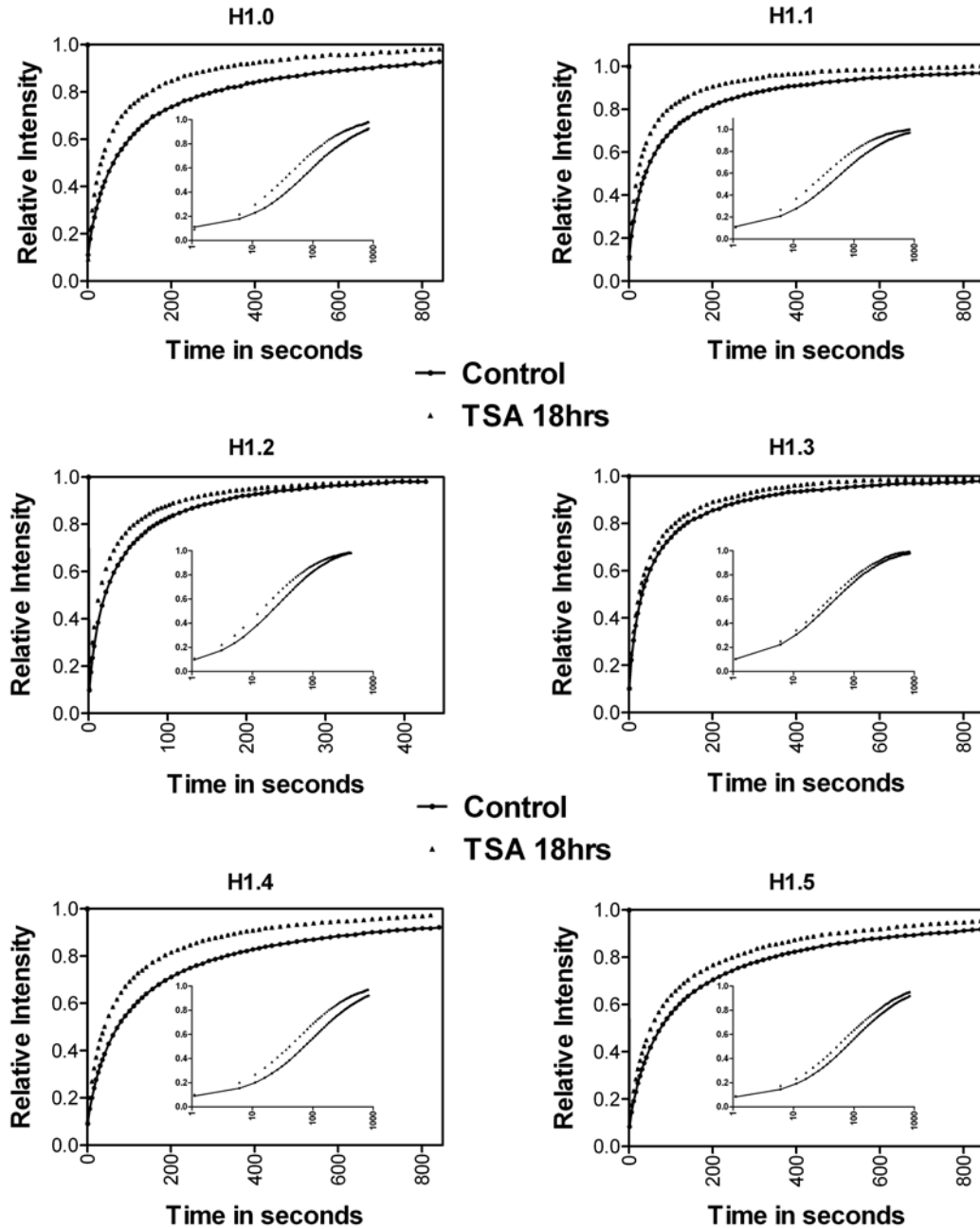


Figure 3.3 - FRAP recovery profiles post induction of core histone hyperacetylation (TSA treatment for 18 hrs). Each FRAP recovery curve shown here is an average from 15 different FRAP experiments, repeated over three times. The plots show the relative intensity versus time (in seconds) for each of the six H1 subtypes. The inset re-plots the recovery profiles as the relative intensity versus the log of time. Note that in most variants, there is a marked change in recovery following core histone hyper-acetylation. This is most prominently seen in H1.0, H1.1, H1.4 and H1.5.

3.3.5 - Heterochromatin vs. Euchromatin

Several studies have shown that specific H1 variants have preferential localization within the nucleus, some showing greater enrichment in euchromatin, while others in heterochromatin (Parseghian & Hamkalo, 2001; Th'ng et al, 2005). Using GFP tagged H1 variants and Hoechst staining, we had previously shown that in MEFs, H1.0, H1.1, H1.2 and H1.3 had a preferential enrichment in euchromatin, while H1.4 and H1.5 showed greater enrichment in heterochromatin (Th'ng et al, 2005). A similar pattern was found in human fetal fibroblasts using immuno-precipitation experiments (Parseghian et al, 2000).

To quantify the changes in recovery patterns in these sub-domains upon treatment with TSA, we photo-bleached a spot of 1 μ m in diameter, specifically targeted to regions that were densely stained with Hoechst (heterochromatin) and those that weren't (euchromatin). The mouse embryonic fibroblasts show visually distinct heterochromatin and euchromatin regions (Th'ng et al, 2005). Hoechst did not affect the binding of H1 at the concentrations used in this study (Supplementary Figure. 3.3).

a. Control cells. Statistically significant differences in t_{50} were found between heterochromatin and euchromatin enriched pools for each variant, with the euchromatin enriched H1 molecules recovering much faster (lower t_{50}) than those enriched in heterochromatin (Figure 3.4a). Similar changes were observed in t_{90} values, although the change in mobility between heterochromatin and euchromatin is most distinct in H1.3, H1.4 and H1.5 (Figure 3.4b). The significant changes seen in the t_{50} value for all variants suggests that the major contributor to

the kinetic disparities between heterochromatin and euchromatin enriched H1 molecules stems from the low-affinity sub-population of linker histones. Only histones H1.3, H1.4, and H1.5 showed a statistically significant difference in the t_{90} value, suggesting a physical difference in the HA sites for these histones in euchromatin versus heterochromatin.

b. *Induction of hyperacetylation.* To analyze the effect of core histone acetylation and hyper-acetylation on the binding of H1 population between the euchromatin and heterochromatin, we treated MEF cells with TSA for 1hr and 18hrs, respectively, and then specifically measured the recovery rates in the euchromatin and heterochromatin regions. Similar to the results in Figure 3.1, the 1hr TSA treatment did not cause any statistically significant changes in t_{50} or t_{90} values for all the variants (Figures 3.4c-f, FRAP curves are shown in Supplementary Figures 3.4-7). However, the values were reduced in a manner that is consistent with the trend previously observed after 18 hours of treatment.

Following treatment with TSA for 18hrs, statistically significant decreases in t_{50} in the euchromatin pool were observed for all of the H1 variants (Figures 3.4c and 3.4d). When the time was represented in the log scale, significant changes seen in the low-affinity H1 population were obvious (Supplementary Figure 3.4). In heterochromatin-enriched pools of H1, however, there were also differences in the FRAP recovery profiles. A statistically significant decrease in t_{50} was observed for all of the variants, except for H1.2 (Figures 3.4e and 3.4f). The decline, however, was not as prominent as that observed in euchromatin. The t_{90} measurements showed that not all variants responded to the 18-hr TSA

treatment according to their affinities. The t_{90} values of the low-affinity H1.2 and high-affinity H1.4 were not affected by the TSA. The absence of an effect in the H1.2 was also observed in the t_{50} measurements, but the heterochromatin-enriched H1.4 showed an initial decline in t_{50} values. Similar to H1.0, the other heterochromatin-enriched variant, H1.5, showed a steep decline in t_{90} value. H1.0, H1.1 and H1.5 display a trend that is very similar to the population enriched in euchromatin.

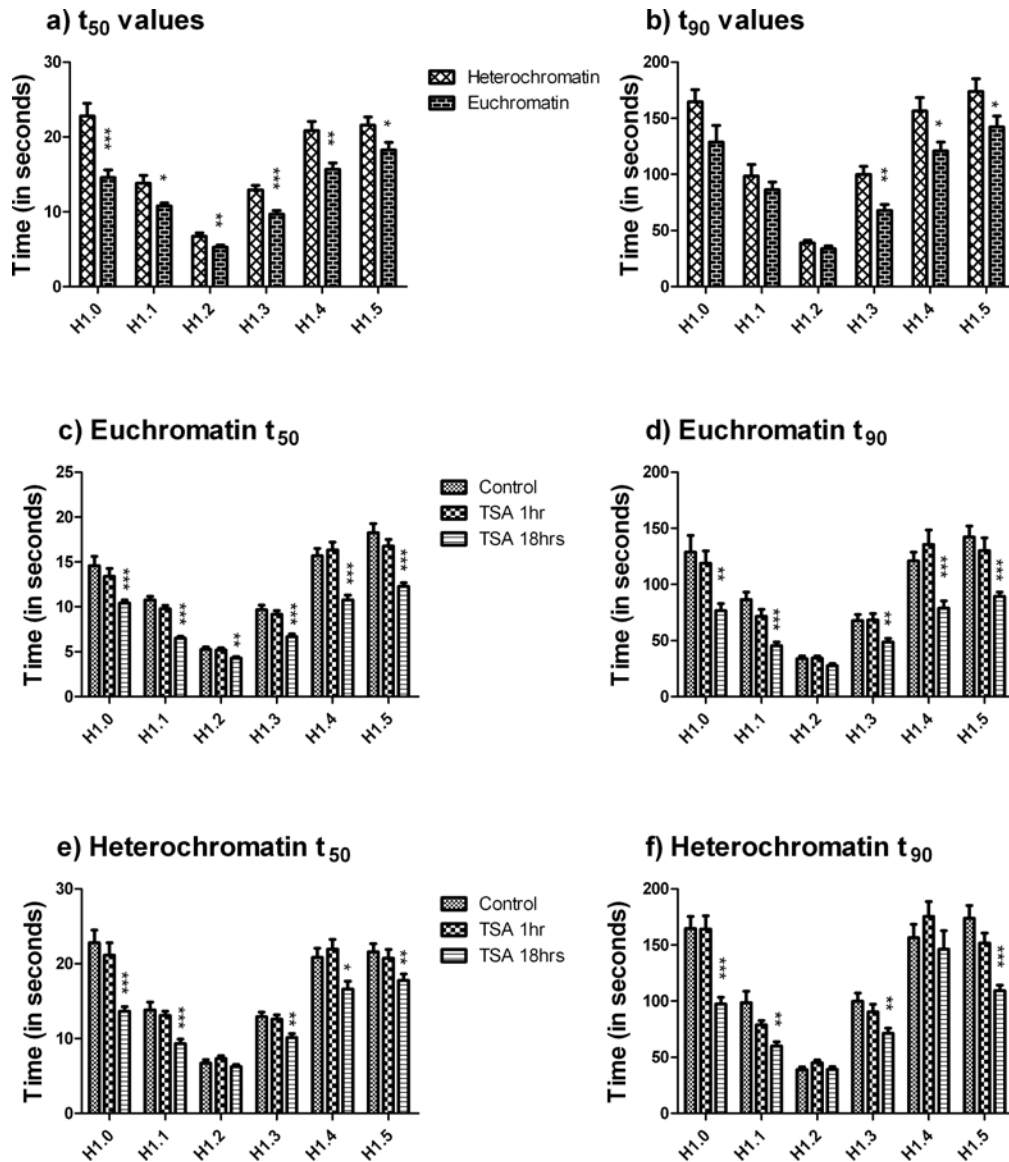


Figure 3.4 - Comparison of t_{50} and t_{90} values between heterochromatin and euchromatin enriched H1 variants. a) the t_{50} values obtained from the FRAP recovery profiles of the different variants following a spot-bleach that specifically targeted either euchromatin or heterochromatin regions (ascertained via staining with Hoechst 33342). b) the t_{90} values from the same. c) and d) the t_{50} and t_{90} values following spot-bleach in euchromatin regions, respectively, after 1-hr and 18hrs TSA treatment. e) and f) the t_{50} and t_{90} values following spot-bleach in heterochromatin regions of the nucleus, after 1-hr and 18-hrs TSA treatment. Each bar represents an average (\pm SEM) from 15 different FRAP experiments. Significance between control vs. TSA (1hr or 18hrs) was analyzed using unpaired t-test (95% confidence interval). [(***) $p < 0.001$, (**) $0.001 < p < 0.01$, (*) $0.01 < p < 0.05$].

3.3.6 - H1 hybrids and their response to hyperacetylation

Both the globular domain and the CTD have an impact on H1 binding, with the CTD being the primary determinant for HA binding (Brown et al, 2006; Hendzel et al, 2004). In order to understand which domain of H1 played a role in influencing the behavior of H1 variants towards core histone hyperacetylation, we constructed H1 hybrids, which have the CTD and globular domain swapped between different variants (Th'ng et al, 2005). For example H1.1-1.4, has the globular domain of H1.1 and the CTD of H1.4. Should the CTD be the primary determinant that influences the changes seen upon core histone hyper acetylation, then all hybrids that harbor the same CTD should give a similar kinetic response. Since the globular domain is identical in H1.1-H1.5, the only other difference between the variants is restricted to the short amino-terminal domain (NTD). Differences between the behavior of the CTD in the native histone versus the hybrid, then, would imply a role for the NTD in the acetylation response.

In all of the H1 hybrids analyzed (H1.1-1.4, H1.4-1.1, H1.5-1.1, H1.1-1.5), we observed a decrease in t_{50} and t_{90} values, consistent with those observed for their “parent” molecules (Figure 3.5). There was a consistent decrease in effective diffusion coefficient, upon core histone hyperacetylation in all the hybrids. Hybrids H1.4-1.1 and H1.5-1.1, which share the same CTD of H1.1, also share a similar kinetic response seen in native H1.1, with a decrease in residence time and a stable proportion of strongly bound molecules being maintained. The change in the HA kinetic parameters, however, cannot be entirely explained by the sequence of the CTD. Hybrid H1.1-1.4, which shares the CTD of H1.4, did maintain a

stable pool of strongly bound molecules. However, the rapid fall of residence time seen in native H1.4 upon core histone hyperacetylation is not seen in hybrid H1.1-1.4. In H1.5, where no change in residence time was observed following core histone hyperacetylation, a significant decrease is observed when coupled with the globular domain of H1.1. This suggests that the NTD can make a subtle contribution to the influence of acetylation on histone H1 binding.

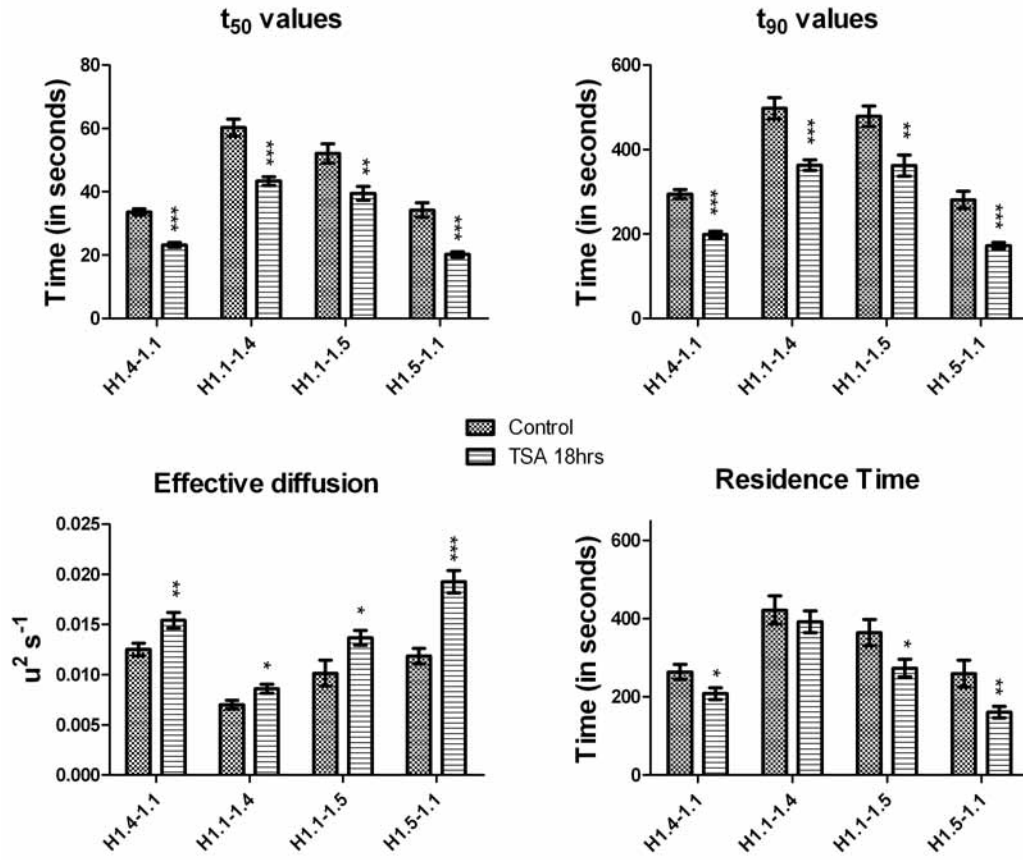


Figure 3.5 - Comparison of t_{50} , t_{90} , and kinetic parameters of H1 hybrids following core histone hyperacetylation (TSA 18hrs). All the hybrids showed a drop in t_{50} , t_{90} and $Deff$ values, similar to the response seen in their “parent” H1 sub-types. The change in residence time, however, was varied.

3.3.7 - Hyperacetylation changes the cooperativity of H1 binding to chromatin

Recent evidence suggests that the contributions of the CTD and globular domains to histone H1 binding are more than just additive. The globular domain, which contains two defined DNA binding sites, only binds with one site in the absence of the CTD. In the presence of the CTD, both sites are engaged. The result is that the globular domain and the CTD bind to chromatin cooperatively (Stasevich et al, 2010). We therefore wished to test whether or not cooperativity was altered in the presence of histone acetylation. For the following cooperativity experiments, H1.1 was selected as a prototype for other H1 variants, given its mid-range affinity to chromatin and similar amino acid length to H1.2 (213 AA compared to 215 in H1.1) and H1.4 (219 AA). Before we measured the change in cooperativity in the entire H1.1 molecule, we measured the binding affinities of the individual sub-domains in the presence of hyperacetylation. We found that the globular domain and the CTD (of H1.1) by themselves, failed to show a change in recovery following treatment with TSA (18hrs) (Figure 3.6e-f). This is in contrast to the increase in effective diffusion and reduction of residence time when the domains are coupled (as in WT H1). We then compared the kinetics of the H1 molecule with key mutations in the individual sites of the globular domain. The globular domain consists of two sites, Site I and II, which are critical in binding to DNA (Brown et al, 2006). Site I is thought to bind DNA near the nucleosomal dyad, while site II is thought to interact with linker DNA. As has already been shown in msH1⁰ (R42A Site II and K73A Site I), mutation of critical residues in

these sites in H1.1 (R57A Site II and K88A Site I) also leads to significant change in recovery (Figure 3.6a). Note that these mutants still have an intact CTD. Interestingly, mutations at either site in the globular domain abrogate the response to core histone hyperacetylation (Figure 3.6b-d), with no effect on the effective diffusion coefficient being observed. The removal of the CTD (R57A Δ CTD, R57AK88A Δ CTD) did not alter the effective diffusion coefficient in the presence of hyperacetylation.

These results suggest that the only way histone hyperacetylation may be able to impact H1 dynamics is by decreasing the cooperativity in binding to chromatin. Cooperativity in binding is present when the binding of one domain influences (in a positive or a negative manner) the binding of the other domain. A mathematical model for assessing cooperativity was recently described (Stasevich et al, 2010). The degree of cooperativity (γ) is proportional to the difference in the ratio of the bound and freely diffusing sub-population in the complete protein (WT protein) and the sum of the ratios of the individual binding domains (Stasevich et al, 2010).

Since the individual domains (CTD, Globular domain, Site I & II) do not change their kinetics upon hyperacetylation, the change in cooperativity ($\Delta\gamma$) is just proportional to the change in the ratio of bound to free WT H1 molecules upon hyperacetylation. A mathematical formula for measuring the change in cooperativity is given in the Supplementary information. If there is no change in cooperativity ($\Delta\gamma=0$) then there is no change in how the two domains bind following the modification (i.e. hyperacetylation). On the other hand, if there were

a negative change ($\Delta\gamma < 0$), then the binding of one domain would not support the binding of the other domain in the presence of the modification (i.e. hyperacetylation). Based on our calculations on the change in cooperativity, all H1 variants and hybrids undergo a negative change in cooperative binding upon hyperacetylation (Figure 3.7).

As per the existing model of H1 binding to chromatin, the CTD establishes initial contact, followed by the cooperative binding of either Site-I or Site-II to DNA (Brown et al, 2006; Stasevich et al, 2010). Analyzing the change in recovery of the K88A mutant allowed us to assess the change in cooperation between the CTD and Site II upon H1 binding, while the R57A mutant allowed us to assess the change in cooperation between the CTD and Site I upon H1 binding. Since these two mutants suffer negligible changes to D_{eff} upon hyperacetylation, a change in cooperativity $\Delta\gamma \approx 0$ is seen (a value of -1 ± 4 for R57A and -4 ± 3 for K88A). This implies that the binding of the CTD-Site-I or CTD-Site-II is unaffected by hyperacetylation (Figure 3.8). However, when all the three domains of H1 are present (Site I, Site II and the CTD), there is a significant change in the cooperativity of binding in the presence of hyperacetylation (Figure 3.7). This change therefore occurs during the transition of CTD-Site-I binding or CTD-Site II binding to CTD-Site-I-Site II binding, which eventually paves the way for high-affinity binding. H1.1 undergoes a change of cooperativity by a factor of -60 following hyperacetylation. Note that this decrease is relative to control cells, since the absolute change in cooperativity would depend upon the ratio of bound and free fractions of the individual binding domains of the molecule.

Extrapolating these calculations to other variants and hybrids of H1, we see that all the variants and H1 hybrids show decreased cooperativity, with H1.4 having an almost 100-fold decrease in cooperativity when compared to control cells. This extrapolation is a predicted loss of cooperativity, since we did not directly measure the individual binding domains for other histone H1s. The validity of the extrapolation rests on the assumption that the individual binding domains of the variants, like H1.1, do not undergo a change in cooperativity, and that the change is observed only in the intact molecule.

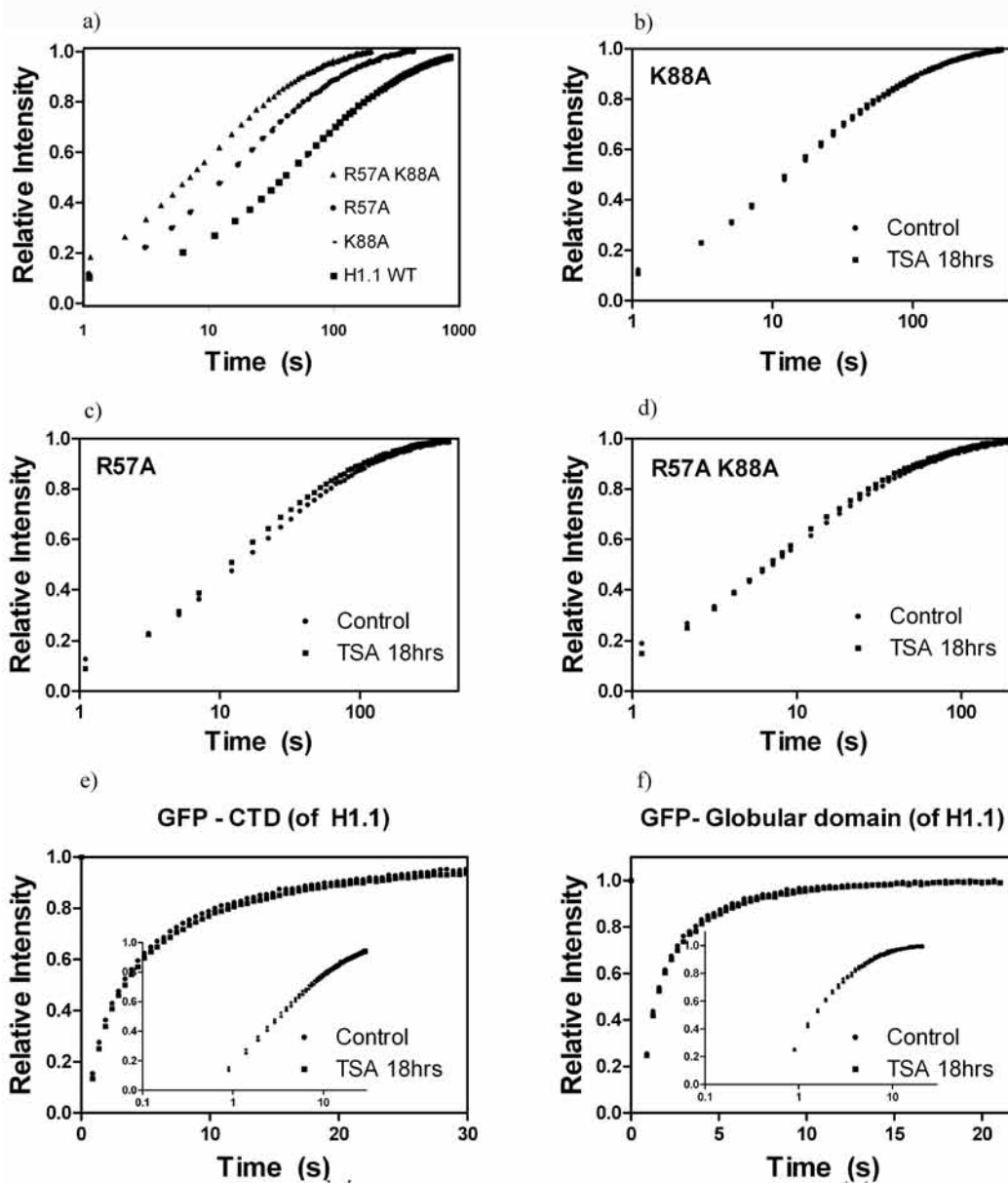


Figure 3.6 - Behavior of individual domains of H1 to hyperacetylation. a) Key residues within the globular domain (site I, site II or both) were mutated and their recovery was monitored with FRAP. This is a comparison in untreated cells (basal levels of acetylation). b-d) FRAP recovery curves of the mutants following an induction of hyperacetylation. Note that mutation of just one residue in the globular domain can entirely abrogate the kinetic response to hyperacetylation. e-f) Both the globular domain and the CTD (of H1.1) by themselves, fail to show a change in recovery following hyperacetylation.

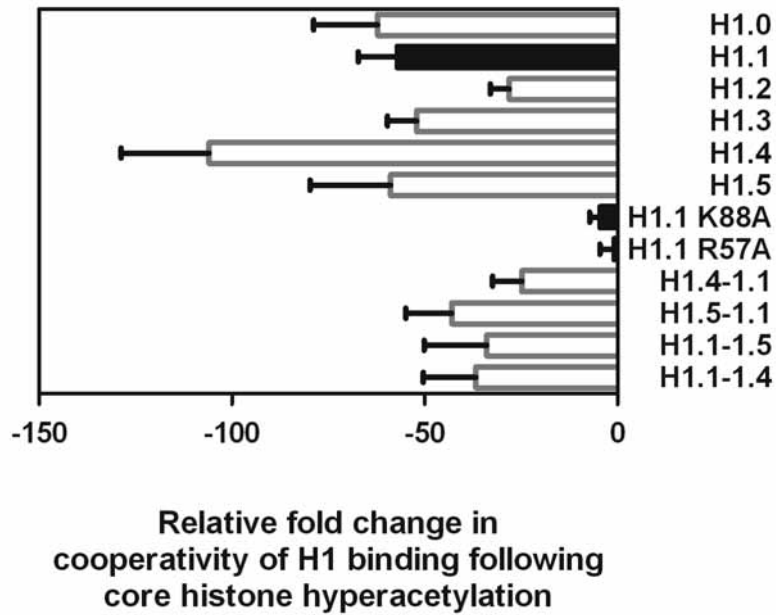


Figure 3.7 – Cooperativity in H1 binding is reduced following hyperacetylation. The change in cooperativity ($\Delta\gamma$) is a function of the difference of the reciprocal product of effective diffusion coefficient and fraction that is effectively diffusing following hyperacetylation (provided the individual domains do not change their affinity). Based on this relation, H1.1 undergoes a 60-fold decrease in cooperativity, while H1.4 is predicted to have a 100-fold decrease in cooperative binding. Predicted values are shown in gray bars, while calculated values are shown in black.

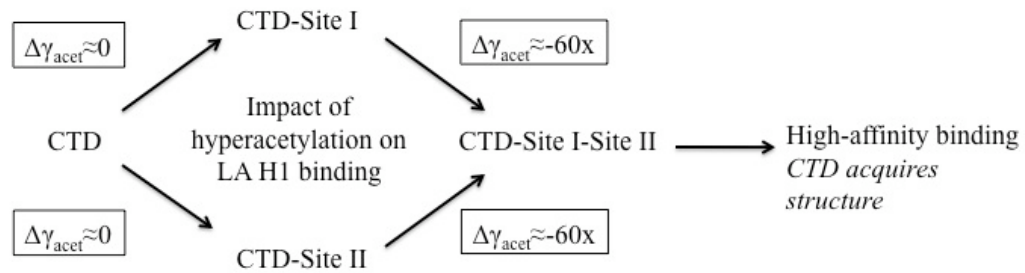


Figure 3.8 - Impact of hyperacetylation on LA and HA sites. Following the initial interaction of the CTD, either site-I or site-II of the globular domain interacts with their respective binding sites. This step is not significantly affected by hyperacetylation, as judged by the response of R57A, K88A H1.1 mutants to hyperacetylation. The transition from this state to a state that allows all the domains of H1 to be cooperatively bound is most affected by hyperacetylation (60 fold decrease in H1.1). Once the three dimensional structure of the CTD is acquired, hyperacetylation acts on decreasing either the residence time, transition time or the proportion of strongly bound H1 molecules in a variant-specific manner.

3.4 - Discussion

Core histone acetylation has been shown to modify the structure of the chromatin fiber (Carruthers & Hansen, 2000; Fletcher & Hansen, 1995; Garcia-Ramirez et al, 1995; Wang et al, 2001). Biochemical evidence suggests that hyperacetylation causes a moderate loosening of chromatin (Annunziato et al, 1988; McGhee et al, 1983). The loosening of chromatin is consistent with weaker DNA-histone interactions seen in the thermal denaturation profile and increased DNase I susceptibility of nucleosome particles following hyperacetylation (Ausio & van Holde, 1986). From these studies, it can be inferred that core histone acetylation should impact all histone H1 variants equally through the potential disruption of the histone H1 binding site on the surface of the nucleosome. Instead, based on our results, we find significant differences in the relative change in cooperativity and the variant-specific changes in HA population. This suggests that either a) disruption of the H1 binding site by acetylation is not the sole mechanism explaining the influence of acetylation on H1 binding or b) different H1 subtypes have different requirements for binding to the surface of the nucleosome.

The caveats of studying core histone acetylation in the context of living cells is that, addition of HDACi can have indirect effects on H1 mobility and chromatin structure. In addition to the reported expression of H1.0 under the influence of HDACi (Girardot et al, 1994), and observed H1 dephosphorylation, we cannot rule out the possibility of other non-histone proteins changing their acetylation patterns upon induction of acetylation. For example, addition of HDACi may

impact the interaction of histone chaperones and other histone modifying enzymes, which rely on the acetylation status of histones (reviewed in (Hansen et al, 2010)). Furthermore, we cannot rule out indirect effects caused due changes in the expression levels of genes, sensitive to core histone acetylation (Van Lint et al, 1996).

There have been previous attempts to address the influence of histone acetylation on the binding of H1 histones in living cells (Misteli et al, 2000; Rao et al, 2007). Following a 2-hour incubation with TSA, mouse H1.2 (H1c) and H1.0 (H1^o) were found to have significantly shorter residency time in both euchromatin and heterochromatin regions. We chose to examine cells after 1-hour treatment with TSA and after 18 hours treatment with TSA. This was chosen to preferentially reflect the separate kinetic pools of acetylated histones (Reviewed (Davie & Hendzel, 1994)). Brief periods of incubation with deacetylase inhibitors impact primarily euchromatic pools of histones while much longer incubations are required to impact heterochromatin regions. Surprisingly, the 1-hour treatment with TSA had no significant impact on the recovery of histone H1 in euchromatin. This may be a reflection of the relatively low abundance of hyperacetylated chromatin in euchromatin. A 1 μm circle necessary for conducting the FRAP experiment may limit the sensitivity to detect these smaller pools of chromatin. The failure to alter the recovery in heterochromatin following a 1-hour treatment with TSA was expected based on the slow kinetics of acetylation, even in the presence of TSA.

Induction of core histone hyperacetylation by longer treatments evoked marked changes in mobility of all H1 variants analyzed, with a consistent change in the effective diffusion coefficient being observed for all H1 variants tested. The effective diffusion coefficient reflects the combined contributions of both a small freely diffusing pool and a much larger weakly bound (LA) population that constitutes the bulk of the histone H1 nuclear pool for all variants. The increased effective diffusion coefficient can arise through two (or more) mutually inclusive mechanisms. The number of H1 binding sites may be reduced by disruption of chromatin structure and, in particular, the trajectory of the DNA at the entry and exit points of the nucleosome. This would result in an increase in the freely diffusing pool of H1. The other way effective diffusion coefficient can increase is if H1 is engaged in LA interactions and is unable to progress to HA interactions with chromatin. This implies that H1 cycles rapidly back and forth between freely diffusing and LA interactions, upon hyperacetylation. This is almost certainly the case in this instance because the population of freely diffusing histone H1 is so small that these measurements are not sensitive enough to detect even a several-fold change in freely diffusing H1.

The changes imparted to the HA H1 population are more varied. Unexpectedly, the distribution of histone H1 between HA and LA sites is largely unchanged. The exception is histone H1.2, where the proportion of molecules bound to HA sites decreases by approximately 30%. Interestingly, H1.2 is also unique in that the transition time and the residence time in the HA sites is unchanged. Thus, for histone H1.2, the recycling at LA sites is increased but the duration of time it

takes for an individual histone H1.2 molecule to convert to a HA site remains the same. Histone H1.2, commonly the most abundant histone H1 in the cell, may see a reduction in available binding sites as a result of changes in chromatin and nucleosome structure upon histone hyperacetylation.

The transition time reflects the duration that an individual histone H1 molecule spends cycling between LA binding sites and unbound diffusing states before engaging in a HA interaction that provides a relative immobilization of the histone H1 molecule. It reflects the likelihood that an interaction will be of high affinity. For H1.1 and H1.5 the transition time decreases. The increased cycling (the effective diffusion coefficient is increased) implies that the probability of engaging in a HA interaction may not have changed significantly for these two variants. For the remaining H1s, however, the transition time remains unchanged. With the increased cycling of these variants, this implies that the probability of either directly engaging or, more likely, converting from LA to HA binding is significantly lower following TSA treatment. Nonetheless, the proportion of HA binding sites remains the same.

The residence time is a measure of the binding affinity of histone H1 at sites where it binds with relatively high stability. For most H1 subtypes, the residence time of an H1 molecule at a high affinity site is dramatically reduced. This illustrates that hyperacetylation has a very significant effect on the ability of histone H1 to be retained at sites of high affinity binding. The exceptions to this are H1.2 and H1.5. The binding of H1.5 seems remarkably robust in spite of hyperacetylation.

H1 binding to chromatin is largely mediated by the cooperative binding of the H1 CTD and globular domain (Stasevich et al, 2010). These individual domains do not alter their kinetics upon hyperacetylation. Since there is a dramatic effect when these individual domains are combined in the wild-type protein, we concluded that it is the cooperativity of binding that is impaired upon hyperacetylation. In the case of H1.1, acetylation led to decreased cooperativity and the primary indicator of this change was the effective diffusion coefficient. This implies that the transition from a state partially bound by two domains, either CTD-Site-I or CTD-Site-II, to a state bound by all three domains, CTD-Site-I-Site-II, is impaired (by a factor of 60x in H1.1 and a predicted value of 100x for H1.4). The latter state would pave the way for the acquisition of the three-dimensional structure of the CTD allowing for high-affinity binding. The transition to a state in which both globular domain sites and the CTD are bound occurs less frequently, leaving more H1 in LA and freely diffusing states. From a structural perspective, this implies that the CTD-Site I or CTD-Site II binding state is unable to undergo a conformational change that would bring the nucleosome entry and the exit linker DNA stems together, which is a prerequisite for high affinity H1 binding, and indeed, higher order chromatin structure.

In conclusion, we have shown that core histone acetylation plays a pivotal role in regulating the dynamics of all histone H1 family members tested. However, once H1 binds to chromatin, the effect of core histone hyperacetylation becomes varied. It can affect the residence time, transition time or the proportion of HA

molecules in a variant-specific manner. In all cases, there is a significant reduction in the cooperativity of binding.

3.5 – Supplementary Material: Core histone hyperacetylation impacts cooperative behavior and high affinity binding of Histone H1 to chromatin.

3.5.1 - Assessing the change in cooperativity of H1 binding to chromatin, following hyperacetylation.

It has been shown that H1 exists in three distinct kinetic populations at any given time - freely diffusing (f), bound to chromatin with low-affinity (b_l) and bound to chromatin with high-affinity (b_s) (Carrero et al, 2004a; Carrero et al, 2004b; Carrero et al, 2003; Carrero, 2009). The low-affinity H1 molecules, together with the freely diffusing H1, constitute an effective-diffusive state (Carrero et al, 2004a; Carrero, 2009; Sprague et al, 2004). This proportion is represented by f_{eff} and is just the sum of the fraction that is freely diffusing state and low-affinity H1 molecules.

$$f_{eff} = b_l + f$$

If the total H1 population is represented as one, then

$$b_s + f_{eff} = 1$$

$$b_s + b_l + f = 1 \tag{Eqn.1}$$

The freely diffusing population is, thus, a sub-fraction of the molecules that are effectively diffusing. This population is shown to be less than 0.2%, rendering most of the H1 molecules in the nucleus to be in a chromatin bound-state (Carrero et al, 2004a). The effective diffusion coefficient, D_{eff} , is a kinetic parameter used to describe f_{eff} fraction (Beaudouin et al, 2006; Carrero et al, 2004a; Carrero, 2009; Sprague et al, 2006). D_{eff} can be described in terms of the actual diffusion coefficient, D , by the following relation -

$$D_{eff} = D(f / f_{eff})$$

Rearranging the terms, and using Eqn.1, we get,

$$f = f_{eff}(D_{eff}/D) = (1 - b_s)(D_{eff}/D) \quad (\text{Eqn.2})$$

The degree of cooperation, γ , is defined in terms of the ratio of H1 molecules that are bound and those that are freely diffusing, both in the wild-type protein and in the individual domains that make up the wild-type protein (Stasevich et al, 2010). A mathematical relation equating cooperativity in terms of the bound/free population is derived in (Stasevich et al, 2010). Assuming the binding of H1 is influenced by the CTD and the globular domain, then the cooperativity in H1 binding will be defined by the difference of the (bound/free fraction) in the wild-

type protein, and the sum of the (bound/free fraction) of the individual domains (Stasevich et al, 2010). Mathematically, γ can be represented as

$$\gamma = \frac{(b/f)_{wt} - (b/f)_c - (b/f)_g}{(b/f)_c(b/f)_g} \quad (\text{Eqn.3})$$

(Stasevich et al, 2010)

Following induction of core histone hyperacetylation, the new cooperativity in H1 binding will be represented by γ^* , which is defined as -

$$\gamma^* = \frac{(b/f)^*_{wt} - (b/f)^*_c - (b/f)^*_g}{(b/f)^*_c(b/f)^*_g} \quad (\text{Eqn.4})$$

The change in cooperativity following acetylation is given as $\Delta\gamma = \gamma^* - \gamma$. Here γ just represents the cooperativity in H1 binding at basal levels of core histone acetylation, while γ^* represents the cooperativity in H1 binding, following an induction of core histone hyperacetylation (TSA 18hrs). If $\Delta\gamma > 0$, then the cooperativity in H1 binding is enhanced upon acetylation, whereas, if the value is less than 0, then the cooperativity is diminished.

As shown in Fig (6), core histone hyperacetylation does not produce a change in the kinetic parameters of the binding of the CTD or the globular domain by itself. There is no statistically significant change in D_{eff} , residence time, transition time or the proportion of strongly bound molecules. This implies that,

$$(b/f)^*_c \approx (b/f)_c \quad \text{and} \quad (b/f)^*_g \approx (b/f)_g \quad (\text{Eqn.5})$$

Using Eqn.3, 4 and 5 the change in cooperativity reduces to

$$\Delta\gamma = \frac{(b/f)^*_{wt} - (b/f)_{wt}}{(b/f)_c(b/f)_g} \quad (\text{Eqn.6})$$

The ratio of bound H1 molecules and the freely diffusing H1 molecules can now be expressed entirely in terms of the freely diffusing population, using the relation given in Eqn. 1.

$$(b/f) = \frac{(b_l + b_s)}{(f)}$$

$$(b/f) = \frac{(1-f)}{(f)} = 1/f - 1 \quad (\text{Eqn. 7})$$

Substituting Eqn.7, in Eqn.6, we can express the change in cooperativity in terms of the proportion of freely diffusing population (f).

$$\Delta\gamma = \frac{(1/f)^*_{wt} - (1/f)_{wt}}{(b/f)_c(b/f)_g}$$

The freely diffusing population can be expressed in terms of D_{eff} and the proportion of H1 molecules that are strongly bound, using Eqn. 2 as follows -

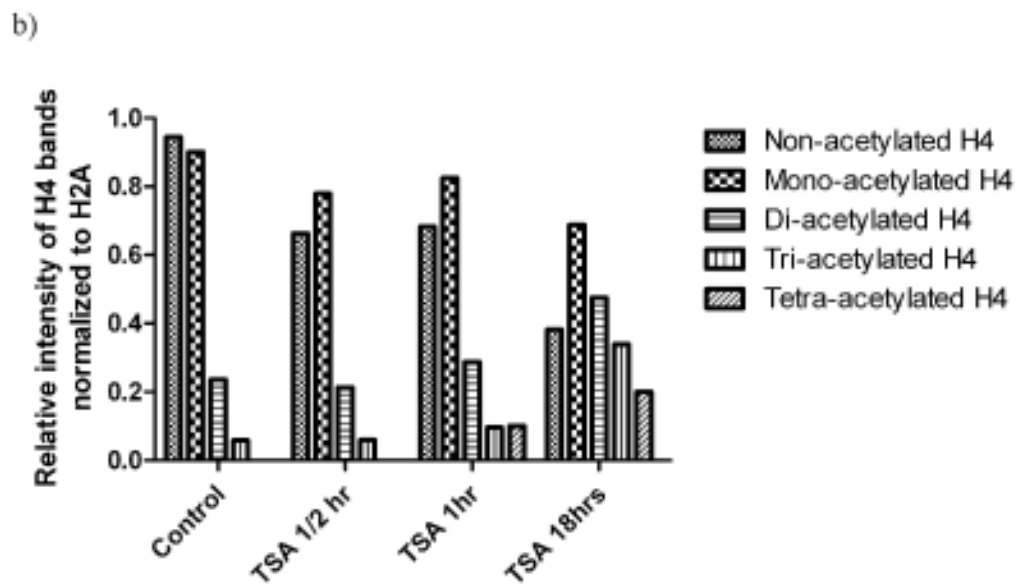
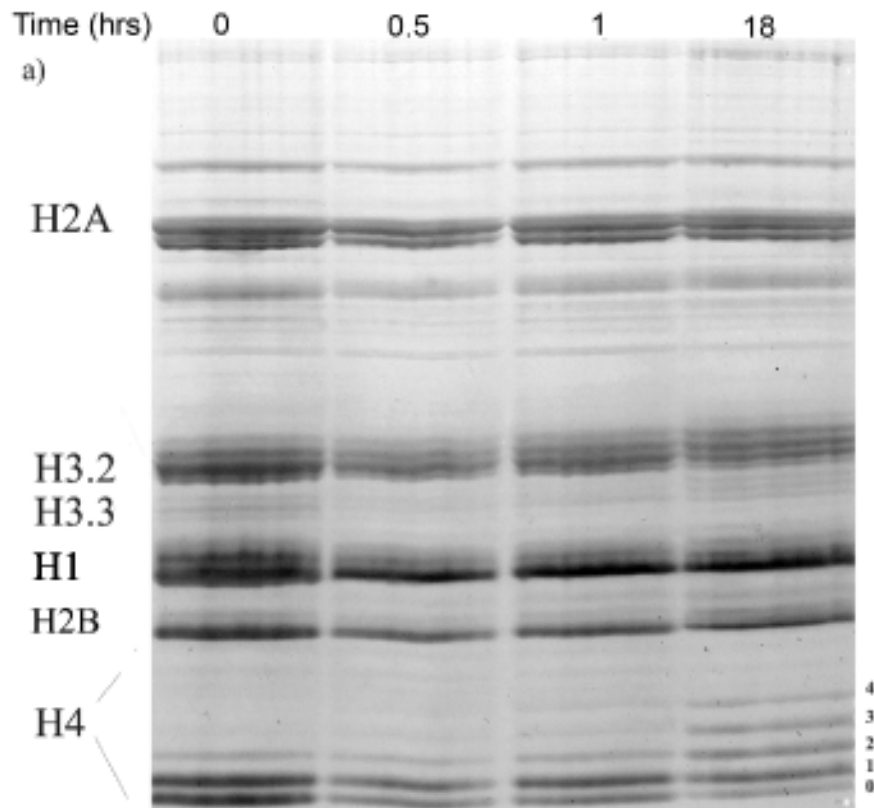
$$\Delta\gamma = \frac{[D/D_{eff}(1-b_s)]^*_{wt} - [D/D_{eff}(1-b_s)]_{wt}}{(b/f)_c(b/f)_g} = D \frac{[1/D_{eff}(1-b_s)]^*_{wt} - [1/D_{eff}(1-b_s)]_{wt}}{(b/f)_c(b/f)_g}$$

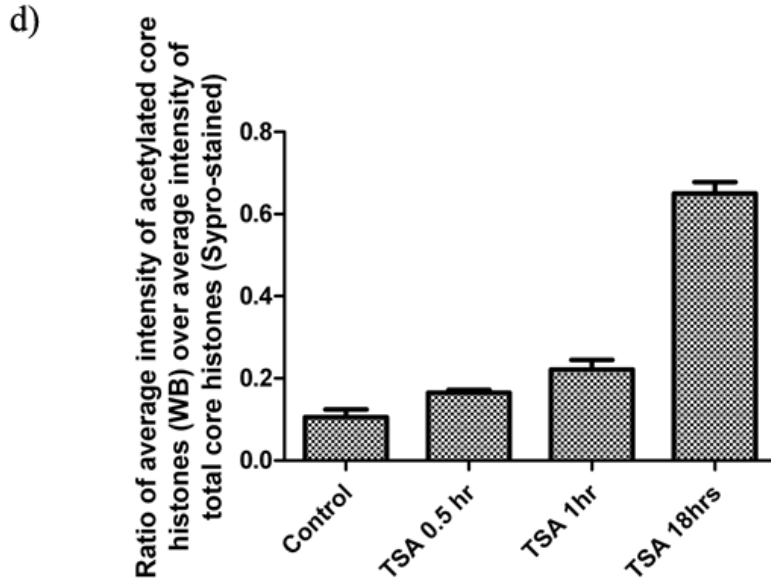
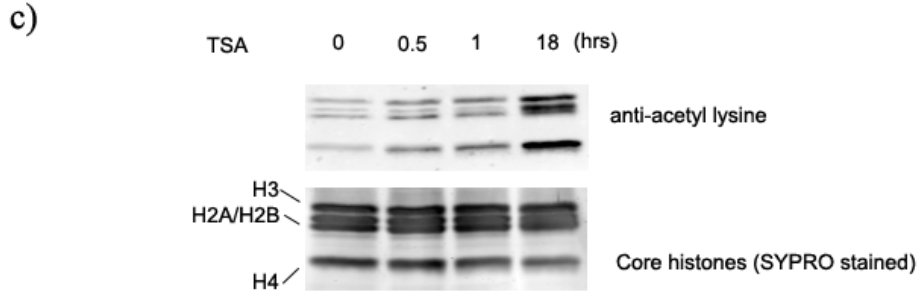
The terms $D, (b/f)_c, (b/f)_g$ are constants for a given temperature and variant. Thus, the change in cooperativity for a particular variant can be expressed as a function of the difference of the reciprocal product of effective diffusion coefficient and fraction that is effectively diffusing, before and after a change of conditions - core histone acetylation. The fraction that is effectively diffusing, f_{eff} , can also be expressed as $1-b_s$, where the total H1 content is expressed as 1.

$$\Delta\gamma \propto \{ [1/D_{eff}(1-b_s)]^* - [1/D_{eff}(1-b_s)] \} \quad (\text{Eqn. 8})$$

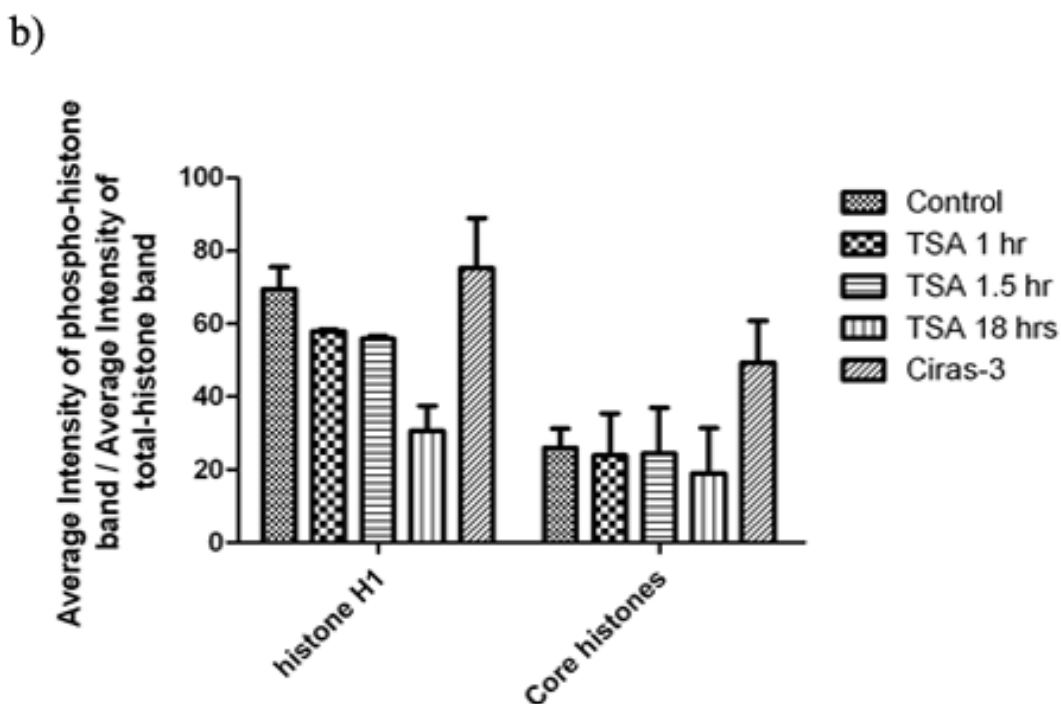
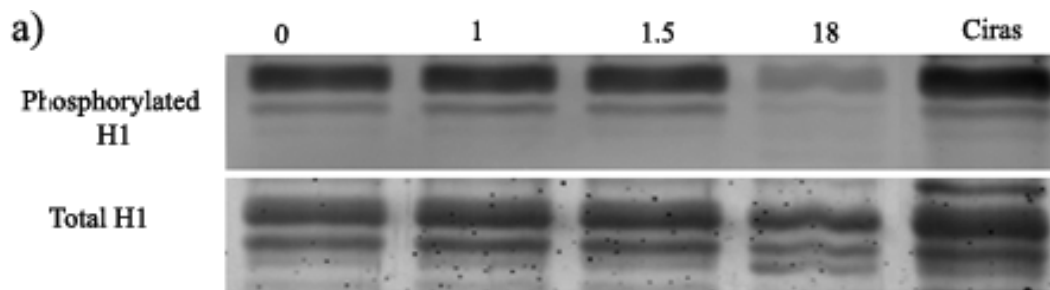
Note that this relation is only true if the individual domains themselves do not suffer a change in dynamics upon the change in conditions, for which cooperativity is being assessed. Should the individual domains change their kinetics, then this change must be taken into account prior to assessing the change in cooperativity.

3.5.2 - Supplementary Figures



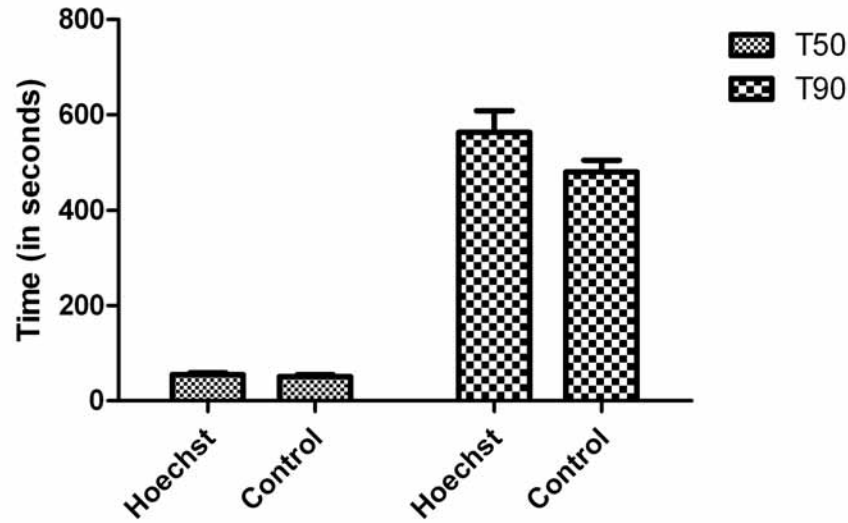


Supplementary Figure 3.1 – TSA increases core histone acetylation levels (a) illustrates a coomassie-stained AUT gel that shows the histones separated on the basis of their charge and mass. Nuclei were extracted at various time points (0, 0.5, 1 and 18hrs) after TSA treatment. Increase in H4 acetylation, which is most prominently seen as a laddering of the bands, is visible most distinctly after 18hr time point, although smaller increases are visible at the 1hr time-interval. The laddering of the H4 band was quantified using MetaMorph software, and normalized to the intensity of the H2A band (Sup. Figure 3.1b). (c) a western blot following separation of core histones (acid-extraction) on an 18% SDS-gel, probed with anti-acetyllysine antibody. (d) quantification of the change in acetylation following TSA treatment for 0.5hrs, 1hr and 18hrs.

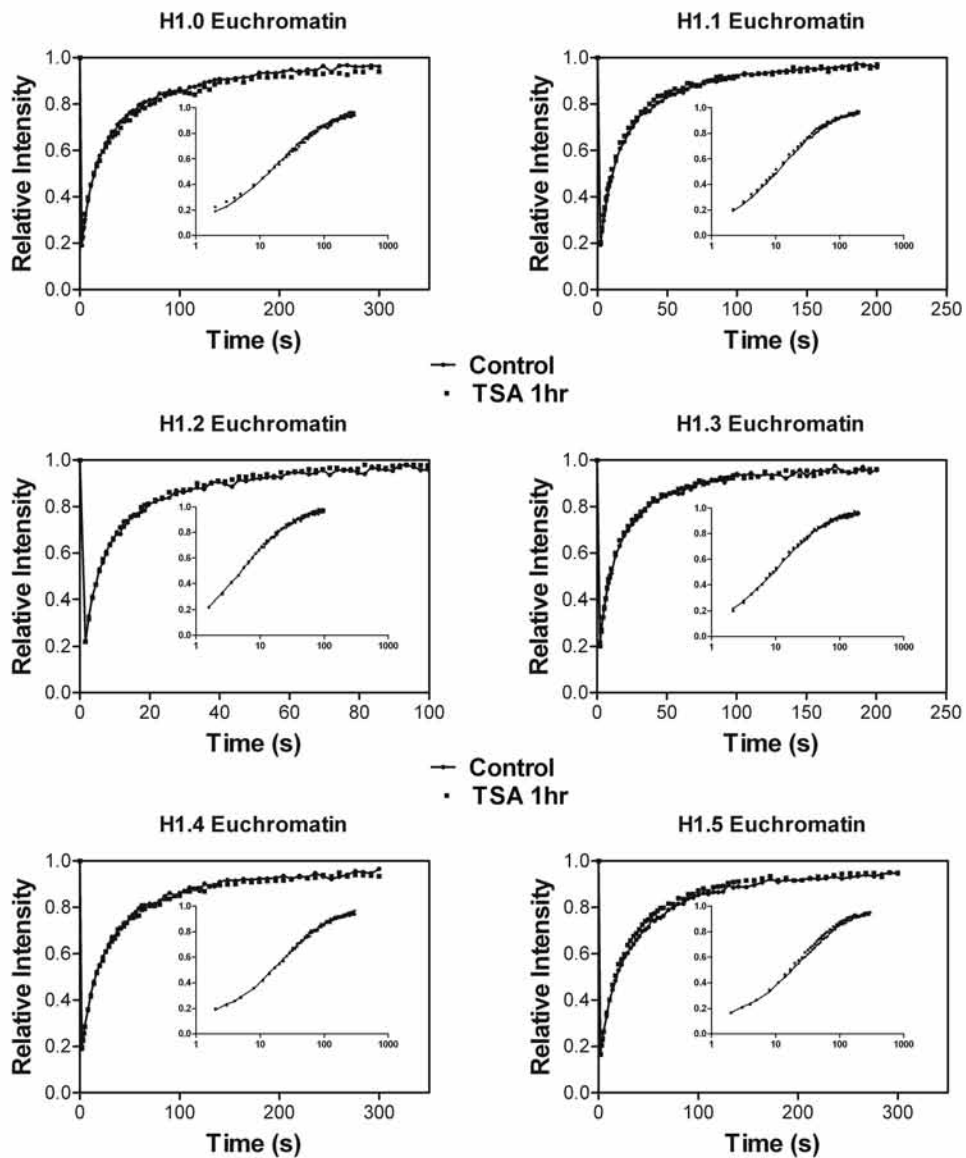


Supplementary Figure 3.2 – Linker histone and core histone phosphorylation status upon TSA treatment. (2a) shows phosphorylated proteins as stained with ProQ Diamond Blot stain, followed by a SYPRO Ruby Protein Blot stain that detects total protein content. (2b) plots the average intensity of phosphorylated H1 over the average intensity of total H1 bands and phosphorylated core histone bands over total amount of core histones present. H1 phosphorylation suffers a decline in its phosphorylation following incubation with TSA for 18hrs. Core histones undergo a relatively modest change in total phosphorylation levels. No such change is observed following shorter durations of TSA treatment (1, 1.5hrs). Ciras-3 cells, which have heightened levels of histone phosphorylation, are used as a positive control.

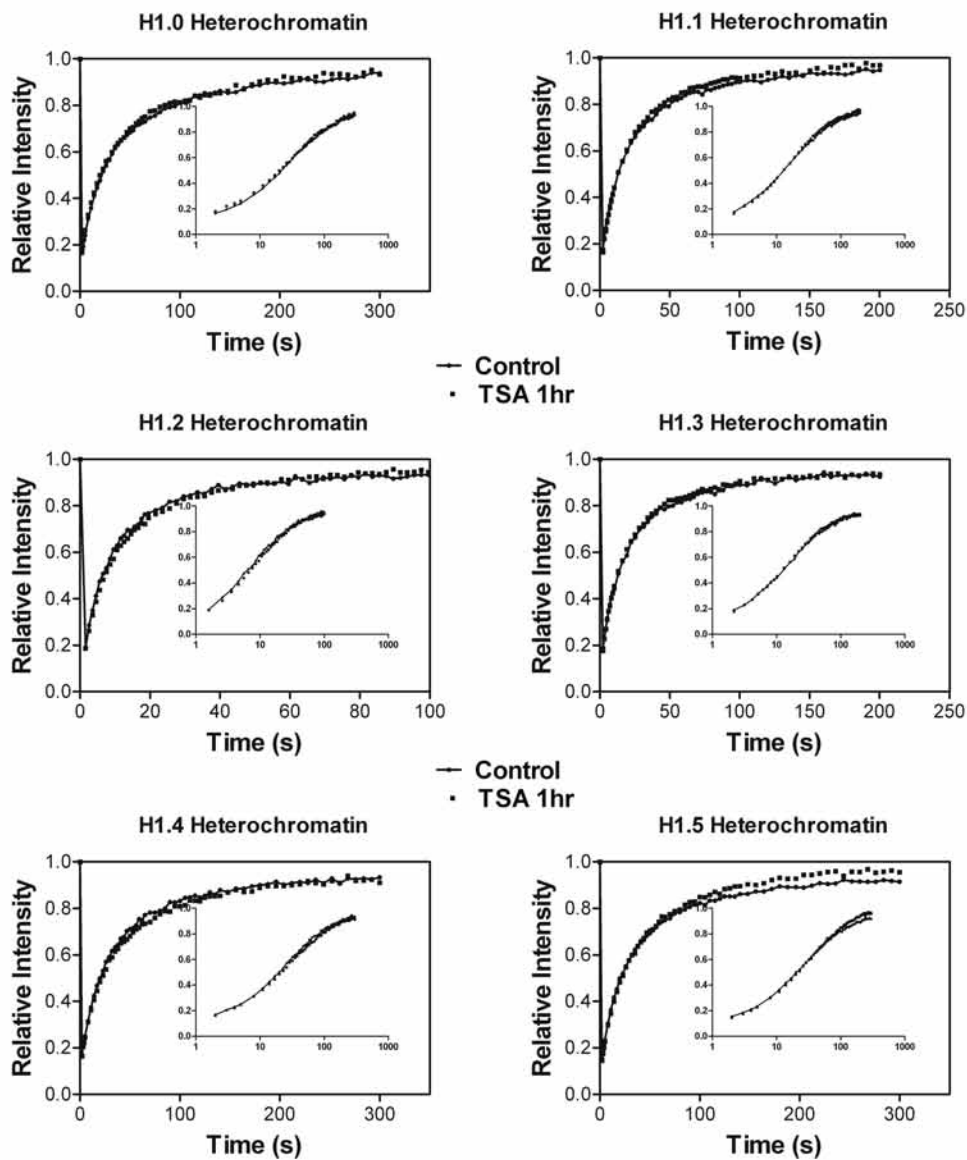
**Comparison of t_{50} and t_{90} values
in cells treated with Hoechst and untreated cells,
transfected with H1.4.**



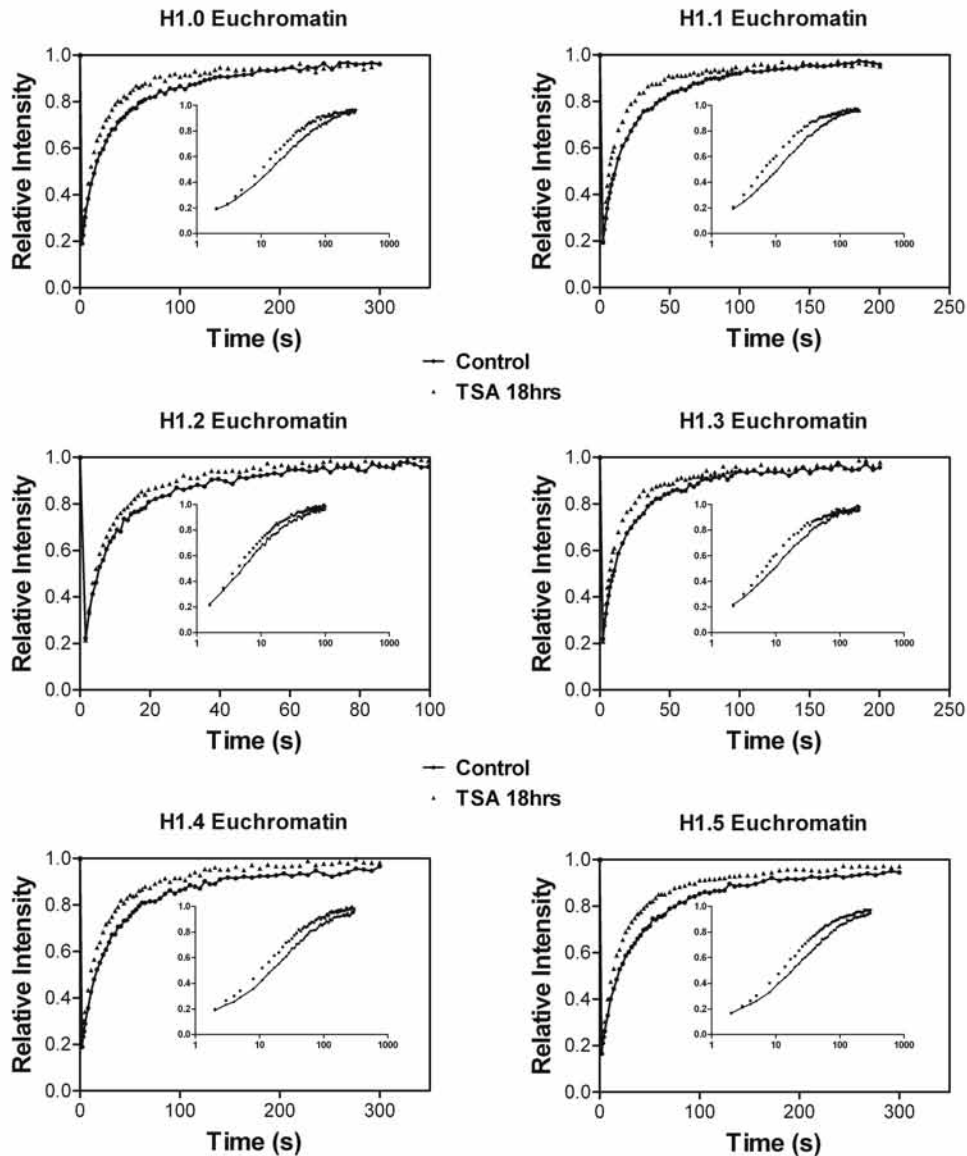
Supplementary Figure 3.3 – Analyzing whether addition of Hoechst 33342 affects H1 mobility. Shown here are the t_{50} and t_{90} values following FRAP experiments on H1.4 transfected cells. There are no significant differences in values before and after addition of Hoechst.



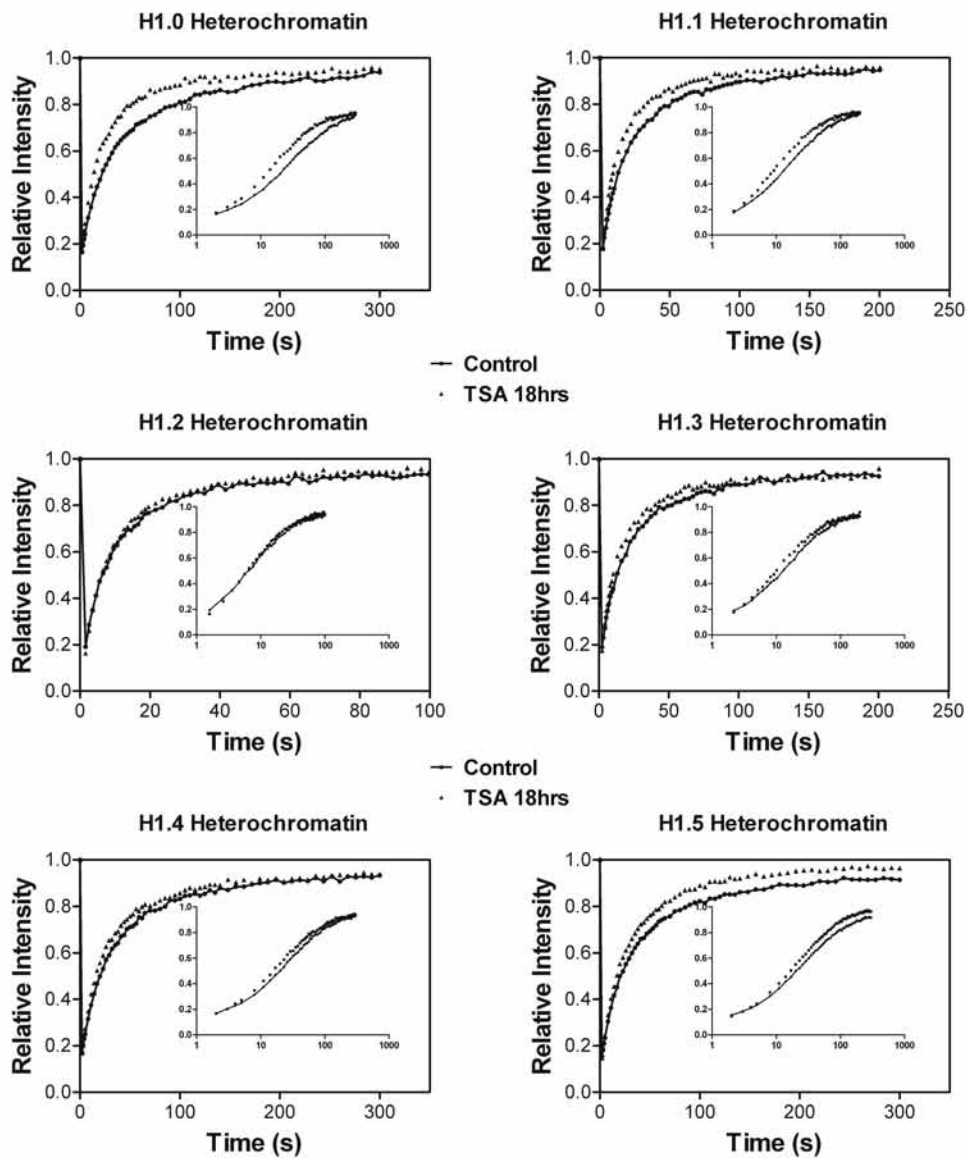
Supplementary Figure 3.4 - FRAP recovery profiles of H1 variants post induction of core histone acetylation (TSA treatment for 1hr) enriched in euchromatin. Each FRAP recovery curve shown here is an average from 15 different FRAP experiments, repeated over three times. The plots show the relative intensity versus time (in seconds) for each of the six H1 subtypes. The inset re-plots the recovery profiles as the relative intensity versus the log of time.



Supplementary Figure 3.5 - FRAP recovery profiles of H1 variants post induction of core histone acetylation (TSA treatment for 1hr) enriched in heterochromatin. Each FRAP recovery curve shown here is an average from 15 different FRAP experiments, repeated over three times. The plots show the relative intensity versus time (in seconds) for each of the six H1 subtypes. The inset re-plots the recovery profiles as the relative intensity versus the log of time.



Supplementary Figure 3.6 - FRAP recovery profiles of H1 variants post induction of core histone hyper-acetylation (TSA treatment for 18hrs) enriched in euchromatin. Each FRAP recovery curve shown here is an average from 15 different FRAP experiments, repeated over three times. The plots show the relative intensity versus time (in seconds) for each of the six H1 subtypes. The inset re-plots the recovery profiles as the relative intensity versus the log of time.



Supplementary Figure 3.7 - FRAP recovery profiles of H1 variants post induction of core histone hyper-acetylation (TSA treatment for 18hrs) enriched in heterochromatin. Each FRAP recovery curve shown here is an average from 15 different FRAP experiments, repeated over three times. The plots show the relative intensity versus time (in seconds) for each of the six H1 subtypes. The inset re-plots the recovery profiles as the relative intensity versus the log of time.

**Chapter IV - Pin1 promotes chromatin condensation and regulates histone
H1 dephosphorylation and chromatin binding ***

* A version of this chapter has been submitted for publication

4.1 – Abstract

Histone H1 plays a crucial role in stabilizing higher order chromatin structure. Transcriptional activation, DNA replication, and chromosome condensation all require changes in chromatin structure and are correlated with the phosphorylation of histone H1. In this study, we describe a novel interaction between Pin1, a phosphorylation-specific prolyl isomerase, and phosphorylated histone H1. A sub-stoichiometric amount of Pin1 stimulated the dephosphorylation of H1 *in vitro* and modulated the structure of the C-terminal domain of H1 in a phosphorylation-dependent manner. Depletion of Pin1 destabilized H1 binding to chromatin leading to chromatin decondensation. Pin1 recruitment and localized histone H1 phosphorylation correlated with transcriptional activation but did not depend on RNA polymerase II transcription. Thus, we have identified a novel form of histone H1 regulation through proline isomerization and shown that this correlates with a more compact chromatin structure, an expected consequence of increased histone H1 binding.

4.2 - Introduction

Histone H1 has an important role in the formation and mechanical stability of the 30nm chromatin fiber by facilitating folding and increasing internucleosomal contacts (Kruithof et al, 2009; Robinson & Rhodes, 2006). Reversible phosphorylation is the most extensively studied post-translational modification of linker histone H1. It is maintained by the antagonistic actions of protein phosphatases and CDC2/CDK2 kinase activities (Herrera et al, 1996; Paulson et al, 1996; Roth et al, 1991; Swank et al, 1997). The kinases require the presence of a consensus sequence (T/S)PXZ, where X can be any amino acid and Z represents a basic amino acid (Moreno & Nurse, 1990). Different variants of H1 have different numbers of these motifs. For example, H1.1 has two T/SPKK sites, while H1.5 has five (Parseghian & Hamkalo, 2001). Additionally, while interphase phosphorylation of H1 is restricted to Ser residues, both Thr and Ser residues are phosphorylated in mitosis (Sarg et al, 2006; Zheng et al, 2010), resulting in a maximally phosphorylated state at the G2-M transition (Bradbury, 1992; Roth & Allis, 1992; Talasz et al, 1996; Th'ng et al, 1994).

Histone H1 phosphorylation has been studied in a wide range of cellular processes. Increased levels of H1 phosphorylation are observed in cells that express several oncogenes correlating with a relaxed chromatin structure (Chadee et al, 1995; Taylor et al, 1995). H1 phosphorylation promotes chromatin decondensation that allows access to other DNA binding proteins (Hohmann, 1983; Roth & Allis, 1992). For example, phosphorylated H1 is associated with decondensed transcriptionally active sites (Chadee et al, 1995; Lu et al, 1995a).

While our interpretation of the function of histone H1 phosphorylation has largely been dominated by the assumption that electrostatic processes are regulated by phosphorylation, the recent recognition of the C-terminal domain (CTD) of histone H1 as an intrinsically disordered structure that adopts a more structured state when it interacts with DNA or nucleosomes necessitates other considerations (Caterino et al, 2011; Fang et al, 2011; Roque et al, 2005). Proline isomerization is a mechanism that alters the structure of a protein in a single enzymatic step. Interestingly, the phosphorylation sites within the CTD of H1 are all adjacent to prolines and match the known target sequence of the Pin1 phosphorylation-directed proline isomerase (Lu et al, 1999; Verdecia et al, 2000).

In this study, we examined whether or not phosphorylated S/T-Pro residues on H1 act as substrates for Pin1, a peptidyl-prolyl isomerase (PPIase). Pin1 recognizes and catalyzes the interconversion between the *cis* and *trans* conformations of the peptidyl prolyl bond. Pin1 is a highly abundant nuclear protein that is essential for progression through the cell cycle and has been shown to interact with a host of proteins, including RNA Polymerase II and Cdc25 (Albert et al, 1999; Lu et al, 1996; Stukenberg & Kirschner, 2001). Pin1 has two domains, an N-terminal WW domain that recognizes and binds phosphorylated Ser/Thr-Pro residues and a C-terminal PPIase domain. Isomerization can induce a conformational change in the protein backbone of a substrate which has been shown to alter the catalytic activity, localization, stability, as well as, the kinetics of phosphorylation and dephosphorylation events (Stukenberg & Kirschner, 2001; Zhou et al, 2000).

In this study, we found that Pin1 binds to histone H1 in a phosphorylation-dependent manner. Using FRET, we determined that Pin1 could directly alter the conformation of the phosphorylated but not the non-phosphorylated H1 CTD when bound to nucleosomes *in vitro*. Sub-stoichiometric levels of Pin1 were found to promote H1 dephosphorylation *in vitro*, consistent with an isomer preference for H1 phosphatase activity. Pin1 stabilized the binding of H1 on chromatin by increasing its residence time. Depletion of Pin1 resulted in a relaxed chromatin structure demonstrating the importance of Pin1 function in chromatin condensation. Pin1 and H1 phosphorylation levels were found to increase early following transcriptional activation, which is consistent with H1 phosphorylation playing a crucial role in transcription (Koop et al, 2003; Lamy et al, 1977; Langan, 1969; Zheng et al, 2010). In the absence of Pin1, transcriptionally active and inactive sites decondensed and H1 mobility was increased. Together, our results implicate Pin1 and phosphorylation-dependent proline isomerization as a chromatin regulatory mechanism that promotes a compacted chromatin state. The only histone protein containing Pin1 target sites is H1, the Pin1-dependent regulation of histone H1, stimulating its dephosphorylation and promoting its binding to chromatin, is therefore a promising mechanism to explain Pin1's function as a chromatin modifier.

4.3 - Results

4.3.1 - Pin1 interacts with histone H1

We first tested whether or not Pin1 physically interacts with histone H1 in co-immunoprecipitation experiments using antibodies specific to H1 or Pin1

bound to magnetic Dynabeads to immunoprecipitate proteins from nuclear extracts. The beads did not bind any detectable amount of either H1 or Pin1 in the absence of antibodies (Figure 4.1A). Anti-H1 antibodies co-immunoprecipitated Pin1 in 10T1/2 cells (Figure 4.1B) and Ciras-3 cells (Figure 4.1C). In the reciprocal experiment, H1 co-immunoprecipitated with Pin1 in 10T1/2 and Pin1wt cells (Figure 4.1D). Pin1 antibody did not pull down H1 in Pin1^{-/-} cells (Liou et al, 2002) (Figure 4.1E). We confirmed that Pin1 was physically bound to GFP-H1.1, utilizing extracts from T98G cells that stably express GFP-H1.1. This interaction was dependent upon the phosphorylation status of H1, since treatment of the nuclear extracts with calf-intestinal phosphatases prior to immunoprecipitation prevented Pin1 from binding to GFP-H1.1 (Figure 4.1F). These observations are consistent with a previous report that used liquid chromatography tandem mass-spectroscopy to show that H1 is a substrate of Pin1 (Tatara et al, 2010).

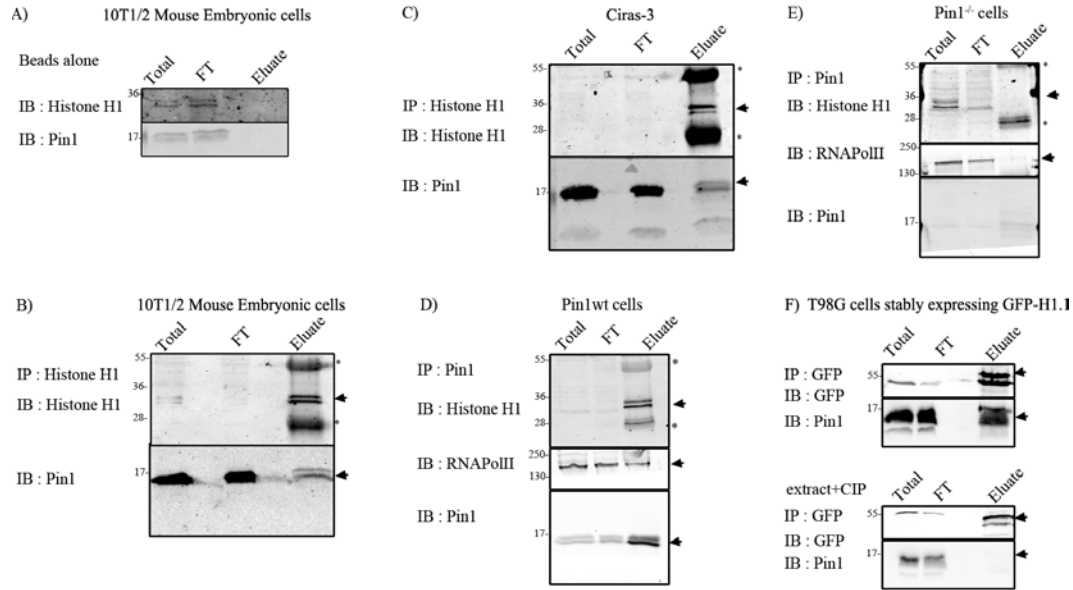


Figure 4.1 – Pin1 interacts with histone H1. Co immunoprecipitation experiments were carried out to test whether Pin1 and H1 interacted with each other *in vitro*. Total refers to the total nuclear extract prior to the addition of the antibody, while FT refers to flow-through (approximately 6% of the total volume). Black lines indicate that intervening lanes were spliced out, while arrows indicate bands that correspond to the protein being IB. Asterisks indicate heavy/light chain IgG antibodies that form part of the eluate. (A) Under the conditions used both histone H1 and Pin1 did not bind beads non-specifically. Histone H1 antibodies were used to immunoprecipitate (IP) H1 from mouse embryonic cells (B) and from Ciras-3 cells (C). Immunoblots (IB) reveals pulldown of Pin1 along with histone H1 demonstrating their association *in vitro*. Reciprocal experiments were carried out using Pin1 antibody to pull down Pin1 from extracts prepared from Pin1wt cells (D) and Pin1^{-/-} cells (E). RNA Polymerase II, which is an established substrate for Pin1, was used as a positive control. Both H1 and RNA Polymerase II form a part of the eluate in Pin1wt cells and not in Pin1^{-/-} cells, demonstrating specific interactions mediated by Pin1. Top panel in (F) shows the interaction between Pin1 and GFP-H1.1 in extracts prepared from T98G cells stably expressing GFP-H1.1. GFP-H1.1 was immunoprecipitated using GFP-antibody coupled to magnetic particles (GFP-Trap). This interaction is dependent on the phosphorylation status of proteins (E, lower panel) as treatment of the extracts with Calf Intestinal Phosphatase (CIP), a general non-specific protein phosphatase, abrogated the interaction between H1 and Pin1.

4.3.2 - Pin1 promotes the dephosphorylation of H1

Pin1 has been shown to promote the dephosphorylation of substrates, such as Cdc25 and Tau proteins (Zhou et al, 2000). Elegant *in vitro* experiments found that the major proline-directed protein phosphatase PP2A specifically dephosphorylates the *trans*-isomer of the pSer/Thr-Pro bond (Zhou et al, 2000), thereby imparting a post-phosphorylation, conformation-specific regulatory step to Pin1 substrates. The *cis* isomer has to achieve the right conformation either through slow spontaneous isomerization, or through Pin1 mediated isomerization in order to be a substrate of phosphatases. We hypothesized that a similar Pin1-mediated regulatory mechanism may also exist for H1.

We first determined whether or not steady-state H1 phosphorylation levels were altered in Pin1^{-/-} cells compared to their wild-type counterparts. We probed both total H1 phosphorylation levels using a general phospho-specific stain, and site/variant specific (H1.2/H1.5 pS173, H1.4 pS187) phosphorylation levels in Pin1wt and Pin1^{-/-} cells (Figure 4.2A). We found that Pin1^{-/-} cells had higher total levels of phosphorylated H1 histones including pS173 and pS187 levels compared to the Pin1wt cells. Ciras-3 cells, murine embryonic fibroblasts with an activated ras-pathway, were used as positive control.

The higher levels of phosphorylated H1 molecules in Pin1^{-/-} cells compared to Pin1wt cells could be due to higher levels of cdk2 activity, lower activity of PP2A, or perhaps, due to a conformation-specific post-phosphorylation step imparted by Pin1. To examine these possibilities, we first determined whether or not the levels of cdk2 were similar in both Pin1wt and Pin1^{-/-} cells (Figure 4.2B).

We further tested the activity of cdk2 extracted from either Pin1wt or Pin1^{-/-} cells to determine the ability of each to phosphorylate H1 (Supplementary Figure 4.1). The kinetics of H1 phosphorylation, as measured by the relative levels of pS173, pS187 and pT146, was similar in extracts containing cdk2 immunoprecipitated from either Pin1wt or Pin1^{-/-} cells. Omission of ATP from the reaction buffer resulted in cdk2 being unable to phosphorylate H1. These results suggest that cdk2 activity was not compromised in Pin1^{-/-} cells.

PP2Ac levels were also found to be similar in both Pin1wt and Pin1^{-/-} cells (Figure 4.2B). We then tested whether PP2A activity was altered after Pin1 knockdown. We immunoprecipitated PP2Ac from either Pin1^{-/-} cells or Pin1wt cells and monitored their ability to dephosphorylate H1. The kinetics of H1 dephosphorylation, as measured by the relative levels of pS187, was very similar in both groups (Figure 4.2C, E). Upon modeling the curves based on a one-phase decay, we found the rate of dephosphorylation in PP2Ac extracted from Pin1^{-/-} cells to be $0.019 \pm 0.006 \text{ min}^{-1}$, while the extract from Pin1wt cells registered a dephosphorylation rate of $0.014 \pm 0.003 \text{ min}^{-1}$. This suggested that PP2A activity was not compromised in Pin1^{-/-} cells.

To test if Pin1 was able to impose a post-phosphorylation regulatory step, we carried out the same dephosphorylation assay as described above but in the presence of increasing amounts of Pin1 (Figure 4.2D,F,G). We found that at sub-stoichiometric concentrations (molar ratio of H1: Pin1 1: 0.0005 to 1:0.1), Pin1 increased the rate of H1 dephosphorylation. The rate of H1 dephosphorylation increased from $0.019 \pm 0.006 \text{ min}^{-1}$ observed in the absence of Pin1, to

0.0291±0.0003 min⁻¹ at a molar stoichiometry of H1: Pin1 1:0.005 (0.04ug of Pin1) (Figure 4.2H). This suggested that sub-stoichiometric levels of Pin1 are able to promote H1 dephosphorylation *in vitro*. At higher levels of Pin1, with the molar stoichiometry approaching 1:1, we noticed that the rate of H1 dephosphorylation approached that seen in the absence of Pin1. This was probably due to competition between Pin1 and PP2A for binding to the H1 substrate. Note that the stoichiometries listed above are strictly molar stoichiometries, however, each H1 molecule may have multiple residues that are phosphorylated, and hence, may have multiple sites of interaction with Pin1/PP2A.

To investigate whether or not Pin1 promoted H1 dephosphorylation in living cells, we utilized roscovitine, a competitive inhibitor of cdk2 activity, and measured the rate of *in vivo* pS187 dephosphorylation kinetics in both Pin1^{-/-} and Pin1wt cells. Histones were extracted using 0.4N H₂SO₄ at regular time intervals following roscovitine treatment and were then separated by electrophoreses. Histone H2A was used as a loading control. Consistent with the role of Pin1 in regulating the kinetics of Cdc25 and tau protein phosphorylation, we observed the rate of H1 dephosphorylation of pS187 was faster in Pin1wt cells, compared to that of Pin1^{-/-} cells (Supplementary Figure 4.2). Fitting these curves using a one-phase decay kinetics we found a higher half-life for H1 phosphorylation of 72.81 min in Pin1^{-/-} cells compared to 58.93 min in Pin1wt cells, explaining the higher steady state levels of pS187 observed in Pin1^{-/-} cells. This suggested that Pin1 promoted the dephosphorylation of these Ser residues on H1. Similarly, the level

of pT146 was higher in Pin1^{-/-} cells but, in contrast to pS187, displayed a similar apparent rate of dephosphorylation compared to wt cells. However, it was difficult to assess the initial rate of dephosphorylation given the rapid rate at which Thr residues are dephosphorylated (an estimated half-life of 7-8 min compared to 59-72 min for Ser residues).

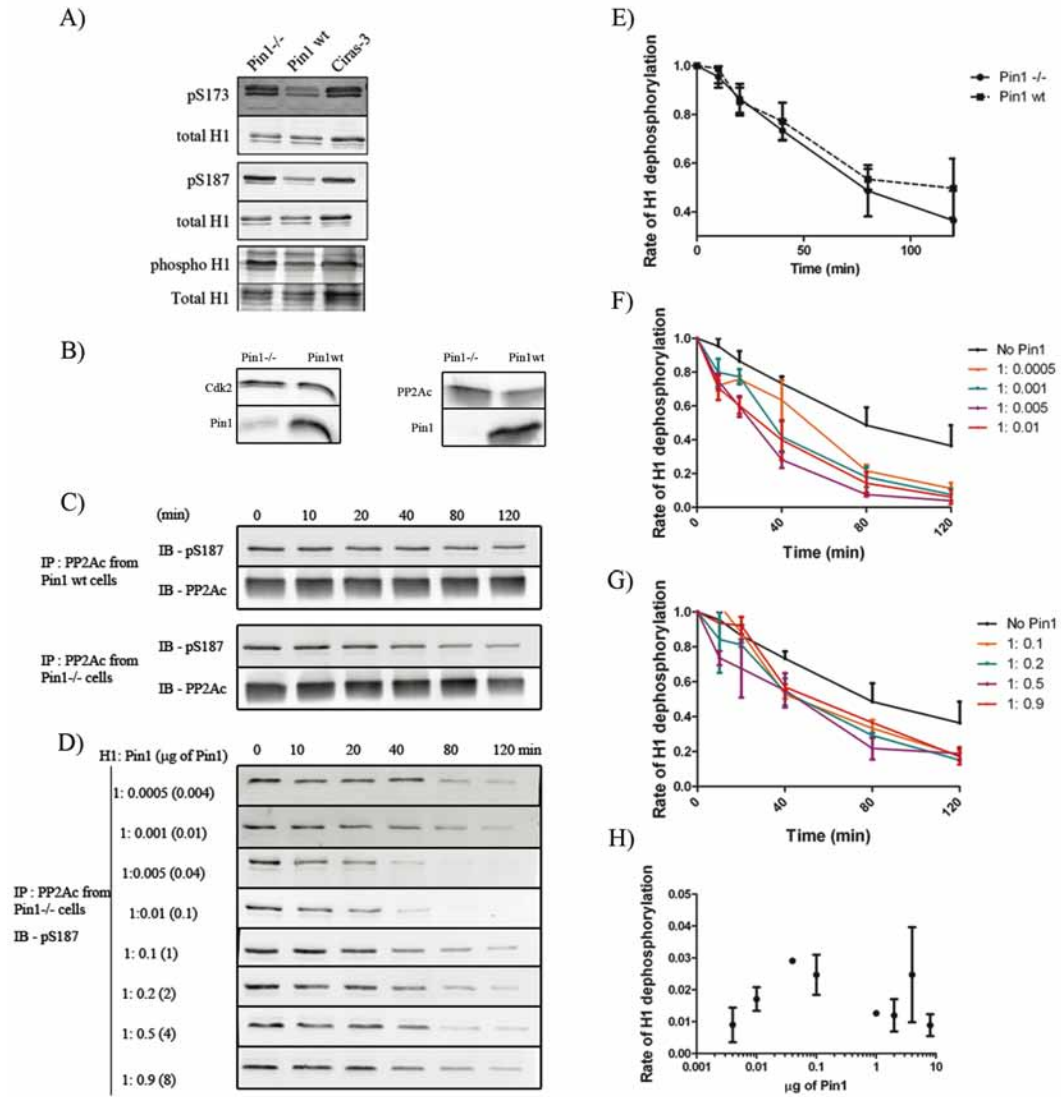


Figure 4.2 – Pin1 promotes H1 dephosphorylation. (A) Histones were extracted from Pin1^{-/-}, Pin1wt and Ciras-3 cells and were run on 18%-acrylamide gels. The blots were then probed with pS173(H1.2/H1.5), pS187(H1.4), and a phospho-specific stain that labels all phosphorylated proteins or with a stain that labels total protein. Levels of pS173, pS187 and net H1 phosphorylation levels were found to be higher in Pin1^{-/-} cells as compared to Pin1wt cells, similar to those observed in Ciras-3 cells (positive control). (B) Nuclear extracts from Pin1^{-/-} cells and Pin1wt cells revealed that the levels of cdk2 and PP2Ac were found to be similar in both cells. (C) The dephosphorylation activity of PP2Ac activity was analyzed using purified H1 as a substrate. PP2Ac was immunoprecipitated from either Pin1wt cells or Pin1^{-/-} cells and resuspended in dephosphorylation buffer to which purified H1 was added. The reaction was stopped at the time intervals indicated by the addition of SDS-loading buffer. The mixture was then run on 18% acrylamide gels and probed for pS187 levels. The kinetics of this dephosphorylation reaction are plotted in (E) with each dot/square representing the average H1 phosphorylation level obtained from at least three independent experiments. The average intensity from the zero-minute time point is set as the maximum, against which all other time points are compared. (D) PP2Ac was immunoprecipitated from Pin1^{-/-} cells and was mixed with a constant amount of H1, while levels of purified Pin1 were varied from 0.004μg to 8μg. The former corresponds to a molar stoichiometry of H1: Pin1 1: 0.0005, while the latter corresponds to H1:Pin1 1:0.9. The reaction was stopped by the addition of SDS loading buffer at defined time intervals and the extracts were probed with pS187 antibody. The kinetics of dephosphorylation is plotted in (F, G), with the average intensity at the zero-minute time point set to 1. These curves were then submitted to a one-phase decay curve analysis and the rate obtained was plotted as a function of the amount of Pin1 added to the reaction (H).

4.3.3 - Phosphorylation of H1 and Pin1 cause conformational changes in H1 CTD

The H1 CTD adopts a random disordered structure in solution, while in the presence of DNA and nucleosomes it is thought to assume characteristics of classical secondary structures, such as α -helices and β -sheets (Caterino et al, 2011; Clark et al, 1988; Roque et al, 2005; Roque et al, 2007). Phosphorylation of H1 increases the proportion of β -sheets at the expense of α -helices (Roque et al, 2008). Recently, H1 labeled with Cy3 and Cy5 on either end of the CTD in the same molecule was used to show that H1 binding to nucleosomes brings the two ends of the CTD into close proximity resulting in significant fluorescent resonance energy transfer (FRET)(Fang et al, 2011). The same level of FRET was not attained with H1 in solution, consistent with the prevailing view that the H1 CTD is intrinsically disordered and acquires structure only upon interaction with DNA (Clark et al, 1988; Lu et al, 2009a; Roque et al, 2005; Roque et al, 2008; Roque et al, 2007). Given these studies, we tested whether or not phosphorylation of labeled H1 and Pin1 would alter FRET levels, reflecting a change in the conformation of the CTD. We used purified H1 that was directly labeled with either Cy3 or Cy5 or both on either end of the CTD, as shown in Figure 4.3A. These proteins were diluted to a concentration of 26nM and the solution was spread on a glass-bottomed dish. Fluorescence emission spectra were recorded with excitation at 514nm and 633nm with 5-nm slit width. Excitation of H1-Cy5 at 514nm was minimal, while H1-Cy3 produced a spectra characteristic of a Cy3 signal (Supplementary Figure 4.3B). Excitation of H1 Cy3Cy5 with 633nm also

produced an emission spectra characteristic of H1Cy5 indicating that the addition of a Cy3 tag did not compromise the emission spectra of Cy5 (Supplementary Figure 4.3C). Consistent with previous results, H1Cy3 and H1Cy5 mixed at a 1:1 stoichiometry showed minimal inter-molecular FRET, as judged by the small amount of Cy5 emission at 671nm in the presence of nucleosomes. This signal increased dramatically when both Cy3 and Cy5 were present on the same molecule, as seen in the emission spectra for free H1Cy3Cy5. There is a further increase in FRET when the same molecules are mixed in the presence of reconstituted nucleosomes suggesting a change in the conformation of the CTD upon binding nucleosomes (Figure 4.3C).

Next, H1Cy3Cy5 was treated with cdk2 immunoprecipitated from Pin1^{-/-} cells in the presence or absence of ATP, as described above. Phosphorylation of H1 in the presence of ATP and cdk2 was confirmed following separation on an acrylamide gel, and phospho-specific staining (Figure 4.3B). Addition of labeled in vitro phosphorylated H1 to reconstituted nucleosomes led to higher levels of FRET signal when compared to labeled H1 that was not phosphorylated (incubated in buffer containing cdk2 devoid of ATP). This change in FRET signal between phosphorylated and non-phosphorylated H1 was not observed when H1 molecules were in solution devoid of nucleosomes, indicating that changes in the conformation of the H1 CTD induced by H1 phosphorylation, occur only in nucleosome-bound H1 (Figure 4.3D). The difference in Cy5 emission at 671nm between phosphorylated H1 molecules and non-phosphorylated H1 molecules, upon binding of nucleosomes, was significantly reduced in the presence of

stoichiometric levels of Pin1 (0.1 μ g of Pin1 or 1:1.4 H1:Pin1 molar ratio). In fact, FRET levels of phosphorylated H1 molecules were restored to the levels seen in non-phosphorylated H1 molecules in the presence of Pin1. For example, the FRET efficiency calculated using the RatioA method (Clegg, 1992; Fang et al, 2011; Poirier et al, 2009) increases from 0.222 \pm 0.008 to 0.27 \pm 0.01 upon phosphorylation of H1 (Supplementary Figure 4.3D). This data demonstrates a decrease in the separation between the Cy3 and Cy5 tags from 6.18 \pm 0.05nm in the non-phosphorylated state to 5.94 \pm 0.06nm in the phosphorylated state. Upon addition of Pin1, the FRET efficiency of phosphorylated H1 molecules bound to nucleosome was reduced to 0.24 \pm 0.01, increasing the apparent separation between Cy3 and Cy5 to 6.09 \pm 0.08nm. Adding Pin1 did not change the FRET levels of non-phosphorylated H1, suggesting that the interaction of H1 and Pin1 was dependent on H1 phosphorylation.

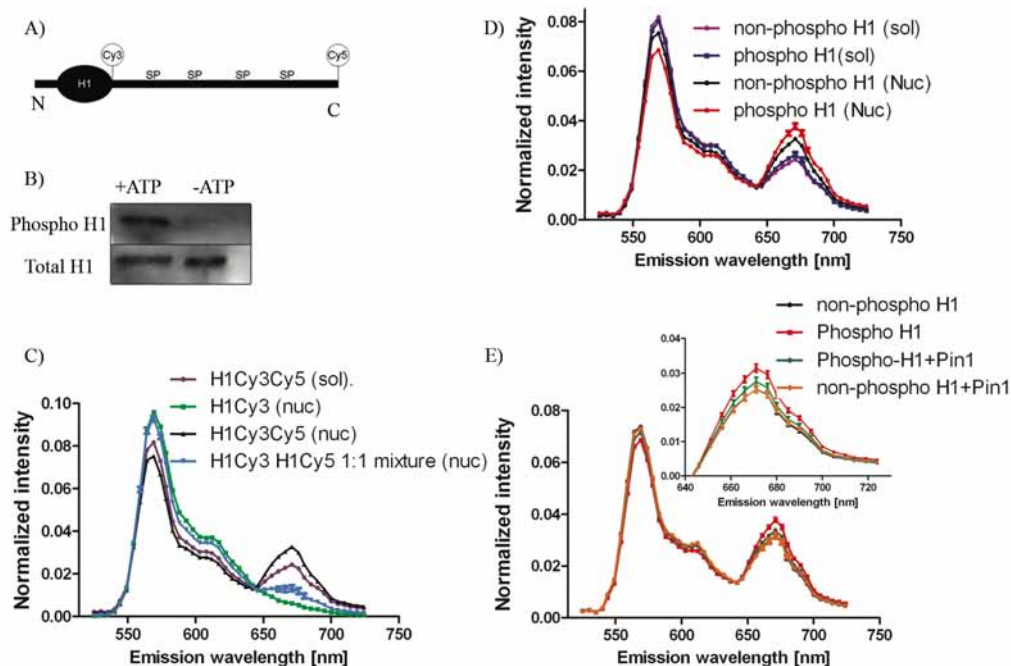


Figure 4.3 – Pin1 and H1 phosphorylation change the structure of the CTD.

(A) H1 labeled with Cy3 and Cy5 were treated with cdk2 immunoprecipitated from Pin1^{-/-} cells in the presence or absence of ATP. Part of the extract was then run on 18% acrylamide gel, transferred onto nitrocellulose membranes and probed with a phospho-specific stain (imaged at 302nm UV lamp). These blots reveal successful phosphorylation of H1 in the presence of ATP (now referred to as phosphoH1) while cdk2 was unable to phosphorylate labeled H1 molecules in the absence of ATP (now referred to as non-phospho H1). (B) The position of the Cy3 and Cy5 label are indicated in relation to the whole H1 molecule (N=N-terminal and C= C-terminal). The phosphorylation sites are marked with SP (Ser-Pro). (C) Labeled phospho H1 molecules were then diluted either in solution (sol.) or with reconstituted nucleosomes (nuc) and placed on a coverslip. A 514nm laser was then used to excite the molecules and fluorescence emission spectra was obtained from 525-724nm (5nm slit-width). Fluorescence intensity was normalized to the total fluorescence intensity obtained from each spectrum. The spectra show a slight increase in FRET signal (peak at 671nm) in the mono-labeled H1's (either Cy3 or Cy5) mixed with each other in 1:1 stoichiometry together with nucleosomes, indicating inter-molecular FRET, while this signal increases dramatically when both Cy3 and Cy5 are on the same H1 molecule. (D) FRET signal was compared between phosphorylated H1 and non-phosphorylated H1 in solution vs. these molecules added to reconstituted nucleosomes. While FRET signal remains the same when H1 is in solution, FRET signal is dependent on the phosphorylation status of H1 in the presence of reconstituted nucleosomes. (E) FRET signal was compared between phosphorylated H1 and non-phosphorylated H1 with reconstituted nucleosomes in the presence or absence of Pin1. While phosphorylation alone increases the FRET signal, addition of Pin1 reduces this signal towards that of the non-phosphorylated H1 molecules.

4.3.4 - Pin1 modulates the dynamics of H1.1 and H1.5

To determine whether or not Pin1 regulates H1 binding *in vivo*, we tested the contribution of Pin1 to histone H1 binding by performing fluorescence recovery after photobleaching (FRAP) experiments with N-terminally GFP-tagged H1.1 (enriched in euchromatin) and H1.5 (enriched in heterochromatin (Th'ng et al, 2005)). H1.1 has one Thr-Pro site (TP), and one Ser-Pro site (SP) on its CTD at positions 152 and 183, respectively. In contrast, H1.5 has the highest number of T/SP sites amongst known H1 variants, having 3 TP and 3 SP sites. We measured the *in vivo* H1 FRAP recovery kinetics and its dependence on Pin1, in Pin1wt and Pin1^{-/-} cells. The resulting FRAP curves were then subjected to mathematical modeling, and kinetic parameters such as effective diffusion coefficient (*Deff*), residence time, transition times and the percentage of H1 molecules that are engaged with high affinity to chromatin, were obtained (Carrero et al, 2004a; Carrero et al, 2004b). The *Deff* is a measure of the freely diffusing population and the molecules bound with low-affinity, while the residence time (time engaged in an high affinity interaction, and inversely proportional to the dissociation rate) and transition time (time between two high-affinity interactions and inversely proportional to the association rate/affinity) reflect kinetic properties of a high-affinity population (Carrero et al, 2004a; Carrero et al, 2004b).

The dynamics of H1.1 and H1.5 were markedly different when compared in the presence or absence of Pin1 (Figure 4.4a,b). In cells expressing GFP-H1.1, the recovery was much faster in the absence of Pin1, as measured by FRAP. For instance, the t_{50} values of H1.1 decreased from 37 ± 2 sec in Pin1wt cells to 23 ± 1

sec in Pin1^{-/-} cells (Figure 4.4c,d). In Pin1wt cells expressing GFP H1.5, we observed a t_{50} value of 80 ± 5 seconds, which was half of that observed in Pin1^{-/-} cells, where a t_{50} value of 40 ± 3 seconds was observed. Thus both H1.1 and H1.5 molecules are more mobile in the absence of Pin1.

Upon mathematical modeling of the FRAP curves, we observed that Pin1 induces a significant increase in the residence time of H1.1, from 140 ± 13 sec in Pin1^{-/-} cells to 277 ± 44 sec in Pin1wt cells, and of H1.5 molecules, 464 ± 32 sec in Pin1wt cells to that of 292 ± 24 sec in Pin1^{-/-} cells (Figure 4.4 e, f, Supplementary table 4-I). This suggests that the H1.1 molecules were able to engage in high-affinity interactions for longer durations in the presence of Pin1. However, there were no increases in the percentage of H1.1 or H1.5 molecules involved in high-affinity interactions with chromatin. Furthermore, a steep reduction in the effective diffusion coefficient of H1.1 and H1.5 in the presence of Pin1 was observed. Given that the diffusion rate is unlikely to change, the reduction in effective diffusion coefficient could imply a greater proportion of H1 pool bound to chromatin or, alternatively but not mutually exclusive, that there is an increase in the affinity of the weakly bound fraction. Additionally, once H1.1 engages in a high-affinity interaction with chromatin, Pin1 can further stabilize the interaction leading to longer residence times.

We tested the impact of other known peptidyl-prolyl cis-trans isomerases, the Cyclophilins and FKBP, on H1 mobility, by selectively inhibiting these classes of proteins using Cyclosporine A and Rapamycin, respectively. A 1hr-incubation of 10T1/2 cells in the presence of either drug produced no change in H1.1 dynamics

(Supplementary Figure 4.4). These results show that among the classes of prolyl-isomerases, only Pin1 affects the mobility of H1 in a significant manner.

In order to determine if the changes in H1 mobility in Pin1^{-/-} and Pin1wt cells could be due to other chromatin modifications that have the potential to modify H1 mobility, we analyzed the composition of core histones and the level of histone acetylation by acetic acid-urea-Triton X100 PAGE and found each to be similar in both Pin1^{-/-} and Pin1wt cells (Supplementary Figure 4.5). These results help confirm that the changes seen in H1 mobility are a direct consequence of an interaction between H1 and Pin1.

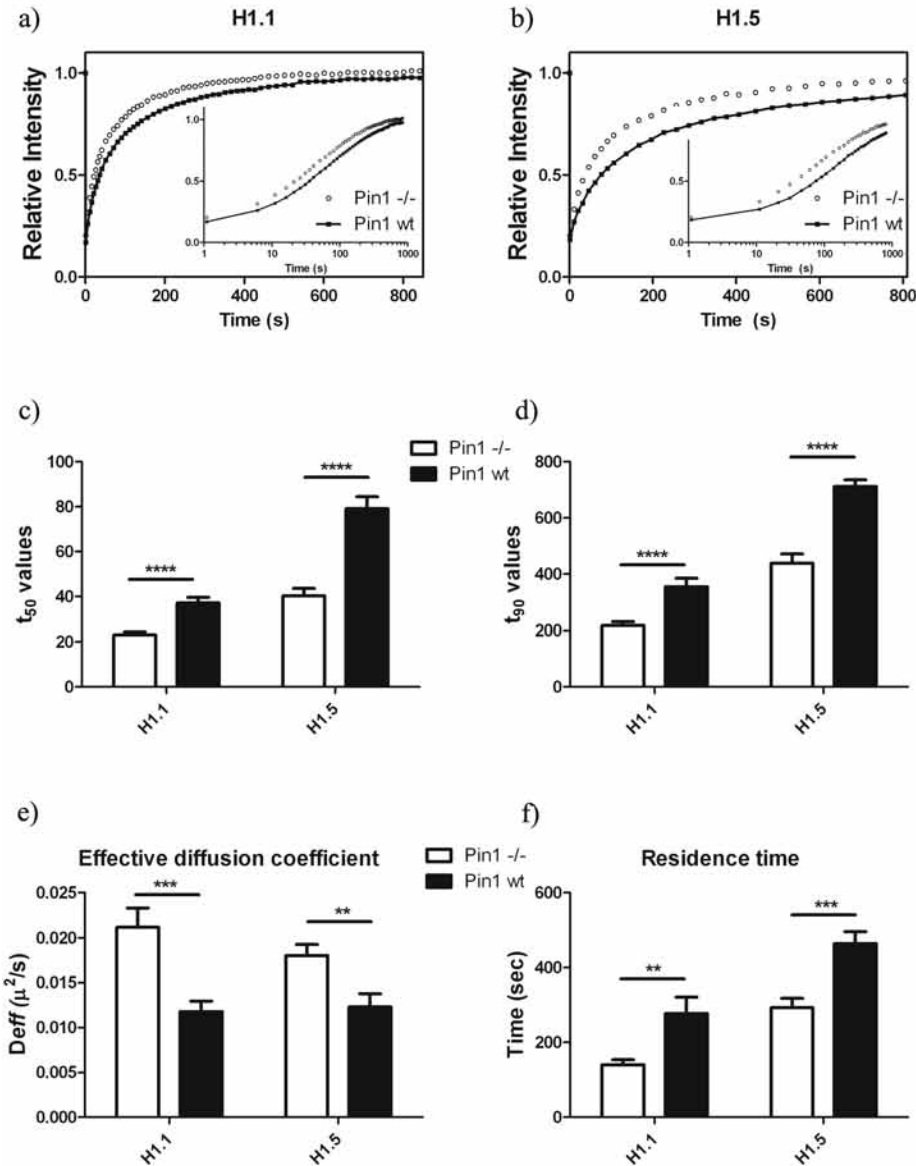


Figure 4.4 – Pin1 stabilizes GFP-H1.1 and GFP-H1.5 dynamics. GFP H1.1 (a) or GFP-H1.5 (b) were expressed either in Pin1^{-/-} cells or Pin1wt cells. FRAP experiments were carried out to measure the dynamics of H1, each curve represents an average of approximately 20 cells (total) in three independent experiments. The inset represents the same FRAP curve with the x-axis in log(time) to highlight changes in the earlier phases of the FRAP curve. Both H1.1 and H1.5 recover much faster in Pin1^{-/-} cells as compared to Pin1wt cells. This trend was affirmed with a statistically significant increase in both t₅₀ (c) and t₉₀ (d) values in the presence of Pin1. FRAP curves were then submitted to mathematical modeling from which kinetic parameters such as effective diffusion coefficient (e) and residence times were obtained. Pin1 causes a decrease in effective diffusion coefficient, a measure of the freely diffusing and low-affinity population, while at the same time causes increases residence time of the high-affinity H1 population.

4.3.5 - Distinct effects of Ser at position 152 vs. 183 in H1.1

Our results show that Pin1 interacts with and stabilizes H1 binding to chromatin. During interphase, serine residues proximal to the C-terminal end of H1 are exclusively phosphorylated, whereas during mitosis, Thr residues proximal to the globular domain are also phosphorylated (Sarg et al, 2006; Zheng et al, 2010). However, the contributions that these Ser/Thr residues make to Pin1-mediated H1 stabilization have not been addressed. Since H1.1 has just one SP and one TP site, we mutated either Ser 183 or Thr 152 to Ala and analyzed whether these mutants could be phosphorylated *in vivo*, when expressed in either Pin1^{wt} or Pin1^{-/-} cells. We transfected FLAG-tagged versions of the H1.1 mutants in these cells, and extracted histones using 0.4N sulfuric acid. The histones were then separated on a 10% SDS-gel ± Phostag. Phostag is a phosphate-binding molecule that, when supplemented in an acrylamide gel, retards phospho-proteins, thus providing a shift in the bands (Kinoshita et al, 2009; Kinoshita et al, 2008).

We found that in the absence of Phostag, all FLAG-H1.1 mutants migrate as single bands; however, in the presence of Phostag, there is a mutant-specific shift in the migration. Wild-type H1.1, for example, migrates as two distinct species, a lower non-phosphorylated band and an upper mono-phosphorylated band (Supplementary Figure 4.6).

The Thr at position 152 in H1.1 was first mutated to Ala (T152A). This rendered position 152 devoid of phosphorylation and thus independent of Pin1-mediated isomerization. In this mutant, the only position where Pin1 can play a potential role is at position Ser 183. We found that this mutant had a similar pattern of

migration on a Phostag gel to that of wt H1.1, suggesting that the Thr at 152 is not phosphorylated to a significant extent in the wt protein. To evaluate if the T152A mutation resulted in a change in the dynamics of H1.1 and the contributions that Pin1 has on the mobility of T152A, we transfected a GFP-tagged version of this mutant in Pin1wt and Pin1^{-/-} cells and analyzed its mobility, by FRAP (Figure 4.5b). The t_{50}/t_{90} values along with the results of mathematical modeling can be found in Supplementary Figure 4.7 and Supplementary Table 1. In Pin1wt cells expressing GFP-H1.1 T152A, the FRAP recovery rates were significantly slower than when GFP-H1.1 T152A was expressed in Pin1^{-/-} cells. The t_{50} values increased from 25 ± 1 sec in Pin1^{-/-} to 43 ± 3 sec in Pin1wt cells. Similar to the pattern seen in H1.1wt, we observed a significant decrease in the effective diffusion coefficient and increase in residence time of H1.1 T152A in the presence of Pin1. The only significant difference we detected between wt H1.1 and H1.1T152A was that the latter had an increase in the time between two consecutive high affinity interactions when Pin1 was present. This implies that in the presence of Pin1, most of the H1.1T152A molecules are bound to chromatin with low-affinity and upon transition to a high affinity state, Pin1 further stabilized H1 binding resulting in higher residence times.

We then switched the position of Ser and Ala, generating a H1.1 mutant that had Ser at position 152 and Ala at position 183 (T152S S183A) (Figure 4.5c). This mutant migrated as two distinct species, suggesting that the Ser at position 152, unlike the Thr at the same position, was indeed phosphorylated (Supplementary Figure 4.6). From FRAP analysis, we observed H1.1T152S S183A to recover

slower in Pin1wt cells as opposed to Pin1^{-/-} cells. This was accompanied by a statistically significant increase in both t_{50} and t_{90} values. Upon kinetic modeling of the FRAP curves, however, we observed that the only kinetic parameter to change was the effective diffusion coefficient, which is decreased in the presence of Pin1. There was no significant difference detected in residence time or transition time for H1.1T152S S183A when expressed in either Pin1wt or Pin1^{-/-} cells. The change in effective diffusion coefficient implies that most of the H1.1 T152S S183A molecules are present in a low-affinity chromatin bound state in the presence of Pin1, following a transition from the freely diffusing pool.

Next, we substituted the Thr at position 152 to Ser, creating a double-serine H1.1 mutant T152S (Figure 4.5d). This mutant produces three distinct bands, suggesting the presence of non-phosphorylated, mono- and di-phosphorylated molecules. We observed that H1.1 T152S recovers slower in Pin1wt cells as compared to Pin1^{-/-} cells. Upon kinetic modeling, we once again observed a drop in effective diffusion coefficient, suggesting an increase in Pin1-mediated conversion from a freely diffusing population to low-affinity chromatin-bound H1 molecules. Surprisingly, H1.1 T152S fails to alter its residence time or transition time in the presence of Pin1, although this mutation does lead to an increase in the strongly bound population in the presence of Pin1.

Our results imply that the action of Pin1 on H1 dynamics is dependent upon the location of its action. Having a potential Pin1 site of action at position 152 can shift the equilibrium from freely diffusing towards a low-affinity population. On the other hand, a Pin1 substrate at site 183 can also have the effect of converting a

freely diffusing H1 molecule to a low-affinity state and keeping it in that state. Once a high affinity state is reached, Pin1 has an additional effect of stabilizing that high-affinity state, an effect that is not seen when Pin1 acts at position 152.

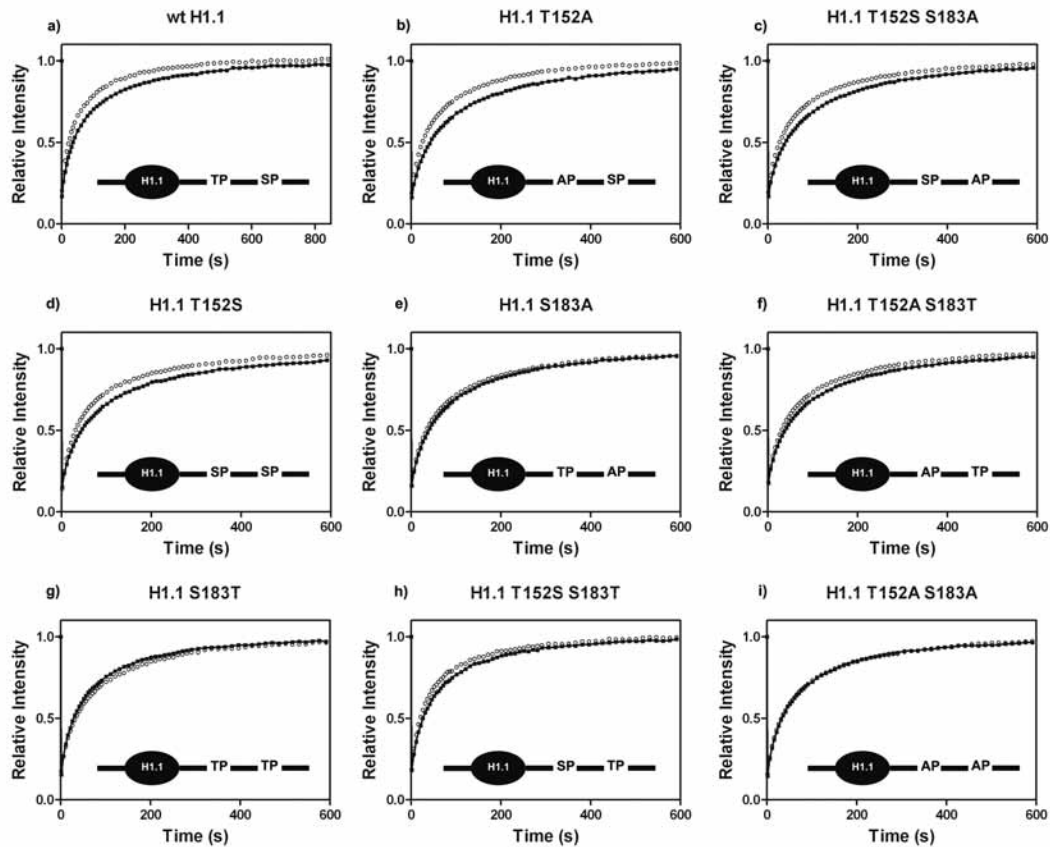


Figure 4.5 – Pin1 primarily acts at phosphorylated position S183 on H1.1. GFP H1.1 (a) or GFP H1.1 mutants (b-i) were expressed either in Pin1wt (black filled circles) or Pin1^{-/-} (open circles) cells. FRAP experiments were carried out to measure the dynamics of the H1 molecules. Each curve represents an average of approximately 20 cells (total), three independent experiments. The inset is a diagrammatic representation of the genetic alteration and relative position of serines (S), threonines (T), prolines (P) and alanines (A). Panels (b-d) allude to the role played by serine at either position 183 or 152 in contributing towards Pin1 mediated changes in H1 dynamics. Panels (e-g) show the role played by altering the Thr residue on H1.1 in Pin1 mediated changes in H1 dynamics. Panel (h) shows the recovery of H1.1 when the ser and thr positions are switched, while Panel (i) shows the lack of any change in H1 dynamics when both the ser and thr residues are changed to ala.

4.3.6 - Distinct effects of Thr at position 152 vs. 183 in H1.1

Our results lead us to conclude that the Thr at position 152 may not be phosphorylated during interphase and therefore may not be a substrate for Pin1 during interphase. We next characterized the effects of Thr further, by inserting Ala/Ser at sites where Thr is normally present in H1.1 and compared histone dynamics in Pin1^{wt} and Pin1^{-/-} cells. (The FRAP curves are shown in Figure 4.5. The t_{50} and t_{90} values and results of mathematical modeling of data obtained from these curves are shown in Supplementary Figure 4.7, Supplementary Table 4-I.)

We first mutated the Ser at position 183 to Ala, creating a H1.1S183A mutant (Figure 4.5e). Thus, any Pin1 dependent change in H1 dynamics would be caused by isomerization of TP at site 152. There was no upward mobility shift seen in Phostag gel analysis (Supplementary Figure 4.6). We observed no change in H1 dynamics when expressed either in Pin1^{wt} or Pin1^{-/-} cells. There were no statistically significant changes in t_{50} , t_{90} , effective diffusion coefficient, residence time or transition times, confirming that Thr at site 152 is not phosphorylated in interphase and, thus, is not a substrate for Pin1.

We next switched the positions of Ala and Thr to generate a H1.1T152A S183T mutant (Figure 4.5f). Once again, there were no detectable upward shifts in electrophoretic mobility, however, H1.1T152A S183T displays a statistically significant increase in t_{50} , t_{90} , and residence times in Pin1^{wt} cells compared to Pin1^{-/-} cells. However, unlike all of the Ser mutants discussed above, there were no changes in effective diffusion coefficient. The increase in residence time indicates that high affinity H1.1T152A S183T molecules bind for a longer

duration in the presence of Pin1. The change in dynamics indicate that Thr at position 183 might be phosphorylated to a low degree and could be a potential substrate for Pin1. However, the changes imparted to H1 are not as dramatic as when a Ser occupies the same position (compare H1.1T152A to H1.1T152A S183T).

Position 183 was mutated to a Thr, keeping position 152 intact, generating a H1.1 S183T mutant (Figure 4.5g). Compared to wt H1.1 and H1.1T152A, H1.1S183T had a modest change in recovery in the presence of Pin1. There were statistically significant changes to the t_{50} values and effective diffusion coefficient, while the rest of the kinetic parameters remained unchanged.

Lastly, mutation of both the Ser and Thr residues to Ala abrogated the change in H1.1 dynamics seen in Pin1^{wt} and Pin1^{-/-} cells, suggesting that at least one phosphorylation-competent residue on the H1 molecule is required in order for Pin1 to mediate changes in H1 dynamics (Figure 4.5i).

4.3.7 - Pin1 depletion relaxes chromatin and causes decondensation

Several *in vitro* experiments have shown the pivotal role played by H1 in condensing chromatin (Bednar et al, 1998; Carruthers et al, 1998). Changes in histone H1 levels and changes in H1 phosphorylation levels have been shown to cause changes in the level of chromatin condensation (Fan et al, 2005; Herrera et al, 1996; Roth & Allis, 1992). Polynucleosomes extracted from cells with an approximately 50 percent reduction of H1, as a result of knockout of three of the 6 somatic H1 subtypes, were found to be heterogeneous and less compact (Fan et al, 2005), while higher levels of H1 phosphorylation corresponded to increased

nuclease sensitivity to chromatin (Chadee et al, 1995; Herrera et al, 1996). We hypothesized that if Pin1 could alter H1 dynamics then it could also alter chromatin condensation levels. In order to test this, Pin1^{-/-} and Pin1wt cells were imaged by transmission electron microscopy (TEM) and examined for differences in chromatin ultrastructure (Figure 4.6 A, B). In contrast to Pin1wt cells, we found that the euchromatin in Pin1^{-/-} cells had a more dispersed appearance. (Figure 4.6 C, D). A line scan of approximately 2µm in length drawn across the nucleus showed that Pin1wt cells had a high frequency of peaks (chromatin fibers) compared to Pin1^{-/-} cells (Figure 4.6E, F). This suggested that there was a reduction in the efficiency with which higher order chromatin structures were formed in the nucleus. Fourier transformation of 2D high-resolution images (n=36) from both Pin1^{-/-} cells and Pin1wt cells was carried out and the resulting power spectra plotting the intensity of the signal at a particular spatial frequency is shown in Figure 6G. The analysis demonstrates that the major differences in chromatin structure between Pin1^{-/-} cells and Pin1wt cells arise in the region between 10-30nm range, with Pin1wt cells having a higher frequency of these structures compared to Pin1^{-/-} cells.

We then analyzed whether knockdown of Pin1 can induce chromatin decondensation in living cells. This is of particular relevance to processes such as transcription, which has been shown to induce chromatin decondensation (Elgin, 1990; Ericsson et al, 1989; Hu et al, 2009; Tumber et al, 1999). In order to study the role of Pin1 in chromatin decondensation *in vivo*, we used the lac array system developed by the Belmont lab and, more specifically, an array system constructed

by the Spector and Janicki labs (Janicki et al, 2004; Rafalska-Metcalf et al, 2010; Robinett et al, 1996; Tsukamoto et al, 2000). The system is comprised of 256 repeats of the lac operon, followed by 96 repeats of tet-responsive elements that are upstream of a minimal CMV promoter, which drives transcription of the CFP-SKL gene. Transcription is activated by adding Tamoxifen, which binds mcherry-ER-tTA causing it to relocalize to the nucleus and bind the tet-responsive elements and subsequent RNA Polymerase II accumulation (Rafalska-Metcalf et al, 2010), (Supplementary Figure 4.9). To visualize transcriptionally inactive chromatin, we transfected cells with mcherry-LacR alone (Rafalska-Metcalf et al, 2010). In accordance with published literature, we observed that transcriptionally elongating chromatin was more decondensed compared to chromatin in a transcriptionally inactive state (Hu et al, 2009; Janicki et al, 2004; Muller et al, 2001; Rafalska-Metcalf et al, 2010; Robinett et al, 1996; Tumber et al, 1999) (Supplementary Figure 4.10). The transcriptionally activated lac-array occupied an approximately 40% greater nuclear volume compared to its transcriptionally inactive state. Chromatin decondensation was strictly dependent on elongation induced by RNA Polymerase II. Overnight treatment with α -amanitin (Supplementary Figure 4.9) completely abolished the decondensation induced by targeting mcherry-ER-tTA to the lac arrays (Figure 8A)(Muller et al, 2001). Pin1 knockdown had a maximal effect on the nuclear volume occupied by the lac arrays (Figure 6H). Under reduced Pin1 levels, the lac arrays increased in volume by approximately 40%, compared to Pin1 proficient cells. Similarly, after induction of transcription, the nuclear volume occupied by the arrays in Pin1-

deficient cells was 40% higher than the transcriptionally active locus in Pin1 proficient cells.

Our results analyzing the chromatin ultrastructure as well as results measuring the chromatin condensation state in living cells reveal an important role for Pin1 in maintaining a more compact chromatin structure in both transcriptionally inactive and transcriptionally active genes.

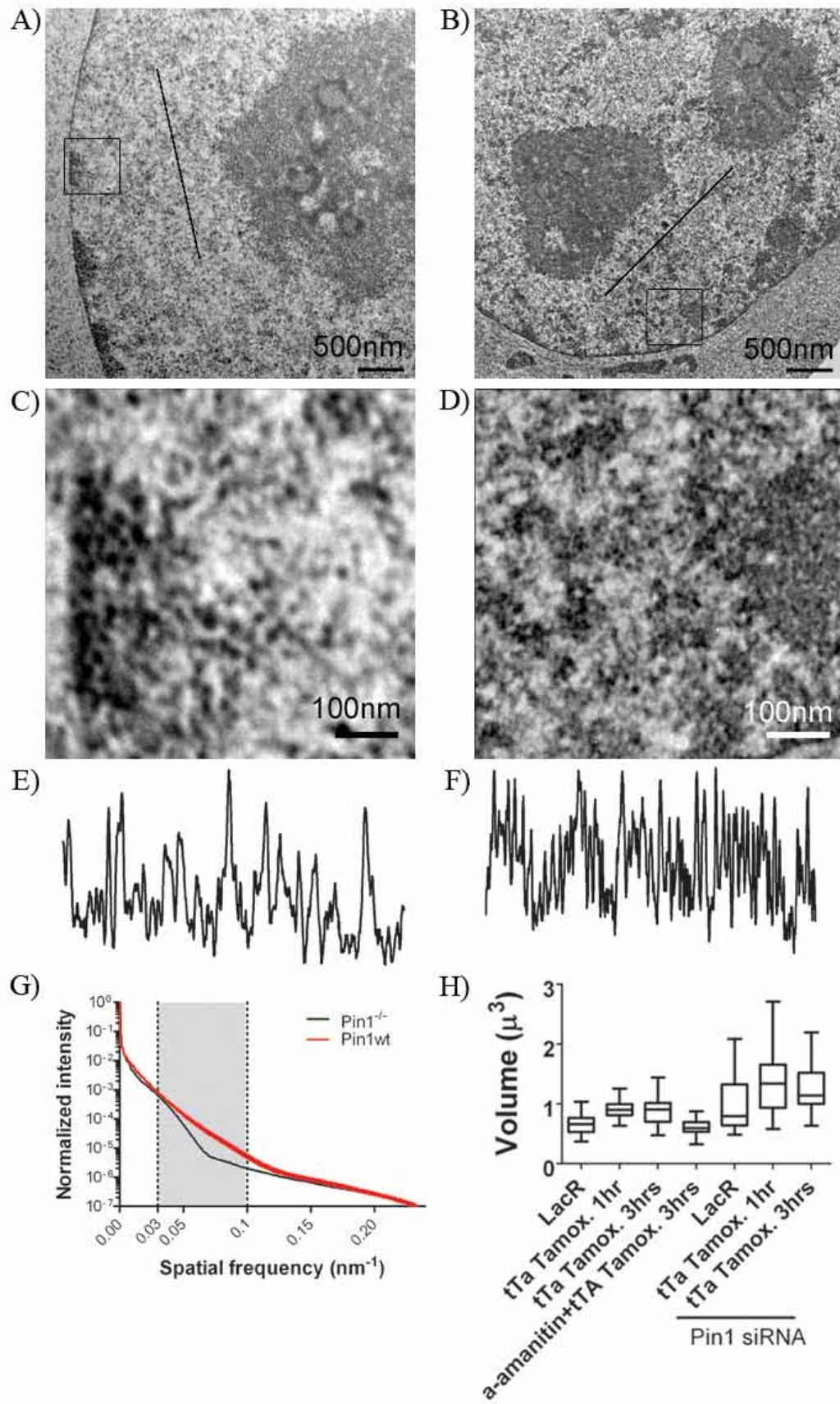


Figure 4.6 – Pin1^{-/-} cells have a relaxed chromatin structure. The chromatin structure of Pin1^{-/-} cells (A) and Pin1wt cells (B) were analyzed by TEM. The same images in much greater detail can be viewed below. Panels (C) and (D) show the chromatin morphology of the boxed region in panel (A/B), in greater detail. Pin1^{-/-} cells have a more homogenous appearance in the region surrounding the heterochromatin. A line scan drawn across the nucleus in panel (A/B) is shown in panel (E) and (F), and demonstrates the coarse texture of chromatin present in Pin1wt cells. Similar 2D high-resolution images of Pin1^{-/-} and Pin1 wt cells were then analyzed by Fourier transformation and rotationally averaged to yield a one-dimensional plot of the power (normalized intensity \pm SEM) and spatial frequency (reciprocal nm). Much of the deviation in the power spectra of Pin1^{-/-} cells and Pin1wt cells occur in the range of 10-30nm, with Pin1wt cells having a higher frequency of these structures. (H) U2OS 263 cells harboring the lac-arrays were transfected with mcherry-LacR or mcherry-ER-tTA. The volume occupied by the arrays was measured in both the transcriptionally inactive state (mcherry-LacR alone) and in the transcriptionally active state (addition of Tamoxifen to cells expressing mcherry-ER-tTA for either 1hr/3hrs). Volume was measured through rapid acquisition of z-stacks in living cells. While transcription caused an increase in the volume occupied by the arrays, treatment of cells with α -amanitin led to compact arrays. Both transcriptionally active and inactive arrays were found to occupy larger volumes when Pin1 was depleted by Pin1siRNA treatment.

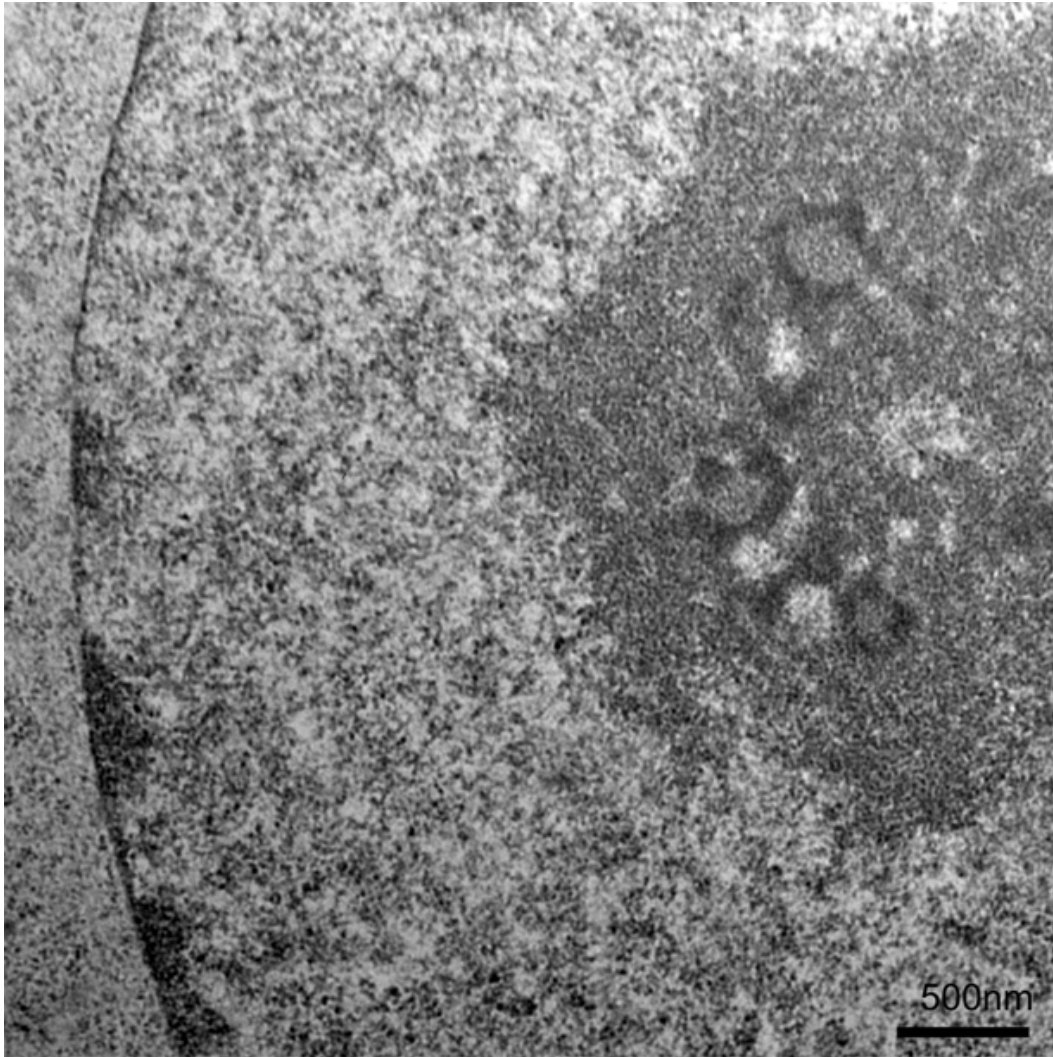


Figure 4.6 (A) – Ultrastructure of Pin1 knockout cell. EM of Pin1 knockout cells show decondensed chromatin architecture and homogenous appearance of chromatin fibers, compared to Pin1 wild-type cells. One factor that might contribute to such a phenotype might be the reduced binding of histone H1 molecules. H1 has been shown to be a key architectural protein that stabilizes the folding of the 30nm chromatin fiber.

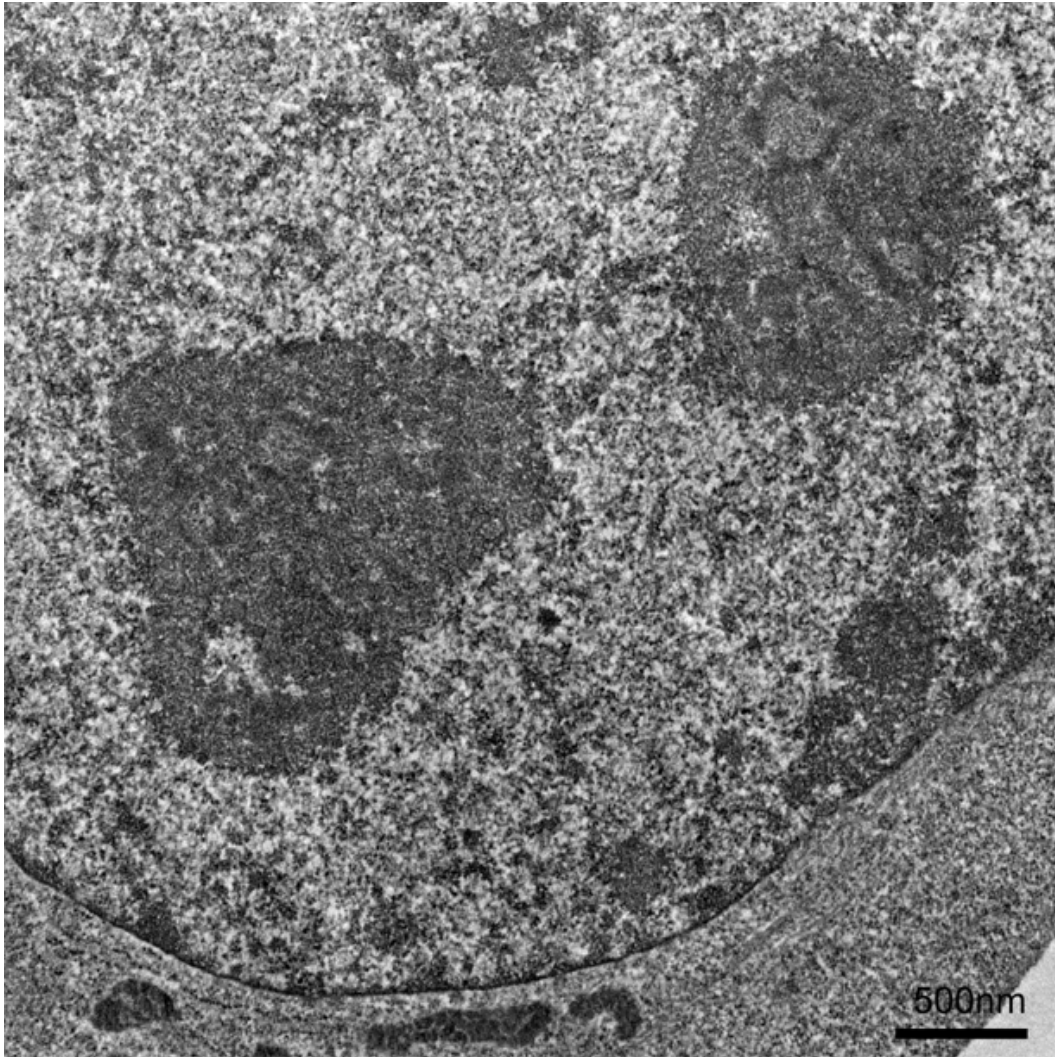


Figure 4.6 (B) – Ultrastructure of Pin1wt cell. The ultrastructure of Pin1 wild-type cells shows a heterogeneous or coarse chromatin structure, compared to Pin1 knockout cells (previous image) that are more homogeneous or "smooth" in appearance.

4.3.8 - Role of Pin1 in transcription

Phosphorylated histone H1 molecules are enriched at sites of active transcription and *in vitro* studies show that phosphorylation of H1 is one of the prerequisite steps for gene induction (Koop et al, 2003; Vicent et al, 2011; Zheng et al, 2010). In addition, Pin1 interacts with proteins involved in transcription, most notably RNA Polymerase II (RNA Polymerase II) (Xu & Manley, 2007b). We quantified the levels of Pin1, H1 phosphorylation and the dynamics of H1 at transcriptionally silent vs. active chromatin to determine how Pin1 modulated these events associated with transcription.

Upon activation of transcription, we found that there was at least a 2-fold increase in the levels of H1 phosphorylation at the lac arrays (Figure 4.7, Supplementary Figure 4.8). This increase was significantly higher than H1 phosphorylation levels seen at transcriptionally inactive sites, using mcherry-LacR as a marker. This is consistent with several *in vitro* as well as *in vivo* studies (Dou et al, 1999; Koop et al, 2003; Zheng et al, 2010). Surprisingly, we found that the increase in H1 phosphorylation levels was independent of transcript elongation by RNA Polymerase II, since overnight pre-treatment with α -amanitin prior to the activation of transcription by Tamoxifen led to the accumulation of high levels of H1 phosphorylation at the lac arrays (Figure 4.7, Supplementary Figure 4.9).

Consistent with the increase in H1 phosphorylation, we also observed an increase in the relative amounts of Pin1 at sites of transcription (Figure 4.7, Supplementary Figure 4.8). The modest increase in Pin1 is significant given the high abundance of Pin1 in the nucleus. The increase in Pin1 was also independent of RNA

Polymerase II, since overnight treatment with α -amanitin prior to the addition of Tamoxifen led to high levels of Pin1 being targeted to the mcherry-ER-tTA sites. This suggests that Pin1 accumulation and an increase in H1 phosphorylation are marks of transcriptionally competent chromatin.

In order to analyze H1 mobility at sites of transcription, we co-transfected GFP-H1.5 and mcherry-ER-tTA in cells housing the lac arrays (Figure 4.8A). Following addition of Tamoxifen (1hr/3hrs), a circular spot of 0.7 μ m diameter was photobleached and the intensity of GFP-H1.5 was monitored over time. The region photobleached coincided with the mcherry-ER-tTA region within the nucleus, while a second circular spot of the same dimension and Y-axis position was simultaneously photo-bleached and served as an internal control. To control for transcription-dependence, parallel experiments were done in cells co-transfected with mcherry-LacR and GFP-H1.5, conditions where the array is not transcriptionally active. H1 kinetics, measured by FRAP is shown in Figure 4.8C, while the t_{50} values obtained from these curves is shown in Figure 4.8B.

First, we measured the kinetics of H1.5 at the lac arrays in the absence of transcriptional stimulation (Figure 4.8Ci). H1.5 kinetics was only slightly faster at the arrays compared to internal control. We next stimulated transcription at the arrays by transfecting mcherry-ER-tTA and incubating these cells in the presence of Tamoxifen for 1hr/3hrs. Despite the increase in levels of Pin1, H1 phosphorylation and decondensed chromatin following the addition of Tamoxifen (1hr/3hrs), we found H1 mobility to be similar to that observed in transcriptionally inactive chromatin (Figure 4.8C ii,iii). For example, following

1hr of transcriptional activation at the lac-arrays, H1.5 was found to bind more stably than that observed at transcriptionally silent chromatin (Figure 4.8B, 4.8Cii). However, after a longer treatment with Tamoxifen (3hrs), there was no difference in the FRAP recovery profiles of H1.5 observed at transcriptionally inactive vs. transcriptionally elongating chromatin (Figure 4.8B, 4.8Ciii). This trend was seen with other variants of H1, such as GFP-H1.1 and GFP-H1.2, which are enriched in euchromatin (Th'ng et al, 2005). The mobility of these molecules remains unchanged following activation of transcription (Supplementary Figure 4.11).

Our earlier experiments suggested that Pin1 played a role in modifying chromatin as well as in stabilizing H1 binding. We next wished to determine whether reducing the level of Pin1 would destabilize H1 at sites of transcription. Using siRNA directed against Pin1, we reduced Pin1 to 50-60% of its original level. Under these conditions, there was a statistically significant increase in the phosphorylation levels of H1 at transcriptionally inactive chromatin (Supplementary Figure 4.8). Note that this increase was in the absence of any transfected transcriptional activators, such as mcherry-ER-tTA. This suggested that Pin1 depletion was able to increase the steady-state levels of H1 phosphorylation, consistent with our earlier observation in Pin1^{-/-} cells. When transcription was induced in Pin1 siRNA-treated cells through transfection of mcherry-ER-tTA and Tamoxifen, H1 phosphorylation was found to further increase to levels seen in Pin1 proficient cells. This suggested that Pin1 had no

effect on the activity of the enzyme that phosphorylates H1 during transcriptional induction, namely Cdk2.

We then analyzed the dynamics of H1 at transcriptionally inactive vs. active sites (Figure 4.8B, 4.8C iv-ix). We found H1.5 mobility at the arrays to be similar to the internal controls (chromatin sites away from the lac arrays) irrespective of whether the site was transcriptionally active or not (Figure 4.8B, 4.8C iv-vi). A major difference in H1 mobility was seen when the kinetics were compared in Pin1-proficient cells compared to Pin1-deficient cells (Figure 4.8B, 4.8C vii-ix). This difference was maintained irrespective of transcriptional status. Our results imply that Pin1 plays a role in promoting chromatin condensation and stabilizing H1 binding at both transcriptionally active and inactive chromatin sites.

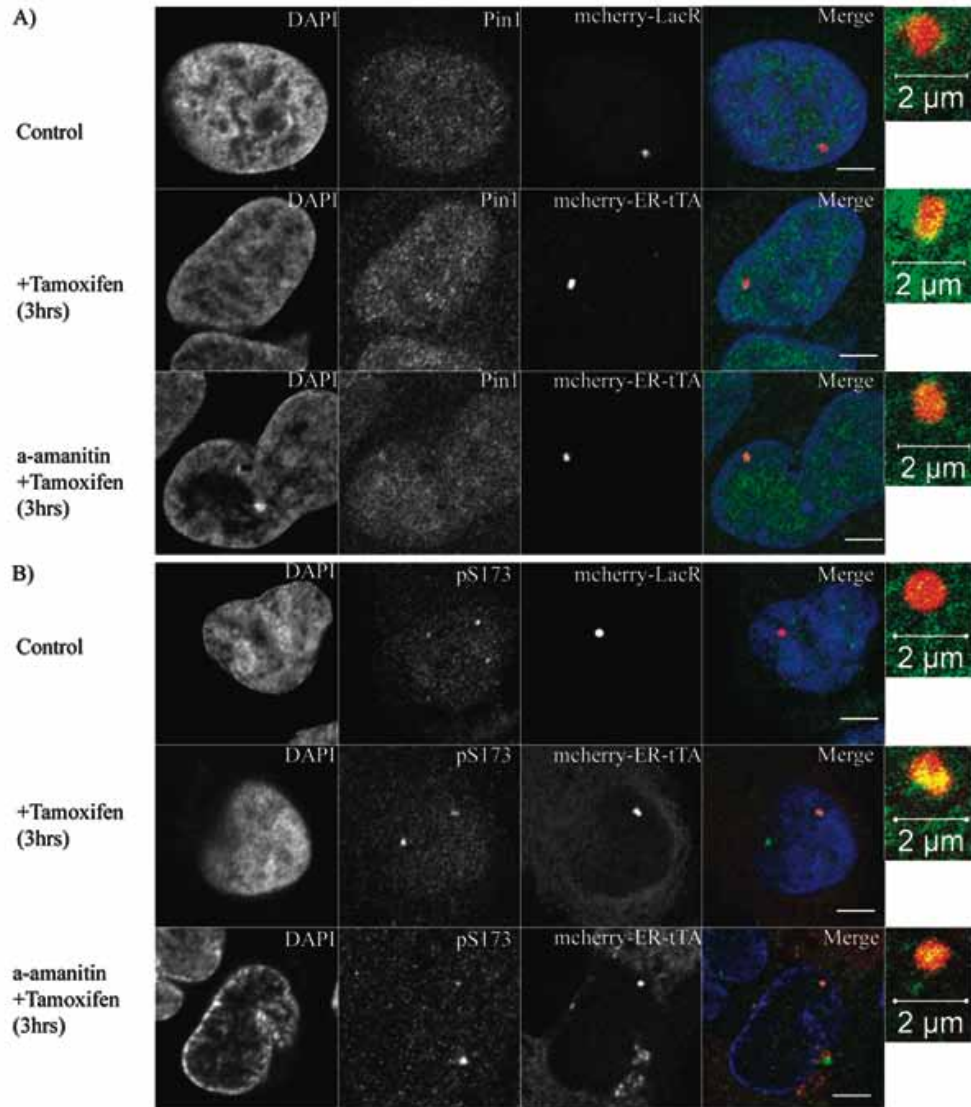


Figure 4.7 – Pin1 and H1 phosphorylation are marks of transcriptionally competent chromatin. U2Os 263 cells harboring lac arrays followed by TRE, CMV promoter, and CFP-SKL gene were either transfected with mcherry LacR or mcherry ER-tTA. The former represented the transcriptionally inactive state while addition of Tamoxifen (3hrs) to the latter represented the transcriptionally active state of chromatin. Pin1 levels (A) and pS173H1.2 levels (B) were measured using immunofluorescence. Both Pin1 and pS173H1.2 levels were found to increase at sites of active transcription. α -amanitin, was used to deplete RNA Polymerase II levels in the cells. When transcription was activated in these competent, yet transcriptionally silent cells, Pin1 and H1 phosphorylation levels were elevated suggesting that these were early events in the initiation of transcription. Unless otherwise specified, scale bar represents 5 μ m.

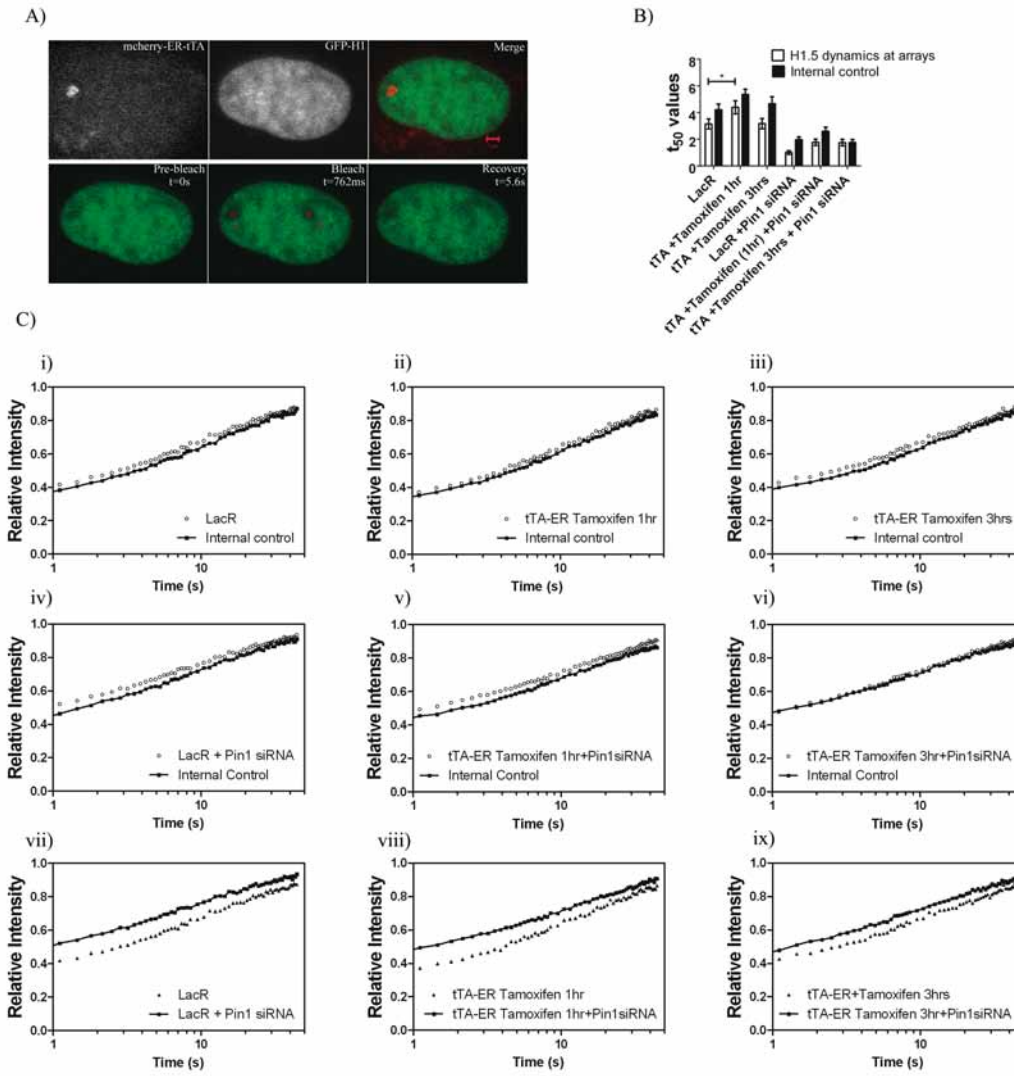


Figure 4.8 – Pin1 stabilizes H1 binding at sites of transcription. (A) GFP-H1.5 was co-transfected with either mcherry LacR or mcherry-ER-tTA in U2OS 263 cells harboring the arrays. H1 dynamics were monitored using FRAP with two separate regions in the nucleus being photo-bleached. One bleached region corresponded to either the mcherry LacR (transcriptionally inactive site) or mcherry-ER-tTA (transcriptionally active site) and photo-bleached region 2 corresponded to a random site within the nucleus in the same horizontal plane. (B) T_{50} values of the FRAP curves (C) show that H1.5 dynamics at the lac arrays is fairly similar to those of internal controls, in the transcriptionally uninduced state (Ci) The same trend is seen even when transcription is stimulated by transfection of mcherry-ER-tTA and Tamoxifen is added for either 1hr (Cii) or 3hrs (Ciii). Similar experiments were carried out in cells treated with Pin1siRNA (Civ-Cvi). Major differences in H1 mobility can be observed when comparing the recovery rate in Pin1 proficient cells vs. those seen in Pin1 deficient cells (Cvii-ix). The increase in H1.5 dynamics upon Pin1 depletion is independent of transcriptional activity.

4.4 - Discussion

In this study, we have shown an interaction between phosphorylated H1 molecules and Pin1 and have examined the implications of this interaction. We define a novel role for Pin1 in interphase as a chromatin modifier, through its association with histone H1. Lack of Pin1 lead to a relaxed, decondensed chromatin structure, which was coupled with reduced H1 retention on chromatin and reduced turnover of the phosphorylated state of H1. At transcriptionally active sites, where both H1 phosphorylation and Pin1 levels are elevated, Pin1 serves to stabilize the binding of H1 and correlated with a reduction in chromatin decondensation.

4.4.1 - Histone H1 interacts with Pin1

Our current understanding of how H1 phosphorylation affects its binding centers around electrostatic repulsions between negatively charged phosphorylation residues and the high degree of negative charge associated with the DNA backbone (Dou et al, 2002; Dou & Gorovsky, 2000). Our data favor a model that is a product of several biophysical studies describing the CTD of H1 as intrinsically disordered (Clark et al, 1988; Hansen et al, 2006; Roque et al, 2005; Roque et al, 2008; Roque et al, 2007). The CTD condenses and acquires classical secondary structures such as α -helices and β -sheets upon interaction with DNA or nucleosomes (Caterino et al, 2011; Fang et al, 2011; Roque et al, 2005). Interestingly, the proportions of CTD secondary structures appear to be dependent upon the phosphorylation status of H1 (Roque et al, 2008). The acquisition of structure is thought to further determine the strength of H1 binding to chromatin,

with high affinity H1 particles having a more folded structure compared to freely diffusing molecules (Misteli et al, 2000; Raghuram et al, 2009; Stasevich et al, 2010). In this study, we have shown that Pin1, through its interaction with the phosphorylated residues on H1, can modulate the conformation of the CTD, thereby influencing the binding dynamics of H1. We previously showed that variants of H1 bind chromatin with differing affinity, where the affinity roughly correlates with the length of the CTD (Hendzel et al, 2004). This correlation can be further extended to the residues that are phosphorylated on H1. For example, in interphase, H1.1 is mono-phosphorylated, while H1.5 can exist as a tri-phosphorylated species (Sarg et al, 2006). This implies that the higher the number of phosphorylated residues on H1, greater is the amount of stabilization mediated by Pin1. This argument is consistent with the fact that H1.5 has a much higher residence time compared to H1.1.

We have demonstrated that Pin1 and histone H1 interact with each other only when H1 is phosphorylated. This interaction leads to a conformation of the H1 CTD that is more conducive for dephosphorylation by PP2A, thereby causing a reduction in the half-life of H1 phosphorylation in Pin1wt cells

4.4.2 - Pin1 as a chromatin modifier

Histone H1 has been shown to stabilize chromosome architecture and play a crucial role in the formation of the 30nm chromatin fiber (Bednar et al, 1998; Carruthers et al, 1998; Robinson et al, 2006; Robinson & Rhodes, 2006; Woodcock et al, 2006). Elegant single-molecule force spectroscopy experiments have shown that binding of H1 increases the mechanical stability of the chromatin

fiber (Kruithof et al, 2009). It has long been known that in native and reconstituted chromatin, phosphorylation of H1 destabilizes chromatin structure (Hill et al, 1991). In this study, we have shown that depletion of Pin1 leads to an increase in H1 phosphorylation levels and more rapid H1 dynamics, as analyzed by FRAP.

We also find that Pin1 promotes chromatin condensation in both a model gene array system and by transmission electron microscopy of Pin1 wild type and Pin1 null cells. Pin1 has previously been shown to participate in chromosome condensation (Xu & Manley, 2007c). This effect was attributed to a role in regulating the association of TopoII α with chromosomes (Xu & Manley, 2007c). However, Histone H1 is also required for chromosome condensation (Maresca et al, 2005) and mitosis is a period of maximal H1 phosphorylation. Thus, the regulation of histone H1 represents an alternative or additional target of Pin1 that may mediate requirement in mitotic chromosome condensation. Similarly, other targets that could contribute to the Pin1-mediated regulation of interphase chromatin structure that we observe. Given the ubiquitous nature of both Pin1 and histone H1 in the nucleus, coupled with the classical role ascribed to H1 in condensing chromatin and maintaining 30nm chromatin fibers, the simplest explanation is that the interaction of Pin1 with H1 is an important factor in regulating chromatin condensation. This is consistent with Pin1-mediated phosphorylation-dependent changes in the H1 CTD that we observed by FRET *in vitro*. The role of Pin1 as a chromatin modifier is consistent with recent developments in the field where a member of FKBP class of prolyl-isomerases

(Fpr4 in yeast) was able to alter transcription and chromatin through its histone (H3, H4) isomerase activity (Nelson et al, 2006). Our study adds Pin1, a member of the Parvulin class of peptidyl-isomerases, into this list of histone isomerases.

4.4.3 - Histone H1 phosphorylation, Pin1 and transcription

A well-characterized target of Pin1 in transcription is the CTD of RNA Polymerase II. Pin1 modulates the CTD phosphorylation status and, thus, RNA Polymerase II activity. Here we show that Pin1 recruitment to sites of transcription is independent of RNA Polymerase II. The increase in Pin1 parallels the increase in H1 phosphorylation at these transcriptionally competent sites. Increases in H1 phosphorylation during the early stages of transcriptional initiation may act to recruit Pin1 to these sites. The recruitment of Pin1 establishes a dynamic cycle of H1 phosphorylation and dephosphorylation at sites of transcription.

It has been a decade since the rapid mobility of H1 in the nucleus was established (Lever et al, 2000; Misteli et al, 2000). However, our immunofluorescence experiments demonstrate a localized increase in H1 phosphorylation upon induction of transcription, despite its rapid mobility. A similar result was obtained when LacR-Cdk2 was targeted to Lac arrays, wherein H1 phosphorylation increased locally as opposed to the spreading of H1 phosphorylation from a focal point (Alexandrow & Hamlin, 2005). These data collectively confirm the stringent spatial regulation of H1 phosphorylation and dephosphorylation *in vivo*. The early recruitment of Pin1 to sites of transcription helps to promote H1

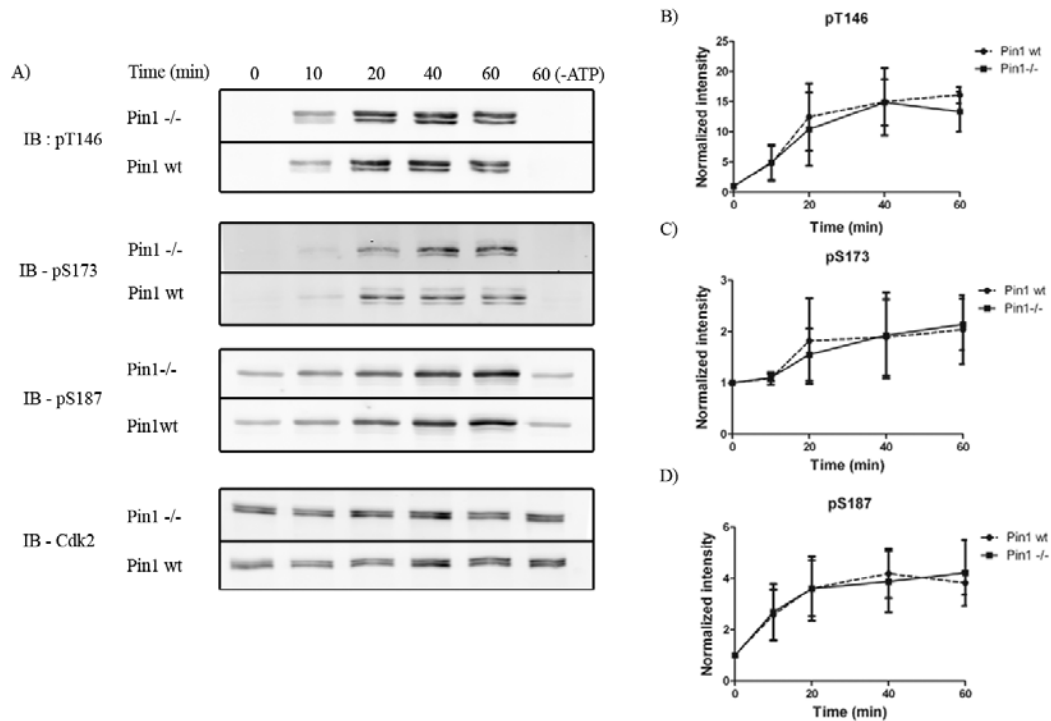
dephosphorylation and stabilize its binding, a mechanism that may prevent inappropriate transcriptional activation of adjacent genes.

The lack of any real change in H1 dynamics when chromatin is subject to strong transcriptional activators contradicts *in vitro* experiments that suggest H1 to be displaced upon initiation of transcription. This, however, could be due to the limitations of *in vitro* systems to replicate *in vivo* complexity. In recent *in vitro* transcription assays where such complexity was established using reconstituted chromatin assembled from purified core histones, H1, and histone chaperones (Li et al, 2010), the level of compaction approximated that of the 30nm fiber and H1 molecules were found to be present throughout a complete cycle of elongation, including the preceding changes to chromatin that are associated with transcriptional activation (Li et al, 2010). These results complement electron microscopy data showing H1 to be present in all stages of transcription from the Balbiani ring genes (Ericsson et al, 1990). The presence of H1 from initiation to elongation, even at very high frequencies of transcription (1 Polymerase II enzyme/100bp of DNA) suggests a role for H1 in the process of transcription (Ericsson et al, 1990). Furthermore, *in vivo* transcription of a model DHFR gene has been shown to occur in chromatin structures that were much more condensed than a 30nm fiber (Hu et al, 2009; Tumber et al, 1999). Induction of transcription did lead to decondensation, however, the resulting chromatin was significantly more compact than expected of a 30nm fiber conformation (Hu et al, 2009).

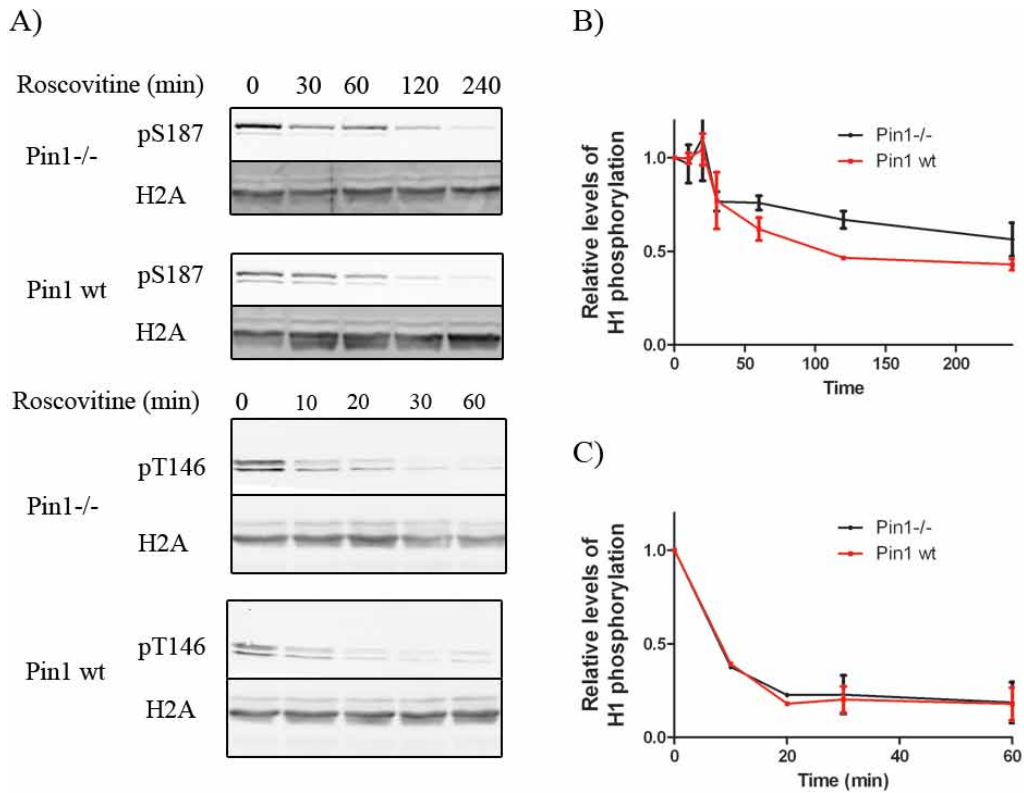
Pin1 could play a pivotal role in stabilizing H1 at transcriptionally active sites. Reduction in the level of Pin1 led to an increase in H1 mobility that was

accompanied by chromatin decondensation. Transcriptionally active regions undergo an additional increase in chromatin decondensation that parallels a further increase in H1 phosphorylation. Furthermore, transcriptionally active regions in Pin1 competent cells bind H1 with a higher affinity compared to Pin1 deficient cells, suggesting that Pin1 could play a role in stabilizing H1 at sites of transcription. However, it remains to be seen if additional factors play a role in this process, or if it is a direct consequence of Pin1 acting on H1.

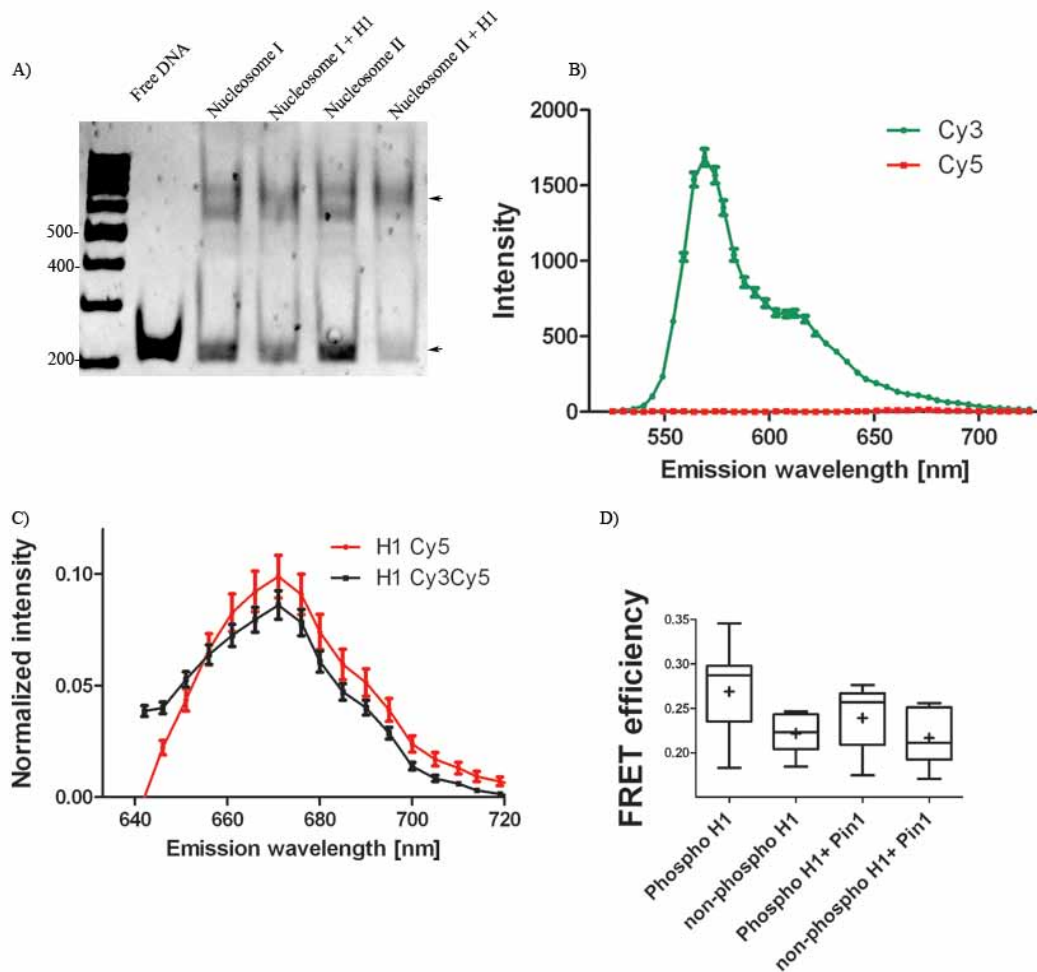
4.5 – Supplementary Figures



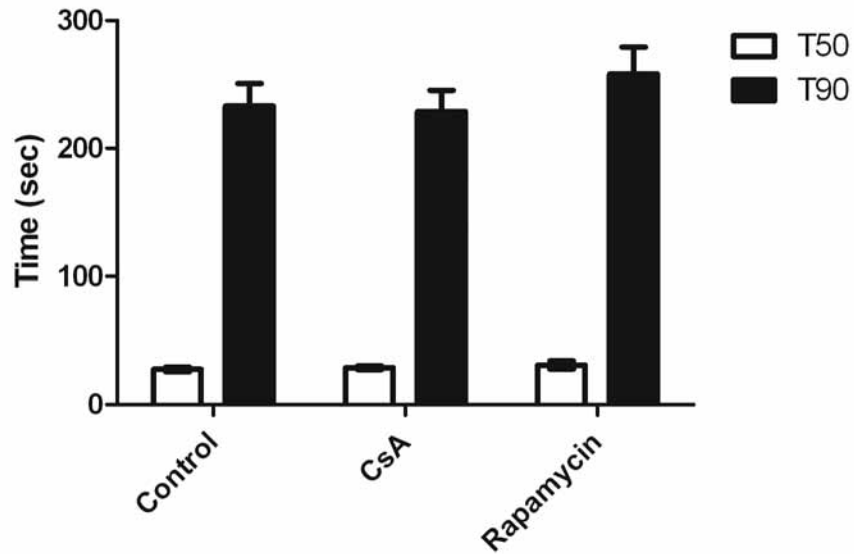
Supplementary Figure 4.1 – Activity of Cdk2 extracted from Pin1wt and Pin1^{-/-} cells. (A) Cdk2 was immunoprecipitated from either Pin1^{-/-} cells or Pin1 wt cells and diluted in H1 kinase buffer along with purified H1^{+/-} ATP. The phosphorylation reaction was stopped at regular time intervals with the addition of SDS loading buffer. The extracts were then run on 18% acrylamide gels and probed for changes in pT146, pS173, and pS187 levels. The changes in the intensity are plotted in (B-D), with the intensity measured at time zero, set to 1.



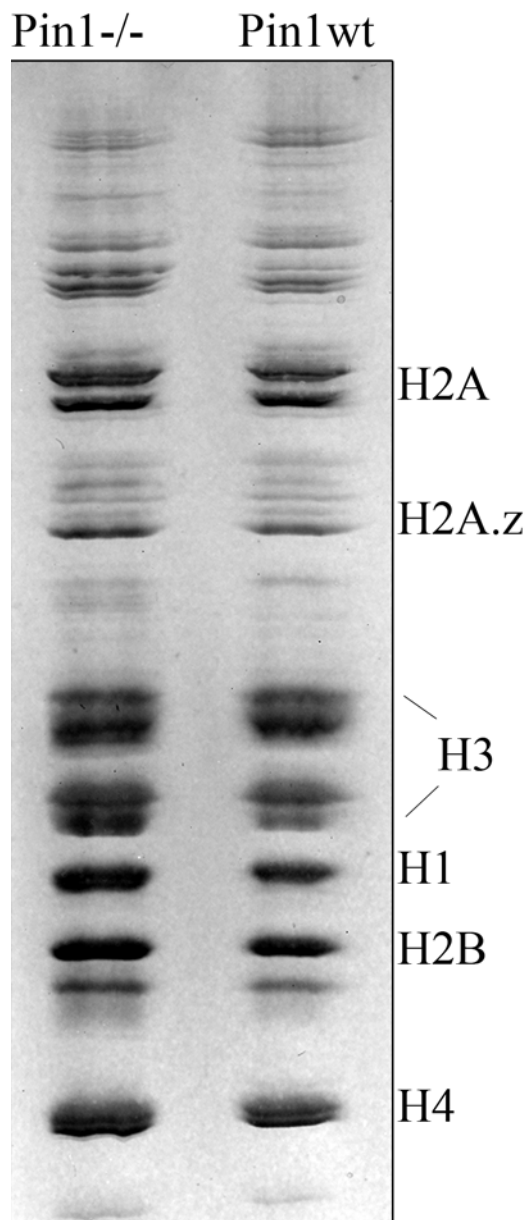
Supplementary Figure 4.2 – Pin1 promotes H1 dephosphorylation of Ser residues *in vivo*. (A) Pin1^{-/-} cells and Pin1 wt cells were treated with roscovitine for defined time intervals, following which the nuclei were harvested. Histones were extracted using 0.4N H₂SO₄ and run on 18% acrylamide gels. Blots were probed against pS187 levels and pT146 levels. H2A was used as a loading control. (B) Plot of pS187 levels and pT146 (C) against duration of Roscovitine treatment. Note that the H1 levels are corrected for load and normalized such that intensity measured at time zero was set as 1.



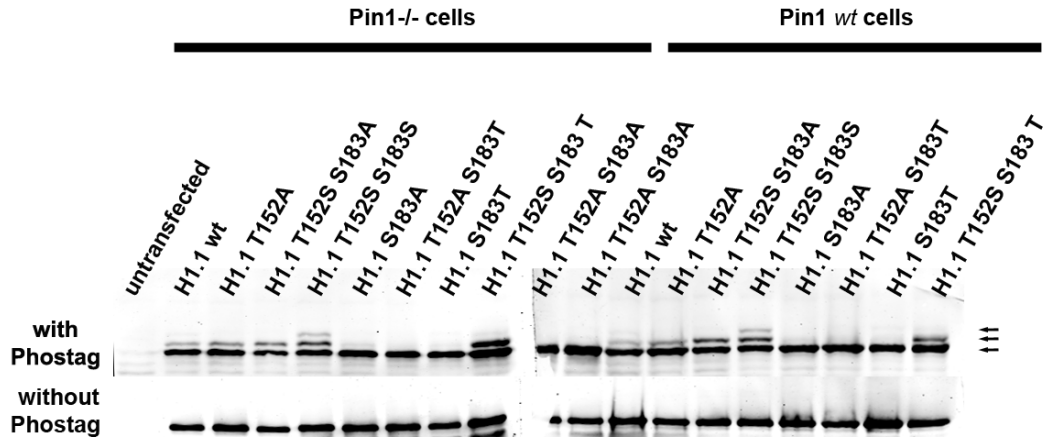
Supplementary Figure 4.3 – FRET controls and FRET efficiency. (A) Nucleosome reconstitution was carried out as described in materials and methods. Free DNA and two different batches of reconstituted nucleosomes were run on 5% native gels with 0.5%TBE running buffer. H1Cy3Cy5 were added in a 1:1 molar stoichiometry in samples run on lanes (4 and 5). Addition of nucleosomes causes a characteristic shift in the migration of DNA around 600bp mark. (B) H1Cy3 and H1 Cy5 emission spectra when excited with 514nm laser. Note that there is very little emission of Cy5 at the 671nm range (peak for Cy5), while there is a slight “shoulder” still present for Cy3 emission spectra at this wavelength. (C) H1Cy5 and H1Cy3Cy5 emission spectra when excited at 633nm laser. Similar emission spectra suggest that the addition of a Cy3 tag does not interfere with Cy5 emission. (D) Changes in FRET efficiencies upon phosphorylation of H1 and addition of Pin1 in H1Cy3Cy5 constructs. Formula for the measurements can be found in materials and methods and references within. Plus sign indicates the mean while the horizontal line in between the boxes represents the median.



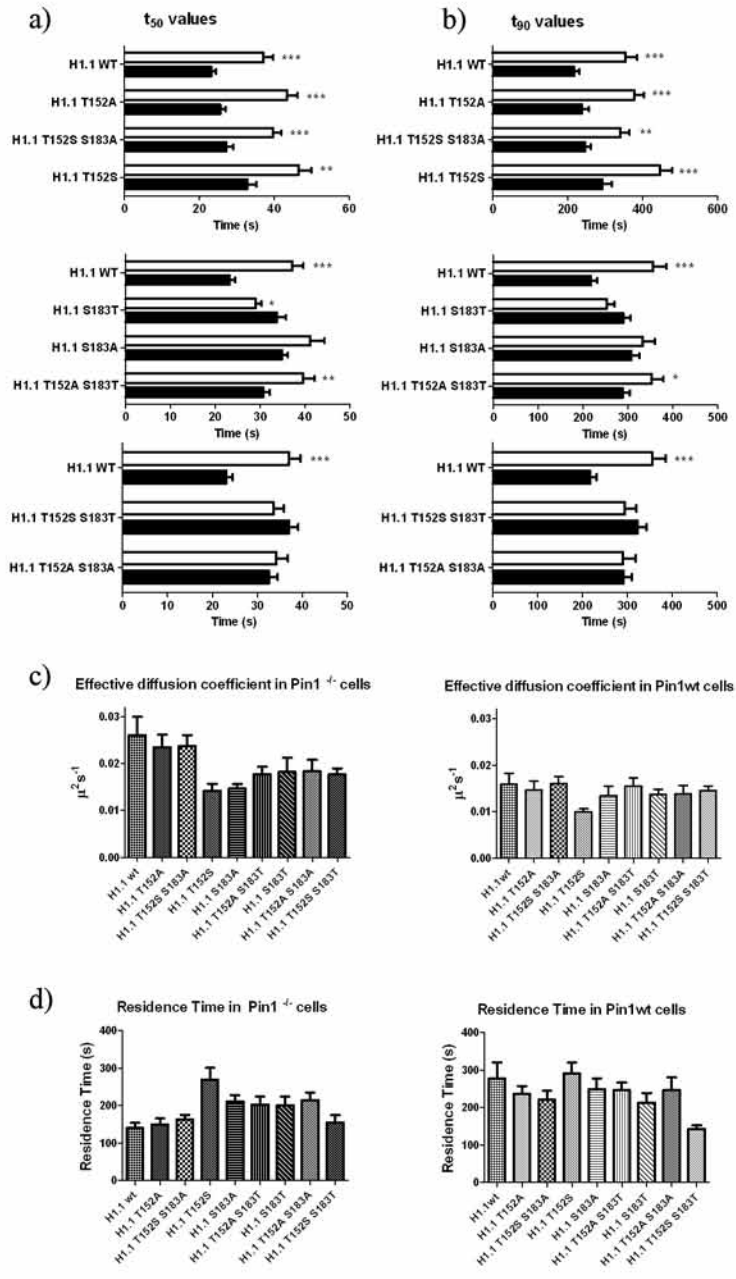
Supplementary Figure 4.4 – Effect of Cyclosporine and Rapamycin on H1 dynamics. GFP H1.1 was transfected in 10T1/2 mouse embryonic cells and were treated with either 1hr of Cyclosporine A or Rapamycin following which H1 dynamics was measured with FRAP. T_{50} and t_{90} values were quantified, however, there were no statistically significant changes in the dynamics of H1 following such treatment.



Supplementary Figure 4.5 – Core histone and H1 composition in Pin1wt vs. Pin1^{-/-} cells. Histones were extracted from Pin1^{-/-} cells and Pin1 wt cells using 0.4N H₂SO₄ and run on an AUT gel at 200V for 3.5hrs at 4°C. Gels were then stained with coomassie brilliant blue. Core histone composition and other post-translational modifications, such as acetylation of H4 (which usually appears as ladders) were found to be very similar.

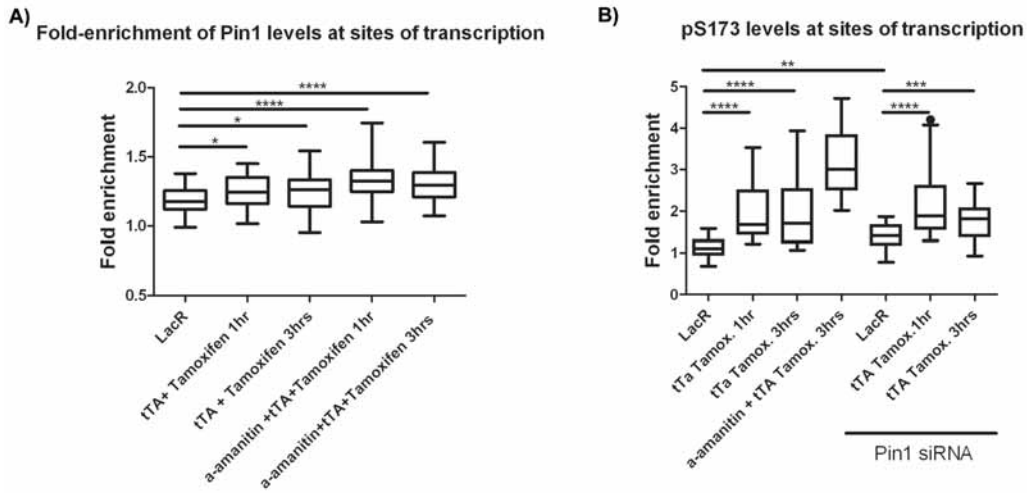


Supplementary Figure 4.6 - Mobility shift assay for detecting phosphorylated H1. FLAG tagged H1.1 wt and H1.1 mutants were transfected in Pin1^{-/-} and Pin1wt cells. Histones were then extracted using 0.4N H₂SO₄ and the extracts were then run a 10% acrylamide gel +/- Phostag. Phostag is a ligand that interacts with phosphate molecules imparting shifts in mobility. H1.1wt migrates as two distinct species in the presence of phostag, while H1.1T152S migrates as three distinct species. In the absence of Phostag, all mutants migrate as a single band.

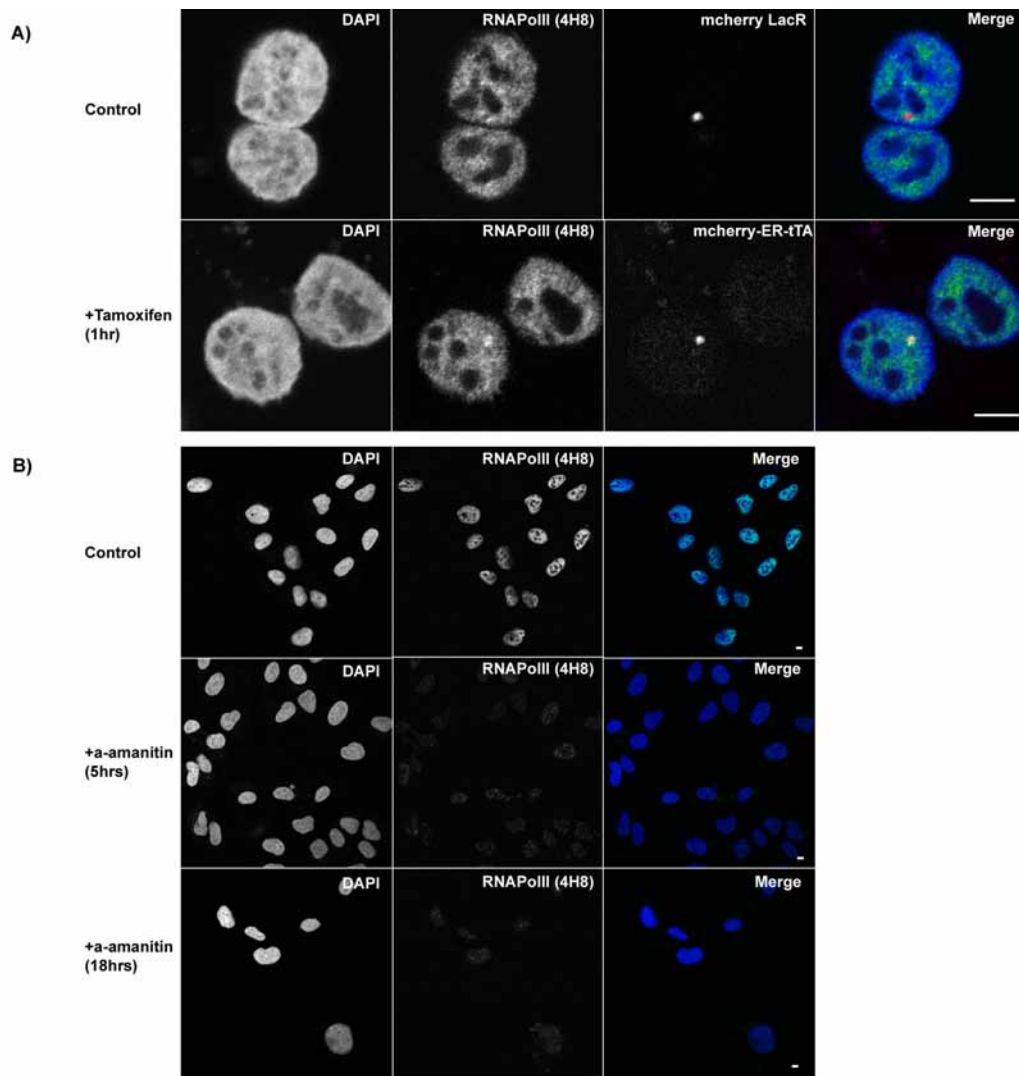


Supplementary Figure 4.7 – Mathematical modeling data derived from H1.1mut FRAP curves. (a, b) GFP-H1.1 wt and GFP-H1.1mut were transfected in Pin1wt (white bars) and Pin1^{-/-} cells (black bars) and their kinetics was analyzed by FRAP. The t_{50} and t_{90} values obtained from these FRAP curves are reported here. Student t-tests were carried out to analyze significance of the differences between data (*denotes a p-value between 0.01 to 0.05, ** denotes a p-value between 0.001 to 0.01 and *** denotes a p-value of less than 0.001). These FRAP curves were further submitted to mathematic modeling which revealed further kinetic parameters such as effective diffusion coefficient (c) and residence times of the high affinity H1 population (d) were obtained. Note that most of the changes in both these kinetic parameters stem from mutating the serine residues at position 183 or shifting the serine to position 152. These mutants have higher effective diffusion coefficient (larger pool of freely diffusing or low-affinity H1 population) and shorter residence time in the absence of Pin1, compared to their Pin1wt counterparts.

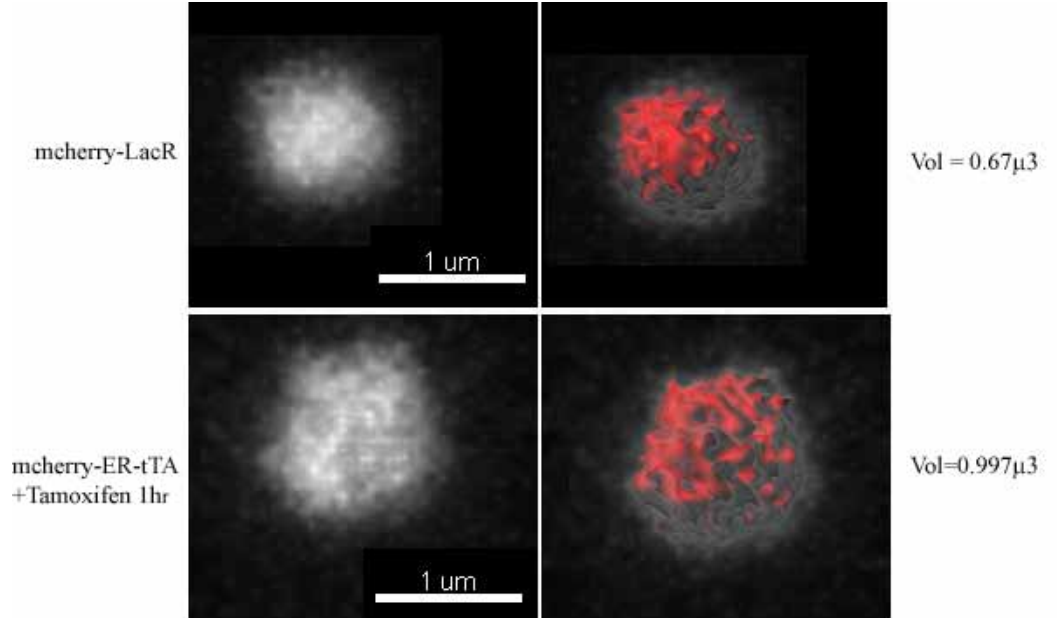
Supplementary Figure 9



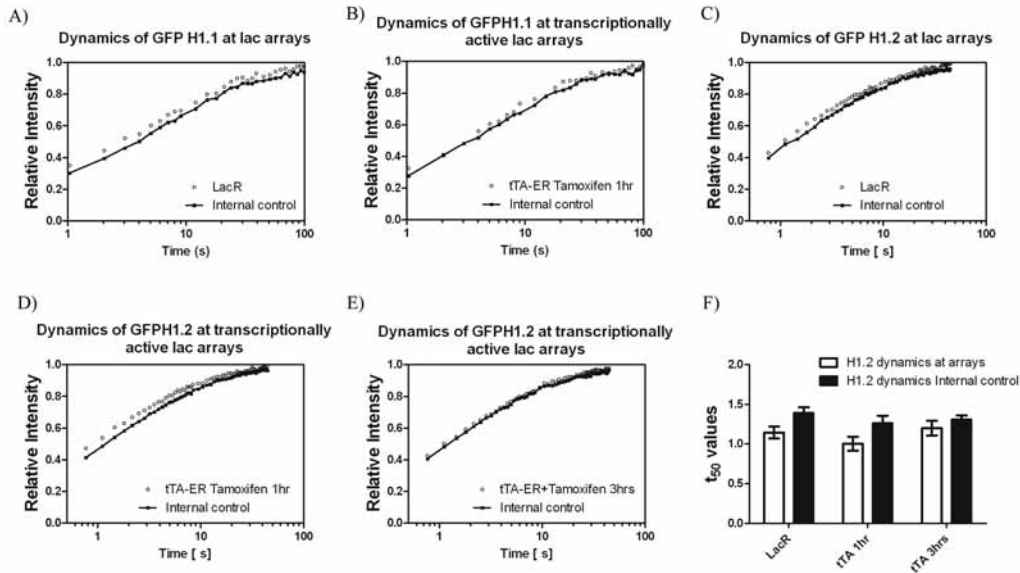
Supplementary Figure 4.8 – Quantification of Pin1 and pS173 levels at lac arrays. Pin1 levels and H1.2/H1.5 pS173 levels were measured by using the mcherry-LacR or mcherry-ER-tTA as a mask to define regions of interest. The intensity obtained from this channel was measured against the average intensity of the entire nucleus to obtain fold enrichment. Each dataset is an average value reported from more than 30 cells compiled from two or more independent experiments. These experiments clearly show the increase in Pin1 levels and pS173 levels at sites of transcription, with this increase being independent of RNA Polymerase II.



Supplementary Figure 4.9 – Accumulation of RNA Polymerase II at sites of transcription and the affect of a-amanitin on its levels. (A) U2Os 263 cells were transfected with either mcherry-LacR or mcherry-ER-tTA following which Tamoxifen was added to stimulate the translocation of the mcherry-ER-tTA to the nucleus. This is accompanied by an accumulation of RNA Polymerase II at the lac arrays. Mcherry-LacR fails to recruit any RNA Polymerase II alluding towards a transcriptionally silent chromatin state. (B) U2Os 263 cells were treated with a-amanitin for either 5hrs or 18hrs in order to deplete the pool of RNA Polymerase II. At the 5hr time point, some RNA Polymerase II foci were still observed, however, at the 18hr time point, these were significantly reduced.



Supplementary Figure 4.10 – Chromatin decondensation upon transcriptional activation. U2Os 263 cells were transfected with either mcherry-LacR or mcherry-ER-tTA, following which transcription was induced with the help of Tamoxifen. These cells (living) were then placed under a confocal microscope and subject to z-stacks (50 slices in 9sec). The stacks were then analyzed on Imaris surface rendering software and the volume occupied by the arrays were measured. Examples illustrated here show the “puffing” of the arrays upon transcriptional induction. The average volume (more than 60 cells) increases from $0.67\mu^3$ to $0.997\mu^3$ upon activation of transcription.



Supplementary Figure 4.11 - Dynamics of H1.1 and H1.2 at sites of transcription. U2OS 263 cells were co-transfected with either GFP H1.1 or GFP H1.2 and mcherry-LacR or mcherry-ER-tTA. The dynamics of GFP H1.1 were measured at the lac arrays at transcriptionally inactive sites (A) and when the same was activated with transcription (B) with Tamoxifen (1hr). Similarly, the dynamics of another euchromatin enriched H1 variant H1.2 was measured at transcriptionally inactive (C), and when transcriptionally activated with Tamoxifen for 1hr (D) and 3hrs (E). The t_{50} values from the FRAP curves are shown in (F).

H1 variant transfected	Cellular background	Effective diffusion coefficient (μ^2/s)		Residence time (s)		Transition time (s)		Strongly bound population (%)	
		Mean \pm SEM	p-value	Mean \pm SEM	p-value	Mean \pm SEM	p-value	Mean \pm SEM	p-value
H1.1	Pin1 -/-	0.02115 \pm 0.002	0.0009	140 \pm 13	0.0045	297 \pm 52	0.1703	38 \pm 3	0.3818
	Pin1wt	0.01176 \pm 0.001		277 \pm 44		427 \pm 81		34 \pm 3	
H1.5	Pin1 -/-	0.01801 \pm 0.001	0.0049	293 \pm 24	0.0001	352 \pm 42	0.0016	40 \pm 3	0.52
	Pin1wt	0.01228 \pm 0.001		464 \pm 32		663 \pm 76		43 \pm 2	
H1.1 T152A	Pin1 -/-	0.02351 \pm 0.003	0.0004	150 \pm 16	0.0045	204 \pm 31	0.0055	40 \pm 3	0.4201
	Pin1wt	0.01178 \pm 0.001		225 \pm 19		387 \pm 54		37 \pm 3	
H1.1 T152S S183A	Pin1 -/-	0.02376 \pm 0.002	0.0094	163 \pm 12	0.6217	355 \pm 59	0.2322	37 \pm 2	0.4755
	Pin1wt	0.01606 \pm 0.001		171 \pm 10		266 \pm 33		39 \pm 2	
H1.1 T152S	Pin1 -/-	0.01419 \pm 0.001	0.0093	269 \pm 31	0.8384	712 \pm 154	0.481	26 \pm 3	0.0257
	Pin1wt	0.009587 \pm 0.0005		261 \pm 21		597 \pm 83		35 \pm 2	
H1.1 S183A	Pin1 -/-	0.01472 \pm 0.0009	0.5602	210 \pm 18	0.2508	510.0 \pm 74	0.4986	31 \pm 2	0.3284
	Pin1wt	0.01350 \pm 0.002		249 \pm 29		599.0 \pm 110		34 \pm 3	
H1.1 T152A S183T	Pin1 -/-	0.01776 \pm 0.002	0.764	187.3 \pm 16	0.0334	354 \pm 53	0.1875	35 \pm 2	0.274
	Pin1wt	0.01694 \pm 0.002		246.6 \pm 20		482 \pm 75		38 \pm 2	
H1.1 S183T	Pin1 -/-	0.01603 \pm 0.002	0.1588	200 \pm 24	0.7322	394 \pm 79	0.3103	34 \pm 3	0.1826
	Pin1wt	0.01298 \pm 0.0008		213 \pm 26		527 \pm 95		30 \pm 2	
H1.1 T152S S183T	Pin1 -/-	0.01770 \pm 0.001	0.0652	155 \pm 19	0.5914	413 \pm 102	0.78	32 \pm 3	0.6296
	Pin1wt	0.01454 \pm 0.001		143 \pm 9		380 \pm 64		34 \pm 3	
H1.1 T152A S183A	Pin1 -/-	0.01839 \pm 0.002	0.1595	214 \pm 21	0.4242	373 \pm 68	0.5009	34 \pm 3	0.5189
	Pin1wt	0.01380 \pm 0.002		246 \pm 34		612 \pm 140		32 \pm 3	

Supplementary Table I – Mathematical modeling data of H1.1, H1.5 and H1.1mut. Kinetic parameters such as effective diffusion coefficient, residence time, transition time and the percentage of strongly bound population were derived from modeling the FRAP curves shown in Figure 4.5. Statistically significant values are shown in bold.

4.6 - Supplementary unpublished results and discussion

4.6.1 – H1 dynamics at sites of replication

Histone H1 has higher levels of phosphorylation at sites of DNA replication and leads to chromatin decondensation (Alexandrow & Hamlin, 2005; Chadee et al, 1997; Yasuda et al, 1981). We wished to investigate the role that Pin1 played in influencing the dynamics of H1 at the sites of replication. In order to accomplish this, we cotransfected Pin1^{wt} and Pin1^{-/-} cells with RFP-PCNA and GFP-H1 and spot-bleached sites that were enriched with PCNA, and monitored the recovery of H1. PCNA (proliferating cell nuclear antigen), a polymerase clamp, forms distinct replication foci allowing easy visualization of the sites of DNA replication (Leonhardt et al, 2000a; Sporbert et al, 2005; Sporbert et al, 2002). It is an essential protein for ensuring processivity of DNA replication and is commonly used as a marker for replication foci/factories (Jonsson & Hubscher, 1997; Leonhardt et al, 2000b; Wyman & Botchan, 1995). We used PCNA foci as a mask to photobleach GFP-H1 at the sites of replication, and then monitored the dynamics of these proteins, by FRAP. We were able to increase the number of S-phase cells by carrying out a single-thymidine block, which gave us a mixture of early to late S-phase cells.

Wild-type H1.1 associated with sites of replication, recovered faster in the absence of Pin1 than when Pin1 was present (Supplementary Figure 4.12 A). This pattern was similar to that observed earlier in asynchronous population of cells. However, when we mutated the Thr site to Ala (T152A) (Supplementary Figure 4.12 B), we observed very little change in recovery profiles in the presence or

absence of Pin1. A similar recovery pattern was obtained when site 183 was substituted with Thr (T152A S183T) (Supplementary Figure 4.12 C). This suggested to us that neither Ser nor Thr were subject to Pin1 dependent isomerization at position 183, in the absence of Thr at site 152. It also alludes towards the crucial role played by Thr at site 152 in influencing H1 dynamics. This is in stark contrast to the pivotal role played by Ser at position 183 and the minimalistic role played by Thr 152, when we analyzed the global changes in H1 dynamics in interphase cells. Interphase cells do contain a sizable population of S-phase cells, however, analyzing the changes in H1 mobility at localized regions (such as sites of replication) is more sensitive to localized changes, that would otherwise, be missed in the global analysis of H1 population.

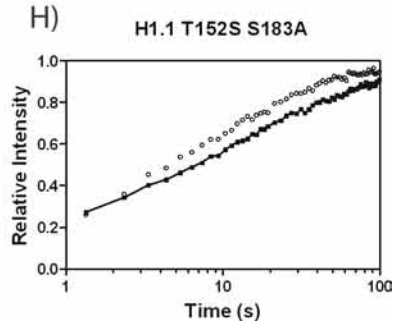
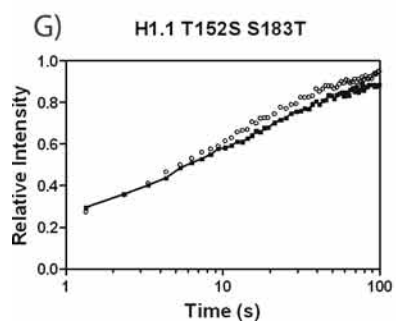
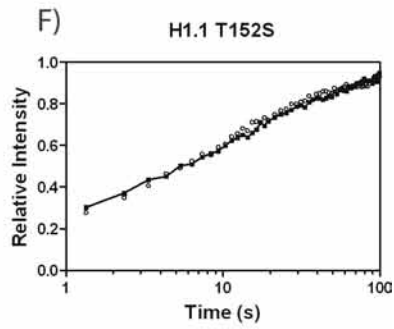
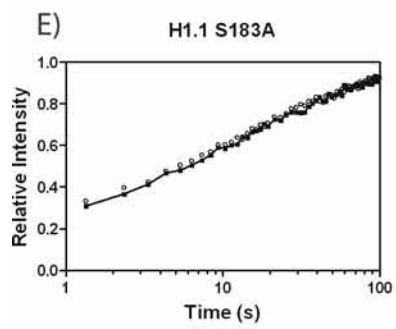
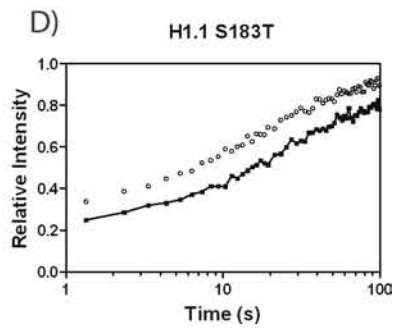
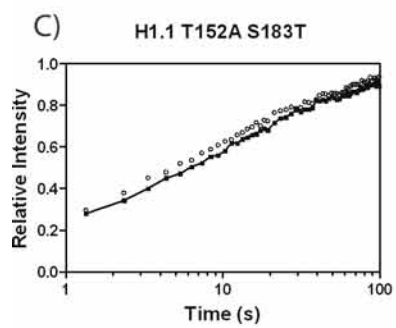
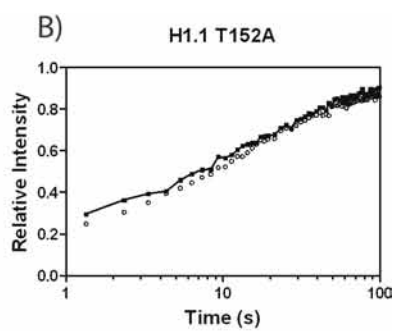
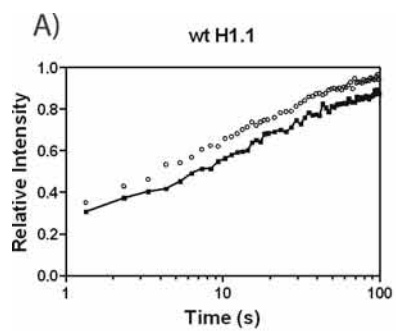
We next targeted site 183 and replaced it with Thr, producing H1.1 (S183T) (Supplementary Figure 4.12 D) mutant and monitored the recovery at sites of replication. We found that this mutant showed a significant decrease in mobility in the presence of Pin1, similar to the response seen in wtH1.1, although completely different from the H1.1S183T kinetics seen in asynchronous populations. The marked change in kinetics was abrogated when one of the Thr at site 183 was changed to Ala (S183A) (Supplementary Figure 4.12 E). This suggests that phosphorylation of Thr at 152 is dependent upon the presence of a phosphorylated residue at site 183.

Next we substituted Ser at site 152 (T152S) (Supplementary Figure 4.12 F). Unlike H1.1 S183T, H1.1 T152S showed no change in FRAP recovery profiles in Pin1^{wt} vs. Pin1^{-/-} cells. However, this failed to elicit any response in the presence

of Pin1. A similar response was seen in H1.1 T152S S183T (Supplementary Figure 4.12 G). However, H1.1 T152S S183A (Supplementary Figure 4.12 H) had a recovery pattern like wtH1.1. This suggests that either H1.1T152S is not phosphorylated, or may have counter-balancing changes in binding/unbinding rates.

We haven't been able to show the presence of Thr phosphorylations at sites of replication, due to the incompatibility of site-specific antibodies for immunofluorescence experiments. For the interpretations made below, we assume that variants that show a change in H1 dynamics between Pin1^{-/-} and Pin1wt cells to be phosphorylated, and that the change in dynamics is due to the phosphorylation dependent Pin1 mediated stabilization in binding. A lack of any change in dynamics between Pin1^{-/-} and Pin1wt cells would imply that the H1 variant is not phosphorylated. While such an approach was validated by our analysis of H1 mutants in an asynchronous population, it is an indirect approach, and more direct approaches to monitor Thr phosphorylation needs to be adopted.

If our above assumption is valid, then it would appear that at sites of replication, additional rules that need to be followed for Pin1 mediated stabilization of H1 – A. Thr at position 152 is absolutely necessary for phosphorylation, whereas, Ser is incompatible for phosphorylation at this position. B. Phosphorylation of Thr at position 152 is dependent on a phospho-compatible (either Ser/Thr) residue at position 183. However, it must be emphasized that these rules are based on the assumption that the sites are phosphorylated, and more experiments are warranted to test our hypothesis.



Supplementary Figure 4.12 – H1.1 dynamics at sites of replication. GFP-H1.1 was co-transfected with RFP-PCNA in Pin1^{-/-} (open circles) and Pin1wt cells (filled circles) , and the cells were enriched in S-phase using a double thymidine block. RFP-PCNA was used as a mask to photobleach GFP-H1 molecules at the sites of replication and the recovery was compared against a background of Pin1 depletion. (A) Wildtype H1.1 shows faster recovery in the absence of Pin1 at the sites of replication, however, mutation of the Thr residue at position 152 (B) completely abolishes the change in dynamics upon Pin1 depletion, which suggests the crucial role played by Thr at this position. Substitution of Thr at position 183 (C & D), however, showed that Pin1 mediated stabilization is only possible if a Thr occupies position 152, proving the greatest Pin1 mediated stabilization. However, Thr at 152 is not sufficient for Pin1 mediated stabilization as mutation of position 183 to Ala abrogates this effect (E). The importance of Thr at position 152 is further highlighted by the fact that mutation of this residue to Ser, once again, abrogates the Pin1 mediated stabilization (F-H).

4.6.2 - Focal accumulation of Pin1 alters chromatin condensation

Our results so far have alluded towards elevated Pin1 levels and H1 phosphorylation levels at a transcriptionally competent chromatin state. In order to understand what these two key events play in establishing this state, we engineered a LacR-mcherry (or CFP) –Pin1 construct, and transfected these to 263 cells harboring the lac array system described above. Two other constructs, LacR-mcherry-Pin1 R68,69A and LacR-mcherry-Pin1 C113A (Stukenberg & Kirschner, 2001; Zhou et al, 2000) (referred to as LacR-Pin1*mut*) were generated to investigate whether the isomerase activity of Pin1 was needed to accomplish its role in establishing a transcriptionally competent state.

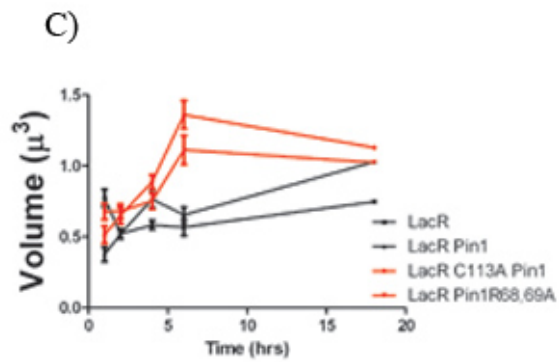
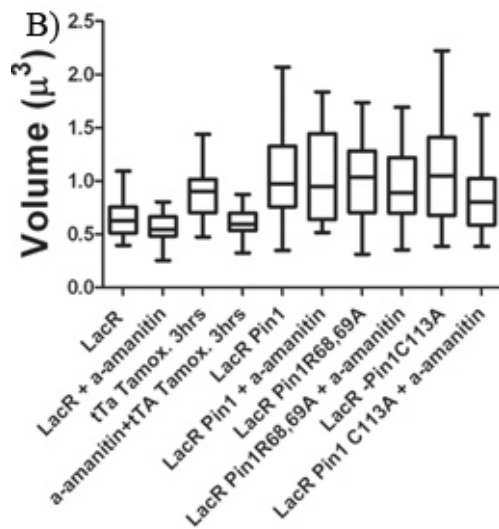
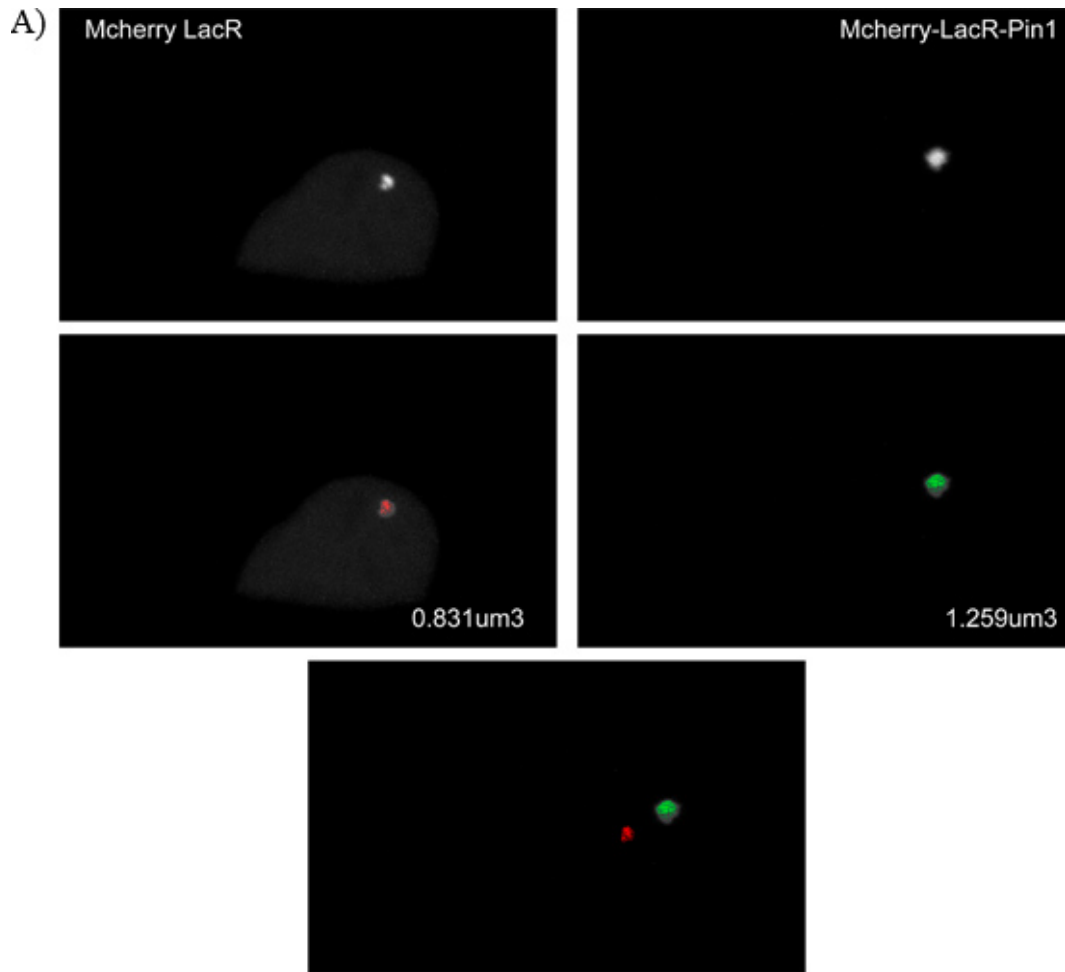
Our previous results with Pin1^{-/-} and Pin1 siRNA studies alluded towards the potential role of Pin1 in influencing chromatin condensation levels (Figure 4.6). Here, we wished to investigate if a local increase in Pin1 concentration would achieve a similar effect and the consequences of such a change. We transfected the 263 cells with either mcherry-LacR, mcherry-LacR-Pin1, mcherry-LacR-Pin1 R68,69A or mcherry-LacR-Pin1 C113A (Supplementary Figure 4.13A, B). We observed that the Pin1 constructs (both wildtype and mutants) lead to increased chromatin decondensation, as compared to mcherry-LacR alone. These experiments were done in the absence of any added transcriptional activators (such as mcherry-ER-tTA) or Tamoxifen. The decondensation levels were similar to that seen in transcriptionally elongating chromatin (mcherry-ER-tTA + Tamoxifen 3hrs). However, unlike the decondensation seen in the presence of transcriptional activators (mcherry-ER-tTA+Tamoxifen), which are sensitive to

the presence of α -amanitin, the decondensation seen in the presence of LacR-Pin1 and LacR-Pin1*mut* were found to be insensitive to α -amanitin (Supplementary Figure 4.13B). α -amanitin causes the degradation of RNA Polymerase II (Nguyen et al, 1996), hence, this suggested that the decondensation induced by LacR-Pin1 (and Pin1*mut*) were independent of RNA Polymerase II.

The observed chromatin decondensation in both LacR-Pin1 and LacR-Pin1*mut* could be either due to the decondensation being independent of the isomerase activity and Pin1 being a scaffold for other chromatin modifiers, or perhaps, due to a difference in the rate at which the decondensation is achieved. To test these models, we transfected cells with the LacR-Pin1*wt* and LacR-Pin1*mut* as described above, but in the presence of IPTG. IPTG is a strong inhibitor of LacR and prevents its binding to DNA (Hu & Davidson, 1987). In the presence of IPTG, LacR-constructs adopt a uniform nuclear distribution, as opposed to concentrating at the lac-arrays. Following 24hrs of transfection, cells were washed three times with PBS and grown in media devoid of IPTG. Following regular time intervals, we measured the volume occupied by the lac arrays using rapid z-stacks on living cells, as described above (Supplementary figure 4.13C). The 18-hour time point is taken as the final steady state level, and measured in cells without any added IPTG (overnight transfection).

As can be seen in Supplementary Figure 4.13C, both the LacR-Pin1*mut* lead to chromatin decondensation much more rapidly than LacR-Pin1*wt*. The difference is obvious at 6hrs post removal of IPTG, wherein LacR-Pin1*mut* achieve steady state chromatin decondensation levels seen at the 18hr time point. Chromatin

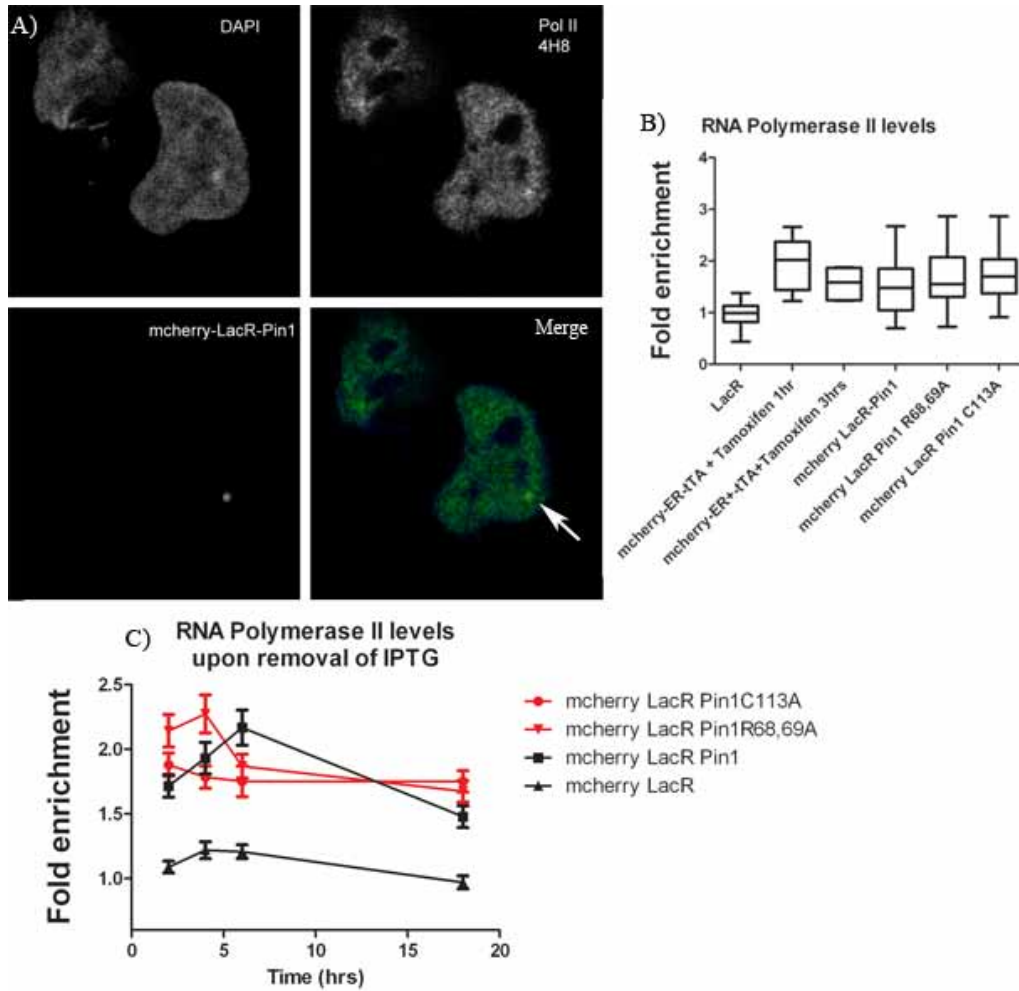
decondensation mediated by LacR-Pin1 $_{wt}$ is much slower compared to the catalytically inactive mutants. These experiments suggested that the isomerase activity (or lack thereof) is important in promoting chromatin decondensation.



Supplementary Figure 4.13 – Focal accumulation of Pin1 and Pin1mut causes chromatin decondensation at lac arrays. (A) U2OS 263 cells were transfected with either LacR or LacR Pin1 and the changes to the volume occupied by the lac arrays was monitored in living cells. Raw image of the lac array obtained from a representative sample is shown in the top panel, while the same image series, upon volume rendering is shown in the middle panel. As can be seen in these representative images, upon tagging Pin1 to lacR, the volume of the lac arrays increases from $0.831\mu\text{m}^3$ when transfected with just lacR to $1.259\mu\text{m}^3$ in the presence of lacR-Pin1. (B) Quantification of the changes in the volume occupied by the arrays when transfected with either LacR, LacR-Pin1, LacRPin1mut or with tTA-ER+ Tamoxifen, in the presence/absence of α -amanitin. Decondensation of chromatin seen in the presence of transcriptional activation (tTA-ER+Tamoxifen) is abolished when treated with α -amanitin. However, chromatin decondensation caused by LacR-Pin1, or LacR-Pin1mut is relatively unaffected by the presence of α -amanitin. (C) Mcherry-LacR-Pin1 and mcherry-LacR-Pin1mut were transfected in U2OS cells housing the lac arrays and incubated with IPTG for 24hrs. The next day, the IPTG was washed away and the decondensation of the array was monitored with time. As can be seen, LacR and LacR-Pin1 cause very little change in the decondensation of the array from 2-6hrs following IPTG withdrawal. LacR-Pin1mut on the other hand, induces rapid decondensation of the arrays in the same time frame. Overnight transfection of these constructs (18hrs), in the same cell-line, however, causes the similar amounts of decondensation both in lacR-Pin1 and lacR-Pin1mut constructs.

4.6.3 – Focal accumulation of Pin1 recruits RNA Polymerase II

The decondensation of chromatin by LacR-Pin1 and LacR-Pin1mut to levels seen in transcriptionally elongating chromatin raised the possibility that accumulation of LacR-Pin1 and the LacR-Pin1mut were sufficient to induce transcriptional elongation. In order to test this, we tested whether there was an increased accumulation of RNA Polymerase II at these sites. Indeed, local enrichment of LacR-Pin1 and LacR-Pin1mut did lead to increased RNA Polymerase II accumulation (Supplementary Figure 4.14A, B). The enrichment of RNA Polymerase II was at levels similar to those observed at transcriptionally elongating chromatin (arrays targeted by mcherry-ER-tTA+Tamoxifen). However, the accumulation of RNA Polymerase II, was independent of the isomerase activity of Pin1. Following transfection of LacR-Pin1 and LacR-Pin1mut, growth in IPTG and PBS washes, RNA Polymerase II accumulation was monitored at regular time intervals (Supplementary Figure 4.14C). We found no differences in the rate at which Polymerase II accumulates at arrays targeted by either LacR-Pin1 or LacR-Pin1mut.

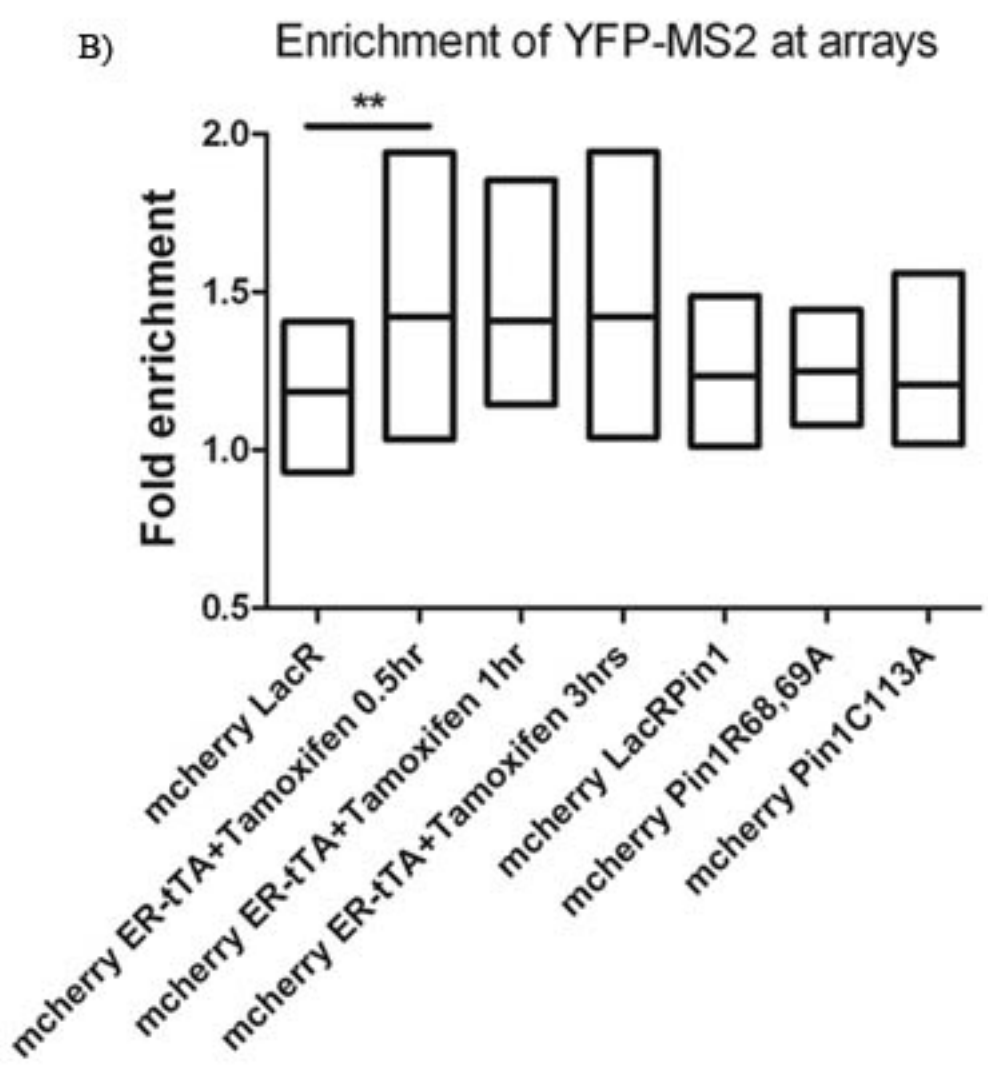
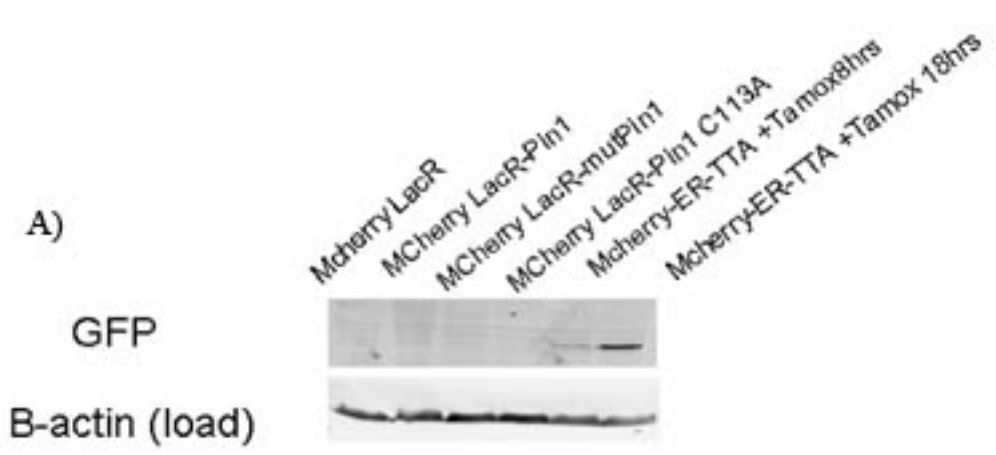


Supplementary Figure 4.14 – Focal accumulation of Pin1 leads to recruitment of RNA Polymerase II in an isomerase independent manner. (A) LacR-Pin1 was transfected into U2OS 263 cells housing the lac arrays. Immunofluorescence experiments were carried out to test the recruitment of RNA Polymerase II at these sites of increased Pin1 accumulation. The arrow shows that even in the absence of added transcriptional activators, RNA Polymerase levels increase at these sites. (B) Accumulation of RNA Polymerase II levels were quantified following transfection of LacR-Pin1 or LacR-Pin1*mut* in U2OS 263 cells. RNA Polymerase II levels rose to the same extent in LacR-Pin1 and LacR-Pin1*mut* as actively transcribing chromatin (mcherry-ER-tTA + Tamoxifen (1hr/3hrs). Basal level of RNA Polymerase II was observed when just mcherry-LacR was transfected in these cells. (C) Kinetics of RNA Polymerase II recruitment following focal accumulation of Pin1. Mcherry-LacR-Pin1 and mcherry-LacR-Pin1*mut* were transfected in U2Os 263 cells with IPTG overnight. Next day, the IPTG was washed away and the kinetics of RNA Polymerase II was monitored using time-course immunofluorescence experiments. Both LacR-Pin1 and LacR-Pin1*mut* were able to recruit RNA Polymerase II at similar rates and quantities, suggesting that this mechanism was independent of isomerase activity.

4.6.4 – Focal accumulation of Pin1 does not lead to transcriptional elongation

The decondensation, increased H1 phosphorylation and elevated RNA Polymerase II accumulation at the lac arrays following transfection of LacR-Pin1 (and LacR-Pin1mut) alluded towards Pin1, in itself, being able to initiate transcriptional elongation. However, we could not find evidence for high levels of elongation at the lac arrays with just LacR-Pin1/LacR-Pin1mut. There was no increase in YFP-MS2 colocalization at these sites. Accordingly, there was a lack of a translational product (CFP-SKL) when the arrays were targeted with LacR-Pin1/LacR-Pin1mut. This is in comparison to high levels of YFP-MS2 colocalization at the lac arrays and CFP-SKL product being formed when transcription is activated by mcherry-ER-tTA and Tamoxifen (Supplementary Figure 4.15A, B, C).

This suggested that the transcriptionally competent chromatin setup by Pin1 accumulation needed an additional factor (such as transcriptional activator) to initiate elongation. When we co-transfected LacR-CFP-Pin1, LacR-CFP-Pin1mut and mcherry-ER-tTA we found the chromatin to undergo 30% more decondensation upon addition of Tamoxifen, than those that were transfected with GFP-LacR and mcherry-ER-tTA (Supplementary Figure 4.16).



C

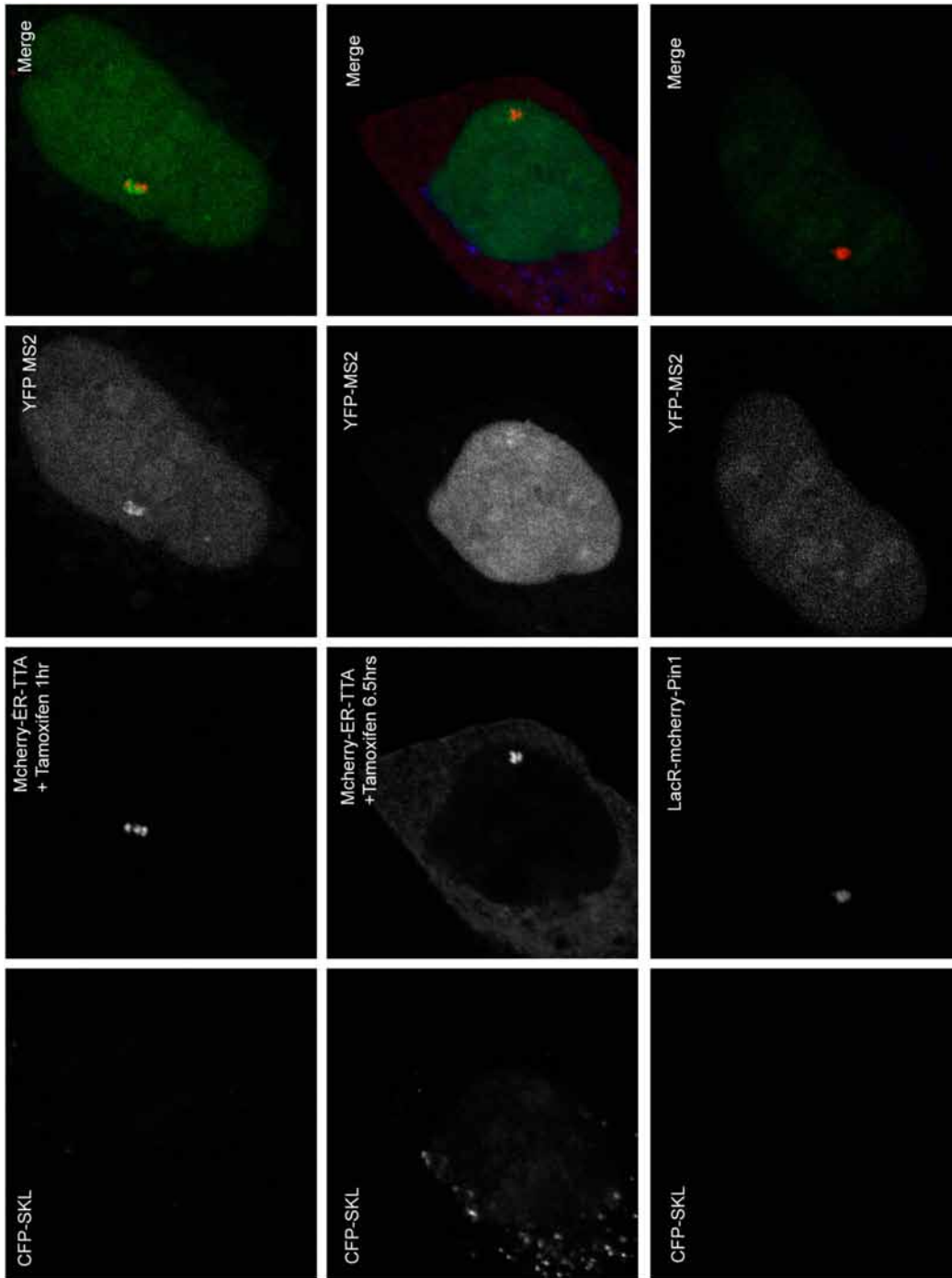


Figure 4.15 – Focal accumulation of Pin1 or Pin1mut does not lead to transcriptional elongation. (A) Upon transcriptional activation of the lac arrays, the system is designed to drive to expression of an artificial CFP-SKL gene. Transfection of LacR-Pin1 (and Pin1mut) does not lead to accumulation of the translational product of the arrays (CFP-SKL). Transfection of mcherry-ER-tTA along with Tamoxifen induces a strong expression of the CFP-SKL translational product. β -actin is used as a loading control. (B) Transcriptional activation drives the expression of CFP-SKL gene that also contains MS2 repeats. Transfected YFP-MS2 binds the MS2 repeats on the transcribed mRNA resulting in localized accumulation of YFP MS2 at these sites. While mcherry-ER-tTA+Tamoxifen induces a strong enhancement of the YFP MS2 signal at these sites, mcherry-Pin1 (and Pin1mut) show no increase in YFP MS2 enrichment at the lac arrays. (** denotes statistical significance with p-value less than 0.5, greater than 0.001, while the horizontal line in the boxes represents the median value of the population). (C) Representative images showing the accumulation of CFP-SKL and YFP MS2 when transcriptionally activated using the mcherry-ER-tTA construct + Tamoxifen (1hr, top panel and 6.5hrs midpanel). The CFP-SKL product is seen to accumulate at peroxisomes, given the SKL peroxisome-targeting motif present in this protein. There is no accumulation of CFP-SKL or YFP MS2 at LacR-Pin1 sites, suggesting that these sites are not transcriptionally active in the absence of transcriptional activators.

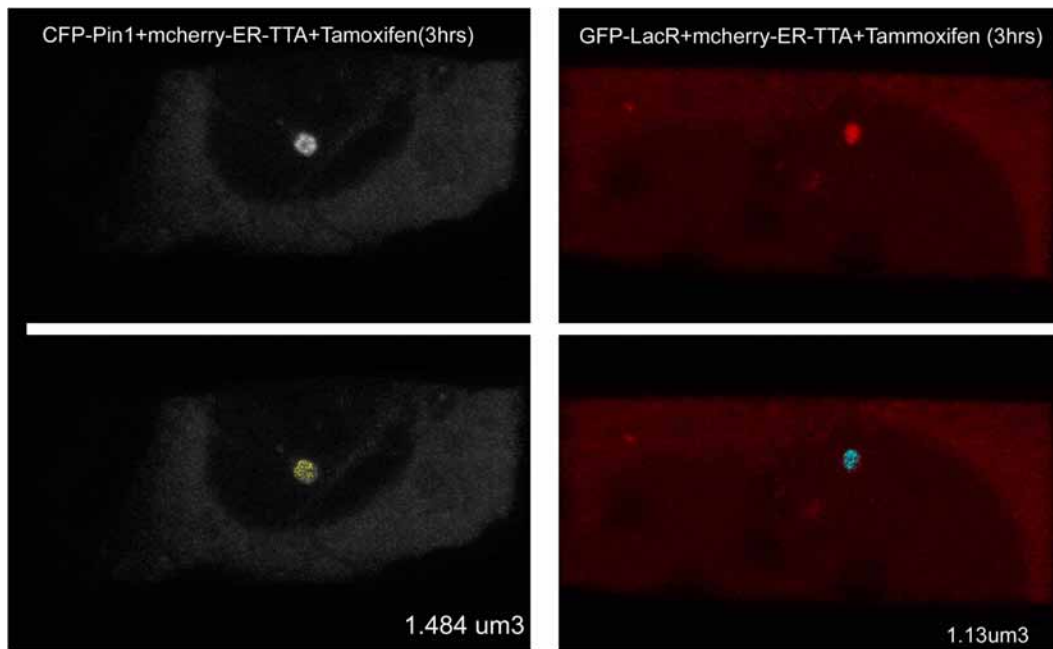


Figure 4.16 – Transcriptional activation at sites of Pin1 accumulation leads to increased chromatin decondensation. Transfection of LacR-Pin1 to lac arrays leads to chromatin decondensation, however it does not, by itself, lead to transcriptional activation. When such sites are transcriptionally activated by transfecting mcherry ER-tTA+ Tamoxifen, further chromatin decondensation is seen. For example, the representative image (above) shows that in the absence of any ‘priming’ from Pin1, chromatin decondenses to $1.13\mu\text{m}^3$. When cells are transfected with lacR-Pin1 prior to activation of transcription, the lac arrays decondense to occupy a volume of $1.484\mu\text{m}^3$.

Chapter V – Perspectives

5.1 - Synopsis

Compared to the regulation of core histones by post-translational modifications, the regulation of H1 has received much less attention. Core histone acetylation and H1 phosphorylation are critical events during transcriptional activation. Furthermore, both core histone acetylation and H1 phosphorylation are mis-regulated during oncogenesis further emphasizing the need for detailed mechanistic insight into their regulation and their impact on chromatin structure. From our studies involving core histone acetylation and H1, we discovered the mechanisms whereby this modification has an impact on the mobility of low-affinity H1 population, while having variant-specific effects on the mobility of the high-affinity H1 population. We also found that core histone acetylation significantly reduced the cooperativity of H1 binding. This was a novel finding correlating the changes in chromatin structure to the cooperativity of H1 binding to chromatin. The ability of FRAP to assess cooperativity in H1 binding provides a vehicle for studying different types of H1 binding in living cells.

In our studies with H1 phosphorylation and Pin1, we characterized a novel mechanism of histone H1 regulation--phosphorylation-dependent proline isomerisation. The molecular mechanism behind H1 phosphorylation, a post-translational modification in many different cellular events including transcription, replication and mitosis, is poorly understood. In this study we demonstrated that Pin1 acts on phosphorylated H1 molecules in which it alters the conformation of the C-terminal domain of H1. This conformation stimulated dephosphorylation by PP2A. Furthermore, Pin1-mediated proline isomerisation

promoted H1 binding to chromatin thereby leading to chromatin condensation. This was true even during transcriptional elongation. Our study provided mechanistic insight into the regulation of H1 phosphorylation in interphase cells. Furthermore, we detailed a hitherto unknown function of Pin1. Pin1 modifies chromatin structure by modulating the association of histone H1 with chromatin through isomerisation of the carboxy terminal domain. The role of Pin1 as a chromatin modifier is consistent with recent developments in the field where a member of FKBP class of prolyl-isomerases (Fpr4 in yeast) has been shown to alter both transcription and chromatin structure through its histone (H3, H4) isomerase activity (Nelson et al, 2006). Our study revealed that histone H1 was also a target of proline isomerisation but that, in the case of Pin1, proline isomerization is dependent upon phosphorylation, thereby establishing post-phosphorylation isomerization of the peptidyl proline bond as an important regulatory mechanism in transcription and chromatin condensation. Our study represented a significant advance in our understanding of how the chromatin-dependent functions of H1 are controlled.

5.2 – Comprehensive model

Our studies analyzing the impact of core histone acetylation and proline isomerization of H1 have alluded to a general mechanism whereby posttranslational modifications regulate H1 dynamics. FRAP experiments and the analysis of FRAP data by mathematical modeling have provided us with experimental evidence that H1 binding involves a series of low-affinity interactions with DNA that eventually lead to a high affinity chromatin bound

state. The progression of binding from a freely diffusing state to a high affinity chromatin bound state also correlates with increasing stability of the nucleosomal particle. H1 binding is initiated by the CTD then either site-I or site-II of the globular domain establishes contact with the DNA (Stasevich et al, 2010). This positions the CTD to bind the linker DNA. Following acquisition of structure by the CTD, a high-affinity state is formed (Brown et al, 2006; Stasevich et al, 2010). Our studies found that core histone acetylation altered the cooperativity of H1 binding, which resulted in a reduced efficiency of globular domain binding and subsequent positioning of the CTD of H1 for high affinity interactions. Proline isomerization, on the other hand, was able to alter the conformation of the CTD and stabilize H1 binding to chromatin. Further experiments need to be carried out to elucidate whether Pin1 affects H1 at multiple stages of binding, or whether a single isomerization event is sufficient to stabilize H1. However, our results reveal the general mechanism employed by core histone acetylation and phosphorylation dependent proline isomerization – these act by impeding or stabilizing one or more steps in the H1 binding cycle, thereby affecting H1 function. While impeding a step in the H1 binding cycle, by preventing the transition from low-affinity interactions to high affinity interactions would destabilize H1 and may lead to chromatin decondensation, mechanisms that facilitate this transition or further stabilize the high affinity H1 binding could lead to condensed chromatin structures.

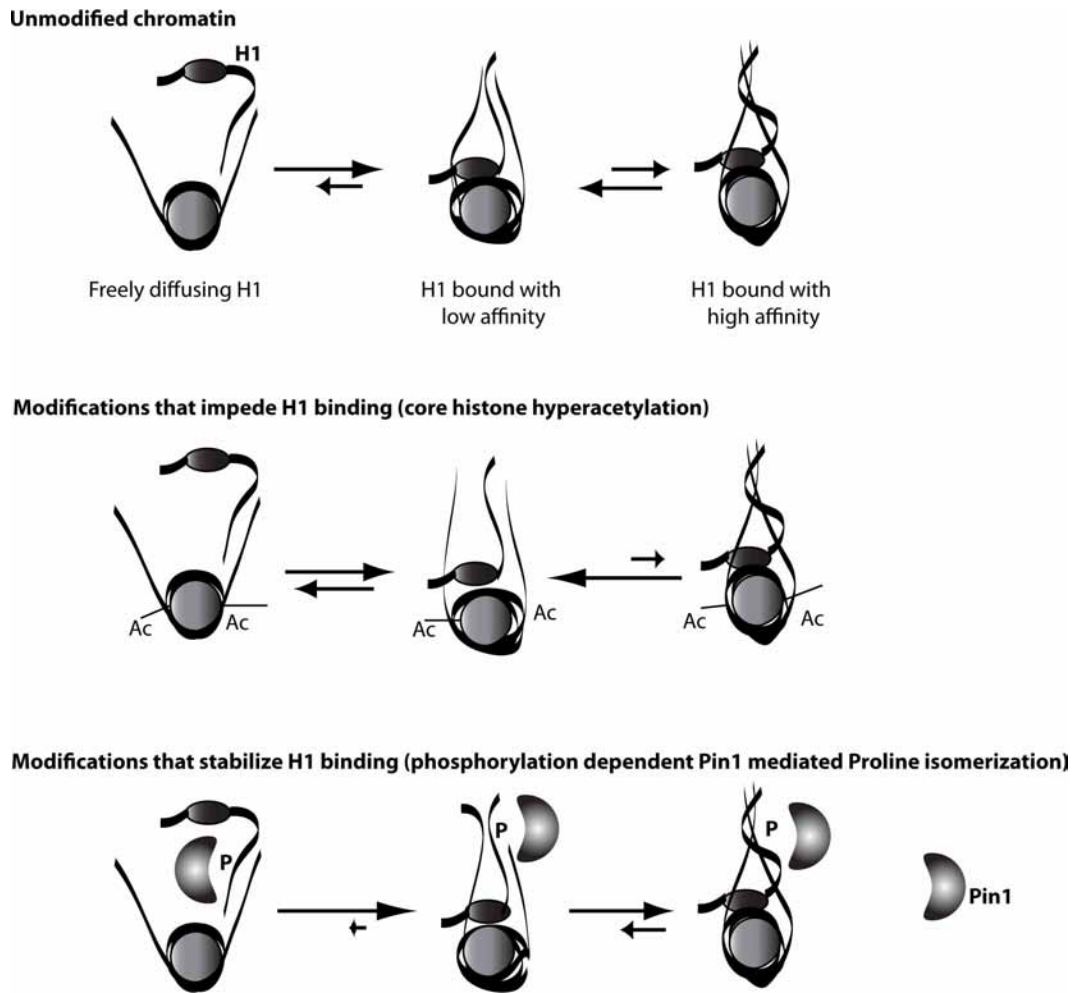


Figure 5.1 – Changes in nucleosomal structure upon induction of transcription-associated post-translational modifications of histones. In the absence of H1 binding, the linker DNA strands are in an “open” configuration given the mutual electrostatic repulsive forces of the linker DNA strands. Binding of H1 to deacetylated chromatin initiates the folding of the linker DNA to form a stem-like motif, thought to be responsible for directing higher order folding of chromatin (Bednar et al, 1998). This structure is thought to be attained when the CTD of H1 acquires a structure upon interacting with DNA, thus establishing a high affinity chromatin bound state for H1. When the core histones are acetylated, we have shown that this modification reduces the cooperativity of H1 binding, which may impede the ability of H1 to bring the linker DNAs together. Phosphorylation dependent proline isomerisation mediated by Pin1 on the other hand, increases the residence time of high affinity H1 population, thereby stabilizing H1 binding. Thus posttranslational modifications, such as core histone acetylation and Pin1 mediated proline isomerisation, affect one or more binding steps of H1 potentially affecting H1 function of condensing chromatin.

5.3 - Applicability to other post-translational modifications –

DNA methylation and H1 – Our studies alluded towards a possible mechanism through which post-translational modifications may change H1 binding. This model can be used to predict the changes in H1 mobility following other chromatin modifications, such as DNA methylation. DNA methylation involves the addition of a methyl group on the cytosine residues of DNA (Hurwitz et al, 1965). This modification does not change the negative charge on the DNA backbone and, consequently would predictably not affect the binding of the CTD or the globular domain, which are primarily mediated by electrostatic charge interactions. The CTD would be in a more hydrophobic molecular environment. One could, therefore, predict a change in the acquisition of CTD structure. Increasing the hydrophobicity within the H1 CTD by deprotonating lysine residues at an alkaline pH increases the folding of the CTD (Roque et al, 2009), alluding towards hydrophobicity being favorable for H1 binding and chromatin compaction. However, it remains to be seen whether increasing the hydrophobicity of the external environment of CTD can alter its structure and thus stabilize or destabilize H1 binding. One could predict from our model that most of the changes in H1 mobility upon DNA methylation would arise from changes in the high-affinity H1 population, while the low-affinity H1 population would remain unaffected.

Consistent with increased hydrophobicity increasing H1 binding to chromatin, DNA methylation induced by 3-aminobenzamide causes chromatin condensation only in the presence of linker histones *in vitro* (Karymov et al,

2001). DNA methylation also induces changes at the nucleosomal level by increasing the rigidity and compactness of the nucleosomes (Choy et al, 2010). However, cells in which DNA methylation is completely knocked out (*Dnmt3a*^{-/-} and *Dnmt3b*^{-/-}), showed that these cells had no change in chromatin compaction but had decreased mobility of H1, as analyzed by FRAP (Gilbert et al, 2007). Compensatory mechanisms might play a role in the complete absence of DNA methylation induced in these cells, which might also explain why an increase in core histone acetylation is also observed in these cells (Gilbert et al, 2007). The latter could also be due to the close association of HDACs with methyl CpG binding proteins. For example, MeCP2 forms a complex with HDAC1 and HDAC2 and is thought to play key roles in transcriptional silencing (Dobosy & Selker, 2001; Jones et al, 1998; Nan et al, 1998). It will be interesting to analyze whether the change in H1 dynamics can be reproduced when DNA methylation is induced in the presence of a drug, such as 3-aminobenzamide.

The example with DNA methylation and H1 dynamics also highlights the limitations of our model. It cannot predict H1 behavior in the presence of multiple pathways that can simultaneously impact H1 behavior. For example, in our studies with TSA and H1 dynamics, we observed that an overnight treatment with TSA led to both core histone hyperacetylation and H1 dephosphorylation. This makes it difficult to predict the changes in H1 behavior upon such a treatment and further experimental evidence may be needed to make accurate predictions of H1 behavior.

5.4 - Implications of the model –

5.4.1 - Core histone hyperacetylation and phosphorylation dependent proline isomerization of H1 modulate the ‘site-exposure’ of chromatosomes.

The sequential binding steps of H1 result in bringing the two linker DNA in close proximity to form a closed stem like structure (Bednar et al, 1998). Post-translational modifications that disrupt H1 binding would impede the processes that bring the linker DNA together in space. The chromatosomes can be thought of being in equilibrium between a conformation with a loosely bound H1 molecule and one in which H1 is strongly bound. Post-translational modifications that impede the binding of H1 would result in a conformation of the chromatosome that is loosely bound with an ‘open’ conformation of linker DNA thereby increasing the ‘exposure’ of the chromatosome. This is of physiological relevance since it would increase the probability of binding by transcription factors or DNA dependent proteins, allowing greater access to DNA.

5.4.2 - Chromatin decondensation and transcription

One of the implications of our model is that H1 is still bound to chromatin following changes to chromatin upon induction of transcription (such as core histone hyperacetylation), albeit with lower affinity. The stably bound H1 population remained fairly constant for all variants regardless of the modification induced. Most of the changes induced either by core histone acetylation or Pin1, included changes in the proportion of low-affinity H1 population and temporal changes (residence time, transition time) to high affinity H1 population. Consistent with this observation, we also found that the affinity of H1 for

chromatin was independent of transcriptional activity. Moreover, others have observed a modest reduction (20% (Ericsson et al, 1990; Kamakaka & Thomas, 1990) – 30% (Ridsdale & Davie, 1987)) in the amount of H1 at sites of transcription. These studies and our observations suggest that chromatin does not require the complete displacement of histone H1 to be transcribed but, rather, H1 is well-retained on transcribed DNA.

This is in contrast to *in vitro* models and some *in vivo* studies that suggested that H1s displacement is a key step in transcriptional elongation (Koop et al, 2003; Vicent et al, 2011) and that chromatin could decondense to the level of nucleosomes during this process (Andersson et al, 1982). Such decondensation is common in polytene chromosomes, which harbor very high rates of transcriptional activity (frequency of 1 RNA Polymerase II/300bp) (Andersson et al, 1982) (Lamb & Daneholt, 1979), but may not be a common feature of eukaryotic transcriptional units (average frequency of 1 RNA Polymerase II/transcriptional unit) (Jackson et al, 2000).

The retention of H1 in chromatin undergoing transcription-associated modifications has implications on the structure of the 30nm fiber under such conditions. The current model describing the changes in chromatin structure upon transcriptional induction (Bassett et al, 2009; Robinson & Rhodes, 2006; Travers, 2009), which will now be referred to as the hierarchical structure model, in order to differentiate it from the dynamic structural model proposed by us, is detailed below. The hierarchical model suggests that in the presence of H1 in a 1:1 stoichiometry to nucleosomes and long nucleosome repeat lengths, the

predominant structure of the 30nm is a one start helical model similar to the one proposed by Robinson & Rhodes (Robinson et al, 2006; Robinson & Rhodes, 2006). This forms the apex of chromatin compaction for the 30nm fiber under physiological conditions, and is thought to be the predominant structure in mitotic chromosomes (Bassett et al, 2009) or transcriptionally inactive chromatin (Robinson & Rhodes, 2006). The 30nm fiber can fold into even higher order structures, although the nature of these structures is unknown. The Robinson & Rhodes model packs in 11 nucleosomes/11nm with a long nucleosome repeat length (187bp) with a near 1:1 nucleosome:H1 stoichiometry (Robinson et al, 2006). Under conditions of suboptimal or shorter nucleosome repeat lengths (167bp), the 30nm structure is thought to decondense and adopt a conformation as suggested by Richmond and colleagues encapsulating 5-6nucleosomes/11nm (Richmond et al, 1984) and forms the second level in the hierarchy. Since nucleosome repeat lengths are variable, the Richmond model is thought to be the default 30nm fiber in a transcriptionally uninduced state.

Eviction of linker histones from this structure is thought to further promote decondensation, which in turn, facilitates transcription. The mechanism of this transformation is thought to involve a change in the DNA trajectory due to the decrease in linker DNA entry/exit angle upon H1 eviction. This induces a decondensation of the chromatin fiber increasing the exposure of the linker DNA (Kepper et al, 2008). Upon transcriptional induction and increases in core histone acetylation, further chromatin decondensation of the chromatin fiber is anticipated, which may be facilitated by the incorporation of histone variants.

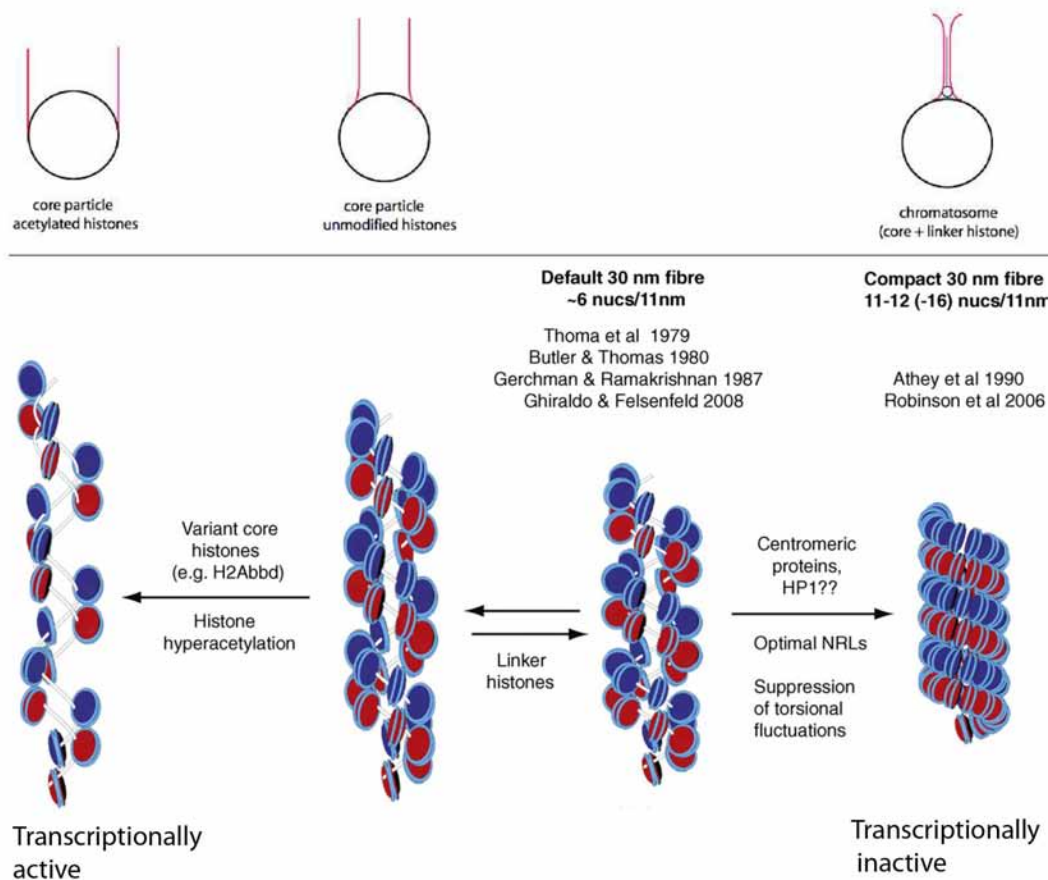


Figure 5.2 – Current model describing the changes in chromatin structure upon transcriptional induction or the hierarchical model of transcription induced changes to chromatin. The top panel illustrates the changes in linker DNA trajectory upon H1 binding. The bottom panel shows the corresponding changes in higher order structure of chromatin. Transcriptionally inactive chromatin is thought to adopt the conformation of chromatin that resembles the model of 30nm structure as reported by Robinson & Rhodes (Robinson et al, 2006). In the absence of optimal nucleosome repeat lengths, the chromatin fiber is thought to adopt a decondensed structure, similar to the two-start helical model reported by Richmond, et al (Schalch et al, 2005). In the absence of linker histones, chromatin is thought to be further decondense. This allows the binding of transcription factors and proteins associated with transcription. Histone acetylation and/or incorporation of histone variants are thought to further decondense the chromatin leading to a transcriptionally active chromatin state. Note that in this model (Bassett et al, 2009; Robinson & Rhodes, 2006; Travers, 2009), only two structures (towards the right, or structures at the apex of the hierarchy) have an active participation of H1. All other structures are devoid of H1, which is inconsistent with our data.

Deficiencies of this model – The hierarchical model does not take into account the dynamic nature of linker histones, or that of the chromatin fiber itself. This model is derived from static images of X-ray crystal structures of tetra-nucleosomes and EM-pictures of fixed chromatosomal arrays and fails to consider the wealth of information gained from kinetic experiments done on nuclear proteins and the nucleosome itself (dynamicity of chromatin is reviewed in (Hubner & Spector, 2010)). Only two structures (of the four proposed) are thought to be in an equilibrium mediated by the presence/absence of H1 binding. Our experiments clearly show the presence of H1 under different chromatin conditions.

Furthermore, whereas the Richmond model is the ‘default’ model for the 30nm fiber, it has been shown that the 30nm fiber adopts a conformation similar to that proposed by Robinson & Rhodes in the presence of H1 and physiologically relevant salt concentrations (Robinson et al, 2006). The Rhodes model is also based on nucleosome repeat lengths most commonly found in nature (178-197bp) while the Richmond model is based on a repeat length of 167bp. The transformation from the compact and thick fibers as suggested by the Rhodes model to the thinner 30nm fibers Richmond model, is assumed to depend upon changes in nucleosome repeat lengths, while it has been shown that nucleosome repeat length does not correlate with the diameter of the fiber (Robinson et al, 2006). Thus, nucleosome repeat length alone cannot be the sole mechanism that can cause the transformation between structures. The deficiencies in this model can be explained if we take into account the dynamic structure of the chromatin

fiber and the contribution that H1 molecules play in influencing the structure, as explained below.

The dynamic chromatin model - Before we describe a model of how chromatin changes upon transcriptional induction and associated post-translational modifications, the structure of the chromatin fiber in the absence of post-translational modifications needs to be described. Numerous biochemical experiments have conclusively shown the presence of H1 at near 0.8-1:1 stoichiometry with core histones in most eukaryotic organisms (reviewed in (Woodcock et al, 2006; Zlatanova & Van Holde, 1992)). With stoichiometric H1 concentrations and chromatin fibers with longer nucleosome repeat lengths, the predominant model is proposed to adopt a one-start helical model as suggested by Robinson & Rhodes (Structure III in Figure 5.3). In the absence of the stabilizing role of H1, this structure forms puddles of nucleosomes and is disorganized, as reported in (Routh et al, 2008) (Structure I). Our model predicts that the ‘default’ chromatin structure is in a state of constant equilibrium between these structures (Structure II).

Ours and several other FRAP experiments on H1 have shown that most of the H1 molecules are bound to chromatin with low affinity (88% by our own estimate) (Carrero et al, 2004a; Carrero et al, 2004b; Misteli et al, 2000). More importantly, H1 is in a state of dynamic equilibrium undergoing complex binding-unbinding events (Lever et al, 2000; Misteli et al, 2000). If we work under the assumption that H1 binding and the consequent changes in linker DNA trajectory has a direct impact on chromatin structure, then it would imply that the chromatin

fiber itself is in a state of dynamic equilibrium that is dictated by the binding of architectural proteins such as H1. This is supported by atomic force spectroscopy experiments that have described the 30nm fiber as being highly compliant and dynamic (Kruithof et al, 2009).

One of the key differences between the two models is that our model places H1's role in stabilizing chromatin fibers as a key feature in shaping different chromatin structures. With a stronger binding of H1 to chromatin, the equilibrium would be shifted to the more compact and ordered structure proposed by Robinson & Rhodes (Structure III), while a relatively weaker binding of H1 would favor the more disorganized structure (Structure I/II). In FRAP or mathematical modeling terms, a stronger binding would imply a greater residence time for high affinity H1 population and/or higher affinity for the freely diffusing pool to chromatin. The transition between chromatin structures can, of course, be enhanced or impeded by other chromatin remodelers or histone variants, which also play a significant role in determining chromatin structures. Unlike the hierarchical model, furthermore, our model does not require eviction of H1 from decondensed structures such as transcriptionally active chromatin. Post-translational modifications, for example, can impede the binding cycle of H1 by preventing the transition from low-affinity to high affinity interactions and push the equilibrium of 30nm structures towards a decondensed state (Structure I). Furthermore, the process of evicting H1 is energetically unfavorable given the strong electrostatic interactions between H1 and DNA.

Our data does not support a complete transformation of the 30nm fiber to the Robinson & Rhodes model (Structure III) in an interphase nuclear environment. Numerous FRAP experiments have established that the majority of H1 molecules are bound to chromatin with low-affinity (Carrero et al, 2004a; Carrero et al, 2004b; Misteli et al, 2000). This assumption in this interpretation is that a complete transformation to the Robinson & Rhodes model would necessitate a high degree of H1 molecules bound with high affinity, to stack and orient successive nucleosomes. Such a high proportion of H1 molecules engaged in high-affinity binding is inconsistent with our FRAP data. Transition to the Robinson model (one-start), however, might be an event seen in condensed chromatin structures, such as in mitotic chromosomes. The proportions of high affinity H1 molecules in condensed chromosomes have not been reported, although they have been observed to still be highly dynamic (Lever et al, 2000). As such, the formation of mitotic structures may require the added contribution of proteins such as condensins and SMCs (Kireeva et al, 2004).

Similarly, our data does not support either a complete disorganization of the structure I. Since H1 is always present, even in structures that are transcriptionally elongating. Hence the ‘default’ model of chromatin is in a constant state of flux. This is in contrast to the hierarchical model that describes an ‘all or none’ effect whereby nucleosomal arrays in the presence of longer nucleosome repeat lengths and H1, radically transform from the Richmond model of 30nm fiber to the Robinson & Rhodes model (Bassett et al, 2009; Robinson & Rhodes, 2006; Travers, 2009). Our model describes a structure of chromatin fiber

that is in a state of dynamic flux between two one-start helices, flux which is dependent on the affinity with which H1 binds. It could be a result of this dynamicity that the structure of the 30nm fiber has been so controversial. Models based on X-ray crystal structures of tetranucleosomes (Schalch et al, 2005) or paraformaldehyde-fixed EM samples (Robinson et al, 2006) represent a conformation of the chromatin that is static and conformationally immobile. Our model is based on the dynamic nature of H1, and hence, is a functionally relevant model. However, it will be interesting to see whether different structures of chromatin are obtained when chromatin fibers are reconstituted with phosphorylated H1 molecules, or when the core histones are acetylated. We will now explore the changes to chromatin structure when such changes are imposed on the chromatin fiber.

Our results would support the 'dynamic chromatin' model for transcription-associated changes in chromatin structure. Upon induction of transcription and accompanying acetylation of histones and phosphorylation of H1, H1 binding is reduced through changes in H1 binding cycle. This change at the nucleosomal level changes the orientation of the linker DNA from a predominantly closed position to a relatively open position. In other words, impeding the H1 binding cycle decreases the linker DNA entry/exit angle. This relaxation in the conformation at the nucleosomal level may be necessary and sufficient to allow higher orders of chromatin structures to decondense, allowing the acquisition of 30nm structures with a lower compaction ratio.

Based on our model in which H1 is always present on chromatin, there are two possible, mutually inclusive, modes through which a compact chromatin fiber with one start helical structure can decondense.

1. A change in entry/exit angle induces a change in chromatin structure with a lower packing ratio. Upon transcriptional activation, and reduced H1 binding, the entry-exit angle decreases, which may be sufficient for changes in the packaging density of the chromatin fiber. Support for this hypothesis comes from Monte-carlo simulations of the one-start helical 30nm fiber, which has revealed that upon decreasing in the entry-exit angle from 104° to 84° , the compaction ratio decreases from 6.6 nucleosomes/11nm to 5.9 nucleosomes/11nm (Kepper et al, 2008).

2. A transformation to the two-start helix through a reduction in nucleosomal repeat length. Although nucleosome repeat lengths from a wide variety of tissues and organisms have revealed these values to vary between 175-190bp, some exceptions to this rule have been reported. Nucleosome repeat lengths in the range of 167bp have been found, so far, only in yeast (165bp) (Downs et al, 2003; Woodcock et al, 2006) and rat neurons (162bp) (Pearson et al, 1984). In such cases, the two-start helix, as proposed by Richmond et al., could be the predominant structure of the 30nm fiber, with lower compaction and longer fiber lengths. Note that such structures have a low dependence for H1 mediated compaction (Routh et al, 2008). The lower compaction may be of benefit for chromatin structures in yeast that experience high rate of transcriptional activity.

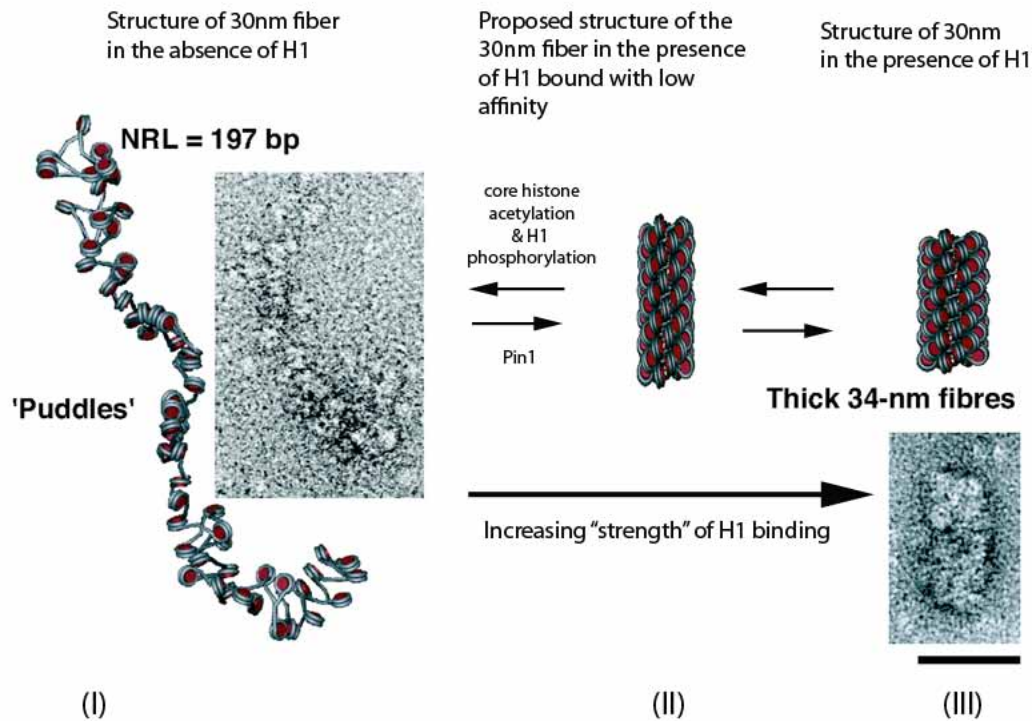


Figure 5.3 – Dynamic chromatin conformation model. This model is based on the dynamic behavior of H1 molecules in the nucleus, coupled with our observation that most changes to chromatin (such as hyperacetylation and Pin1 mediated proline isomerisation) affect the low-affinity H1 binding or alter the residence time of the high affinity population. The proportion of stably bound H1 molecules is fairly consistent among different chromatin environments, even at transcriptionally active chromatin sites. Under conditions of maximal H1 binding which ensures maximal coiling of the linker DNA, we expect the conformation of the 30nm structure to resemble closely the model proposed by Robinson & Rhodes (Structure III) (Robinson et al, 2006). However, under physiological conditions under which most of the linker histones are bound to chromatin with low affinity, the chromatin fiber is expected to decondense, decreasing the packing ratio (Structure II). In the complete absence of H1, the chromatin fiber adopts a disorganized structure, forming puddles of nucleosomes (structure I). Changes such as increased core histone acetylation and H1 phosphorylation change the temporal dynamics of H1. This changes the linker DNA entry/exit angles, allowing a further decrease in compaction ratio. Our data predicts that the majority of the 30nm fibers seen *in vivo* would be in state of equilibrium between structures I and II, with the strength of linker histone binding determining the prevalence of the structure. Euchromatin, which have a higher proportion of weakly bound H1 molecules, would also a higher proportion of Structure I, while heterochromatic structures would be expected to have a higher proportion of Structure II. Structure III could be observed in condensed chromatin structures

such as mitotic chromosomes, while structure I could be observed in regions with very high transcriptional activity, such as Balbiani ring structures (Andersson et al, 1982). The key difference between our model and the one previously suggested is the active participation of H1 molecules in determining the shape of the chromatin structures. Figure adapted from (Routh et al, 2008), with permission from PNAS.

Limitations of our model –

1. Our model is primarily based on the strength of H1 binding *in vivo*, and as such, cannot accurately predict the nature of the fiber itself (such as packing ratio, exact angles of linker DNA entry/exit).
2. There is limited structural information as to the nature of the chromatin fiber under reduced H1 binding. It will be interesting to analyze the nature of the 30nm fiber in the presence of such modifications, either through cryo-EM procedures (Robinson et al, 2006) or molecular simulations on existing models (Kepper et al, 2008). Atomic force spectroscopy can be used to further elucidate the physical properties of the 30nm fiber when nucleosomal arrays are reconstituted with phosphorylated H1 or acetylated core histones.
3. Additionally, our model cannot predict the nature of higher order structures of chromatin (greater than 30nm fibers), although we can postulate that the dynamic nature of the 30nm fiber could be translated to these higher order structures as well.

5.5 - Future directions

5.5.1 - Understanding the role of the NTD of H1

Most of our studies have involved the fusion of the GFP molecule to the NTD of H1 (Hendzel et al, 2004; Th'ng et al, 2005). We, and others, have assumed that the NTD of H1 plays a minimal role in influencing H1 dynamics (Hendzel et al, 2004; Stasevich et al, 2010). We have argued against fusing GFP at the CTD, since it is intrinsically disordered and has been shown to acquire a structure upon interacting with DNA (Raghuram et al, 2009). Placing an ordered GFP molecule

at this end would disrupt the molecular architecture of the protein, consistent with our observation that H1-GFP binds with lower affinity as compared to GFP-H1 (Hendzel et al, 2004). However, it has been shown that the NTD is also intrinsically disordered, and may also play a role in influencing H1 dynamics (Vila et al, 2001). While the NTD lacks the chromatin condensing function that is characteristic of the CTD (Allan et al, 1986), it may play a role in positioning and orienting the globular domain and the CTD, enhancing the binding of the entire molecule (Brown et al, 2006; Vyas & Brown, 2012a). Furthermore, our experiments with the switch mutants of H1 in response to core histone acetylation, suggest that the NTD of H1 may also play a role in influencing the behavior of H1 towards this modification.

In order to test this, we will have to use fluorescent tags that do not compromise the structure of H1. This can be accomplished by introducing artificially labeled H1-Cy3 molecules into living cells (Fang et al, 2011), either with the help of microinjection or protein transfection methods described elsewhere (Gros et al, 2006; Yan et al, 2009). H1 proteins are unique in that there is a complete absence of cysteine residues in the primary sequence of H1. However, cysteine can be introduced by site directed mutagenesis and can be tagged with fluorophores such as Cy3 using the free sulphhydryl group. H1-Cy3 molecules can be microinjected into living cells, and FRAP can be performed as before. The Cy3 tag is considerably smaller than GFP and should offer minimal resistance to H1 binding. The advantage of using the H1-Cy3 label to study the dynamics of H1 is that it

may provide us with the kinetic parameters that would be very close (and perhaps, our best) approximation to that of the endogenous H1 molecules.

The mathematical model that describes the cooperativity of H1 makes an assumption that assigns the globular domain and the NTD as since one binding module (Stasevich et al, 2010). Should the NTD act as an independent binding module, the mathematical model needs to be modified to take into account the contributions of the NTD to H1 binding.

The key limitation to this experimental approach is the efficient delivery of the labeled proteins to the nucleus. Although microinjection has been utilized by several studies, it is fairly invasive.

5.3.2 – Understanding the role of Thr phosphorylations in H1

Thr-Pro sites are located proximal to the globular end of the CTD and in the NTD of some H1 variants (Th'ng et al, 2005). They are exclusively phosphorylated during mitosis (Sarg et al, 2006). Our results showed that Ser in position 183 on H1.1 was phosphorylated during interphase. Our studies with Thr switch mutants, where we switched the positions of Thr and Ser residues revealed several interesting findings. For example, we found that substituting Thr in the position of Ser at 183 in H1.1 (H1.1 S183T), resulted in no phosphorylation in interphase. This suggested that the kinase that phosphorylates H1 in interphase has a strong preference for serine residues at position 183 and not for Thr residues. Thus, it is likely that H1 is phosphorylated by a different kinase (perhaps Cdk1) or a different kinase/cyclin combination (Cdk2 and cyclin E/A). For example, Cdk2 activity is thought to occur throughout G1 while peaking at the G1/S transition

(Paris et al, 1994). Cdk1, on the other hand, is inactive during G1 due to the presence cyclin dependent kinase inhibitors (CKI) and the absence of Cdk1 specific cyclins (Amon et al, 1994). The activity of Cdk1 increases during late G1, and the cyclinB-cdk1 complex is imported into the nucleus prior to nuclear envelope breakdown, where it's active till anaphase (Amon et al, 1994; Schwob et al, 1994). Expression of cyclins also varies with cell cycle. Cyclin A expression can be detected at the onset of S-phase as well as at the G2 phase interacting with both cdk2 and cdc2 (cdk1) (Pagano et al, 1992). Cyclin E, levels peak at the G1/S border (Lew et al, 1991), while cyclin Ds are primarily expressed in G1 phase (Sherr, 1995). This leads us to the simple hypothesis that in G1 phase, cyclin D-Cdk2 primarily target Ser residues of H1 while cyclin E-Cdk2 or cyclin A-Cdk1 target the Thr residues in mitosis.

Our kinetic studies analyzing the rates of H1 phosphorylation, revealed that Thr residues are phosphorylated approximately ten fold faster by immunoprecipitated cdk1/2. Similarly, dephosphorylation rates were higher for Thr residues, compared to Ser residues in cells treated with cdk2 inhibitor, Roscovitine (which also inhibits Cdk1, Cdk5 and cdk7 (Meijer et al, 1997)). Thr residues were rapidly dephosphorylated (10-15 min) while Ser residues took much longer (30-120 min). While we cannot conclude that cdk2 is the sole kinase targeting H1 Ser sites, we can postulate that unlike Ser residues, the Thr sites are rapidly and dynamically modified.

Thr phosphorylated H1 molecules have been observed in mitotic enriched cells (Sarg et al, 2006). Our data analyzing H1 dynamics at sites of replication

alluded towards the possibility that Thr residues may be phosphorylated at these sites. However, neither us nor others have been able to show accumulation of H1 Thr phosphorylation at sites of replication. This is either due to the lack of specific antibodies that recognize this modification, or maybe due to the rapid removal of threonine phosphorylation resulting in very low steady state levels of phosphorylated threonines in interphase. Furthermore, it is currently unknown if H1 is phosphorylated exclusively at sites of replication or if H1 phosphorylation is a global, genome-wide event associated with S-phase. Additionally, little is known about the percentage of H1 molecules undergoing this change during S-phase. Based on our experiments looking at the global changes in H1 dynamics in interphase cells, we observed that Thr residues play no role in phosphorylation dependent proline isomerisation mediated changes in H1 dynamics. Furthermore, in H1 extracted from asynchronous mixtures of cells, Thr residues were not phosphorylated even when otherwise phosphorylated serines were mutated to threonine. This argues against a simple model whereby accessibility limits phosphorylation of the more internal threonines relative to the more external serines during interphase. This apparent contradiction between our global analysis of H1 (which also includes S-phase cells) and replication-specific H1 dynamics, can be resolved if the fraction of H1 molecules undergoing this phosphorylation is small. FRAP experiments analyzing the dynamics of the global population of H1 may not be sensitive enough to detect changes locally. For replication-dependent experiments, H1 mobility has to be monitored both at sites of replication as well

as sites that are not undergoing replication. This can be done using RFP-PCNA as a marker for active replication sites.

Mass-spectroscopy on H1 extracted specifically from S-phase enriched cells would provide us with an answer as to whether Thr sites on H1 are specifically targeted during S-phase. The Thr-specific antibodies used in our studies were unable to detect threonine phosphorylation during interphase in immunofluorescence experiments. Thr-phosphorylation specific H1 antibodies, however, are essential to answering the questions regarding H1 phosphorylation during S-phase and greater emphasis needs to be placed in generating such antibodies. Little is yet known about how H1 phosphorylation can regulate the dynamics of chromatin structure during replication, or whether Pin1 has a role during this crucial process. It would be interesting to see if the replication foci, visualized by RFP-PCNA accumulation increase in size upon depletion of Pin1 (chromatin decondensation) or are subject to changes in H1 phosphorylation, similar to the changes observed during transcriptional activation.

5.3.3 – Does Pin1 recruit RNA Polymerase II to sites of transcription?

Our studies with Pin1 and H1 phosphorylation revealed that these were modifications associated with transcriptionally competent chromatin. We hypothesized that phosphorylation of H1 could be a potential mechanism of recruiting Pin1 to these sites of chromatin. It is possible that Pin1 is responsible for recruiting additional proteins to sites of transcription. The WW domain of Pin1 interacts with a number of different proteins and was initially thought of as a domain that played a role similar to the Src-homology domain (SH2 domain) to

serve as a binding module (Chen & Sudol, 1995). This would imply that local enrichment of Pin1 (and the WW domain) at transcriptionally competent sites would serve to recruit other proteins to initiate transcriptional activation.

Support for our hypothesis comes from studies where we artificially tagged Pin1 to LacR and transfected these into U2OS osteosarcoma cells housing the lac arrays. We found RNA Polymerase II to accumulate at these sites independently of any added transcriptional activators, such as mcherry-ER-tTA. This suggested that a focal accumulation of Pin1 at lac arrays was sufficient to recruit RNA Polymerase II to sites of transcription. We also found that this increase was independent of Pin1 isomerase activity. Critical mutations in the catalytic domain failed to alter recruitment of RNA Polymerase II. Furthermore, we found that the recruitment of RNA Polymerase II in itself was not sufficient for initiation of transcription because no enrichment of YFP-MS2 was found at these sites. We did not find any increase in the amount of translational product, CFP-SKL, being formed upon expression of LacR-Pin1. This is in direct contrast to the high amount of CFP-SKL expressed when transcription is activated upon expression of mcherry-ER-tTA and Tamoxifen (Rafalska-Metcalf et al, 2010).

The recruitment of RNA Polymerase II to sites of Pin1 accumulation independent of Pin1 isomerase activity is surprising. This suggests that the WW domain of Pin1 could play a principal role in recruiting proteins, such as RNA Polymerase II to sites of transcription and/or lac arrays. However, this notion is in contradiction with the phosphorylation cycle of RNA Polymerase II. RNA Polymerase II is heavily phosphorylated only upon transcriptional initiation and elongation. Any

direct interaction between Pin1 and RNA Polymerase II would have to be mediated by the phosphorylated version of RNA Polymerase II due to the strict requirement of Pin1 for phosphorylated substrates. Whether the recruited RNA Polymerase is present in its phosphorylated form or not remains to be determined. More studies need to be carried out to define the recruitment of RNA Polymerase II and other proteins to these sites. It remains possible that the recruitment of RNA Polymerase II is an indirect consequence requiring the presence of an intermediate protein mediator that is present in a phosphorylated form.

Further molecular characterization of the proteins recruited following Pin1 accumulation at transcriptionally active sites is needed to appreciate the role of Pin1 and that of the WW domain at these sites. While the association of RNA polymerase and Pin1 has been studied in the context of transcriptional elongation (Xu & Manley, 2007b), little is known about their function at transcriptionally competent sites. This can be achieved with the help of tethering either Pin1 or the WW domain by itself to LacR and expressing these artificial constructs in U2OS 263 cells. This can be followed up with an examination of the phosphorylation status of RNA Polymerase II and different transcription associated proteins recruited to these sites using immunofluorescence or live cell microscopy. These include TFIIH, TBP and transcription associated histone marks. While TFIIH would help us in understanding the phosphorylation status of the recruited RNA Polymerase II, the presence of TBP would suggest that the accumulation of Pin1 at these sites changes the site-exposure of nucleosomes, allowing sequence specific transcription factors to bind. Acetylated H3 and H4 will allow us to

characterize whether this recruitment of RNA Polymerase II is dependent upon HATs, such as Gcn5, PCAF or p300.

References:

Ajiro K, Borun TW, Cohen LH (1981a) Phosphorylation states of different histone 1 subtypes and their relationship to chromatin functions during the HeLa S-3 cell cycle. *Biochemistry* **20**(6): 1445-1454

Ajiro K, Borun TW, Shulman SD, McFadden GM, Cohen LH (1981b) Comparison of the structures of human histone 1A and 1B and their intramolecular phosphorylation sites during the HeLa S-3 cell cycle. *Biochemistry* **20**(6): 1454-1464

Alami R, Fan Y, Pack S, Sonbuchner TM, Besse A, Lin Q, Grealley JM, Skoultschi AI, Bouhassira EE (2003) Mammalian linker-histone subtypes differentially affect gene expression in vivo. *Proceedings of the National Academy of Sciences* **100**(10): 5920

Albers MW, Walsh CT, Schreiber SL (1990) Substrate specificity for the human rotamase FKBP: a view of FK506 and rapamycin as leucine-(twisted amide)-proline mimics. *The Journal of Organic Chemistry* **55**(17): 4984-4986

Albert A, Lavoie S, Vincent M (1999) A hyperphosphorylated form of RNA polymerase II is the major interphase antigen of the phosphoprotein antibody MPM-2 and interacts with the peptidyl-prolyl isomerase Pin1. *J Cell Sci* **112** (Pt 15): 2493-2500

Albig W, Drabent B, Kunz J, Kalff-Suske M, Grzeschik KH, Doenecke D (1993) All known human H1 histone genes except the H1(0) gene are clustered on chromosome 6. *Genomics* **16**(3): 649-654

Albig W, Kioschis P, Poustka A, Meergans K, Doenecke D (1997a) Human histone gene organization: nonregular arrangement within a large cluster. *Genomics* **40**(2): 314-322

Albig W, Meergans T, Doenecke D (1997b) Characterization of the H1.5 gene completes the set of human H1 subtype genes. *Gene* **184**(2): 141

Alexandrow MG, Hamlin JL (2005) Chromatin decondensation in S-phase involves recruitment of Cdk2 by Cdc45 and histone H1 phosphorylation. *The Journal of Cell Biology* **168**(6): 875-886

Alfageme CR, Zweidler A, Mahowald A, Cohen LH (1974) Histones of *Drosophila* embryos. Electrophoretic isolation and structural studies. *J Biol Chem* **249**(12): 3729-3736

Ali T, Coles P, Stevens TJ, Stott K, Thomas JO (2004) Two homologous domains of similar structure but different stability in the yeast linker histone, Hho1p. *J Mol Biol* **338**(1): 139-148

Allan J, Hartman PG, Crane-Robinson C, Aviles FX (1980) The structure of histone H1 and its location in chromatin. *Nature* **288**(5792): 675-679

Allan J, Mitchell T, Harborne N, Bohm L, Crane-Robinson C (1986) Roles of H1 domains in determining higher order chromatin structure and H1 location. *J Mol Biol* **187**(4): 591-601

Allfrey VG, Faulkner R, Mirsky AE (1964) Acetylation and Methylation of Histones and Their Possible Role in the Regulation of Rna Synthesis. *Proceedings of the National Academy of Sciences of the United States of America* **51**: 786-794

Allis CD, Gorovsky MA (1981) Histone phosphorylation in macro- and micronuclei of *Tetrahymena thermophila*. *Biochemistry* **20**(13): 3828-3833

Amon A, Irniger S, Nasmyth K (1994) Closing the cell cycle circle in yeast: G2 cyclin proteolysis initiated at mitosis persists until the activation of G1 cyclins in the next cycle. *Cell* **77**(7): 1037-1050

Anderson JD, Lowary PT, Widom J (2001) Effects of histone acetylation on the equilibrium accessibility of nucleosomal DNA target sites. *J Mol Biol* **307**(4): 977-985

Anderson JD, Widom J (2000) Sequence and position-dependence of the equilibrium accessibility of nucleosomal DNA target sites. *J Mol Biol* **296**(4): 979-987

Anderson JD, Widom J (2001) Poly(dA-dT) promoter elements increase the equilibrium accessibility of nucleosomal DNA target sites. *Mol Cell Biol* **21**(11): 3830-3839

Andersson K, Mahr R, Bjorkroth B, Daneholt B (1982) Rapid reformation of the thick chromosome fiber upon completion of RNA synthesis at the Balbiani ring genes in *Chironomus tentans*. *Chromosoma* **87**(1): 33-48

Annunziato AT, Frado LL, Seale RL, Woodcock CL (1988) Treatment with sodium butyrate inhibits the complete condensation of interphase chromatin. *Chromosoma* **96**(2): 132-138

Annunziato AT, Seale RL (1983a) Chromatin replication, reconstitution and assembly. *Mol Cell Biochem* **55**(2): 99-112

Annunziato AT, Seale RL (1983b) Histone deacetylation is required for the maturation of newly replicated chromatin. *J Biol Chem* **258**(20): 12675-12684

Archer TK, Cordingley MG, Wolford RG, Hager GL (1991) Transcription factor access is mediated by accurately positioned nucleosomes on the mouse mammary tumor virus promoter. *Molecular and cellular biology* **11**(2): 688

Arevalo-Rodriguez M, Cardenas ME, Wu X, Hanes SD, Heitman J (2000) Cyclophilin A and Ess1 interact with and regulate silencing by the Sin3-Rpd3 histone deacetylase. *EMBO J* **19**(14): 3739-3749

Arevalo-Rodriguez M, Heitman J (2005) Cyclophilin A is localized to the nucleus and controls meiosis in *Saccharomyces cerevisiae*. *Eukaryot Cell* **4**(1): 17-29

Armstrong JA (2007) Negotiating the nucleosome: factors that allow RNA polymerase II to elongate through chromatin. *Biochem Cell Biol* **85**(4): 426-434

Arrio-Dupont M, Foucault G, Vacher M, Douhou A, Cribier S (1997) Mobility of creatine phosphokinase and beta-enolase in cultured muscle cells. *Biophys J* **73**(5): 2667-2673

Ausio J, van Holde KE (1986) Histone hyperacetylation: its effects on nucleosome conformation and stability. *Biochemistry* **25**(6): 1421-1428

Axelrod D, Koppel DE, Schlessinger J, Elson E, Webb WW (1976a) Mobility measurement by analysis of fluorescence photobleaching recovery kinetics. *Biophys J* **16**(9): 1055-1069

Axelrod D, Ravdin P, Koppel DE, Schlessinger J, Webb WW, Elson EL, Podleski TR (1976b) Lateral motion of fluorescently labeled acetylcholine receptors in membranes of developing muscle fibers. *Proc Natl Acad Sci U S A* **73**(12): 4594-4598

Ayala G, Wang D, Wulf G, Frolov A, Li R, Sowadski J, Wheeler TM, Lu KP, Bao L (2003) The prolyl isomerase Pin1 is a novel prognostic marker in human prostate cancer. *Cancer Res* **63**(19): 6244-6251

Baneres JL, Martin A, Parello J (1997) The N tails of histones H3 and H4 adopt a highly structured conformation in the nucleosome. *J Mol Biol* **273**(3): 503-508

- Bao L, Kimzey A, Sauter G, Sowadski JM, Lu KP, Wang DG (2004) Prevalent overexpression of prolyl isomerase Pin1 in human cancers. *Am J Pathol* **164**(5): 1727-1737
- Bassett A, Cooper S, Wu C, Travers A (2009) The folding and unfolding of eukaryotic chromatin. *Curr Opin Genet Dev* **19**(2): 159-165
- Baylin SB, Herman JG (2000) DNA hypermethylation in tumorigenesis: epigenetics joins genetics. *Trends Genet* **16**(4): 168-174
- Beaudouin J, Mora-Bermudez F, Klee T, Daigle N, Ellenberg J (2006) Dissecting the contribution of diffusion and interactions to the mobility of nuclear proteins. *Biophys J* **90**(6): 1878-1894
- Bedford MT, Reed R, Leder P (1998) WW domain-mediated interactions reveal a spliceosome-associated protein that binds a third class of proline-rich motif: the proline glycine and methionine-rich motif. *Proc Natl Acad Sci U S A* **95**(18): 10602-10607
- Bedford MT, Sarbassova D, Xu J, Leder P, Yaffe MB (2000) A novel pro-Arg motif recognized by WW domains. *J Biol Chem* **275**(14): 10359-10369
- Bednar J, Horowitz RA, Grigoryev SA, Carruthers LM, Hansen JC, Koster AJ, Woodcock CL (1998) Nucleosomes, linker DNA, and linker histone form a unique structural motif that directs the higher-order folding and compaction of chromatin. *Proc Natl Acad Sci U S A* **95**(24): 14173-14178
- Bharath MM, Chandra NR, Rao MR (2002) Prediction of an HMG-box fold in the C-terminal domain of histone H1: insights into its role in DNA condensation. *Proteins* **49**(1): 71-81
- Bharath MM, Chandra NR, Rao MR (2003) Molecular modeling of the chromatosome particle. *Nucleic acids research* **31**(14): 4264
- Bird AW, Yu DY, Pray-Grant MG, Qiu Q, Harmon KE, Megee PC, Grant PA, Smith MM, Christman MF (2002) Acetylation of histone H4 by Esa1 is required for DNA double-strand break repair. *Nature* **419**(6905): 411-415
- Blume-Jensen P, Hunter T (2001) Oncogenic kinase signalling. *Nature* **411**(6835): 355-365
- Boffa LC, Walker J, Chen TA, Sterner R, Mariani MR, Allfrey VG (1990) Factors affecting nucleosome structure in transcriptionally active chromatin. Histone acetylation, nascent RNA and inhibitors of RNA synthesis. *Eur J Biochem* **194**(3): 811-823

Bohm L, Mitchell TC (1985) Sequence conservation in the N-terminal domain of histone H1. *FEBS Lett* **193**(1): 1-4

Bradbury EM (1992) Reversible histone modifications and the chromosome cell cycle. *BioEssays: news and reviews in molecular, cellular and developmental biology* **14**(1): 9-16

Bradbury EM, Inglis RJ, Matthews HR (1974a) Control of cell division by very lysine rich histone (F1) phosphorylation. *Nature* **247**(439): 257-261

Bradbury EM, Inglis RJ, Matthews HR, Langan TA (1974b) Molecular basis of control of mitotic cell division in eukaryotes. *Nature* **249**(457): 553-556

Bradbury EM, Inglis RJ, Matthews HR, Sarner N (1973) Phosphorylation of very-lysine-rich histone in *Physarum polycephalum*. Correlation with chromosome condensation. *Eur J Biochem* **33**(1): 131-139

Bresnick EH, Bustin M, Marsaud V, Richard-Foy H, Hager GL (1992) The transcriptionally-active MMTV promoter is depleted of histone H1. *Nucleic acids research* **20**(2): 273

Brotherton TW, Covault J, Shires A, Chalkley R (1981) Only a small fraction of avian erythrocyte histone is involved in ongoing acetylation. *Nucleic Acids Res* **9**(19): 5061-5073

Brown DT, Izard T, Misteli T (2006) Mapping the interaction surface of linker histone H1(0) with the nucleosome of native chromatin in vivo. *Nat Struct Mol Biol* **13**(3): 250-255

Brown NR, Noble ME, Endicott JA, Johnson LN (1999) The structural basis for specificity of substrate and recruitment peptides for cyclin-dependent kinases. *Nat Cell Biol* **1**(7): 438-443

Brownell JE, Zhou J, Ranalli T, Kobayashi R, Edmondson DG, Roth SY, Allis CD (1996) Tetrahymena histone acetyltransferase A: a homolog to yeast Gcn5p linking histone acetylation to gene activation. *Cell* **84**(6): 843-851

Carrero G, Crawford E, Hendzel MJ, de Vries G (2004a) Characterizing fluorescence recovery curves for nuclear proteins undergoing binding events. *Bulletin of Mathematical Biology* **66**(6): 1515-1545

Carrero G, Crawford E, Th'ng J, de Vries G, Hendzel MJ (2004b) Quantification of protein-protein and protein-DNA interactions in vivo, using fluorescence recovery after photobleaching. *Methods in enzymology* **375**: 415

Carrero G, McDonald D, Crawford E, de Vries G, Hendzel MJ (2003) Using FRAP and mathematical modeling to determine the in vivo kinetics of nuclear proteins. *Methods* **29**(1): 14–28

Carrero G, Raghuram, N., Th'ng, J., and Hendzel, M. (2009) A Method for Assessing Kinetic Changes of Histone H1 after Post-Translational Modifications. *AIP Conf Proc* **1168** **2**: 1306-1309

Carruthers LM, Bednar J, Woodcock CL, Hansen JC (1998) Linker histones stabilize the intrinsic salt-dependent folding of nucleosomal arrays: mechanistic ramifications for higher-order chromatin folding. *Biochemistry* **37**(42): 14776

Carruthers LM, Hansen JC (2000) The core histone N termini function independently of linker histones during chromatin condensation. *The Journal of Biological Chemistry* **275**(47): 37285-37290

Caterino TL, Fang H, Hayes JJ (2011) Nucleosome linker DNA contacts and induces specific folding of the intrinsically disordered H1 carboxyl-terminal domain. *Mol Cell Biol* **31**(11): 2341-2348

Catez F, Brown DT, Misteli T, Bustin M (2002) Competition between histone H1 and HMGN proteins for chromatin binding sites. *EMBO Rep* **3**(8): 760-766

Catez F, Ueda T, Bustin M (2006) Determinants of histone H1 mobility and chromatin binding in living cells. *Nat Struct Mol Biol* **13**(4): 305-310

Cayla X, Van Hoof C, Bosch M, Waelkens E, Vandekerckhove J, Peeters B, Merlevede W, Goris J (1994) Molecular cloning, expression, and characterization of PTPA, a protein that activates the tyrosyl phosphatase activity of protein phosphatase 2A. *J Biol Chem* **269**(22): 15668-15675

Cerf C, Lippens G, Muyldermans S, Segers A, Ramakrishnan V, Wodak SJ, Hallenga K, Wyns L (1993) Homo- and heteronuclear two-dimensional NMR studies of the globular domain of histone H1: sequential assignment and secondary structure. *Biochemistry* **32**(42): 11345-11351

Cerf C, Lippens G, Ramakrishnan V, Muyldermans S, Segers A, Wyns L, Wodak SJ, Hallenga K (1994) Homo- and heteronuclear two-dimensional NMR studies of the globular domain of histone H1: full assignment, tertiary structure, and comparison with the globular domain of histone H5. *Biochemistry* **33**(37): 11079-11086

Chadee DN, Allis CD, Wright JA, Davie JR (1997) Histone H1b phosphorylation is dependent upon ongoing transcription and replication in

normal and ras-transformed mouse fibroblasts. *The Journal of biological chemistry* **272**(13): 8113

Chadee DN, Taylor WR, Hurta RA, Allis CD, Wright JA, Davie JR (1995) Increased phosphorylation of histone H1 in mouse fibroblasts transformed with oncogenes or constitutively active mitogen-activated protein kinase kinase. *The Journal of Biological Chemistry* **270**(34): 20098-20105

Chahal SS, Matthews HR, Bradbury EM (1980) Acetylation of histone H4 and its role in chromatin structure and function. *Nature* **287**(5777): 76-79

Chambeyron S, Bickmore WA (2004) Chromatin decondensation and nuclear reorganization of the HoxB locus upon induction of transcription. *Genes Dev* **18**(10): 1119-1130

Che S, Wu W, Nelman-Gonzalez M, Stukenberg T, Clark R, Kuang J (1998) A phosphatase activity in *Xenopus* oocyte extracts preferentially dephosphorylates the MPM-2 epitope. *FEBS Lett* **424**(3): 225-233

Chen HI, Einbond A, Kwak SJ, Linn H, Koepf E, Peterson S, Kelly JW, Sudol M (1997) Characterization of the WW domain of human yes-associated protein and its polyproline-containing ligands. *J Biol Chem* **272**(27): 17070-17077

Chen HI, Sudol M (1995) The WW domain of Yes-associated protein binds a proline-rich ligand that differs from the consensus established for Src homology 3-binding modules. *Proc Natl Acad Sci U S A* **92**(17): 7819-7823

Chicoine LG, Schulman IG, Richman R, Cook RG, Allis CD (1986) Nonrandom utilization of acetylation sites in histones isolated from *Tetrahymena*. Evidence for functionally distinct H4 acetylation sites. *J Biol Chem* **261**(3): 1071-1076

Chien FT, van Noort J (2009) 10 years of tension on chromatin: results from single molecule force spectroscopy. *Curr Pharm Biotechnol* **10**(5): 474-485

Choy JS, Wei S, Lee JY, Tan S, Chu S, Lee TH (2010) DNA methylation increases nucleosome compaction and rigidity. *J Am Chem Soc* **132**(6): 1782-1783

Christoph CW, K (1981) NMR studies of the rates of proline cis-trans isomerization in oligopeptides. *Biopolymers* **20**: 2623-2633

Chuang CH, Carpenter AE, Fuchsova B, Johnson T, de Lanerolle P, Belmont AS (2006) Long-range directional movement of an interphase chromosome site. *Curr Biol* **16**(8): 825-831

Clark DJ, Hill CS, Martin SR, Thomas JO (1988) Alpha-helix in the carboxy-terminal domains of histones H1 and H5. *EMBO J* **7**(1): 69-75

Clarke PR, Hoffmann I, Draetta G, Karsenti E (1993) Dephosphorylation of cdc25-C by a type-2A protein phosphatase: specific regulation during the cell cycle in *Xenopus* egg extracts. *Mol Biol Cell* **4**(4): 397-411

Clegg RM (1992) Fluorescence resonance energy transfer and nucleic acids. *Methods Enzymol* **211**: 353-388

Costello JF, Fruhwald MC, Smiraglia DJ, Rush LJ, Robertson GP, Gao X, Wright FA, Feramisco JD, Peltomaki P, Lang JC, Schuller DE, Yu L, Bloomfield CD, Caligiuri MA, Yates A, Nishikawa R, Su Huang H, Petrelli NJ, Zhang X, O'Dorisio MS, Held WA, Cavenee WK, Plass C (2000) Aberrant CpG-island methylation has non-random and tumour-type-specific patterns. *Nat Genet* **24**(2): 132-138

Cousens LS, Gallwitz D, Alberts BM (1979) Different accessibilities in chromatin to histone acetylase. *J Biol Chem* **254**(5): 1716-1723

Covault J, Chalkley R (1980) The identification of distinct populations of acetylated histone. *J Biol Chem* **255**(19): 9110-9116

Crane-Robinson C (1999) How do linker histones mediate differential gene expression? *BioEssays* **21**(5): 367-371

Crenshaw DG, Yang J, Means AR, Kornbluth S (1998) The mitotic peptidyl-prolyl isomerase, Pin1, interacts with Cdc25 and Plx1. *The EMBO journal* **17**(5): 1315-1327

Cui Y, Bustamante C (2000) Pulling a single chromatin fiber reveals the forces that maintain its higher-order structure. *Proc Natl Acad Sci U S A* **97**(1): 127-132

D'Incalci M, Allavena P, Wu RS, Bonner WM (1986) H 1 variant synthesis in proliferating and quiescent human cells. *European Journal of Biochemistry* **154**(2): 273-279

Daksis JI, Lu RY, Facchini LM, Marhin WW, Penn LJ (1994) Myc induces cyclin D1 expression in the absence of de novo protein synthesis and links mitogen-stimulated signal transduction to the cell cycle. *Oncogene* **9**(12): 3635-3645

Daujat S, Zeissler U, Waldmann T, Happel N, Schneider R (2005) HP1 binds specifically to Lys26-methylated histone H1.4, whereas simultaneous Ser27 phosphorylation blocks HP1 binding. *J Biol Chem* **280**(45): 38090-38095

Davie JR, Hendzel MJ (1994) Multiple functions of dynamic histone acetylation. *J Cell Biochem* **55**(1): 98-105

Davis RJ (1993) The mitogen-activated protein kinase signal transduction pathway. *J Biol Chem* **268**(20): 14553-14556

Dedon PC, Soultz JA, Allis CD, Gorovsky MA (1991) Formaldehyde cross-linking and immunoprecipitation demonstrate developmental changes in H1 association with transcriptionally active genes. *Molecular and cellular biology* **11**(3): 1729-1733

Dilworth D, Gudavicius G, Leung A, Nelson CJ (2012) The roles of peptidyl-proline isomerases in gene regulation. *Biochem Cell Biol* **90**(1): 55-69

Dobosy JR, Selker EU (2001) Emerging connections between DNA methylation and histone acetylation. *Cell Mol Life Sci* **58**(5-6): 721-727

Doenecke D, Albig W, Bode C, Drabent B, Franke K, Gavenis K, Witt O (1997) Histones: genetic diversity and tissue-specific gene expression. *Histochem Cell Biol* **107**(1): 1-10

Doenecke D, Albig W, Bouterfa H, Drabent B (1994) Organization and expression of H1 histone and H1 replacement histone genes. *J Cell Biochem* **54**(4): 423-431

Dokmanovic M, Clarke C, Marks PA (2007) Histone deacetylase inhibitors: overview and perspectives. *Mol Cancer Res* **5**(10): 981-989

Dolinski KJ, Heitman J (1999) Hmo1p, a high mobility group 1/2 homolog, genetically and physically interacts with the yeast FKBP12 prolyl isomerase. *Genetics* **151**(3): 935-944

Dou Y, Bowen J, Liu Y, Gorovsky MA (2002) Phosphorylation and an ATP-dependent process increase the dynamic exchange of H1 in chromatin. *The Journal of cell biology* **158**(7): 1161

Dou Y, Gorovsky MA (2000) Phosphorylation of Linker Histone H1 Regulates Gene Expression In Vivo by Creating a Charge Patch. *Cell* **103**(2): 263

Dou Y, Mizzen CA, Abrams M, Allis CD, Gorovsky MA (1999) Phosphorylation of linker histone H1 regulates gene expression in vivo by mimicking H1 removal. *Molecular cell* **4**(4): 641

Downs JA, Kosmidou E, Morgan A, Jackson SP (2003) Suppression of homologous recombination by the *Saccharomyces cerevisiae* linker histone. *Mol Cell* **11**(6): 1685-1692

- Dunphy WG, Kumagai A (1991) The cdc25 protein contains an intrinsic phosphatase activity. *Cell* **67**(1): 189-196
- Eddidin M, Zagayansky Y, Lardner TJ (1976) Measurement of membrane protein lateral diffusion in single cells. *Science* **191**(4226): 466-468
- Edmondson DG, Smith MM, Roth SY (1996) Repression domain of the yeast global repressor Tup1 interacts directly with histones H3 and H4. *Genes Dev* **10**(10): 1247-1259
- Elgin SC (1990) Chromatin structure and gene activity. *Curr Opin Cell Biol* **2**(3): 437-445
- Ericsson C, Grossbach U, Bjorkroth B, Daneholt B (1990) Presence of histone H1 on an active Balbiani ring gene. *Cell* **60**(1): 73-83
- Ericsson C, Mehlin H, Bjorkroth B, Lamb MM, Daneholt B (1989) The ultrastructure of upstream and downstream regions of an active Balbiani ring gene. *Cell* **56**(4): 631-639
- Ermekova KS, Zambrano N, Linn H, Minopoli G, Gertler F, Russo T, Sudol M (1997) The WW domain of neural protein FE65 interacts with proline-rich motifs in Mena, the mammalian homolog of Drosophila enabled. *J Biol Chem* **272**(52): 32869-32877
- Fan Y, Nikitina T, Morin-Kensicki EM, Zhao J, Magnuson TR, Woodcock CL, Skoultchi AI (2003) H1 Linker Histones Are Essential for Mouse Development and Affect Nucleosome Spacing In Vivo. *Molecular and cellular Biology* **23**(13): 4559-4572
- Fan Y, Nikitina T, Zhao J, Fleury TJ, Bhattacharyya R, Bouhassira EE, Stein A, Woodcock CL, Skoultchi AI (2005) Histone H1 Depletion in Mammals Alters Global Chromatin Structure but Causes Specific Changes in Gene Regulation. *Cell* **123**(7): 1199
- Fang H, Clark DJ, Hayes JJ (2011) DNA and nucleosomes direct distinct folding of a linker histone H1 C-terminal domain. *Nucleic Acids Res*: 1-10
- Feinberg AP, Vogelstein B (1983) Hypomethylation distinguishes genes of some human cancers from their normal counterparts. *Nature* **301**(5895): 89-92
- Filmus J, Robles AI, Shi W, Wong MJ, Colombo LL, Conti CJ (1994) Induction of cyclin D1 overexpression by activated ras. *Oncogene* **9**(12): 3627-3633

Finn RM, Browne K, Hodgson KC, Ausio J (2008) sNASP, a histone H1-specific eukaryotic chaperone dimer that facilitates chromatin assembly. *Biophys J* **95**(3): 1314-1325

Fischer G, Aumuller T (2003) Regulation of peptide bond cis/trans isomerization by enzyme catalysis and its implication in physiological processes. *Rev Physiol Biochem Pharmacol* **148**: 105-150

Fletcher TM, Hansen JC (1995) Core histone tail domains mediate oligonucleosome folding and nucleosomal DNA organization through distinct molecular mechanisms. *The Journal of Biological Chemistry* **270**(43): 25359-25362

Fletcher TM, Hansen JC (1996) The nucleosomal array: structure/function relationships. *Crit Rev Eukaryot Gene Expr* **6**(2-3): 149-188

Flickinger CJ (1965) The fine structure of the nuclei of *Tetrahymena pyriformis* throughout the cell cycle. *J Cell Biol* **27**(3): 519-529

Folco HD, Freitag M, Ramon A, Temporini ED, Alvarez ME, Garcia I, Scazzocchio C, Selker EU, Rosa AL (2003) Histone H1 Is Required for Proper Regulation of Pyruvate Decarboxylase Gene Expression in *Neurospora crassa*. *Eukaryotic Cell* **2**(2): 341-350

Fraga MF, Ballestar E, Villar-Garea A, Boix-Chornet M, Espada J, Schotta G, Bonaldi T, Haydon C, Ropero S, Petrie K, Iyer NG, Perez-Rosado A, Calvo E, Lopez JA, Cano A, Calasanz MJ, Colomer D, Piris MA, Ahn N, Imhof A, Caldas C, Jenuwein T, Esteller M (2005) Loss of acetylation at Lys16 and trimethylation at Lys20 of histone H4 is a common hallmark of human cancer. *Nat Genet* **37**(4): 391-400

Franke K, Drabent B, Doenecke D (1998) Testicular expression of the mouse histone H1.1 gene. *Histochem Cell Biol* **109**(4): 383-390

Galat A (2003) Peptidylprolyl cis/trans isomerases (immunophilins): biological diversity--targets--functions. *Curr Top Med Chem* **3**(12): 1315-1347

Galat A (2004) A note on clustering the functionally-related paralogues and orthologues of proteins: a case of the FK506-binding proteins (FKBPs). *Comput Biol Chem* **28**(2): 129-140

Gallinari P, Di Marco S, Jones P, Pallaoro M, Steinkuhler C (2007) HDACs, histone deacetylation and gene transcription: from molecular biology to cancer therapeutics. *Cell Res* **17**(3): 195-211

Garcia-Manero G, Tambaro FP, Bekele NB, Yang H, Ravandi F, Jabbour E, Borthakur G, Kadia TM, Konopleva MY, Faderl S, Cortes JE, Brandt M, Hu Y, McCue D, Newsome WM, Pierce SR, de Lima M, Kantarjian HM (2012) Phase II Trial of Vorinostat With Idarubicin and Cytarabine for Patients With Newly Diagnosed Acute Myelogenous Leukemia or Myelodysplastic Syndrome. *J Clin Oncol* **30**(18): 2204-2210

Garcia-Ramirez M, Dong F, Ausio J (1992) Role of the histone "tails" in the folding of oligonucleosomes depleted of histone H1. *J Biol Chem* **267**(27): 19587-19595

Garcia-Ramirez M, Rocchini C, Ausio J (1995) Modulation of chromatin folding by histone acetylation. *The Journal of Biological Chemistry* **270**(30): 17923-17928

Gautier J, Solomon MJ, Booher RN, Bazan JF, Kirschner MW (1991) cdc25 is a specific tyrosine phosphatase that directly activates p34cdc2. *Cell* **67**(1): 197-211

Gilbert N, Thomson I, Boyle S, Allan J, Ramsahoye B, Bickmore WA (2007) DNA methylation affects nuclear organization, histone modifications, and linker histone binding but not chromatin compaction. *J Cell Biol* **177**(3): 401-411

Girardot V, Rabilloud T, Yoshida M, Beppu T, Lawrence JJ, Khochbin S (1994) Relationship between core histone acetylation and histone H1(0) gene activity. *Eur J Biochem* **224**(3): 885-892

Gjerset R, Gorka C, Hasthorpe S, Lawrence JJ, Eisen H (1982) Developmental and hormonal regulation of protein H1 degrees in rodents. *Proc Natl Acad Sci USA* **79**(7): 2333-2337

Godde JS, Ura K (2008) Cracking the enigmatic linker histone code. *J Biochem* **143**(3): 287-293

Goelz SE, Vogelstein B, Hamilton SR, Feinberg AP (1985) Hypomethylation of DNA from benign and malignant human colon neoplasms. *Science* **228**(4696): 187-190

Gorovsky MA (1973) Macro- and micronuclei of *Tetrahymena pyriformis*: a model system for studying the structure and function of eukaryotic nuclei. *J Protozool* **20**(1): 19-25

Gorovsky MA, Glover C, Johmann CA, Keevert JB, Mathis DJ, Samuelson M (1978) Histones and chromatin structure in *Tetrahymena* macro- and micronuclei. *Cold Spring Harb Symp Quant Biol* **42 Pt 1**: 493-503

- Gorovsky MA, Keevert JB (1975) Subunit structure of a naturally occurring chromatin lacking histones F1 and F3. *Proc Natl Acad Sci U S A* **72**(9): 3536-3540
- Gorovsky MA, Keevert JB, Pleger GL (1974) Histone F1 of *Tetrahymena* macronuclei: unique electrophoretic properties and phosphorylation of F1 in an amitotic nucleus. *J Cell Biol* **61**(1): 134-145
- Gorovsky MA, Pleger GL, Keevert JB, Johmann CA (1973) Studies on histone fraction F2A1 in macro- and micronuclei of *Tetrahymena pyriformis*. *J Cell Biol* **57**(3): 773-781
- Gothel SF, Marahiel MA (1999) Peptidyl-prolyl cis-trans isomerases, a superfamily of ubiquitous folding catalysts. *Cell Mol Life Sci* **55**(3): 423-436
- Gros E, Deshayes S, Morris MC, Aldrian-Herrada G, Depollier J, Heitz F, Divita G (2006) A non-covalent peptide-based strategy for protein and peptide nucleic acid transduction. *Biochim Biophys Acta* **1758**(3): 384-393
- Grunwald D, Khochbin S, Lawrence JJ (1991) Cell cycle-related accumulation of H1(0) mRNA: induction in murine erythroleukemia cells. *Exp Cell Res* **194**(2): 174-179
- Gurley LR, D'Anna JA, Barham SS, Deaven LL, Tobey RA (1978) Histone phosphorylation and chromatin structure during mitosis in Chinese hamster cells. *European Journal of Biochemistry* **84**(1): 1
- Gurley LR, Walters RA, Tobey RA (1974) Cell cycle-specific changes in histone phosphorylation associated with cell proliferation and chromosome condensation. *J Cell Biol* **60**(2): 356-364
- Han X, Yoon SH, Ding Y, Choi TG, Choi WJ, Kim YH, Kim YJ, Huh YB, Ha J, Kim SS (2010) Cyclosporin A and sangliferrin A enhance chemotherapeutic effect of cisplatin in C6 glioma cells. *Oncol Rep* **23**(4): 1053-1062
- Handsbumacher RE, Harding MW, Rice J, Drugge RJ, Speicher DW (1984) Cyclophilin: a specific cytosolic binding protein for cyclosporin A. *Science* **226**(4674): 544-547
- Hansen JC (2002) Conformational dynamics of the chromatin fiber in solution: determinants, mechanisms, and functions. *Annu Rev Biophys Biomol Struct* **31**: 361-392

Hansen JC, Lu X, Ross ED, Woody RW (2006) Intrinsic protein disorder, amino acid composition, and histone terminal domains. *The Journal of biological chemistry* **281**(4): 1853

Hansen JC, Nyborg JK, Luger K, Stargell LA (2010) Histone chaperones, histone acetylation, and the fluidity of the chromogenome. *J Cell Physiol* **224**(2): 289-299

Hansen JC, Tse C, Wolffe AP (1998) Structure and function of the core histone N-termini: more than meets the eye. *Biochemistry* **37**(51): 17637-17641

Happel N, Schulze E, Doenecke D (2005) Characterisation of human histone H1x. *Biological chemistry* **386**(6): 541

Harding MW, Galat A, Uehling DE, Schreiber SL (1989) A receptor for the immunosuppressant FK506 is a cis-trans peptidyl-prolyl isomerase. *Nature* **341**(6244): 758-760

He X, Ding Y, Li D, Lin B (2004) Recent advances in the study of biomolecular interactions by capillary electrophoresis. *Electrophoresis* **25**(4-5): 697-711

Hebbes TR, Clayton A, AW T, C. C-R (1994a) Core histone hyperacetylation co-maps with generalized DNase I sensitivity in the chicken β -globin chromosomal domain. *EMBO J* **13**(8): 1823-1830

Hebbes TR, Clayton AL, Thorne AW, Crane-Robinson C (1994b) Core histone hyperacetylation co-maps with generalized DNase I sensitivity in the chicken beta-globin chromosomal domain. *EMBO J* **13**(8): 1823-1830

Hebbes TR, Thorne AW, Clayton AL, Crane-Robinson C (1992) Histone acetylation and globin gene switching. *Nucleic Acids Res* **20**(5): 1017-1022

Hebbes TR, Thorne AW, Crane-Robinson C (1988a) A direct link between core histone acetylation and transcriptionally active chromatin. *EMBO J* **7**(5): 1395-1402

Hebbes TR, Thorne AW, Crane-Robinson C (1988b) A direct link between core histone acetylation and transcriptionally active chromatin. *EMBO J* **7**(5): 1395-1402

Hecht A, Laroche T, Strahl-Bolsinger S, Gasser SM, Grunstein M (1995) Histone H3 and H4 N-termini interact with SIR3 and SIR4 proteins: a molecular model for the formation of heterochromatin in yeast. *Cell* **80**(4): 583-592

Hecht A, Strahl-Bolsinger S, Grunstein M (1996) Spreading of transcriptional repressor SIR3 from telomeric heterochromatin. *Nature* **383**(6595): 92-96

Hendzel MJ, Davie JR (1991) Dynamically acetylated histones of chicken erythrocytes are selectively methylated. *Biochem J* **273** (Pt 3): 753-758

Hendzel MJ, Delcuve GP, Davie JR (1991) Histone deacetylase is a component of the internal nuclear matrix. *J Biol Chem* **266**(32): 21936-21942

Hendzel MJ, Kruhlak MJ, Bazett-Jones DP (1998) Organization of highly acetylated chromatin around sites of heterogeneous nuclear RNA accumulation. *Mol Biol Cell* **9**(9): 2491-2507

Hendzel MJ, Lever MA, Crawford E, Th'ng JP (2004) The C-terminal domain is the primary determinant of histone H1 binding to chromatin in vivo. *The Journal of biological chemistry* **279**(19): 20028

Herrera RE, Chen F, Weinberg RA (1996) Increased histone H1 phosphorylation and relaxed chromatin structure in Rb-deficient fibroblasts. *Proceedings of the National Academy of Sciences of the United States of America* **93**(21): 11510

Higurashi M, Adachi H, Ohba Y (1987) Synthesis and degradation of H1 histone subtypes in mouse lymphoma L5178Y cells. *The Journal of biological Chemistry* **262**(27): 13075-13080

Hill CS, Rimmer JM, Green BN, Finch JT, Thomas JO (1991) Histone-DNA interactions and their modulation by phosphorylation of -Ser-Pro-X-Lys/Arg-motifs. *EMBO J* **10**(7): 1939-1948

Hill RJ, Watt F, Wilson CM, Fifis T, Underwood PA, Tribbick G, Geysen HM, Thomas JO (1989) Bands, interbands and puffs in native Drosophila polytene chromosomes are recognized by a monoclonal antibody to an epitope in the carboxy-terminal tail of histone H1. *Chromosoma* **98**(6): 411-421

Hinterdorfer P, Van Oijen A (2009) *Handbook of Single-Molecule Biophysics*: Springer.

Hirose Y, Manley JL (1998) RNA polymerase II is an essential mRNA polyadenylation factor. *Nature* **395**(6697): 93-96

Hohmann P (1983) Phosphorylation of H1 histones. *Mol Cell Biochem* **57**(1): 81-92

Hohmann P, Tobey RA, Gurley LR (1976) Phosphorylation of distinct regions of f1 histone. Relationship to the cell cycle. *J Biol Chem* **251**(12): 3685-3692

Howard BA, Furumai R, Campa MJ, Rabbani ZN, Vujaskovic Z, Wang XF, Patz EF, Jr. (2005) Stable RNA interference-mediated suppression of cyclophilin A diminishes non-small-cell lung tumor growth in vivo. *Cancer Res* **65**(19): 8853-8860

Hu MC, Davidson N (1987) The inducible lac operator-repressor system is functional in mammalian cells. *Cell* **48**(4): 555-566

Hu Y, Kireev I, Plutz M, Ashourian N, Belmont AS (2009) Large-scale chromatin structure of inducible genes: transcription on a condensed, linear template. *J Cell Biol* **185**(1): 87-100

Huang RC, Bonner J (1962) Histone, a suppressor of chromosomal RNA synthesis. *Proc Natl Acad Sci U S A* **48**: 1216-1222

Hubner MR, Spector DL (2010) Chromatin dynamics. *Annu Rev Biophys* **39**: 471-489

Hunter T, Pines J (1994) Cyclins and cancer. II: Cyclin D and CDK inhibitors come of age. *Cell* **79**(4): 573-582

Hurwitz J, Anders M, Gold M, Smith I (1965) The Enzymatic Methylation of Ribonucleic Acid and Deoxyribonucleic Acid. Vii. The Methylation of Ribonucleic Acid. *J Biol Chem* **240**: 1256-1266

Ip YT, Jackson V, Meier J, Chalkley R (1988) The separation of transcriptionally engaged genes. *J Biol Chem* **263**(28): 14044-14052

Ivanov PVaZ, J. S. (1989) Quantitative changes in the histone content of the cytoplasm and the nucleus of germinating maize embryo cells. *Plant Physiol Biochem* **27**: 925-930

Jackson DA, Pombo A, Iborra F (2000) The balance sheet for transcription: an analysis of nuclear RNA metabolism in mammalian cells. *FASEB J* **14**(2): 242-254

Jackson V, Shires A, Tanphaichitr N, Chalkley R (1976) Modifications to histones immediately after synthesis. *J Mol Biol* **104**(2): 471-483

Janicki SM, Tsukamoto T, Salghetti SE, Tansey WP, Sachidanandam R, Prasanth KV, Ried T, Shav-Tal Y, Bertrand E, Singer RH, Spector DL (2004) From silencing to gene expression: real-time analysis in single cells. *Cell* **116**(5): 683-698

Jansen-Durr P, Meichle A, Steiner P, Pagano M, Finke K, Botz J, Wessbecher J, Draetta G, Eilers M (1993) Differential modulation of cyclin gene expression by MYC. *Proc Natl Acad Sci U S A* **90**(8): 3685-3689

Janssens V, Van Hoof C, Merlevede W, Goris J (1998) PTPA regulating PP2A as a dual specificity phosphatase. *Methods Mol Biol* **93**: 103-115

Johmann CA, Gorovsky MA (1976) Immunofluorescence evidence for the absence of histone H1 in a mitotically dividing, genetically inactive nucleus. *J Cell Biol* **71**(1): 89-95

John S, Howe L, Tafrov ST, Grant PA, Sternglanz R, Workman JL (2000) The something about silencing protein, Sas3, is the catalytic subunit of NuA3, a yTAF(II)30-containing HAT complex that interacts with the Spt16 subunit of the yeast CP (Cdc68/Pob3)-FACT complex. *Genes Dev* **14**(10): 1196-1208

Jones PA, Baylin SB (2002) The fundamental role of epigenetic events in cancer. *Nat Rev Genet* **3**(6): 415-428

Jones PA, Laird PW (1999) Cancer epigenetics comes of age. *Nat Genet* **21**(2): 163-167

Jones PL, Veenstra GJ, Wade PA, Vermaak D, Kass SU, Landsberger N, Strouboulis J, Wolffe AP (1998) Methylated DNA and MeCP2 recruit histone deacetylase to repress transcription. *Nat Genet* **19**(2): 187-191

Jonsson ZO, Hubscher U (1997) Proliferating cell nuclear antigen: more than a clamp for DNA polymerases. *Bioessays* **19**(11): 967-975

Jordens J, Janssens V, Longin S, Stevens I, Martens E, Bultynck G, Engelborghs Y, Lescrinier E, Waelkens E, Goris J, Van Hoof C (2006) The protein phosphatase 2A phosphatase activator is a novel peptidyl-prolyl cis/trans-isomerase. *J Biol Chem* **281**(10): 6349-6357

Jouvet N, Poschmann J, Douville J, Bulet L, Ramotar D (2010) Rrd1 isomerizes RNA polymerase II in response to rapamycin. *BMC Mol Biol* **11**: 92

Kamakaka RT, Thomas JO (1990) Chromatin structure of transcriptionally competent and repressed genes. *The EMBO journal* **9**(12): 3997

Kaplan LJ, Bauer R, Morrison E, Langan TA, Fasman GD (1984) The structure of chromatin reconstituted with phosphorylated H1. Circular dichroism and thermal denaturation studies. *The Journal of biological chemistry* **259**(14): 8777

Karaiskou A, Jessus C, Brassac T, Ozon R (1999) Phosphatase 2A and polo kinase, two antagonistic regulators of cdc25 activation and MPF auto-amplification. *J Cell Sci* **112 (Pt 21)**: 3747-3756

Karymov MA, Tomschik M, Leuba SH, Caiafa P, Zlatanova J (2001) DNA methylation-dependent chromatin fiber compaction in vivo and in vitro: requirement for linker histone. *FASEB J* **15(14)**: 2631-2641

Kasinsky HE, Lewis JD, Dacks JB, Ausio J (2001) Origin of H1 linker histones. *FASEB J* **15(1)**: 34-42

Kawasaki H, Eckner R, Yao TP, Taira K, Chiu R, Livingston DM, Yokoyama KK (1998) Distinct roles of the co-activators p300 and CBP in retinoic-acid-induced F9-cell differentiation. *Nature* **393(6682)**: 284-289

Kelly WK, Marks PA (2005) Drug insight: Histone deacetylase inhibitors--development of the new targeted anticancer agent suberoylanilide hydroxamic acid. *Nat Clin Pract Oncol* **2(3)**: 150-157

Kelly WK, O'Connor OA, Krug LM, Chiao JH, Heaney M, Curley T, MacGregore-Cortelli B, Tong W, Secrist JP, Schwartz L, Richardson S, Chu E, Olgac S, Marks PA, Scher H, Richon VM (2005) Phase I study of an oral histone deacetylase inhibitor, suberoylanilide hydroxamic acid, in patients with advanced cancer. *J Clin Oncol* **23(17)**: 3923-3931

Kepper N, Foethke D, Stehr R, Wedemann G, Rippe K (2008) Nucleosome geometry and internucleosomal interactions control the chromatin fiber conformation. *Biophys J* **95(8)**: 3692-3705

Khadake JR, Rao MRS (1995) DNA-and chromatin-condensing properties of rat testes H1a and H1t compared to those of rat liver H1bdec: H1t is a poor condenser of chromatin. *Biochemistry* **34(48)**: 15792-15801

Khochbin S, Wolffe AP (1994) Developmentally regulated expression of linker-histone variants in vertebrates. *FEBS Journal* **225(2)**: 501-510

Kim Y, Yoshida M, Horinouchi S (1999) Selective Induction of Cyclin-Dependent Kinase Inhibitors and Their Roles in Cell Cycle Arrest Caused by Trichostatin A, an Inhibitor of Histone Deacetylase. *Annals of the New York Academy of Sciences* **886(1)**: 200-203

Kim YB, Ki SW, Yoshida M, Horinouchi S (2000) Mechanism of cell cycle arrest caused by histone deacetylase inhibitors in human carcinoma cells. *J Antibiot (Tokyo)* **53(10)**: 1191-1200

Kimura H, Cook PR (2001) Kinetics of Core Histones in Living Human Cells Little Exchange of H3 and H4 and Some Rapid Exchange of H2B. *The Journal of cell biology* **153**(7): 1341

Kingston RE, Bunker CA, Imbalzano AN (1996) Repression and activation by multiprotein complexes that alter chromatin structure. *Genes Dev* **10**(8): 905-920

Kinkade JM, Jr., Cole RD (1966) The resolution of four lysine-rich histones derived from calf thymus. *The Journal of biological chemistry* **241**(24): 5790

Kinoshita E, Kinoshita-Kikuta E, Koike T (2009) Separation and detection of large phosphoproteins using Phos-tag SDS-PAGE. *Nat Protoc* **4**(10): 1513-1521

Kinoshita E, Kinoshita-Kikuta E, Matsubara M, Yamada S, Nakamura H, Shiro Y, Aoki Y, Okita K, Koike T (2008) Separation of phosphoprotein isotypes having the same number of phosphate groups using phosphate-affinity SDS-PAGE. *Proteomics* **8**(15): 2994-3003

Kireeva N, Lakonishok M, Kireev I, Hirano T, Belmont AS (2004) Visualization of early chromosome condensation: a hierarchical folding, axial glue model of chromosome structure. *J Cell Biol* **166**(6): 775-785

Kirschbaum M, Frankel P, Popplewell L, Zain J, Delioukina M, Pullarkat V, Matsuoka D, Pulone B, Rotter AJ, Espinoza-Delgado I, Nademanee A, Forman SJ, Gandara D, Newman E (2011) Phase II study of vorinostat for treatment of relapsed or refractory indolent non-Hodgkin's lymphoma and mantle cell lymphoma. *J Clin Oncol* **29**(9): 1198-1203

Koop R, Di Croce L, Beato M (2003) Histone H1 enhances synergistic activation of the MMTV promoter in chromatin. *The EMBO journal* **22**(3): 588

Kornberg RD, Lorch Y (1999) Twenty-Five Years of the Nucleosome, Review Fundamental Particle of the Eukaryote Chromosome. *Cell* **98**: 285

Kornberg RD, Thomas JO (1974) Chromatin structure; oligomers of the histones. *Science* **184**(4139): 865-868

Kouzarides T (2007) Chromatin modifications and their function. *Cell* **128**(4): 693-705

Krishnamurthy S, Ghazy MA, Moore C, Hampsey M (2009) Functional interaction of the Ess1 prolyl isomerase with components of the RNA polymerase II initiation and termination machineries. *Mol Cell Biol* **29**(11): 2925-2934

Kruithof M, Chien FT, Routh A, Logie C, Rhodes D, van Noort J (2009) Single-molecule force spectroscopy reveals a highly compliant helical folding for the 30-nm chromatin fiber. *Nat Struct Mol Biol* **16**(5): 534-540

Krylov D, Leuba S, van Holde K, Zlatanova J (1993) Histones H1 and H5 interact preferentially with crossovers of double-helical DNA. *Proc Natl Acad Sci U S A* **90**(11): 5052-5056

Kumagai A, Dunphy WG (1992) Regulation of the cdc25 protein during the cell cycle in *Xenopus* extracts. *Cell* **70**(1): 139-151

Laitinen J, Sistonen L, Alitalo K, Holtta E (1990) c-Ha-rasVal 12 oncogene-transformed NIH-3T3 fibroblasts display more decondensed nucleosomal organization than normal fibroblasts. *J Cell Biol* **111**(1): 9-17

Laitinen J, Sistonen L, Alitalo K, Holtta E (1995) Cell transformation by c-Ha-rasVal12 oncogene is accompanied by a decrease in histone H1 zero and an increase in nucleosomal repeat length. *J Cell Biochem* **57**(1): 1-11

Lamb MM, Daneholt B (1979) Characterization of active transcription units in Balbiani rings of *Chironomus tentans*. *Cell* **17**(4): 835-848

Lamy F, Lecocq R, Dumont JE (1977) Thyrotropin stimulation of the phosphorylation of serine in the N-terminal of thyroid H1 histones. *Eur J Biochem* **73**(2): 529-535

Langan TA (1969) Phosphorylation of liver histone following the administration of glucagon and insulin. *Proc Natl Acad Sci U S A* **64**(4): 1276-1283

Langan TA (1978a) Isolation of histone kinases. *Methods Cell Biol* **19**: 143-152

Langan TA (1978b) Methods for the assessment of site-specific histone phosphorylation. *Methods Cell Biol* **19**: 127-142

Lawrie AM, Noble ME, Tunnah P, Brown NR, Johnson LN, Endicott JA (1997) Protein kinase inhibition by staurosporine revealed in details of the molecular interaction with CDK2. *Nat Struct Biol* **4**(10): 796-801

Laybourn PJ, Kadonaga JT (1991) Role of nucleosomal cores and histone H1 in regulation of transcription by RNA polymerase II. *Science* **254**(5029): 238

Lee H, Habas R, Abate-Shen C (2004) MSX1 cooperates with histone H1b for inhibition of transcription and myogenesis. *Science* **304**(5677): 1675-1678

Lee HL, Archer TK (1998) Prolonged glucocorticoid exposure dephosphorylates histone H1 and inactivates the MMTV promoter. *The EMBO journal* **17**(5): 1454

Lee KK, Workman JL (2007) Histone acetyltransferase complexes: one size doesn't fit all. *Nat Rev Mol Cell Biol* **8**(4): 284-295

Lee TH, Pastorino L, Lu KP Peptidyl-prolyl cis-trans isomerase Pin1 in ageing, cancer and Alzheimer disease. *Expert Rev Mol Med* **13**: e21

Lennox RW, Cohen LH (1983) The histone H1 complements of dividing and nondividing cells of the mouse. *The Journal of biological Chemistry* **258**(1): 262-268

Lennox RW, Oshima RG, Cohen LH (1982) The H1 histones and their interphase phosphorylated states in differentiated and undifferentiated cell lines derived from murine teratocarcinomas. *J Biol Chem* **257**(9): 5183-5189

Leonhardt H, Rahn HP, Weinzierl P, Sporbert A, Cremer T, Zink D, Cardoso MC (2000a) Dynamics of DNA replication factories in living cells. *The Journal of Cell Biology* **149**(2): 271-280

Leonhardt H, Rahn HP, Weinzierl P, Sporbert A, Cremer T, Zink D, Cardoso MC (2000b) Dynamics of DNA replication factories in living cells. *J Cell Biol* **149**(2): 271-280

Leulliot N, Vicentini G, Jordens J, Quevillon-Cheruel S, Schiltz M, Barford D, van Tilbeurgh H, Goris J (2006) Crystal structure of the PP2A phosphatase activator: implications for its PP2A-specific PPIase activity. *Mol Cell* **23**(3): 413-424

Lever MA, Th'ng JP, Sun X, Hendzel MJ (2000) Rapid exchange of histone H1.1 on chromatin in living human cells. *Nature* **408**(6814): 873

Lew DJ, Dulic V, Reed SI (1991) Isolation of three novel human cyclins by rescue of G1 cyclin (Cln) function in yeast. *Cell* **66**(6): 1197-1206

Li G, Margueron R, Hu G, Stokes D, Wang YH, Reinberg D (2010) Highly compacted chromatin formed in vitro reflects the dynamics of transcription activation in vivo. *Mol Cell* **38**(1): 41-53

Li H, He Z, Lu G, Lee SC, Alonso J, Ecker JR, Luan S (2007) A WD40 domain cyclophilin interacts with histone H3 and functions in gene repression and organogenesis in Arabidopsis. *Plant Cell* **19**(8): 2403-2416

- Li M, Zhai Q, Bharadwaj U, Wang H, Li F, Fisher WE, Chen C, Yao Q (2006) Cyclophilin A is overexpressed in human pancreatic cancer cells and stimulates cell proliferation through CD147. *Cancer* **106**(10): 2284-2294
- Li Q, Zhou H, Wurtele H, Davies B, Horazdovsky B, Verreault A, Zhang Z (2008) Acetylation of histone H3 lysine 56 regulates replication-coupled nucleosome assembly. *Cell* **134**(2): 244-255
- Liao LW, Cole RD (1981a) Condensation of dinucleosomes by individual subfractions of H1 histone. *The Journal of biological Chemistry* **256**(19): 10124-10128
- Liao LW, Cole RD (1981b) Differences among H1 histone subfractions in binding to linear and superhelical DNA. Sedimentation velocity studies. *The Journal of biological Chemistry* **256**(21): 11145-11150
- Lim SO, Park SJ, Kim W, Park SG, Kim HJ, Kim YI, Sohn TS, Noh JH, Jung G (2002) Proteome analysis of hepatocellular carcinoma. *Biochem Biophys Res Commun* **291**(4): 1031-1037
- Liou YC, Ryo A, Huang HK, Lu PJ, Bronson R, Fujimori F, Uchida T, Hunter T, Lu KP (2002) Loss of Pin1 function in the mouse causes phenotypes resembling cyclin D1-null phenotypes. *Proceedings of the National Academy of Sciences of the United States of America* **99**(3): 1335-1340
- Lippincott-Schwartz J, Snapp E, Kenworthy A (2001) Studying protein dynamics in living cells. *Nat Rev Mol Cell Biol* **2**(6): 444-456
- Liu J, Farmer JD, Jr., Lane WS, Friedman J, Weissman I, Schreiber SL (1991) Calcineurin is a common target of cyclophilin-cyclosporin A and FKBP-FK506 complexes. *Cell* **66**(4): 807-815
- Loidl P (1988) Towards an understanding of the biological function of histone acetylation. *FEBS letters* **227**(2): 91
- Lorch Y, LaPointe JW, Kornberg RD (1987) Nucleosomes inhibit the initiation of transcription but allow chain elongation with the displacement of histones. *Cell* **49**(2): 203-210
- Lorch Y, LaPointe JW, Kornberg RD (1992) Initiation on chromatin templates in a yeast RNA polymerase II transcription system. *Genes Dev* **6**(12A): 2282-2287
- Lowary PT, Widom J (1998) New DNA sequence rules for high affinity binding to histone octamer and sequence-directed nucleosome positioning. *J Mol Biol* **276**(1): 19-42

Lu KP (2004) Pinning down cell signaling, cancer and Alzheimer's disease. *Trends in biochemical sciences* **29**(4): 200-209

Lu KP, Finn G, Lee TH, Nicholson LK (2007) Prolyl cis-trans isomerization as a molecular timer. *Nat Chem Biol* **3**(10): 619-629

Lu KP, Hanes SD, Hunter T (1996) A human peptidyl-prolyl isomerase essential for regulation of mitosis. *Nature* **380**(6574): 544-547

Lu KP, Liou YC, Vincent I (2003) Proline-directed phosphorylation and isomerization in mitotic regulation and in Alzheimer's Disease. *Bioessays* **25**(2): 174-181

Lu KP, Liou YC, Zhou XZ (2002a) Pinning down proline-directed phosphorylation signaling. *Trends Cell Biol* **12**(4): 164-172

Lu KP, Zhou XZ (2007) The prolyl isomerase PIN1: a pivotal new twist in phosphorylation signalling and disease. *Nat Rev Mol Cell Biol* **8**(11): 904-916

Lu MJ, Mpoke SS, Dadd CA, Allis CD (1995a) Phosphorylated and dephosphorylated linker histone H1 reside in distinct chromatin domains in *Tetrahymena* macronuclei. *Molecular biology of the cell* **6**(8): 1077-1087

Lu MJ, Mpoke SS, Dadd CA, Allis CD (1995b) Phosphorylated and dephosphorylated linker histone H1 reside in distinct chromatin domains in *Tetrahymena* macronuclei. *Mol Biol Cell* **6**(8): 1077-1087

Lu PJ, Zhou XZ, Liou YC, Noel JP, Lu KP (2002b) Critical role of WW domain phosphorylation in regulating phosphoserine binding activity and Pin1 function. *The Journal of Biological Chemistry* **277**(4): 2381-2384

Lu PJ, Zhou XZ, Shen M, Lu KP (1999) Function of WW domains as phosphoserine- or phosphothreonine-binding modules. *Science* **283**(5406): 1325-1328

Lu X, Hamkalo B, Parseghian MH, Hansen JC (2009a) Chromatin condensing functions of the linker histone C-terminal domain are mediated by specific amino acid composition and intrinsic protein disorder. *Biochemistry* **48**(1): 164-172

Lu X, Hansen JC (2004) Identification of specific functional subdomains within the linker histone H10 C-terminal domain. *The Journal of biological chemistry* **279**(10): 8701

Lu X, Wontakal SN, Emelyanov AV, Morcillo P, Konev AY, Fyodorov DV, Skoultchi AI (2009b) Linker histone H1 is essential for Drosophila development, the establishment of pericentric heterochromatin, and a normal polytene chromosome structure. *Genes Dev* **23**(4): 452-465

Lufe C, Koh TH, Uchida T, Cao X (2007) Pin1 is required for the Ser727 phosphorylation-dependent Stat3 activity. *Oncogene* **26**(55): 7656-7664

Luger K, Mader AW, Richmond RK, Sargent DF, Richmond TJ (1997) Crystal structure of the nucleosome core particle at 2.8 Å resolution. *Nature* **389**(6648): 251-260

Luger K, Richmond TJ (1998) The histone tails of the nucleosome. *Curr Opin Genet Dev* **8**(2): 140-146

Macleod AR, Wong NC, Dixon GH (1977) The amino-acid sequence of trout-testis histone H1. *Eur J Biochem* **78**(1): 281-291

Mani SA, Guo W, Liao MJ, Eaton EN, Ayyanan A, Zhou AY, Brooks M, Reinhard F, Zhang CC, Shipitsin M, Campbell LL, Polyak K, Brisken C, Yang J, Weinberg RA (2008) The epithelial-mesenchymal transition generates cells with properties of stem cells. *Cell* **133**(4): 704-715

Maresca TJ, Freedman BS, Heald R (2005) Histone H1 is essential for mitotic chromosome architecture and segregation in *Xenopus laevis* egg extracts. *The Journal of cell biology* **169**(6): 859

Marunouchi T, Yasuda H, Matsumoto Y, Yamada M (1980) Disappearance of a basic chromosomal protein from cells of a mouse temperature-sensitive mutant defective in histone phosphorylation. *Biochem Biophys Res Commun* **95**(1): 126-131

Marzluff WF (2005) Metazoan replication-dependent histone mRNAs: a distinct set of RNA polymerase II transcripts. *Curr Opin Cell Biol* **17**(3): 274-280

Masumoto H, Hawke D, Kobayashi R, Verreault A (2005) A role for cell-cycle-regulated histone H3 lysine 56 acetylation in the DNA damage response. *Nature* **436**(7048): 294-298

Mathis DJ, Oudet P, Wasylyk B, Chambon P (1978) Effect of histone acetylation on structure and in vitro transcription of chromatin. *Nucleic Acids Res* **5**(10): 3523-3547

Matsumoto Y, Yasuda H, Marunouchi T, Yamada M (1983) Decrease in uH2A (protein A24) of a mouse temperature-sensitive mutant. *FEBS Lett* **151**(1): 139-142

Matsumoto Y, Yasuda H, Mita S, Marunouchi T, Yamada M (1980) Evidence for the involvement of H1 histone phosphorylation in chromosome condensation. *Nature* **284**(5752): 181-183

Matsuoka S, Ballif BA, Smogorzewska A, McDonald ER, 3rd, Hurov KE, Luo J, Bakalarski CE, Zhao Z, Solimini N, Lerenthal Y, Shiloh Y, Gygi SP, Elledge SJ (2007) ATM and ATR substrate analysis reveals extensive protein networks responsive to DNA damage. *Science* **316**(5828): 1160-1166

McAnaney TB, Zeng W, Doe CF, Bhanji N, Wakelin S, Pearson DS, Abbyad P, Shi X, Boxer SG, Bagshaw CR (2005) Protonation, photobleaching, and photoactivation of yellow fluorescent protein (YFP 10C): a unifying mechanism. *Biochemistry* **44**(14): 5510-5524

McBryant SJ, Hansen JC (2012) Dynamic fuzziness during linker histone action. *Adv Exp Med Biol* **725**: 15-26

McBryant SJ, Lu X, Hansen JC (2010) Multifunctionality of the linker histones: an emerging role for protein-protein interactions. *Cell Res* **20**(5): 519-528

McCracken S, Fong N, Yankulov K, Ballantyne S, Pan G, Greenblatt J, Patterson SD, Wickens M, Bentley DL (1997) The C-terminal domain of RNA polymerase II couples mRNA processing to transcription. *Nature* **385**(6614): 357-361

McGhee JD, Nickol JM, Felsenfeld G, Rau DC (1983) Histone hyperacetylation has little effect on the higher order folding of chromatin. *Nucleic Acids Research* **11**(12): 4065-4075

McManus KJ, Hendzel MJ (2003) Quantitative analysis of CBP- and P300-induced histone acetylations in vivo using native chromatin. *Mol Cell Biol* **23**(21): 7611-7627

McNally JG (2008) Quantitative FRAP in analysis of molecular binding dynamics in vivo. *Methods Cell Biol* **85**: 329-351

Meijer L, Borgne A, Mulner O, Chong JP, Blow JJ, Inagaki N, Inagaki M, Delcros JG, Moulinoux JP (1997) Biochemical and cellular effects of roscovitine, a potent and selective inhibitor of the cyclin-dependent kinases cdc2, cdk2 and cdk5. *Eur J Biochem* **243**(1-2): 527-536

Misteli T (2001) Protein dynamics: implications for nuclear architecture and gene expression. *Science* **291**(5505): 843-847

Misteli T, Gunjan A, Hock R, Bustin M, Brown DT (2000) Dynamic binding of histone H1 to chromatin in living cells. *Nature* **408**(6814): 877

Monje P, Hernandez-Losa J, Lyons RJ, Castellone MD, Gutkind JS (2005) Regulation of the transcriptional activity of c-Fos by ERK. A novel role for the prolyl isomerase PIN1. *J Biol Chem* **280**(42): 35081-35084

Montes de Oca R, Lee KK, Wilson KL (2005) Binding of barrier to autointegration factor (BAF) to histone H3 and selected linker histones including H1.1. *J Biol Chem* **280**(51): 42252-42262

Moore SC, Ausio J (1997) Major role of the histones H3-H4 in the folding of the chromatin fiber. *Biochem Biophys Res Commun* **230**(1): 136-139

Moreno S, Nurse P (1990) Substrates for p34cdc2: in vivo veritas? *Cell* **61**(4): 549-551

Moretto-Zita M, Jin H, Shen Z, Zhao T, Briggs SP, Xu Y (2010) Phosphorylation stabilizes Nanog by promoting its interaction with Pin1. *Proc Natl Acad Sci U S A* **107**(30): 13312-13317

Mori M, Eki T, Takahashi-Kudo M, Hanaoka F, Ui M, Enomoto T (1993) Characterization of DNA synthesis at a restrictive temperature in the temperature-sensitive mutants, tsFT5 cells, that belong to the complementation group of ts85 cells containing a thermolabile ubiquitin-activating enzyme E1. Involvement of the ubiquitin-conjugating system in DNA replication. *J Biol Chem* **268**(22): 16803-16809

Morris DP, Phatnani HP, Greenleaf AL (1999) Phospho-carboxyl-terminal domain binding and the role of a prolyl isomerase in pre-mRNA 3'-End formation. *J Biol Chem* **274**(44): 31583-31587

Mueller F, Mazza D, Stasevich TJ, McNally JG (2010) FRAP and kinetic modeling in the analysis of nuclear protein dynamics: what do we really know? *Curr Opin Cell Biol* **22**(3): 403-411

Mueller JW, Kessler D, Neumann D, Stratmann T, Papatheodorou P, Hartmann-Fatu C, Bayer P (2006) Characterization of novel elongated Parvulin isoforms that are ubiquitously expressed in human tissues and originate from alternative transcription initiation. *BMC Mol Biol* **7**: 9

- Muller WG, Rieder D, Kreth G, Cremer C, Trajanoski Z, McNally JG (2004) Generic features of tertiary chromatin structure as detected in natural chromosomes. *Mol Cell Biol* **24**(21): 9359-9370
- Muller WG, Walker D, Hager GL, McNally JG (2001) Large-scale chromatin decondensation and recondensation regulated by transcription from a natural promoter. *J Cell Biol* **154**(1): 33-48
- Nagaraja S, Delcuve GP, Davie JR (1995) Differential compaction of transcriptionally competent and repressed chromatin reconstituted with histone H1 subtypes. *Biochim Biophys Acta* **1260**(2): 207-214
- Nan X, Ng HH, Johnson CA, Laherty CD, Turner BM, Eisenman RN, Bird A (1998) Transcriptional repression by the methyl-CpG-binding protein MeCP2 involves a histone deacetylase complex. *Nature* **393**(6683): 386-389
- Nelson CJ, Santos-Rosa H, Kouzarides T (2006) Proline isomerization of histone H3 regulates lysine methylation and gene expression. *Cell* **126**(5): 905-916
- Nelson D, Perry ME, Chalkley R (1979) A correlation between nucleosome spacer region susceptibility to DNase I and histone acetylation. *Nucleic Acids Res* **6**(2): 561-574
- Nguyen VT, Giannoni F, Dubois MF, Seo SJ, Vigneron M, Kedinger C, Bensaude O (1996) In vivo degradation of RNA polymerase II largest subunit triggered by alpha-amanitin. *Nucleic Acids Res* **24**(15): 2924-2929
- Nigg EA (2001) Mitotic kinases as regulators of cell division and its checkpoints. *Nat Rev Mol Cell Biol* **2**(1): 21-32
- Nilsson JR (1970) Suggestive structural evidence for macronuclear "subnuclei" in *Tetrahymena pyriformis* GL. *J Protozool* **17**(4): 539-548
- Nishi M, Akutsu H, Masui S, Kondo A, Nagashima Y, Kimura H, Perrem K, Shigeri Y, Toyoda M, Okayama A, Hirano H, Umezawa A, Yamamoto N, Lee SW, Ryo A (2011) A distinct role for Pin1 in the induction and maintenance of pluripotency. *J Biol Chem* **286**(13): 11593-11603
- Noll M, Kornberg RD (1977) Action of micrococcal nuclease on chromatin and the location of histone H1. *J Mol Biol* **109**(3): 393-404
- O'Brien T, Hardin S, Greenleaf A, Lis JT (1994) Phosphorylation of RNA polymerase II C-terminal domain and transcriptional elongation. *Nature* **370**(6484): 75-77

- O'Neill TE, Meersseman G, Pennings S, Bradbury EM (1995) Deposition of histone H1 onto reconstituted nucleosome arrays inhibits both initiation and elongation of transcripts by T7 RNA polymerase. *Nucleic Acids Res* **23**(6): 1075-1082
- Ozawa Y, Towatari M, Tsuzuki S, Hayakawa F, Maeda T, Miyata Y, Tanimoto M, Saito H (2001) Histone deacetylase 3 associates with and represses the transcription factor GATA-2. *Blood* **98**(7): 2116-2123
- Ozdemir A, Masumoto H, Fitzjohn P, Verreault A, Logie C (2006) Histone H3 lysine 56 acetylation: a new twist in the chromosome cycle. *Cell Cycle* **5**(22): 2602-2608
- Pace CN, Scholtz JM (1998) A helix propensity scale based on experimental studies of peptides and proteins. *Biophys J* **75**(1): 422-427
- Pagano M, Pepperkok R, Verde F, Ansorge W, Draetta G (1992) Cyclin A is required at two points in the human cell cycle. *EMBO J* **11**(3): 961-971
- Pal D, Chakrabarti P (1999) Cis peptide bonds in proteins: residues involved, their conformations, interactions and locations. *J Mol Biol* **294**(1): 271-288
- Panyim S, Chalkley R (1969a) A new histone found only in mammalian tissues with little cell division. *Biochem Biophys Res Commun* **37**(6): 1042-1049
- Panyim S, Chalkley R (1969b) High resolution acrylamide gel electrophoresis of histones. *Arch Biochem Biophys* **130**(1): 337-346
- Paris J, Leplatois P, Nurse P (1994) Study of the higher eukaryotic gene function CDK2 using fission yeast. *J Cell Sci* **107** (Pt 3): 615-623
- Parseghian MH, Clark RF, Hauser LJ, Dvorkin N, Harris DA, Hamkalo BA (1993) Fractionation of human H1 subtypes and characterization of a subtype-specific antibody exhibiting non-uniform nuclear staining. *Chromosome research: an international journal on the molecular, supramolecular and evolutionary aspects of chromosome biology* **1**(2): 127
- Parseghian MH, Hamkalo BA (2001) A compendium of the histone H1 family of somatic subtypes: an elusive cast of characters and their characteristics. *Biochemistry and cell biology = Biochimie et biologie cellulaire* **79**(3): 289
- Parseghian MH, Harris DA, Rishwain DR, Hamkalo BA (1994) Characterization of a set of antibodies specific for three human histone H1 subtypes. *Chromosoma* **103**(3): 198

- Parseghian MH, Newcomb RL, Winokur ST, Hamkalo BA (2000) The distribution of somatic H1 subtypes is non-random on active vs. inactive chromatin: distribution in human fetal fibroblasts. *Chromosome research: an international journal on the molecular, supramolecular and evolutionary aspects of chromosome biology* **8**(5): 405
- Pathan N, Aime-Sempe C, Kitada S, Basu A, Haldar S, Reed JC (2001) Microtubule-targeting drugs induce bcl-2 phosphorylation and association with Pin1. *Neoplasia* **3**(6): 550-559
- Patterton HG, Landel CC, Landsman D, Peterson CL, Simpson RT (1998) The biochemical and phenotypic characterization of Hho1p, the putative linker histone H1 of *Saccharomyces cerevisiae*. *J Biol Chem* **273**(13): 7268-7276
- Paulson JR, Patzlaff JS, Vallis AJ (1996) Evidence that the endogenous histone H1 phosphatase in HeLa mitotic chromosomes is protein phosphatase 1, not protein phosphatase 2A. *Journal of cell science* **109** (Pt 6)(Pt 6): 1437
- Pearson EC, Bates DL, Prospero TD, Thomas JO (1984) Neuronal nuclei and glial nuclei from mammalian cerebral cortex. Nucleosome repeat lengths, DNA contents and H1 contents. *Eur J Biochem* **144**(2): 353-360
- Pehrson JR, Cole RD (1982) Histone H1 subfractions and H10 turnover at different rates in nondividing cells. *Biochemistry* **21**(3): 456-460
- Perry CA, Annunziato AT (1989) Influence of histone acetylation on the solubility, H1 content and DNase I sensitivity of newly assembled chromatin. *Nucleic acids research* **17**(11): 4275
- Perry CA, Annunziato AT (1991) Histone acetylation reduces H1-mediated nucleosome interactions during chromatin assembly. *Experimental cell research* **196**(2): 337
- Peters R, Peters J, Tews KH, Bahr W (1974) A microfluorimetric study of translational diffusion in erythrocyte membranes. *Biochim Biophys Acta* **367**(3): 282-294
- Phair RD, Gorski SA, Misteli T (2004a) Measurement of dynamic protein binding to chromatin in vivo, using photobleaching microscopy. *Methods Enzymol* **375**: 393-414
- Phair RD, Misteli T (2000) High mobility of proteins in the mammalian cell nucleus. *Nature* **404**(6778): 604
- Phair RD, Misteli T (2001) Kinetic Modelling Approaches to in vivo imaging. *Nature Reviews Molecular Cell Biology* **2**(12): 898-907

- Phair RD, Scaffidi P, Elbi C, Vecerova J, Dey A, Ozato K, Brown DT, Hager G, Bustin M, Misteli T (2004b) Global Nature of Dynamic Protein-Chromatin Interactions In Vivo: Three-Dimensional Genome Scanning and Dynamic Interaction Networks of Chromatin Proteins. *Molecular and cellular biology* **24**(14): 6393
- Poirier MG, Oh E, Tims HS, Widom J (2009) Dynamics and function of compact nucleosome arrays. *Nat Struct Mol Biol* **16**(9): 938-944
- Polach KJ, Lowary PT, Widom J (2000) Effects of core histone tail domains on the equilibrium constants for dynamic DNA site accessibility in nucleosomes. *J Mol Biol* **298**(2): 211-223
- Polach KJ, Widom J (1995) Mechanism of protein access to specific DNA sequences in chromatin: a dynamic equilibrium model for gene regulation. *J Mol Biol* **254**(2): 130-149
- Pollard KJ, Peterson CL (1997) Role for ADA/GCN5 products in antagonizing chromatin-mediated transcriptional repression. *Mol Cell Biol* **17**(11): 6212-6222
- Poschmann J, Drouin S, Jacques PE, El Fadili K, Newmarch M, Robert F, Ramotar D (2011) The peptidyl prolyl isomerase Rrd1 regulates the elongation of RNA polymerase II during transcriptional stresses. *PLoS One* **6**(8): e23159
- Proudfoot NJ, Furger A, Dye MJ (2002) Integrating mRNA processing with transcription. *Cell* **108**(4): 501-512
- Qiu L, Burgess A, Fairlie DP, Leonard H, Parsons PG, Gabrielli BG (2000) Histone deacetylase inhibitors trigger a G2 checkpoint in normal cells that is defective in tumor cells. *Mol Biol Cell* **11**(6): 2069-2083
- Rafalska-Metcalf IU, Powers SL, Joo LM, LeRoy G, Janicki SM (2010) Single cell analysis of transcriptional activation dynamics. *PLoS One* **5**(4): e10272
- Raghuram N, Carrero G, Th'ng J, Hendzel MJ (2009) Molecular dynamics of histone H1. *Biochemistry and cell biology = Biochimie et biologie cellulaire* **87**(1): 189-206
- Rahfeld JU, Rucknagel KP, Schelbert B, Ludwig B, Hacker J, Mann K, Fischer G (1994a) Confirmation of the existence of a third family among peptidyl-prolyl cis/trans isomerases. Amino acid sequence and recombinant production of parvulin. *FEBS Lett* **352**(2): 180-184

Rahfeld JU, Schierhorn A, Mann K, Fischer G (1994b) A novel peptidyl-prolyl cis/trans isomerase from Escherichia coli. *FEBS Lett* **343**(1): 65-69

Ramachandran GN, Sasisekharan V (1968) Conformation of polypeptides and proteins. *Adv Protein Chem* **23**: 283-438

Ramakrishnan V (1997) Histone H1 and chromatin higher-order structure. *Critical reviews in eukaryotic gene expression* **7**(3): 215

Ramakrishnan V, Finch JT, Graziano V, Lee PL, Sweet RM (1993) Crystal structure of globular domain of histone H5 and its implications for nucleosome binding. *Nature* **362**(6417): 219

Ramon A, Muro-Pastor MI, Scazzocchio C, Gonzalez R (2000) Deletion of the unique gene encoding a typical histone H1 has no apparent phenotype in *Aspergillus nidulans*. *Mol Microbiol* **35**(1): 223-233

Ranganathan R, Lu KP, Hunter T, Noel JP (1997) Structural and functional analysis of the mitotic rotamase Pin1 suggests substrate recognition is phosphorylation dependent. *Cell* **89**(6): 875-886

Rao J, Bhattacharya D, Banerjee B, Sarin A, Shivashankar GV (2007) Trichostatin-A induces differential changes in histone protein dynamics and expression in HeLa cells. *Biochem Biophys Res Commun* **363**(2): 263-268

Rasheed BK, Whisenant EC, Ghai RD, Papaioannou VE, Bhatnagar YM (1989) Biochemical and immunocytochemical analysis of a histone H1 variant from the mouse testis. *J Cell Sci* **94** (Pt 1): 61-71

Rattle HW, Langan TA, Danby SE, Bradbury EM (1977) Studies on the role and mode of operation of the very-lysine-rich histones in eukaryote chromatin. Effect of A and B site phosphorylation on the conformation and interaction of histone H1. *Eur J Biochem* **81**(3): 499-505

Reeves R (1984) Transcriptionally active chromatin. *Biochim Biophys Acta* **782**(4): 343-393

Reits EAJ, Neefjes JJ (2001) From fixed to FRAP: measuring protein mobility and activity in living cells. *Nature cell biology* **3**: E145

Richmond TJ, Finch JT, Rushton B, Rhodes D, Klug A (1984) Structure of the nucleosome core particle at 7 Å resolution. *Nature* **311**(5986): 532-537

Ridsdale JA, Davie JR (1987) Chicken erythrocyte polynucleosomes which are soluble at physiological ionic strength and contain linker histones are highly enriched in beta-globin gene sequences. *Nucleic Acids Res* **15**(3): 1081-1096

Ridsdale JA, Hendzel MJ, Delcuve GP, Davie JR (1990) Histone acetylation alters the capacity of the H1 histones to condense transcriptionally active/competent chromatin. *The Journal of biological chemistry* **265**(9): 5150

Ridsdale JA, Rattner JB, Davie JR (1988) Erythroid-specific gene chromatin has an altered association with linker histones. *Nucleic Acids Res* **16**(13): 5915-5926

Riggs AD, Suzuki H, Bourgeois S (1970) Lac repressor-operator interaction. I. Equilibrium studies. *J Mol Biol* **48**(1): 67-83

Robinett CC, Straight A, Li G, Willhelm C, Sudlow G, Murray A, Belmont AS (1996) In vivo localization of DNA sequences and visualization of large-scale chromatin organization using lac operator/repressor recognition. *J Cell Biol* **135**(6 Pt 2): 1685-1700

Robinson PJ, Fairall L, Huynh VA, Rhodes D (2006) EM measurements define the dimensions of the "30-nm" chromatin fiber: evidence for a compact, interdigitated structure. *Proc Natl Acad Sci U S A* **103**(17): 6506-6511

Robinson PJ, Rhodes D (2006) Structure of the '30 nm' chromatin fibre: a key role for the linker histone. *Curr Opin Struct Biol* **16**(3): 336-343

Roque A, Iloro I, Ponte I, Arrondo JL, Suau P (2005) DNA-induced secondary structure of the carboxyl-terminal domain of histone H1. *The Journal of biological chemistry* **280**(37): 32141

Roque A, Ponte I, Arrondo JL, Suau P (2008) Phosphorylation of the carboxy-terminal domain of histone H1: effects on secondary structure and DNA condensation. *Nucleic Acids Res* **36**(14): 4719-4726

Roque A, Ponte I, Suau P (2007) Macromolecular crowding induces a molten globule state in the C-terminal domain of histone H1. *Biophys J* **93**(6): 2170-2177

Roque A, Ponte I, Suau P (2009) Role of charge neutralization in the folding of the carboxy-terminal domain of histone H1. *J Phys Chem B* **113**(35): 12061-12066

Roth SY (1995) Chromatin-mediated transcriptional repression in yeast. *Curr Opin Genet Dev* **5**(2): 168-173

Roth SY, Allis CD (1992) Chromatin condensation: does histone H1 dephosphorylation play a role? *Trends Biochem Sci* **17**(3): 93-98

Roth SY, Collini MP, Draetta G, Beach D, Allis CD (1991) A cdc2-like kinase phosphorylates histone H1 in the amitotic macronucleus of Tetrahymena. *EMBO J* **10**(8): 2069-2075

Roth SY, Denu JM, Allis CD (2001) Histone Acetyltransferases. *Annual Review of Biochemistry* **70**: 81-120

Routh A, Sandin S, Rhodes D (2008) Nucleosome repeat length and linker histone stoichiometry determine chromatin fiber structure. *Proc Natl Acad Sci U S A* **105**(26): 8872-8877

Ruiz-Carrillo A, Wangh LJ, Allfrey VG (1975) Processing of newly synthesized histone molecules. *Science* **190**(4210): 117-128

Rundquist I, Lindner HH (2006) Analyses of linker histone--chromatin interactions in situ. *Biochem Cell Biol* **84**(4): 427-436

Ryo A, Nakamura M, Wulf G, Liou YC, Lu KP (2001) Pin1 regulates turnover and subcellular localization of beta-catenin by inhibiting its interaction with APC. *Nat Cell Biol* **3**(9): 793-801

Sancho M, Diani E, Beato M, Jordan A (2008) Depletion of human histone H1 variants uncovers specific roles in gene expression and cell growth. *PLoS Genet* **4**(10): e1000227

Sarg B, Helliger W, Talasz H, Forg B, Lindner HH (2006) Histone H1 Phosphorylation Occurs Site-specifically during Interphase and Mitosis: IDENTIFICATION OF A NOVEL PHOSPHORYLATION SITE ON HISTONE H1. *The Journal of biological Chemistry* **281**(10): 6573

Sawa H, Murakami H, Ohshima Y, Sugino T, Nakajyo T, Kisanuki T, Tamura Y, Satone A, Ide W, Hashimoto I, Kamada H (2001) Histone deacetylase inhibitors such as sodium butyrate and trichostatin A induce apoptosis through an increase of the bcl-2-related protein Bad. *Brain Tumor Pathol* **18**(2): 109-114

Schalch T, Duda S, Sargent DF, Richmond TJ (2005) X-ray structure of a tetranucleosome and its implications for the chromatin fibre. *Nature* **436**(7047): 138-141

Schlissel MS, Brown DD (1984) The transcriptional regulation of Xenopus 5S RNA genes in chromatin: the roles of active stable transcription complexes and histone H1. *Cell* **37**(3): 903-913

Schwarz PM, Felthauer A, Fletcher TM, Hansen JC (1996) Reversible oligonucleosome self-association: dependence on divalent cations and core histone tail domains. *Biochemistry* **35**(13): 4009-4015

Schwob E, Bohm T, Mendenhall MD, Nasmyth K (1994) The B-type cyclin kinase inhibitor p40SIC1 controls the G1 to S transition in *S. cerevisiae*. *Cell* **79**(2): 233-244

Sekerina E, Rahfeld JU, Muller J, Fanghanel J, Rascher C, Fischer G, Bayer P (2000) NMR solution structure of hPar14 reveals similarity to the peptidyl prolyl cis/trans isomerase domain of the mitotic regulator hPin1 but indicates a different functionality of the protein. *J Mol Biol* **301**(4): 1003-1017

Seyedin SM, Cole RD, Kistler WS (1981) H1 histones from mammalian testes. The widespread occurrence of H1t. *Exp Cell Res* **136**(2): 399-405

Shahbazian MD, Grunstein M (2007) Functions of site-specific histone acetylation and deacetylation. *Annu Rev Biochem* **76**: 75-100

Sharma N, Nyborg JK (2008) The coactivators CBP/p300 and the histone chaperone NAP1 promote transcription-independent nucleosome eviction at the HTLV-1 promoter. *Proc Natl Acad Sci U S A* **105**(23): 7959-7963

Sharp ZD, Mancini MG, Hinojos CA, Dai F, Berno V, Szafran AT, Smith KP, Lele TP, Ingber DE, Mancini MA (2006) Estrogen-receptor-alpha exchange and chromatin dynamics are ligand- and domain-dependent. *J Cell Sci* **119**(Pt 19): 4101-4116

Shaw BR, Herman TM, Kovacic RT, Beaudreau GS, Van Holde KE (1976) Analysis of subunit organization in chicken erythrocyte chromatin. *Proc Natl Acad Sci U S A* **73**(2): 505-509

Shechter D, Dormann HL, Allis CD, Hake SB (2007) Extraction, purification and analysis of histones. *Nat Protoc* **2**(6): 1445-1457

Shen M, Stukenberg PT, Kirschner MW, Lu KP (1998) The essential mitotic peptidyl-prolyl isomerase Pin1 binds and regulates mitosis-specific phosphoproteins. *Genes & Development* **12**(5): 706-720

Shen X, Gorovsky MA (1996) Linker histone H1 regulates specific gene expression but not global transcription in vivo. *Cell* **86**(3): 475

Shen X, Yu L, Weir JW, Gorovsky MA (1995) Linker histones are not essential and affect chromatin condensation in vivo. *Cell* **82**(1): 47

- Sherr CJ (1995) D-type cyclins. *Trends Biochem Sci* **20**(5): 187-190
- Shogren-Knaak M, Ishii H, Sun JM, Pazin MJ, Davie JR, Peterson CL (2006) Histone H4-K16 acetylation controls chromatin structure and protein interactions. *Science* **311**(5762): 844-847
- Siekierka JJ, Hung SH, Poe M, Lin CS, Sigal NH (1989) A cytosolic binding protein for the immunosuppressant FK506 has peptidyl-prolyl isomerase activity but is distinct from cyclophilin. *Nature* **341**(6244): 755-757
- Simpson RT (1978) Structure of chromatin containing extensively acetylated H3 and H4. *Cell* **13**(4): 691-699
- Simpson RT, Thoma F, Brubaker JM (1985) Chromatin reconstituted from tandemly repeated cloned DNA fragments and core histones: a model system for study of higher order structure. *Cell* **42**(3): 799-808
- Sims RJ, 3rd, Belotserkovskaya R, Reinberg D (2004) Elongation by RNA polymerase II: the short and long of it. *Genes Dev* **18**(20): 2437-2468
- Sirotkin AM, Edelmann W, Cheng G, Klein-Szanto A, Kucherlapati R, Skoultschi AI (1995) Mice develop normally without the H1(0) linker histone. *Proc Natl Acad Sci U S A* **92**(14): 6434-6438
- Sobel RE, Cook RG, Perry CA, Annunziato AT, Allis CD (1995) Conservation of deposition-related acetylation sites in newly synthesized histones H3 and H4. *Proc Natl Acad Sci U S A* **92**(4): 1237-1241
- Spadafora C, Bellard M, Compton JL, Chambon P (1976) The DNA repeat lengths in chromatins from sea urchin sperm and gastrule cells are markedly different. *FEBS Lett* **69**(1): 281-285
- Spector DL, Fu XD, Maniatis T (1991) Associations between distinct pre-mRNA splicing components and the cell nucleus. *EMBO J* **10**(11): 3467-3481
- Spencer VA, Davie JR (2001) Dynamically acetylated histone association with transcriptionally active and competent genes in the avian adult beta-globin gene domain. *J Biol Chem* **276**(37): 34810-34815
- Sporbert A, Domaing P, Leonhardt H, Cardoso MC (2005) PCNA acts as a stationary loading platform for transiently interacting Okazaki fragment maturation proteins. *Nucleic Acids Research* **33**(11): 3521-3528
- Sporbert A, Gahl A, Ankerhold R, Leonhardt H, Cardoso MC (2002) DNA polymerase clamp shows little turnover at established replication sites but

sequential de novo assembly at adjacent origin clusters. *Molecular Cell* **10**(6): 1355-1365

Sprague BL, Muller F, Pego RL, Bungay PM, Stavreva DA, McNally JG (2006) Analysis of binding at a single spatially localized cluster of binding sites by fluorescence recovery after photobleaching. *Biophys J* **91**(4): 1169-1191

Sprague BL, Pego RL, Stavreva DA, McNally JG (2004) Analysis of binding reactions by fluorescence recovery after photobleaching. *Biophys J* **86**(6): 3473-3495

Stanya KJ, Liu Y, Means AR, Kao HY (2008) Cdk2 and Pin1 negatively regulate the transcriptional corepressor SMRT. *J Cell Biol* **183**(1): 49-61

Stasevich TJ, Mueller F, Brown DT, McNally JG (2010) Dissecting the binding mechanism of the linker histone in live cells: an integrated FRAP analysis. *The EMBO journal*

Stavreva DA, McNally JG (2006) Role of H1 phosphorylation in rapid GR exchange and function at the MMTV promoter. *Histochem Cell Biol* **125**(1-2): 83-89

Steger DJ, Workman JL (1999) Transcriptional analysis of purified histone acetyltransferase complexes. *Methods* **19**(3): 410-416

Stewart DE, Sarkar A, Wampler JE (1990) Occurrence and role of cis peptide bonds in protein structures. *J Mol Biol* **214**(1): 253-260

Strahl BD, Allis CD (2000) The language of covalent histone modifications. *Nature* **403**(6765): 41

Strausfeld U, Labbe JC, Fesquet D, Cavadore JC, Picard A, Sadhu K, Russell P, Doree M (1991) Dephosphorylation and activation of a p34cdc2/cyclin B complex in vitro by human CDC25 protein. *Nature* **351**(6323): 242-245

Struhl K (1998) Histone acetylation and transcriptional regulatory mechanisms. *Genes & Development* **12**(5): 599-606

Stukenberg PT, Kirschner MW (2001) Pin1 acts catalytically to promote a conformational change in Cdc25. *Molecular Cell* **7**(5): 1071-1083

Subirana JA (1990) Analysis of the charge distribution in the C-terminal region of histone H1 as related to its interaction with DNA. *Biopolymers* **29**(10-11): 1351-1357

Sudol M (1996) Structure and function of the WW domain. *Prog Biophys Mol Biol* **65**(1-2): 113-132

Sulimova GE, Kutsenko AS, Rakhmanaliev ER, Udina IG, Kompaniytsev AA, Protopopov AI, Mojsjak EV, Klimov EA, Muravenko OV, Zelenin AV, Braga EA, Kashuba VI, Zabarovskiy ER, Kisselev LL (2002) Human chromosome 3: integration of 60 NotI clones into a physical and gene map. *Cytogenet Genome Res* **98**(2-3): 177-183

Sun JM, Chen HY, Moniwa M, Litchfield DW, Seto E, Davie JR (2002) The transcriptional repressor Sp3 is associated with CK2-phosphorylated histone deacetylase 2. *J Biol Chem* **277**(39): 35783-35786

Surmacz TA, Bayer E, Rahfeld JU, Fischer G, Bayer P (2002) The N-terminal basic domain of human parvulin hPar14 is responsible for the entry to the nucleus and high-affinity DNA-binding. *J Mol Biol* **321**(2): 235-247

Suzuki R, Nagata K, Yumoto F, Kawakami M, Nemoto N, Furutani M, Adachi K, Maruyama T, Tanokura M (2003) Three-dimensional solution structure of an archaeal FKBP with a dual function of peptidyl prolyl cis-trans isomerase and chaperone-like activities. *J Mol Biol* **328**(5): 1149-1160

Swank RA, Th'ng JP, Guo XW, Valdez J, Bradbury EM, Gurley LR (1997) Four distinct cyclin-dependent kinases phosphorylate histone H1 at all of its growth-related phosphorylation sites. *Biochemistry* **36**(45): 13761

Takami Y, Nishi R, Nakayama T (2000) Histone H1 Variants Play Individual Roles in Transcription Regulation in the DT40 Chicken B Cell Line. *Biochemical and Biophysical Research Communications* **268**(2): 501-508

Talasz H, Helliger W, Puschendorf B, Lindner H (1996) In vivo phosphorylation of histone H1 variants during the cell cycle. *Biochemistry* **35**(6): 1761

Tanaka M, Hennebold JD, Macfarlane J, Adashi EY (2001) A mammalian oocyte-specific linker histone gene H1oo: homology with the genes for the oocyte-specific cleavage stage histone (cs-H1) of sea urchin and the B4/H1M histone of the frog. *Development (Cambridge, England)* **128**(5): 655

Tanaka M, Kihara M, Hennebold JD, Eppig JJ, Viveiros MM, Emery BR, Carrell DT, Kirkman NJ, Meczekalski B, Zhou J, Bondy CA, Becker M, Schultz RM, Misteli T, De La Fuente R, King GJ, Adashi EY (2005) H1FOO is coupled to the initiation of oocytic growth. *Biology of reproduction* **72**(1): 135

- Tatara Y, Terakawa T, Uchida T (2010) Identification of Pin1-binding phosphorylated proteins in the mouse brain. *Biosci Biotechnol Biochem* **74**(12): 2480-2483
- Taunton J, Hassig CA, Schreiber SL (1996a) A Mammalian Histone Deacetylase Related to the Yeast Transcriptional Regulator Rpd3p. *Science* **272**(5260): 408
- Taunton J, Hassig CA, Schreiber SL (1996b) A mammalian histone deacetylase related to the yeast transcriptional regulator Rpd3p. *Science* **272**(5260): 408-411
- Taylor WR, Chadee DN, Allis CD, Wright JA, Davie JR (1995) Fibroblasts transformed by combinations of ras, myc and mutant p53 exhibit increased phosphorylation of histone H1 that is independent of metastatic potential. *The FEBS journal* **377**(1): 51-53
- Th'ng JP, Guo XW, Swank RA, Crissman HA, Bradbury EM (1994) Inhibition of histone phosphorylation by staurosporine leads to chromosome decondensation. *The Journal of biological chemistry* **269**(13): 9568
- Th'ng JP, Sung R, Ye M, Hendzel MJ (2005) H1 family histones in the nucleus. Control of binding and localization by the C-terminal domain. *The Journal of biological chemistry* **280**(30): 27809
- Thevenaz P, Ruttimann UE, Unser M (1998) A pyramid approach to subpixel registration based on intensity. *IEEE Trans Image Process* **7**(1): 27-41
- Thiagalingam S, Cheng KH, Lee HJ, Mineva N, Thiagalingam A, Ponte JF (2003) Histone deacetylases: unique players in shaping the epigenetic histone code. *Ann N Y Acad Sci* **983**: 84-100
- Thoma F (1979) Involvement of histone H1 in the organization of the nucleosome and of the salt-dependent superstructures of chromatin. *The Journal of Cell Biology* **83**(2): 403-427
- Thoma F, Losa R, Koller T (1983) Involvement of the domains of histones H1 and H5 in the structural organization of soluble chromatin. *J Mol Biol* **167**(3): 619-640
- Thomas JO (1999) Histone H1: location and role. *Current opinion in cell biology* **11**(3): 312
- Travers A (2009) Paradox Regained: a Topological Coupling of Nucleosomal DNA Wrapping and Chromatin Fibre Coiling. *The IMA Volumes in Mathematics and its Applications* **150**: 321-329

- Trieschmann L, Martin B, Bustin M (1998) The chromatin unfolding domain of chromosomal protein HMG-14 targets the N-terminal tail of histone H3 in nucleosomes. *Proc Natl Acad Sci U S A* **95**(10): 5468-5473
- Tse C, Hansen JC (1997) Hybrid trypsinized nucleosomal arrays: identification of multiple functional roles of the H2A/H2B and H3/H4 N-termini in chromatin fiber compaction. *Biochemistry* **36**(38): 11381-11388
- Tse C, Sera T, Wolffe AP, Hansen JC (1998) Disruption of higher-order folding by core histone acetylation dramatically enhances transcription of nucleosomal arrays by RNA polymerase III. *Mol Cell Biol* **18**(8): 4629-4638
- Tsukamoto T, Hashiguchi N, Janicki SM, Tumber T, Belmont AS, Spector DL (2000) Visualization of gene activity in living cells. *Nat Cell Biol* **2**(12): 871-878
- Tumber T, Sudlow G, Belmont AS (1999) Large-scale chromatin unfolding and remodeling induced by VP16 acidic activation domain. *J Cell Biol* **145**(7): 1341-1354
- Uchida T, Fujimori F, Tradler T, Fischer G, Rahfeld JU (1999) Identification and characterization of a 14 kDa human protein as a novel parvulin-like peptidyl prolyl cis/trans isomerase. *FEBS Lett* **446**(2-3): 278-282
- van Holde K, Zlatanova J (1996) What determines the folding of the chromatin fiber? *Proceedings of the National Academy of Sciences* **93**(20): 10548-10555
- Van Holde KE (1988) Chromatin. *Springer series in molecular biology*: 530
- Van Lint C, Emiliani S, Verdin E (1996) The expression of a small fraction of cellular genes is changed in response to histone hyperacetylation. *Gene Expr* **5**(4-5): 245-253
- Van Speybroeck L (2002) From epigenesis to epigenetics: the case of C. H. Waddington. *Ann N Y Acad Sci* **981**: 61-81
- Varga-Weisz P, van Holde K, Zlatanova J (1993) Preferential binding of histone H1 to four-way helical junction DNA. *J Biol Chem* **268**(28): 20699-20700
- Varshavsky AJ, Bakayev VV, Georgiev GP (1976) Heterogeneity of chromatin subunits in vitro and location of histone H1. *Nucleic Acids Res* **3**(2): 477-492

Verdecia MA, Bowman ME, Lu KP, Hunter T, Noel JP (2000) Structural basis for phosphoserine-proline recognition by group IV WW domains. *Nat Struct Biol* **7**(8): 639-643

Vicent GP, Nacht AS, Font-Mateu J, Castellano G, Gaveglia L, Ballare C, Beato M (2011) Four enzymes cooperate to displace histone H1 during the first minute of hormonal gene activation. *Genes Dev* **25**(8): 845-862

Vidali G, Boffa LC, Bradbury EM, Allfrey VG (1978) Butyrate suppression of histone deacetylation leads to accumulation of multiacetylated forms of histones H3 and H4 and increased DNase I sensitivity of the associated DNA sequences. *Proc Natl Acad Sci U S A* **75**(5): 2239-2243

Vidali G, Ferrari N, Pfeffer U (1988) Histone acetylation: a step in gene activation. *Adv Exp Med Biol* **231**: 583-596

Vila R, Ponte I, Collado M, Arrondo JL, Jimenez MA, Rico M, Suau P (2001) DNA-induced alpha-helical structure in the NH2-terminal domain of histone H1. *The Journal of biological chemistry* **276**(49): 46429

Vila R, Ponte I, Jimenez MA, Rico M, Suau P (2002) An inducible helix-Gly-Gly-helix motif in the N-terminal domain of histone H1e: a CD and NMR study. *Protein Sci* **11**(2): 214-220

Vujatovic O, Zaragoza K, Vaquero A, Reina O, Bernues J, Azorin F (2012) Drosophila melanogaster linker histone dH1 is required for transposon silencing and to preserve genome integrity. *Nucleic Acids Res*

Vyas P, Brown DT (2012a) N- and C-terminal domains determine differential nucleosomal binding geometry and affinity of linker histone isotypes H1(0) and H1c. *J Biol Chem* **287**(15): 11778-11787

Vyas P, Brown DT (2012b) N- and C-terminal Domains Determine Differential Nucleosomal Binding Geometry and Affinity of Linker Histone Isotypes H10 and H1c. *J Biol Chem* **287**(15): 11778-11787

Waddington CH (1942) The epigenotype. 1942. *Int J Epidemiol* **41**(1): 10-13

Wang X, Hayes JJ (2008) Acetylation mimics within individual core histone tail domains indicate distinct roles in regulating the stability of higher-order chromatin structure. *Mol Cell Biol* **28**(1): 227-236

Wang X, He C, Moore SC, Ausio J (2001) Effects of histone acetylation on the solubility and folding of the chromatin fiber. *The Journal of Biological Chemistry* **276**(16): 12764-12768

- Wang X, Moore SC, Laszckzak M, Ausio J (2000) Acetylation increases the alpha-helical content of the histone tails of the nucleosome. *J Biol Chem* **275**(45): 35013-35020
- Ward JJ, Sodhi JS, McGuffin LJ, Buxton BF, Jones DT (2004) Prediction and functional analysis of native disorder in proteins from the three kingdoms of life. *Journal of Molecular Biology* **337**(3): 635
- Waterborg JH (2000) Steady-state levels of histone acetylation in *Saccharomyces cerevisiae*. *J Biol Chem* **275**(17): 13007-13011
- Waterborg JH (2001) Dynamics of histone acetylation in *Saccharomyces cerevisiae*. *Biochemistry* **40**(8): 2599-2605
- Weiwad M, Kullertz G, Schutkowski M, Fischer G (2000) Evidence that the substrate backbone conformation is critical to phosphorylation by p42 MAP kinase. *FEBS Lett* **478**(1-2): 39-42
- Wells NJ, Hickson ID (1995) Human topoisomerase II alpha is phosphorylated in a cell-cycle phase-dependent manner by a proline-directed kinase. *Eur J Biochem* **231**(2): 491-497
- Whitlock JP, Jr., Simpson RT (1976) Removal of histone H1 exposes a fifty base pair DNA segment between nucleosomes. *Biochemistry* **15**(15): 3307-3314
- Widlak P, Kalinowska M, Parseghian MH, Lu X, Hansen JC, Garrard WT (2005) The histone H1 C-terminal domain binds to the apoptotic nuclease, DNA fragmentation factor (DFF40/CAD) and stimulates DNA cleavage. *Biochemistry* **44**(21): 7871-7878
- Widom J (1992) A relationship between the helical twist of DNA and the ordered positioning of nucleosomes in all eukaryotic cells. *Proc Natl Acad Sci USA* **89**(3): 1095-1099
- Widom J (1998) Structure, dynamics, and function of chromatin in vitro. *Annual Review of Biophysics and Biomolecular Structure* **27**: 285
- Winkler KE, Swenson KI, Kornbluth S, Means AR (2000) Requirement of the prolyl isomerase Pin1 for the replication checkpoint. *Science* **287**(5458): 1644-1647
- Wintjens R, Wieruszeski JM, Drobecq H, Rousselot-Pailley P, Buee L, Lippens G, Landrieu I (2001) 1H NMR study on the binding of Pin1 Trp-Trp domain with phosphothreonine peptides. *J Biol Chem* **276**(27): 25150-25156

- Wolffe A (1998) *Chromatin: Structure and Function*: Academic Press London.
- Wolffe AP, Hayes JJ (1999) Chromatin disruption and modification. *Nucleic acids research* **27**(3): 711
- Wolffe AP, Khochbin S, Dimitrov S (1997) What do linker histones do in chromatin? *BioEssays : news and reviews in molecular, cellular and developmental biology* **19**(3): 249
- Wolffe AP, Kurumizaka H (1998) The nucleosome: a powerful regulator of transcription. *Progress in nucleic acid research and molecular biology* **61**: 379
- Won J, Yim J, Kim TK (2002) Sp1 and Sp3 recruit histone deacetylase to repress transcription of human telomerase reverse transcriptase (hTERT) promoter in normal human somatic cells. *J Biol Chem* **277**(41): 38230-38238
- Woodcock CL, Ghosh RP (2010) Chromatin higher-order structure and dynamics. *Cold Spring Harb Perspect Biol* **2**(5): a000596
- Woodcock CL, Skoultchi AI, Fan Y (2006) Role of linker histone in chromatin structure and function: H1 stoichiometry and nucleosome repeat length. *Chromosome Res* **14**(1): 17-25
- Workman JL, Kingston RE (1992) Nucleosome core displacement in vitro via a metastable transcription factor-nucleosome complex. *Science (New York, NY)* **258**(5089): 1780
- Wu C (1997) Chromatin remodeling and the control of gene expression. *The Journal of biological chemistry* **272**(45): 28171
- Wu M, Allis CD, Richman R, Cook RG, Gorovsky MA (1986) An intervening sequence in an unusual histone H1 gene of *Tetrahymena thermophila*. *Proceedings of the National Academy of Sciences of the United States of America* **83**(22): 8674
- Wulf G, Finn G, Suizu F, Lu KP (2005) Phosphorylation-specific prolyl isomerization: is there an underlying theme? *Nature cell biology* **7**(5): 435-441
- Wulf GM, Liou YC, Ryo A, Lee SW, Lu KP (2002) Role of Pin1 in the regulation of p53 stability and p21 transactivation, and cell cycle checkpoints in response to DNA damage. *The Journal of Biological Chemistry* **277**(50): 47976-47979
- Wulf GM, Ryo A, Wulf GG, Lee SW, Niu T, Petkova V, Lu KP (2001) Pin1 is overexpressed in breast cancer and cooperates with Ras signaling in

increasing the transcriptional activity of c-Jun towards cyclin D1. *The EMBO journal* **20**(13): 3459-3472

Wyman C, Botchan M (1995) DNA replication. A familiar ring to DNA polymerase processivity. *Curr Biol* **5**(4): 334-337

Xu YX, Manley JL (2007a) New insights into mitotic chromosome condensation: a role for the prolyl isomerase Pin1. *Cell Cycle* **6**(23): 2896-2901

Xu YX, Manley JL (2007b) Pin1 modulates RNA polymerase II activity during the transcription cycle. *Genes Dev* **21**(22): 2950-2962

Xu YX, Manley JL (2007c) The prolyl isomerase Pin1 functions in mitotic chromosome condensation. *Mol Cell* **26**(2): 287-300

Yaffe MB, Schutkowski M, Shen M, Zhou XZ, Stukenberg PT, Rahfeld JU, Xu J, Kuang J, Kirschner MW, Fischer G, Cantley LC, Lu KP (1997) Sequence-specific and phosphorylation-dependent proline isomerization: a potential mitotic regulatory mechanism. *Science* **278**(5345): 1957-1960

Yamamoto T, Horikoshi M (1996) Cloning of the cDNA encoding a novel subtype of histone H1. *Gene* **173**(2): 281

Yamanaka S (2009) A fresh look at iPS cells. *Cell* **137**(1): 13-17

Yan M, Du J, Gu Z, Liang M, Hu Y, Zhang W, Priceman S, Wu L, Zhou ZH, Liu Z, Segura T, Tang Y, Lu Y (2009) A novel intracellular protein delivery platform based on single-protein nanocapsules. *Nat Nanotechnol* **5**(1): 48-53

Yan W, Ma L, Burns KH, Matzuk MM (2003) HILS1 is a spermatid-specific linker histone H1-like protein implicated in chromatin remodeling during mammalian spermiogenesis. *Proc Natl Acad Sci U S A* **100**(18): 10546-10551

Yang WM, Inouye CJ, Seto E (1995) Cyclophilin A and FKBP12 interact with YY1 and alter its transcriptional activity. *J Biol Chem* **270**(25): 15187-15193

Yang WM, Yao YL, Seto E (2001) The FK506-binding protein 25 functionally associates with histone deacetylases and with transcription factor YY1. *EMBO J* **20**(17): 4814-4825

Yao TP, Oh SP, Fuchs M, Zhou ND, Ch'ng LE, Newsome D, Bronson RT, Li E, Livingston DM, Eckner R (1998) Gene dosage-dependent embryonic development and proliferation defects in mice lacking the transcriptional integrator p300. *Cell* **93**(3): 361-372

Yasuda H, Matsumoto Y, Mita S, Marunouchi T, Yamada M (1981) A mouse temperature-sensitive mutant defective in H1 histone phosphorylation is defective in deoxyribonucleic acid synthesis and chromosome condensation. *Biochemistry* **20**(15): 4414-4419

Yeh E, Cunningham M, Arnold H, Chasse D, Monteith T, Ivaldi G, Hahn WC, Stukenberg PT, Shenolikar S, Uchida T, Counter CM, Nevins JR, Means AR, Sears R (2004) A signalling pathway controlling c-Myc degradation that impacts oncogenic transformation of human cells. *Nat Cell Biol* **6**(4): 308-318

Yeh ES, Lew BO, Means AR (2006) The loss of PIN1 deregulates cyclin E and sensitizes mouse embryo fibroblasts to genomic instability. *J Biol Chem* **281**(1): 241-251

Yoo CB, Jones PA (2006) Epigenetic therapy of cancer: past, present and future. *Nat Rev Drug Discov* **5**(1): 37-50

Yoshida M, Horinouchi S (1999) Trichostatin and leptomycin. Inhibition of histone deacetylation and signal-dependent nuclear export. *Ann N Y Acad Sci* **886**: 23-36

Yoshida M, Kijima M, Akita M, Beppu T (1990) Potent and specific inhibition of mammalian histone deacetylase both in vivo and in vitro by trichostatin A. *J Biol Chem* **265**(28): 17174-17179

Zhang CL, McKinsey TA, Chang S, Antos CL, Hill JA, Olson EN (2002) Class II histone deacetylases act as signal-responsive repressors of cardiac hypertrophy. *Cell* **110**(4): 479-488

Zhang D, Nelson DA (1986) Histone acetylation in chicken erythrocytes. Estimation of the percentage of sites actively modified. *Biochem J* **240**(3): 857-862

Zhang DE, Nelson DA (1988a) Histone acetylation in chicken erythrocytes. Rates of acetylation and evidence that histones in both active and potentially active chromatin are rapidly modified. *Biochem J* **250**(1): 233-240

Zhang DE, Nelson DA (1988b) Histone acetylation in chicken erythrocytes. Rates of deacetylation in immature and mature red blood cells. *Biochem J* **250**(1): 241-245

Zheng H, You H, Zhou XZ, Murray SA, Uchida T, Wulf G, Gu L, Tang X, Lu KP, Xiao ZX (2002) The prolyl isomerase Pin1 is a regulator of p53 in genotoxic response. *Nature* **419**(6909): 849-853

Zheng Y, John S, Pesavento JJ, Schultz-Norton JR, Schiltz RL, Baek S, Nardulli AM, Hager GL, Kelleher NL, Mizzen CA (2010) Histone H1 phosphorylation is associated with transcription by RNA polymerases I and II. *J Cell Biol* **189**(3): 407-415

Zhou XZ, Kops O, Werner A, Lu PJ, Shen M, Stoller G, Kullertz G, Stark M, Fischer G, Lu KP (2000) Pin1-dependent prolyl isomerization regulates dephosphorylation of Cdc25C and tau proteins. *Molecular Cell* **6**(4): 873-883

Zhou XZ, Lu PJ, Wulf G, Lu KP (1999) Phosphorylation-dependent prolyl isomerization: a novel signaling regulatory mechanism. *Cell Mol Life Sci* **56**(9-10): 788-806

Zlatanova J, Doenecke D (1994) Histone H1 zero: a major player in cell differentiation? *FASEB J* **8**(15): 1260-1268

Zlatanova J, Van Holde K (1992) Histone H1 and transcription: still an enigma? *Journal of cell science* **103 (Pt 4)**(Pt 4): 889

Zlatanova J, van Holde K (1996) The linker histones and chromatin structure: new twists. *Progress in nucleic acid research and molecular biology* **52**: 217-259

Zlatanova JS (1980) Synthesis of histone H1(0) is not inhibited in hydroxyurea-treated Friend cells. *FEBS Lett* **112**(2): 199-202